Solubilisation and stabilisation of MRP4 using novel detergents for function and structural studies

David Hardy

Doctor of Philosophy

Aston University

September 2018

Aston University

"Solubilisation and stabilisation of MRP4 using novel detergents for functional and structural studies" by David Hardy for the degree of Doctor of Philosophy in Biochemistry, 2018.

Knowledge of membrane protein function and structure is limited due to the complications in the production of stable, functional membrane proteins that can be used in functional and structural studies. These limitations are due to their location within a lipid bilayer and this creates challenges at almost every stage including expression, solubilisation, stabilisation and purification of membrane proteins. This study aimed to combat some of these limitations for the human membrane protein ABCC4/MRP4 (multidrug resistance protein 4) from the ABC superfamily, in particular focusing on the solubilisation and stabilisation aspects.

MRP4 was expressed in *Spodoptera frugiperda* (*Sf* 9) insect cells, *Pichia pastoris* yeast cells and Human Embryonic Kidney (HEK) cells. It was found that the highest level of expression was achieved using *Sf* 9 insect cells. MRP4 was then tested for functionality using a fluorescent vesicular transport assay that was developed within this study and shown to be functional. It was found that Calixarene C4C7 and the polymer SMA 2000 were both more efficient at solubilising and stabilising MRP4 than conventional detergents. Conditions for purification with both C4C7 and SMA 2000 were optimised, and were able to produce protein at ~40% and ~70% purity and concentrations of ~400 µg/mL and ~25 µg/mL respectively. Following purification it was determined, using tryptophan fluorescence quenching binding assays, that the SMA purified MRP4 bound ligands and retained increased stability compared to conventional detergents. Preliminary studies were performed using electron microscopy, which showed potential for this approach in the future. The techniques and methods developed in this study can be used by others in the future to gain better structural and functional knowledge of MRP4 and can also be applied to the study of other membrane proteins.

Membrane proteins, expression, purification, Calixar, SMALP

Acknowledgements

First and fore most I would like to thank my supervisor, Dr Alice Rothnie, for her support, guidance, patience and dedication during my PhD.

Thank you to my co-supervisor, Prof Roslyn Bill, for her help and guidance.

I would like to thank Anass Jawhari for his expertise and giving me the opportunity to gain valuable industrial experience at Calixar. And to everyone at Calixar for their help and support.

Thank you to Dr Ian Kerr at Nottingham University and Phd students: Aaron and Meg, for helping me out with difficult molecular biology.

Thank you to Prof. Susan Cole for providing the MRP4-his_6 baculovirus plasmid.

A special massive thank you to all my close friends; Chris Burton, Hanna Burton, Allan Cameron, Laura Feather, Rory McLean, Shaun Fell, Marta Amaral, Cian Spaine and Elisa Spaine for making the PhD truly fantastic. Thank you to everyone in the lab for making it an very fun and enjoyable place to work. Of course, thank you to my family for their support and helping me out at difficult times.

And thank you to everyone else who has made this PhD an incredible experience and great start to my research career.

List of contents

List of abbreviations

Sf 9 - *Spodoptera frugiperda*

P. pastoris - *Pichia pastoris*

HEK - Human embryonic kindey

SMA - styrene maleic acid

SMALP - styrene maleic acid lipid particle

C4Cn – calixar[4]erene (n = 1 – 12)

DDM- *n*-Dodecyl β-D-maltoside

CP – creatine phosphatase

CK – creatine kinase

ABC – ATP binding cassette

SDS- Sodium dodecyl sulfate

LSB – Laemmli sample buffer

PVDF - polyvinylidene difluoride

TBSt – Tris buffer saline tween

TAE – Tris acetic acid EDTA

EDTA - Ethylenediaminetetraacetic acid

BMGY - Buffered Glycerol-complex Medium

BMMY - Buffered Methanol-complex Medium

YNB – Yeast nitrogen base

ATP – Adenosine Triphosphate

AMP – Adenosine Monophosphate

Fluo-cAMP - 8- (2-[Fluoresceinyl]aminoethylthio) adenosine- 3', 5'- cyclic monophosphate

TSB – Tris sucrose buffer

CMC – critical micelle concentration

SEC – Size exclusion chromatography

List of table and figures

1. Introduction

1.1 Membrane Proteins

Membrane proteins are localised in the membranes of cells and make up between 20 and 30% of all proteins in eukaryotic cells (Wallin and von Heijne 1998). They can be localised in the cell surface membranes, membranes of organelles such as mitochondria or vesicular membranes. Membrane proteins have a wide range of functions and are present in both prokaryotes and eukaryotes. The defining characteristic of membrane proteins is that a portion of the protein must interact with the membrane directly or indirectly. The general structure and way in which they interact with the lipid bilayer means they can be classed into two general groups: integral or intrinsic and peripheral or extrinsic. The lipid bilayer is a complex environment made up of many different types of phospholipids each containing a hydrophobic fatty acyl chain which faces inwards and a hydrophilic polarised head group on the surface. Extrinsic or peripheral proteins are not embedded in the hydrophobic core of the lipid bilayer and do not interact with the hydrophobic fatty acyl chains of the phospholipids. As their name suggests they are on the periphery of the lipid bilayer and are anchored into the lipid bilayer via a variety of means: the attachment to integral membrane proteins, covalently bound to membrane lipids, by having hydrophobic loops inserted into the membrane, or amphiphilic α-helixes of ionic interactions with phospholipids. Integral membrane proteins have at least one domain embedded in the lipid bilayer and can have transmembrane domains that span the entire bilayer which contain hydrophobic side chains. These hydrophobic side chains can interact with the fatty acyl chains of the phospholipids due to their hydrophobic nature securing them in the lipid bilayer. The transmembrane domains of intrinsic membrane proteins are either α-helices or β-sheets and can weave their way in and out of the membrane creating polytopic membrane domains.

Transmembrane spanning proteins that contain both extra and intracellular domains as well as transmembrane domains are often involved in the transport of molecules across the membrane or cell signalling (Figure 1.1). Transporters are the gate keepers of the cells and allow certain molecules into and out of the cell. The extracellular domain of a receptor can sense changes in the environment around the cell and convey the message to the intracellular domain and down a signalling pathway, allowing the cell to respond to these changes. Other transmembrane proteins are involved in enzymatic functions catalysing reactions and allowing intracellular signalling pathways to be triggered. Some transmembrane proteins are anchoring proteins holding the cytoskeleton in place.

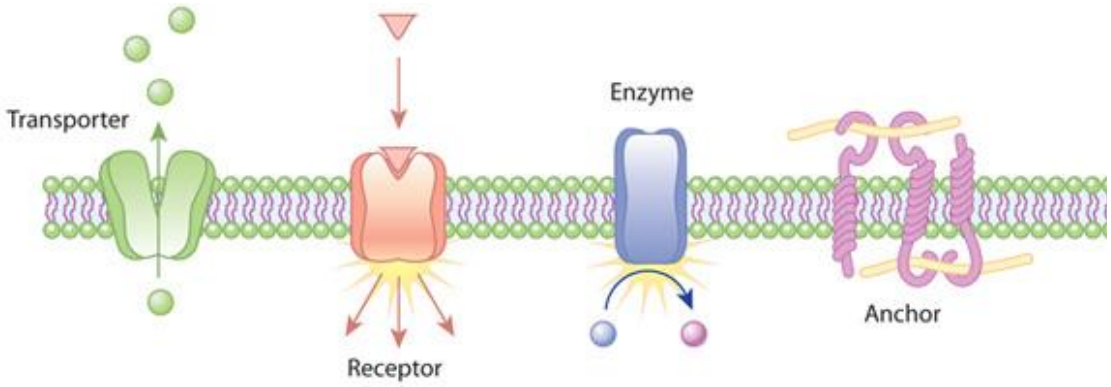

Figure 1.1: Examples of integral transmembrane proteins and their functions. *Transporters and channels are capable of transporting molecules across the lipid membrane. Receptors are able to bind extracellular molecules and translate them into intracellular processes. Enzymes catalyse the transformation of a molecule. Anchoring proteins can link intra and extra cellular proteins to the lipid membrane.(Bruce Alberts 2009)*

Human membrane proteins can be found all over the body in every cell type and are vital for any cells survival, and thus for keeping the cells in the body functioning properly. When there are mutations in membrane proteins, it can cause severe disease states such as cystic fibrosis and Alzheimer's disease (Lichtenthaler, Ida et al. 1997, Vankeerberghen, Cuppens et al. 2002). They are potential drug targets for many conditions. One class of membrane proteins, the G-protein coupled receptors (GPCRs) are already the target of ~34% of current drugs (Hauser, Chavali et al. 2018) but the insight into these membrane proteins is ever expanding through developments in

membrane protein structural biology. Understanding the structure and function of membrane proteins, especially those involved in diseases, is a key step in developing new targeted therapies for many conditions.

1.2 The topology and structure of membrane proteins.

A very crude idea of the general structure of membrane proteins can be obtained from topology predictions. The topology of membrane proteins is predicted using two factors of membrane proteins, the hydrophobicity and charge (van Geest and Lolkema 2000). Which regions of the protein are hydrophobic are determined simply by analysing the amino acid sequence. The more hydrophobic regions are more likely to be located within the membrane as they will favour the hydrophobic environment of the lipid bilayer and make up the transmembrane domains (Vonheijne and Gavel 1988). The segments that are not translocated into the lipid membrane can help determine the orientation of the membrane protein. This is to do with the charges on the membrane protein as it will follow the "positive inside" rule describe by Gunnar von Heijne. This rule states the non-translocated segments contain positive charged residues. These factors have led to software that can predict the structure of membrane proteins which has been a valuable tool in membrane protein structural biology (Claros and Vonheijne 1994).

To date there are over 863 structures of unique membrane proteins in the database " Membrane proteins of known 3D structure" (http://blanco.biomol.uci.edu/mpstruc/). This may seem like the field has come along way since 1985 when the first X-ray crystal structure of a membrane protein was produced, but the vast majority of the structures in the database are prokaryotic membrane proteins. Considering that around 25% of the human genome codes for proteins are membrane proteins, equating to around 5500 membrane proteins there is a long way to go in discovering and understanding human membrane proteins (Fagerberg, Jonasson et al. 2010). The amount of structures is increasing but not as fast as soluble proteins. The reasons why

there are so few membrane protein structures especially human membrane proteins are due to limitations encountered at every stage of the process including overexpression, solubilisation, stabilisation, purification and sample preparation (Table 1).

Process	**Limitation**
Expression	• Naturally low in abundance • Membrane proteins have to be made into recombinant proteins • Overexpression can lead to misfolded and non-functional membrane proteins
Solubilisation and stabilisation	• Loss of native lipid membrane reduces lateral pressure causing protein to collapse and aggregate • Detergent solubilisation can lead to denaturing proteins • Membrane proteins have to be stable and maintain native conformation
Purification	• Weak binding of membrane proteins • Detergents must be present in all solutions • Samples have to be homogeneous and in high concentration for functional and structural studies
Functional and Structural Studies	• Detergents can cause loss of function • Only detergent solubilised membrane proteins have been crystallized in 3D • Producing 3D crystals requires a highly stable and homogenous sample

Table 1: The limitations of membrane protein structural biology.

1.3 Limitations of membrane protein structural biology

1.3.1 Expression

The first limitation of membrane protein structural biology is producing the membrane protein of interest. It is not only about expressing the protein of interest but also expressing it to a high level in its native conformation(s). Most membrane proteins are naturally expressed in low levels, and so obtaining sufficient amounts of the native membrane proteins to conduct structural studies from natural sources would require large amounts of that cell type. This can lead to very costly and time consuming experiments, and is really only realistic for proteins which are naturally abundant in certain cell types such as rhodopsin in the retina (Kobilka 2007).

To overcome the problem of low natural expression, recombinant overexpression can be performed, increasing the yield per cell (Tate 2001). Another advantage of recombinant expression is the ability to easily add tags to enable efficient separation of the target protein from the other membrane proteins. Common purification tags include histidine, strep and flag tags which can increase the purity and yield though affinity purification (Kimple, Brill et al. 2013). However, it is important these tags do not interfere with the function of the protein. Other common recombinant membrane protein changes include attaching green fluorescent protein (GFP) to the membrane protein. GFP can be used for quantitative measurements such as expression levels (Drew, Slotboom et al. 2005). It can be used to establish where the protein is being expressed to make sure it is located in the correct membrane, and allows tracking of the target protein throughout the solubilisation and purification procedure (Bird, Rada et al. 2015). One problem that may arise when using GFP fusion protein is the expression levels and function of the membrane protein may change.

Effective recombinant membrane protein expression requires finding a suitable host. If the membrane protein is a prokaryotic protein then *E. coli* could potentially be used. The advantages of using of *E.coli* for recombinant overexpression of membrane proteins is that it can be carried

out quickly as they have a high growth rate, high quantities of cells are easily achieved and they only require cheap nutrient broth for growth. This makes them very easy to grow requiring minimal specialised equipment and are simple to culture in large quantities (Rosano and Ceccarelli 2014).

If your target protein is eukaryotic, such as human membrane proteins, then *E.coli* often does not work. Instead, a eukaryotic host such as yeast, insect cells or mammalian cells can be used. Yeast cells are able to grow to very high cells densities very quickly and cost efficiently similarly to *E.coli* cells. Two main strains of yeast have been used for membrane protein expression, *Pichia pastoris* and *Sacchromyces cerevisiae*. *Pichia pastoris* requires the integration of the recombinant gene of interest into the yeast genome allowing a stable strain to be produced but it is not possible to control the number of copies or location of the recombinant gene. However the advantages of using *Pichia* are the high cells densities it can grow to with exceptionally high yields of correctly folded protein meaning large amount of recombinant protein can be produced (Dilworth, Piel et al. 2018). In contrast *Sacchromyces cerevisiae* expression tends to use plasmids containing the gene of interest, similarly to *E.coli*. Although the promoter maybe 10-100 fold weaker in *S. cerevisiae* then in *P.pastoris* there can be high copy numbers of the plasmid. The genetics of *S. cerevisiae* are also better understood allowing for the production of thousands of mutant strains to improve the expression (Dilworth, Piel et al. 2018). This means there are many different strains that can be used to improved expression yield compared to *P. pastoris* so there is more chance of finding a strain that will allow overexpression the membrane proteins.

Insect cell expression is a commonly used expression system for recombinant mammalian membrane proteins. These cells can also been grown in suspension cultures to high cell densities in large volumes and are simple to culture. They require the production of a recombinant baculovirus carrying the gene of interest, and infection of the insect cells with this virus leads to protein expression. There are three main types of insect cells used for recombinant mammalian membrane protein expression: *Sf* 9, *Sf* 21 and High Five. These insect cells are only able to

perform simple mannose glycosylation but a new strain *Sf*SWT-5 has been produced to overcome this problem by including six key glycogenes (McKenzie and Abbott 2018). There are a large number of baculovirus expression vectors that have aided in the high level of protein expression. Inclusion bodies are rarely formed with the baculovirus expression system in insect cells unlike in *E.coli (*Jarvis *2009)*. This system has also been beneficial in the production of multiprotein subunit complexes (Berger, Fitzgerald et al. 2004, Kost, Condreay et al. 2005).

Mammalian cell expression offers potentially the most relevant cellular environment for human membrane proteins. However, cell culturing techniques are often much more costly and time consuming. Many mammalian cell lines have to grow in monolayers, not suspension cultures like *E.coli* and yeast, and can often be very slow growing. Specialised equipment such as micro flow hoods and incubators with gas exchange are need. Certain cell lines are hard to culture needing constant care and attention making them a much harder way of producing large quantities of membrane protein. Two of the most common mammalian cell line used are human embryonic kidney (HEK) and Chinese hamster ovary (CHO) cells (Pham, Kamen et al. 2006). The HEK cell line was chosen for this study as these cells naturally express MRP4 showing that their cellular environment is optimised for producing functional MRP4 (Massimi, Ciuffetta et al. 2015). HEK cells can be made to overexpress recombinant membrane proteins by either producing a transient or stable cell lines (Vatandoost J 2017). Transient transfections involve the production of a plasmid and then transfection, with many different plasmids and transfection reagents available to increase the expression. Stable cell lines often produce higher yields than transient transfections but producing a stable cell line can be time consuming (McKenzie and Abbott 2018). Once a stable cell line is produced the HEK cell can grow in suspension to high cell densities increasing the yield.

When a suitable host is found the membrane protein expressed must not be toxic to the cell – this is often particularly problematic for ion channels as overexpression can disrupt the electrochemical gradients essential for the cell survival. The expressed membrane protein has to be folded correctly and post translational modification is an important consideration for this.

Finding the balance between overexpression and quality needs to be obtained, it is quite possible that reducing the expression level may increase the quality of the membrane protein as the recombinant membrane protein expressed maybe harmful to the cell at high yields leading to cell death. Also compared to proteins overexpressed in the cytosol or secreted there is limited space in the plasma membrane when over expressing membrane proteins, reducing the yield (Hardy, Bill et al. 2016).

1.3.2 Extraction and Stabilisation

1.3.2.1 Detergents

The overexpressed membrane protein has to be extracted/solubilised from the membrane as they are naturally surrounded by lipids, which are not soluble in aqueous solutions due to their hydrophobic nature. Maintaining protein stability whilst extracting it from its native environment has been a major problem in membrane protein structural biology since it began and is the key area of this project. Solubilisation is required for downstream processing such as purification and many structural techniques. The conventional and most commonly used method for solubilising membrane protein is using detergents. These amphipathic molecules are able to mimic the lipid bilayer by forming micelles around the membrane protein allowing it to become soluble in aqueous solutions. The two main components of detergents are the hydrophilic polar head group and the hydrophobic hydrocarbon tail (Seddon, Curnow et al. 2004). These two features allow these molecules to be amphipathic and are capable of solubilising membrane proteins in three main steps. First, they destabilise the lipids found in the membrane and then they are able to bind to the membrane protein. The hydrophobic hydrocarbon chain of the detergent is able it bind to the hydrophobic transmembrane region of the membrane protein. The detergent surrounds the membrane protein by creating a micelle around the protein allowing the hydrophilic head groups to interact with the aqueous solution creating a soluble membrane protein (le Maire, Champeil et

al. 2000). A defining characteristic of detergents is their critical micelle concentration (CMC). This is the minimal concentration at which a detergent will spontaneously form a micelle in water. Not all detergents have the same CMC with higher CMC equating to more detergent needed to reach the CMC and short chain detergents having high CMC values (Prive 2007). Most membrane protein solubilisation is carried out using concentrations well above the CMC value of the detergent to ensure maximum solubilisation efficiency. After solubilisation the concentration of detergent present has to be kept high enough to maintain solubility (Lin and Guidotti 2009). If the CMC value for a given detergent is very high, more will be needed and some detergents are very costly, potentially making this a very expensive process.

Detergents can be classed into three main types; ionic, non-ionic and zwitterionic (Seddon, Curnow et al. 2004). They have a range from harsh denaturing to soft non-denaturing detergents. The size and charge of the head group has an influence on the harshness with the smaller charged head groups being harsh and larger uncharged ones being softer (le Maire, Champeil et al. 2000). The other contributing factor is the length of the acyl tail with shorter lengths 3-8 carbons being harsh and longer 10-12 carbons being softer (Prive 2007). There is a fine balance between solubilisation and denaturing membrane proteins. The lipid-protein interactions need to be broken but not the protein-protein interactions as these help hold the membrane protein in the correct conformation (Stetsenko and Guskov 2017).

Ionic detergents have a polar head group that is either cationic or anionic and either a hydrocarbon or steroidal backbone that is hydrophobic. They are very effective at solubilising membrane proteins but are also denaturing, making them a harsh detergent. Sodium dodecyl sulfate (SDS) is one of the most commonly known detergents that falls into this category (Figure 1.3.2.1). SDS is used in biological techniques such as SDS polyacrylamide gel electrophoresis as it is capable of denaturing proteins by breaking protein-protein interactions allowing for greater separation of proteins. The denaturing effects of ionic detergents such as SDS can be reversed by renaturing the membrane protein as demonstrated with bacteriorhodopsin (Booth, Flitsch et al.

1995)but is usually met with limited success. SDS has been used in NMR studies of transmembrane peptides as it is used as a membrane mimetic environment (le Maire, Champeil et al. 2000).

Non-ionic detergents are generally milder detergents with solubilising capabilities but are not as denaturing as ionic detergents. They contain either a polyoxyethylene or glycosidic uncharged hydrophilic head group. Non-ionic detergents with polyoxyethylene head groups include the Tween and Triton series of detergents. Ones with glycosides have sugars as their uncharged head groups such as maltoside or glucoside. It is the length of the hydrophobic chain in non-ionic detergents that determines how denaturing the detergent is. Non-ionic detergents with short hydrocarbon chains (C_7-C_{10})such as octylglucoside(OG) (Figure 1.3.2.1) often lead to denaturing and inactivation of the membrane protein compared to longer hydrocarbon chains (C_{12}-C_{14}) (Lund, Orlowski et al. 1989). Other non-ionic detergents such as n-dodecyl-β-D-maltoside (DDM) are capable of solubilising membrane proteins and keeping them in the active state (Fleming, Ackerman et al. 1997). DDM is actually the most commonly used detergent in membrane protein structural studies (Stetsenko and Guskov 2017). The larger head group of DDM and its longer hydrocarbon chain may be what makes this detergent so successful at solubilising, but at the same time not denaturing, membrane proteins. The difference between DDM and n-decyl-β-D-maltopyranoside (DM) is a good example of how even the slightest change in a detergent can have an effect on its CMC. By just adding two carbons to the DM molecule creating DDM the CMC value drops from 2.2 mM to 0.18 mM (le Maire, Champeil et al. 2000).

Zwitterionoic detergents are generally more inactivating than non-ionic detergents but have still been used in structural studies. For example N,N-Dimethyldodecylamine N-oxide (DDAO) (Figure

1.3.2.1) has been used in the crystallization of the photosynthetic reaction centre from Rhodopseudomonas viridis (Deisenhofer, Epp et al. 1985).

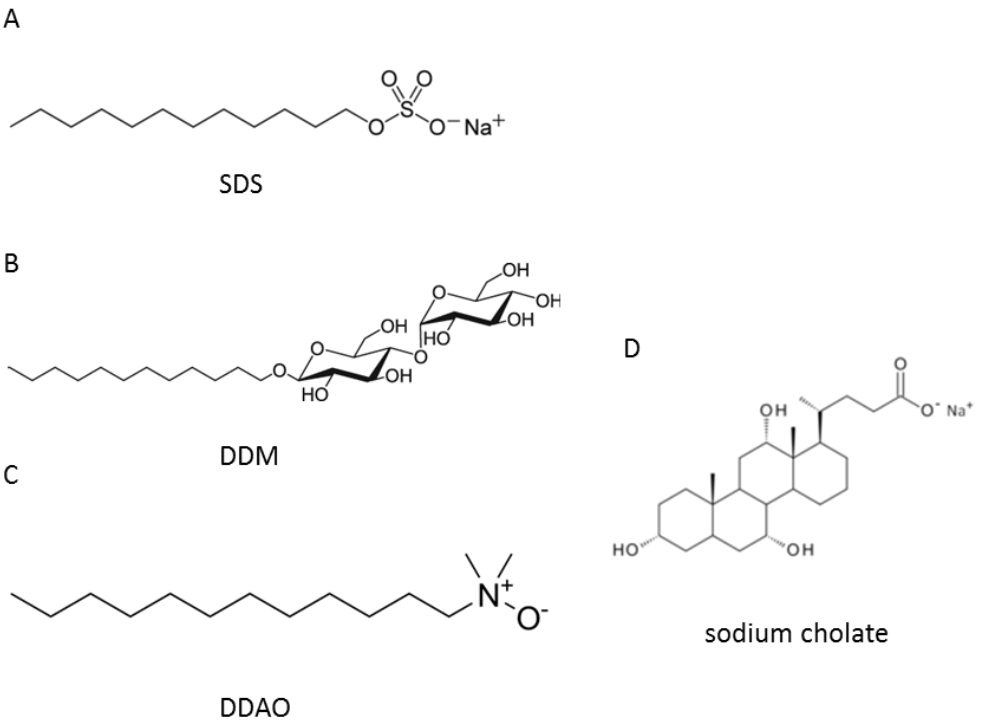

Figure 1.3.2.1: The structures of conventional detergents used in membrane protein solubilisation*. A shows the structure of sodium dodecyl sulfate (SDS), B) n-dodecyl-h-d-maltoside (DDM), C) N,N-Dimethyldodecylamine N-oxide (DDAO) and D) sodium cholate.*

Unfortunately many detergents do not maintain the structure and function of membrane proteins. The micelle is not a perfect mimic for the lipid bilayer, and there is a loss of lateral pressure. As different detergents have varying characteristics it is hard to predict which detergent will be optimal for the membrane protein in question. Therefore finding the optimal detergent via detergent screens is required, which can be time consuming and laborious. In addition the best detergents for initial solubilisation may not be suitable for downstream processes. Short chain detergents have a low solubility efficiency but they are better for crystallization whereas long chain detergents interfere with protein-protein interactions needed for crystallization. Also what works for one protein may not necessarily work for another as each membrane protein is unique making the optimal detergent protein specific (Seddon, Curnow et al. 2004).

Because of the larger variety of detergents available and as there is no universal detergent to solubilise all membrane proteins, detergent screening is needed. The most commonly used technique is through ultra-centrifugation. If a membrane protein has been effectively solubilised it would be in the soluble supernatant with all insoluble material being pelleted. This is a very simple technique that is fairly accurate but can be very lengthy if a large panel of detergents is needed to be screened. An alternative high throughput method is using the 96 well plate dot blot method (Eshaghi, Hedren et al. 2005). By utilising the 96 well plate format a large number of detergents can be screened at once. It is not as accurate as ultra-centrifugation as only the soluble fraction is examined. However it is able to give a general idea to which detergents are capable of solubilising your membrane protein to allow you rule out detergents that don't work. This method has been used in finding the most suitable detergents for solubilising and purifying other ABC transporters such as ABCB4 and ABCB11 (Ellinger, Kluth et al. 2013). Ultra-centrifugation can then be performed on a smaller panel of detergents using SDS PAGE or Western Blot analysis. If the insoluble and soluble fractions are measured the solubilisation efficiency can be calculated. An alternative method for detergent screening is to exploit the use of GFP fusion protein. Because of it fluorescent properties GFP fusion proteins are visible on SDS polyacrylamide gels allowing for rapid detection of that specific protein. The solubility of GFP fusion proteins using different detergents can also be assessed using SEC with a fluorescence detector by showing which has the least amount of aggregation and best monodispersity (Kawate and Gouaux 2006).

1.3.2.2 Approaches to stabilise detergent-solubilised proteins

Other conventional methods of stabilising membrane proteins are through the use of orthologues, ligand binding, mutagenesis and protein engineering but these also come with their own set of problems. The expression of human membrane proteins can be problematic as they must be expressed in a eukaryotic expression system. Finding orthologues especially those that

are able to be expressed in prokaryotes can simplify the expression. But no two proteins are 100% alike especially when switching between species and finding an orthologue of a human protein will not represent the actual structure of the human protein (Hardy, Bill et al. 2016).

Many membrane proteins are able to bind ligands and this binding of the ligand that can help stabilise the membrane proteins. It can be used to give the protein more rigidity but in doing so can also change the conformation of the membrane protein. The ligand bound state of a membrane protein will only reflect one conformation, and whilst this can be extremely useful, for determining specific ligand interactions it limits you to a single snap shot of a highly dynamic process.

Mutagenesis and protein engineering are ways of producing more stable membrane proteins by creating mutations within the protein or by coupling it to another protein. Mutations can be made within the protein, for example through alanine mutagenesis screening and then analysis of the mutants for stability in detergents. The most stable mutations can be combined together to form the most stable protein (Scott, Kummer et al. 2013). This approach has been extensively used with GPCRs and has led to several structures being determined (Heydenreich, Vuckovic et al. 2015) but because the mutated protein doesn't have the same amino acid sequence as the native membrane protein, and sometimes is not fully functional, one can't be certain that it represents the true native structure. With protein engineering additions to the membrane protein can be made. This is usually in the form of fusion proteins such as attaching T4 lysozyme (Moraes, Evans et al. 2014). However, fusion proteins can also increase stability of membrane proteins. The idea behind this is that T4 lysozyme is able to crystallise easily and helps crystallize the native membrane protein. This does mean fusing the native protein onto another protein may disrupt its conformation. This is the problem with all of these methods as they may not represent the native membrane protein and therefore the correct structure might not be elucidated.

1.3.2.3 Novel Methods

Although conventional detergents remain the most widely used method of membrane protein solubilisation their stabilising capabilities can be poor. Maintaining the stability of membrane protein in their native conformation is an integral part of membrane protein structural studies. Novel detergents that are able to not only solubilise but also stabilise membrane proteins have been developed. Many of these novel detergents are built on previous conventional detergents utilising their solubilisation capabilities but also enhancing their stabilising properties. Two of the novel detergents are glucose or maltose neopentyl glycols and calixarenes based detergents (Chae, Rasmussen et al. 2010, Matar-Merheb, Rhimi et al. 2011, Chae, Rana et al. 2013). Other novel approaches for maintaining membrane proteins stability deviate from detergents. Polymers such as styrene maleic acid (SMA), amphipols and membrane scaffold proteins (MSP) form nanoparticles around the protein which maintains the lateral pressure around the membrane protein keeping it stable (Tribet, Audebert et al. 1996, Leitz, Bayburt et al. 2006, Dorr, Scheidelaar et al. 2016).

1.3.2.3.1 New Detergents

Glucose Neopentyl Glycol (GNG) and Maltose Neopentyl Glycol (MNG) are two classes of amphiphiles built around a central quaternary carbon atom as shown in figure 1.3.2.3.1. They are structurally similar with the hydrophilic groups of GNG derived from glucose and MNG being derived from maltose. The difference between these detergents and other conventional detergents with similar structures such as DDM is the central quaternary carbon atom that is derived from neopentyl glycol. This allows for the addition the two hydrophobic and hydrophilic groups whereas DDM is linear and only contains a singular hydrophobic hydrocarbon chain and a singular hydrophilic maltose (Chae, Rasmussen et al. 2010). GNG has four different variations involving the attachment of the hydrophobic chain to the quaternary carbon with GNG-1 and GNG-2 having an ether link and GNG-3 and GNG-4 having direct contact (Chae, Rana et al. 2013). There are three different forms of MNG (1-3), which also vary the attachment of the hydrophobic

chain to the quaternary carbon, with MNG-1 comprising of an amide link, MNG-2 with an ether linkage and MNG-3 having a direct connection. MNG-3 has demonstrated great solubilisation and stabilisation characteristics (Cho, Husri et al. 2015).

A

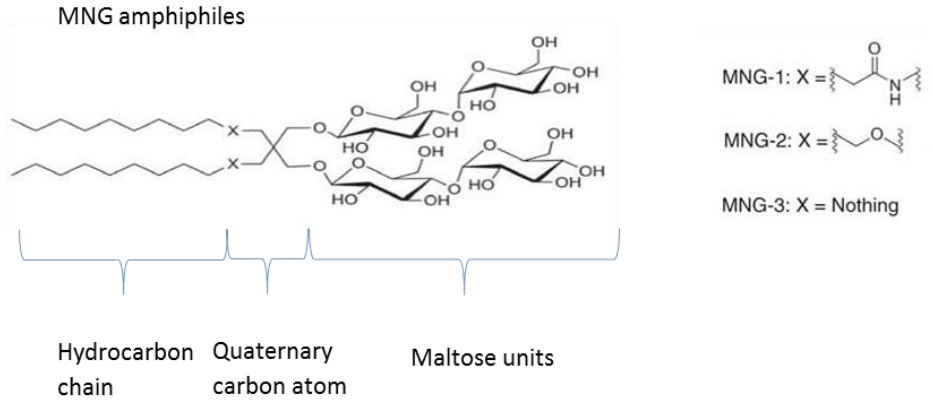

B

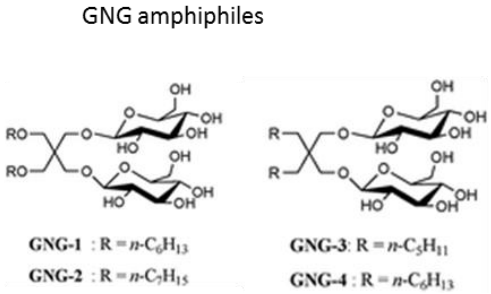

Figure 1.3.2.3.1 A: MNG and GNG structures*. A) shows the structure of MNG with the hydrocarbon chain far left, the quaternary carbon atom in the middle and the maltose unit far right. The type of bonds showing the attachment of the hydrocarbon chains to the quaternary carbon atom (MNG 1-3)are shown next to the structure (Chae, Rasmussen et al. 2010). B) shows the structures of the four GNG (GNG 1-4) with the composition of their R groups (Chae, Rana et al. 2013).*

Another novel series of detergents developed are the Calixarenes that contain a calixarene platform. These detergents still have the same general structure of conventional detergents, with a hydrophilic head group and hydrocarbon chain but also contain a calixarene platform of aromatic rings. This calixarene platform comprises of four aromatic rings, three in the para

position and the fourth attached to the hydrocarbon chain (Figure 1.3.2.3.1 B). They are capable of not only interacting with the hydrophobic transmembrane domains of membrane proteins but also the basic residues that are at the cytosol-membrane interface. This interaction with the basic residues is through the formation of salt bridges and is able to strengthen the packing of the membrane domain making the membrane protein more stable (Matar-Merheb, Rhimi et al. 2011). The lengths of the hydrocarbon chain can also be varied to change the solubilising properties of this detergent.

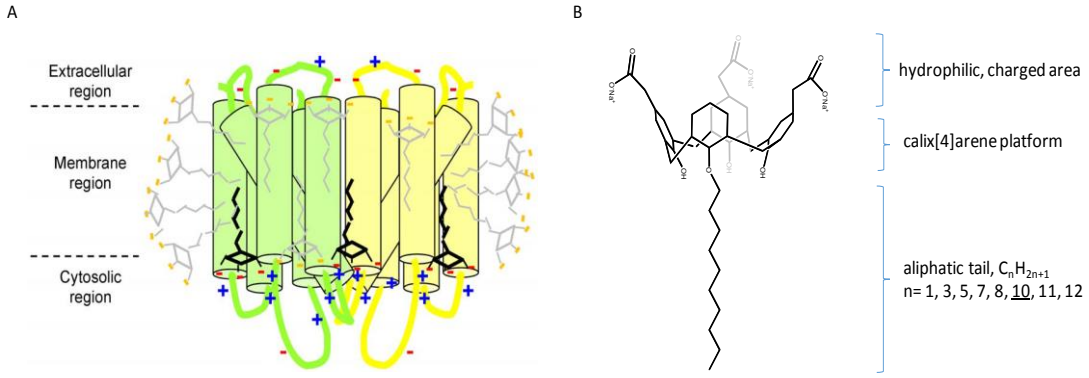

Figure 1.3.2.3.1 B: The structure and function of the calixarenes based detergent*. A) shows a diagram of the detergent interacting with a membrane protein. The grey molecules show the detergent characteristics and the black molecules showing the form of salt bridges at the membrane-cytosolic interface. B) shows a chemical structure in the calix[4]arene based detergent. The molecule is comprised of a hydrophobic tail of varying carbon lengths which is attached to the calix[4]arene platform that supports a hydrophilic charged head group (Matar-Merheb, Rhimi et al. 2011)*

A study conducted by Matar-Merheb et al in 2011 examined the properties of these detergents. They were able to confirm the interactions of these detergents with basic amino acids by showing a reduction in surface tension. The different lengths of hydrocarbon chains had an effect on the surface tension and size of the micelle. The solubility of various membrane proteins expressed in both prokaryotes and eukaryotes was also evaluated and the lengths of hydrocarbon chains had a dramatic effect. When the hydrocarbon chain length was 1 or 3 carbons there was poor solubility of membrane proteins. Increasing the hydrocarbon chain length to 7 carbons showed complete solubilisation of some membrane proteins and partial solubilisation of others. When compared to

controls of DDM and FC12 the solubilisation of all membrane proteins in the study was either equal to or greater than the controls. Not only were they predominately more soluble but the activity of the membrane protein was preserved. One protein tested for functionality was BmrA and upon extraction with C4C7 (calixarene containing 7 carbon length hydrocarbon chain) it maintained 50% function whereas DDM and FC12 extraction showed a 90-99% loss of function. These detergents are also capable of being exchanged with other detergent to help with solubility, stability and functionality. Calixarene detergents have also been used in the stabilisation of a native GPCR ($A_{2A}R$) and was capable of maintaining ligand binding capacity and used in saturation-transfer difference nuclear magnetic resonance (STD-NMR) (Igonet, Raingeval et al. 2018). The potassium chloride co-transporter KCC2 was also solubilised and purified in calixarene detergents used to measure binding using surface plasmon resonance (SPR) and structural analysis with negative stain electron microscopy (Agez, Schultz et al. 2017).

Facial amphiphiles represent a slightly different approach to maintaining membrane protein stability (Figure 1.3.2.3.1 C). These molecules are comprised of a hydrophobic sterol backbone capable of solubilisation attached to different head groups many of which are maltose based (Lee, Bennett et al. 2013). They deviate from the traditional detergent structure of polar head group and move towards a polar side groups. Many facial amphiphiles are based on the CHAPS detergent, by using the same cholic acid backbone and instead of adding a polar head group to make CHAPS, polar side groups are added (Zhang, Ma et al. 2007). They can form a belt around the hydrophobic domains of the membrane proteins allowing it to be soluble in aqueous solutions. Facial amphiphiles have been shown to solubilise membrane proteins such as the ABC transporter MsbA from *Escherichia coli* and the human gap junction channel composed of connexin 26 (Cx26) expressed in *Sf* 9 insect cells, also aiding in the crystallisation of these two proteins (Lee, Bennett et al. 2013). Facial amphiphiles have further been modified to create tandem facial amphiphiles and are able to span the width of a lipid bilayer. These tandem facial

amphiphiles increased membrane protein stability compare to conventional detergents (Chae, Gotfryd et al. 2010).

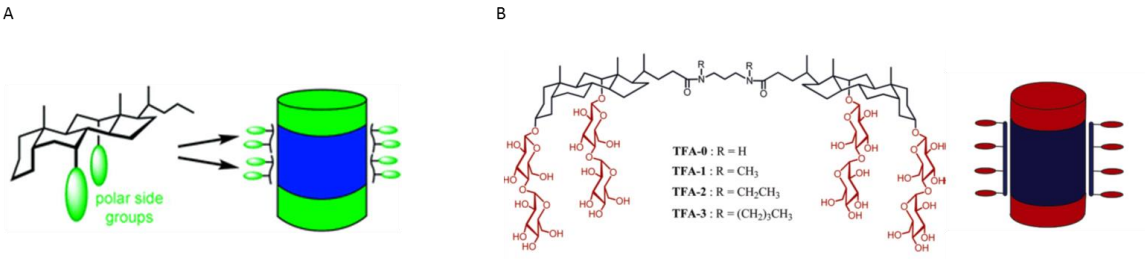

Figure 1.3.2.3.1 C: Schematics of facial amphiphiles. *A) shows facial amphiphiles by with green polar side groups and how they would arrange around a membrane protein (Zhang, Ma et al. 2007). B) shows the structure of tandem facial amphiphiles with different R groups and how they would arrange around a membrane protein spanning the hydrophobic domains (Chae, Gotfryd et al. 2010).*

1.3.2.3.2 Membrane scaffolding proteins (MSP)

Nanodiscs formed using membrane scaffolding proteins (MSPs) were first reported in 2002 (Bayburt, Grinkova et al. 2002). MSPs are based on the amphipathic α-helical protein that naturally occurs in apolipoprotein A1 and are capable of self-assembling into discoidal nanoparticles in the presence of synthetic phospholipids (Bayburt, Grinkova et al. 2002) . They were later able to reconstitute the membrane protein bacteriorhodopsin (bR) from *Halobacterium salinarum* into nanodiscs using the membrane scaffolding protein (Bayburt and Sligar 2003). The method works by forming a nanodisc of about 150 phospholipid molecules arranged in a bilayer that will encapsulate the membrane protein, thus providing the protein with a lipid environment making it stable and soluble (Figure 1.3.2.3.2). This has the advantage over detergents that it mimics the native environment much better than detergent micelles; it retains lateral pressure, and allows interactions between the protein and lipids, which are often important for function. Membrane proteins encapsulated in MSP-based nanodiscs can be used for a range of functional and biophysical studies (Bayburt and Sligar 2010). However, the formation of the MSP nanodiscs does require initial detergent solubilisation and purification before

reconstitution into the nanodisc. In addition, as the technique involves the use of a protein surrounding the nanodisc this technique is not suitable for x-ray crystallography or CD spectroscopy. There are now two constructs that are available for purchase MSP1D1 and MSP1E3D1 that generate a nanodisc size of ~10.6 and ~12.9 nm in diameter respectively.

Figure 1.3.2.3.2: Diagram of membrane scaffolding protein (MSP) forming a nanodisc. *The diagram shows the MSP (purple) wrapping around a core of lipids (red) containing a transmembrane protein (green). The size of the MSP is shown to be between 10.5 and 12.9 nm wide and 4.5 to 5.6 nm in height.(Leitz, Bayburt et al. 2006)*

1.3.2.3.3 Amphipols

Amphipols have been used in the stabilisation of membrane proteins for many years. These amphipathic molecules are able to wrap around the membrane protein by interacting with the hydrophobic core domains (Tribet, Audebert et al. 1996). They are not able to solubilise membrane proteins from their lipid environment so just like MSP the membrane protein must be first be solubilised from the membrane. Detergents must be removed prior to using amphipols as any surfactant present in the solution will destabilise the amphipols from the membrane proteins (Zoonens, Giusti et al. 2007). One of the most common amphipols used is A8-35 but there is now

a whole plethora available. Although initial solubilisation is required amphipols have aided in many different techniques involving membrane proteins including: functional studies, optical/infrared spectroscopy, solution NMR, electron microscopy and mass spectrometry (Le Bon, Marconnet et al. 2018). Not only do amphipols stabilise membrane proteins they can also be used in refolding and insertion into lipid bilayers (Nagy, Hoffmann et al. 2001). Some amphipols like A8-35 are sensitive to pH and divalent cations but other amphipols have been produced in order to overcome this problem such as sulfonated, zwitterionic (using a phosphocholine head group) and non-ionic containing sugar groups. Other additions of amphipols have also been made including spin labelled, fluorescent, affinity tagged and isotopically labelled (Le Bon, Marconnet et al. 2018).

1.3.2.3.4 Saposin based nanodiscs

Saposin based nanodiscs are a new way of stabilising membrane proteins in a lipid environment. Saposins are family of proteins that are known to have modulating properties of lipid membranes (Bruhn 2005). They are able to form lipid complexes such as saposin lipid-nanoparticles and incorporate membrane proteins into them creating a saposin lipoprotein nanoparticle (Jens Frauenfeld 2016). However, just like MSP and amphipols, membrane proteins must first requires initial detergent solubilisation and purification. Also just as MSP, saposins have to be overexpressed and purified prior to their use (Lyons, Boggild et al. 2017). Detergent purified membrane proteins are incubated with lipids and saposin and after detergent removal, saposins will retain the membrane protein in a lipid disc (saposin lipoprotein nanoparticle). These nanoparticles can have a range of different size by modulating stoichiometric ratio of lipid and saposin components and have allowed for reconstitution of many different sized membrane proteins domains (Flayhan, Mertens et al. 2018). The archaeal mechanosensitve channel T2 was successfully transferred into a saposin lipoprotein nanoparticle after which no detergent was needed to maintain the stability (Jens Frauenfeld 2016). This means structural studies can be

conducted in a detergent free environment. The sarco-endoplasmic reticulum calcium ATPase (SERCA) was reconstituted into saposin lipoprotein nanoparticles and analysed using negative stain electron microscopy (Lyons, Boggild et al. 2017). A bacterial peptide transporter POT1 in saposin lipoprotein nanoparticles have been used in cryo-EM studies (Jens Frauenfeld 2016).

1.3.2.3.5 Styrene maleic acid lipid particles (SMALPs)

Styrene maleic acid (SMA) is a copolymer made up of alternating units of styrene and maleic acid. When mixed with lipid bilayers or membranes the SMA polymer inserts into the membrane and forms small nanodiscs of membrane with the polymer wrapped around the outside (Dorr, Scheidelaar et al. 2016). These particles are termed SMA lipid particles (SMALPs), and are typically ~10nm in diameter (Lee and Pollock 2016).

The precursor to SMA is styrene maleic anhydride and through hydrolysis of the anhydride group SMA is formed. The styrene to maleic acid ratio can be altered but the way in which the styrene and maleic groups are positioned is random and does not follow a specific pattern. The length of the polymer is not tightly controlled during synthesis meaning a distribution of varying lengths of the polymer will exist (Dorr, Scheidelaar et al. 2016) . The most commonly used and well established SMA is SMA 2000, which has a 2:1 ratio of styrene to maleic acid, and an average molecular weight of 7.5kDa. Other SMA polymers are shown in table 1.3.2.3.5.

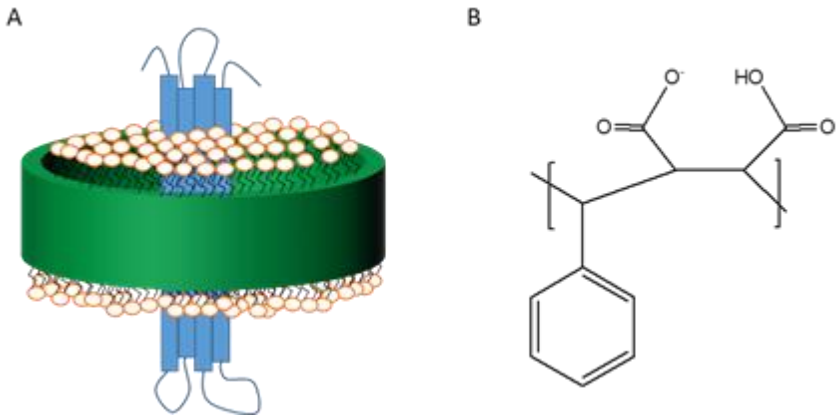

***Figure 1.3.2.3.5: Diagram of SMALPs**. A) This diagram shows the SMA (green) wrapping around a central core of lipids (red) with the membrane protein (blue) in the middle of the lipid core. B) Chemical structure of styrene maleic acid.*

SMA solubilises the membrane forming SMALPs, most of them will encapsulate a membrane protein. The particles formed are much like nanodiscs formed using MSPs, however unlike MSP nanodiscs this is done without the need of detergents to solubilise the membrane protein and the membrane proteins are kept in their native lipid environment. There is also no need to supplement buffers during purification, as there is when using detergents because once formed the SMALPs are stable. The membrane protein that is encompassed inside the SMALPs is stable in its native lipid environment, and allows access to both side of the membrane protein aiding in functional studies and structural studies. There has been a range of different membrane proteins that SMA has successfully been able to solubilise including ABC transporters, GPCRs and ion channels from all expression systems. SMA had successfully been able to extract P-gp from High Five cells, MRP1 from both H69AR and HEK cells, MRP4 from both HEK and *Sf* 9 cells, CFTR from *S. cerevisiae* and ABCG2 from High Five, HEK and MCF7-FLV (Gulati, Jamshad et al. 2014, Rothnie 2016). SMA has been used in ligand binding studies of ABC transporters as well as nucleotide binding studies. Binding studies have also been done on SMA solubilised and purified GPCRs from HEK and *P.pastoris* (Jamshad, Charlton et al. 2015). SMA could be used in the lipid analysis and functional reconstitution of KscA into planar lipid bilayers for functional characterization through single channel conductivity (Dorr, Koorengevel et al. 2014). Many of these proteins have also had increased thermostability when solubilised and purified in SMA compared to detergents (Gulati,

Jamshad et al. 2014, Morrison, Akram et al. 2016). These examples show the versatility of the SMA polymer in aiding functional understand of membrane proteins.

Current limitations to the SMA approach include the disc size. The typical size is 10-12 nm diameter, which may mean some large proteins or protein complexes will not fit. However, recent reports have suggested there is some flexibility with this. If the membrane protein is just about large enough to fit there may not be much lipid surrounding the protein which may affect its stability or function. The rigidity of the lipids within the SMALP is still under investigation but if the particle is too tightly packed the membrane protein may not be functional (Pollock, Lee et al. 2018). SMA is also sensitive to divalent cations such as magnesium and calcium (Morrison, Akram et al. 2016). If these ions are needed in order for the membrane protein to function, such as Mg^{2+} needed for proteins that bind and hydrolyse ATP, this will become problematic.

	Polymer name	Percent of maleic acid content (%)	Average molecular mass (kDa)
Cray Valley	SMA 100	50	5.5
	SMA 2000	33	7.5
	SMA 3000	25	9.5
Polyscope	XZ09006	40	7.5
	XZ09008	25	10
	SZ40005	42	5
	SZ25010	25	10
	SZ42010	42	10
	SZ33030	33	30
	SZ28065	28	65
	SZ28110	28	110

Table 1.3.2.3.5: SMA polymers. *This table shows the percent of maleic acid content and average molecular mass (kDa) for each polymer produced by Cray Valley or Polyscope(Stroud, Hall et al. 2018).*

Alternative SMA like polymers such as styrene maleimide SMI and diisobutylene -maleic acid (DIBMA) are also being developed which are reported to overcome the divalent cation sensitivity by replacing the maleic acid with either maleimide (SMI) or replacing the styrene with diisobutylene (DIBMA) (Oluwole, Klingler et al. 2017, Hall, Tognoloni et al. 2018).

Until recently, the mode of action that allows SMA copolymer to insert itself into the lipid bilayer of cells has been poorly understood. There is a three step model that explains how SMA is able to form SMALPs as shown in figure 1.3.2.3.5 (Scheidelaar, Koorengevel et al. 2015). The first step is membrane binding where the SMA copolymer binds to the lipid membrane through hydrophobic and electrostatic interactions. The electrostatic interactions between the SMA copolymer and the anionic lipid at the membrane surface are actually repulsive and can control the intensity of membrane binding. It is the stronger hydrophobic force from the interaction between the styrene moiety of the SMA copolymer and the lipid acyl chains that is driving the insertion of the SMA copolymer into the lipid membrane. Once bound to the surface of the lipid membrane it can insert itself and destabilise the membrane. The forces governing the ease with which the SMA copolymer can do this are lateral pressure and packing defects of the lipid membrane. When the membrane is above its transition/melting temperature (Tm) the lateral pressure is lower and insertion is made easier. Below the Tm the lateral pressure is higher as the lipids are more tightly packed in gel phase making it increasingly hard for SMA insertion. The final step is the formation of nanodisc or SMALPs. The SMALPs are able to stay stable because of the way in which the SMA copolymer inserts itself into the lipid bilayer. The phenyl groups are able to insert themselves between the lipid acyl chains holding the SMALPs together (Jamshad, Grimard et al. 2015).

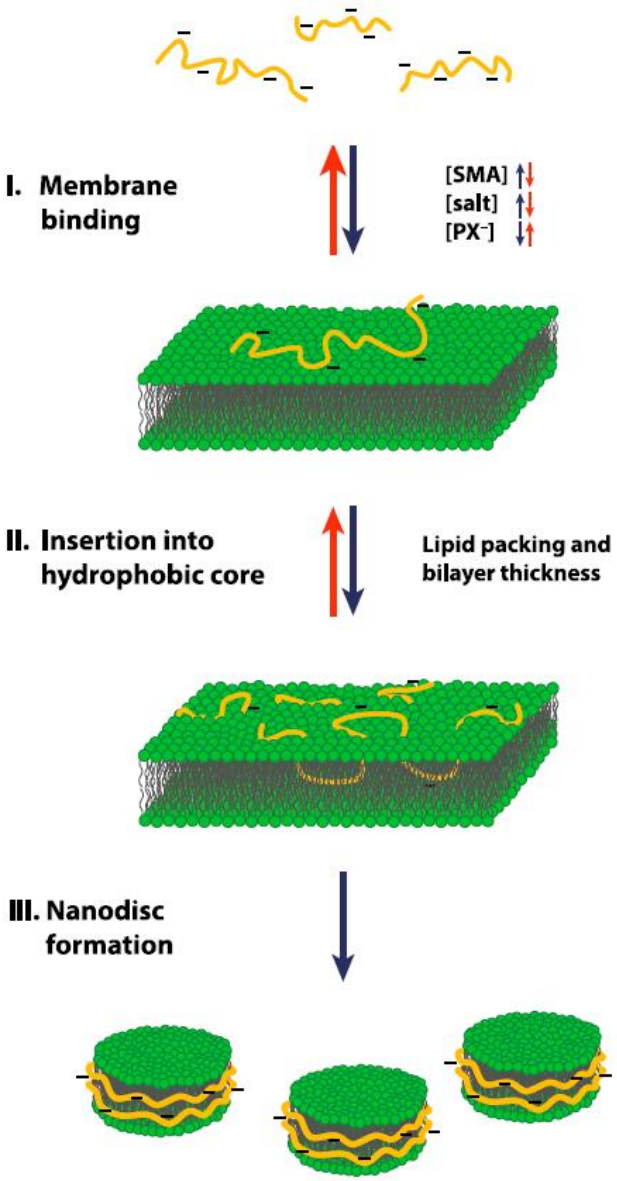

Figure 1.3.2.3.6: SMA insertion into lipid membrane. *Diagram showing the steps of SMA insertion into a lipid membrane. I) SMA first initially binds to the surface of the membrane and is influenced by SMA and salt concentrations along with negatively charged lipids. II) Hydrophobic forces drives SMA into the lipid bilayer and is modulated by lipid packing and bilayer thickness. III) Membrane solubilisation and nanodisc/SMALP formation. (Dorr, Scheidelaar et al. 2016)*

1.3.3 Purification

The third step in the process is the purification of the solubilised membrane protein. The protein of interest need to be separated from the rest of the proteins that reside in the membrane. Also the protein of interest needs to be kept stable though out the purification process for downstream processing. Purification can be achieved through a variety of different chromatographic techniques such as size exclusion, ion-exchange and affinity. These purification techniques work by taking advantage of different properties that proteins possess.

Affinity chromatography is based on the principal that the membrane protein, which is being overexpressed, will have an affinity to the purification matrix. Antibodies that can bind to a specific epitope on the membrane protein can be used. If the membrane protein has a specific substrate with high affinity or a receptor that can bind to its ligand these can also be used. However it is most commonly done through the addition of an affinity tag attached to the membrane protein of interest. Many affinity tags exist, including FLAG, Strep, MBP and GST but the most commonly utilised is the his-tag (Pollock, Lee et al. 2018). A his-tag is a string of histidine amino acid positioned at either the C of N terminal end of the membrane protein. The histidine tag is usually between 6 and 12 histidines long. These histidines are able to bind with high affinity to divalent cations such as nickel and cobalt. Once bound, following wash steps to remove contaminants, the membrane protein is able to be eluted from the column using imidazole. Sometimes affinity tags may affect a protein's function and structure. In which case cleavage sites may be introduced between the membrane protein and its affinity tag in order to cleave off the tag after purification (Kimple, Brill et al. 2013).

Size exclusion chromatography (SEC) works on the principal of separating proteins by size. As there are many membrane proteins in any given sample, many of which will have similar molecular masses, purification using this as a primary step is generally not effective. More often,

it is used as a secondary purification technique to remove contaminating proteins after initial purification. This can work very efficiently if there are contaminating proteins that have a different molecular weight to the membrane protein of interest. If there are different oligomeric states of the membrane protein then these can be separated out as well. SEC is also a good technique for investigating the stability and monodispersity of proteins after purification. If the membrane proteins become aggregated during purification they will form large aggregates and will elute faster than non-aggregated protein. SEC can also be used for buffer and/or detergent exchange allowing the switch from one buffer to another depending on the end goal.

Ion-exchange chromatography works based on the net charge a protein exhibits. Depending on the isoelectric point of the membrane protein the pH can be altered to create a net negative or positive charge. Then depending on the net charge either an anionic or cationic ion exchange column can be used. Binding of the membrane protein to the column will occur thorough electrostatic interactions. Unfortunately if the isoelectric point of the membrane protein is unknown then finding a condition where the membrane is able to bind can be time consuming. Again this technique is normally used as a secondary technique to help remove any contaminating proteins

The solubilisation approach chosen will have an effect on which purification technique(s) are possible. Complete solubilisation often occurs above the CMC so when using detergents all the buffers used in these chromatography techniques have to be supplemented with detergent above the CMC to maintain solubility (Garavito and Ferguson-Miller 2001). This can be very expensive depending on the volume of buffer required, the CMC of the detergent, and how much the detergent costs. Detergents can also interfere with the binding of membrane proteins to affinity columns such as those used in nickel affinity chromatography. Reduced binding arises from reduced accessibility of the purification tag, such as the (histidine) can become masked and therefore reducing binding. To overcome this issue longer histidine tags with 8, 10 or 12 histidines

or creating a linker protein or peptide between the purification tag and membrane protein could be used (Kimple, Brill et al. 2013).

The uses of polymers such as SMA have the huge advantage of being used in “detergent free” purification. When SMA polymers are used to solubilise membrane proteins the SMA lipid particle (SMALP), which contains the membrane protein, is in a highly stable state. SMA does not detach from the lipids and therefore no additional SMA is needed in any of the buffers during purifications (Lee, Knowles et al. 2016, Rothnie 2016). Not only is SMA cheaper than many detergents but buffers do not need to be supplemented with it, keeping cost down. One reported disadvantage of SMA during purification is that excess free SMA from the initial solubilisation may interact with the chromatography column reducing binding efficiency (Pollock, Lee et al. 2018). Sometimes the free SMA has to be removed prior to binding to the affinity column (Bersch, Dorr et al. 2017). SMA has previously been shown to improve the purity of several membrane proteins compared to conventional detergents with a single affinity chromatography purification step (Morrison, Akram et al. 2016). However, for SMALP encapsulated proteins, ion exchange chromatography cannot be used due to the high negative charge of the maleic acid groups, thus not allowing separation.

1.3.4 Structural Analysis

For all structural techniques a homogenous and stable pure membrane protein sample must be obtained. This is why maintaining the stability of the membrane protein throughout the purification process is vital. The membrane protein needs to be kept in it native conformation so accurate structural data can be obtained.

The two main structural techniques commonly utilised for membrane protein structural determination are X-ray crystallography and electron microscopy (EM). NMR has also been used for some membrane protein structural determination but generally only works for small proteins

under 20kDa. The CXCR1 chemokine GPCR structure elucidated by rotationally aligned solid state NMR is one of the largest reported (Park, Das et al. 2012) but the majority of membrane proteins are just too large for structural determination by NMR.

1.3.4.1 X-ray Crystallography

X-ray crystallography has historically been the pinnacle in terms of determining high resolution structures of membrane proteins and is the technique by which the vast majority of membrane protein structures have been determined. Producing 3D protein crystals that will diffract x-rays requires a membrane protein that is highly stable and homogenous. These two factors are key in producing a viable 3D crystal for X-ray crystallography as unstable membrane proteins and heterogeneous membrane protein samples will not be able to form a crystalline structure. Another key problem in X-ray crystallography is the high concentration of the membrane protein that is needed for crystallization. Typically a minimal concentration of 10mg/mL is required and relatively large volumes are also needed for the screening of different crystallisation conditions. Concentrating detergent solubilised protein is notoriously difficult, since proteins often aggregates or sticks to filters, and often due to the size of detergent micelles the detergent is often concentrated at the same time. Increasing the concentration of detergent present can have detrimental effects on the protein stability and free micelles can cause problems with crystal formation (Loll 2014).

Almost all x-ray crystallography structures of membrane proteins have been determined using detergents. The optimal detergents used to solubilise and stabilise membrane protein are not necessarily the same as the detergents best for 3D crystal formation. Generally speaking detergents with smaller micelle structures are preferred during crystallography as they allow for more protein-protein interactions (Prive 2007, Loll 2014). However, out of the large variety of detergents DDM has been by far the most used for x-ray crystallography (Stetsenko and Guskov

2017). Although to date most structures have utilised conventional detergents, the novel detergents are now starting to produce structures. In particular, the neo-pentyl glycols have been successful. GNG-3 has been used to produce the structures of Na+ -pumping pyrophosphatase (Kellosalo, Kajander et al. 2012) and *E. coli* acetate transporter (Chae, Rana et al. 2013) and MNG-3 was used for the determination of high resolution structures for more than 10 GPCRs (Cho, Husri et al. 2015).

Facial amphiphiles have also been shown to enhance crystallization(Lee, Bennett et al. 2013). Whilst SMALP purified protein is unlikely to be useful in vapour diffusion unless a way to remove the SMA belt is found, SMALP purified proteins have been successfully used for lipidic cubic phase crystallization, leading to the 2.0 Å structure of bacteriorhodopsin from *Haloquadratum walsbyi* (Broecker, Eger et al. 2017).

1.3.4.2 Electron Microscopy

Until recently the use of electron microscopy (EM) as a structural technique for membrane proteins has been limited by low resolution. There are a few different types of EM that have been used to study membrane proteins; single particle (negative stain and cryo-EM) and electron crystallography. Recent technical advances in microscopes, classification methods to sort particles and the stabilisation and preparation of membrane proteins has led to improvements in resolution (Rawson, Davies et al. 2016). Single particle EM can determine the structure of a membrane protein by imaging individual particles. The membrane protein particles can be prepared either by negative stain or freezing in vitreous ice (Rubinstein 2007). Negative staining is produced by embedding the membrane protein in a heavy metal salt solution which stains the area around the protein but will not penetrate the protein itself due to the hydrophobic nature (Boekema, Folea et al. 2009). The contrast is therefore enhanced and protein envelopes can be determined as stain surrounding the particle scatters the electrons. Cryo-EM of proteins is done in

ice that has been rapidly cooled to form a non-crystalline, vitreous ice. This allows the preservation of the membrane protein structure and is able to be imaged by the scattering of electron from the membrane protein. There is less artefactual information produced from cryo-EM but negative staining has the advantage of having highly stable sample specimens that are less sensitive to radiation (Rubinstein 2007). Images of membrane proteins through single particle EM can be enhanced by averaging (Boekema, Folea et al. 2009). As the particles are all in random orientations it is necessary to average images of hundreds or thousands of particles to gain a more defined electron density map. These electron density maps or electron micrographs can be used to obtain a 3D density map of the membrane protein using imaging process software such as SPIDER (Shaikh, Gao et al. 2008).

Traditionally detergents have been used in the solubilisation of membrane proteins for electron microscopy and have led to many structures of membrane proteins but do not come without complications. For example detergents that are capable of solubilising membrane proteins are not always the most optimal in electron microscopy (Rawson, Davies et al. 2016). Detergents that form micelles at low concentration are more desirable in cryo-EM allowing reduced scattering of electrons. New ways of solubilising and stabilising membrane proteins such as amphipols, nanodiscs and SMA polymers have helped overcome some of the problems faced with detergents in cryo-EM and been able to producing high resolution structures. Amphipols and nanodiscs have been used in the structural analysis of mammalian endo-lysosomal TRPML1 channel and due to low resolution there is no detectable difference in the structure of the channel of this membrane proteins in the two systems (Zhang, Li et al. 2017). Nanodiscs have also been able to reveal different conformational states of the MsbA transporter (Mi, Li et al. 2017). SMA has been used in determining the structures of alternative complex III to a 3.4 angstrom resolution (Sun, Benlekbir et al. 2018) and AcrB to a 8.8 angstrom resolution (Parmar, Rawson et al. 2018).

The other ways of electron scattering to produce structures of membrane proteins is through electron crystallography. Here membrane proteins form thin layers of planar, two-dimensional (2D) crystals which are then able to scatter electrons (Goldie, Abeyrathne et al. 2014). The technique has been used to obtain atomic resolution of several membrane proteins including bacteriorhodopsin and aquaporins. Electron crystallography can produce structures of membrane proteins in membranes which provides a near to native environmental state (Fujiyoshi 2011). Although both sides of the membrane protein are kept open and crystal packing has less of an influence there is still a need to produce high quality crystal for the best resolution possible.

1.4 ABC transporters

In order to try and overcome some of these limitations of membrane protein structural biology a model membrane protein had to be chosen. For this study an integral membrane protein from the ATP-binding cassette (ABC) superfamily, namely ABCC4/MRP4 (multidrug resistance protein 4) was chosen as a model membrane protein. A large multi transmembrane human membrane protein was chosen to enhance the progression of the techniques and approaches beyond prokaryotic proteins.

The ABC superfamily of integral membrane proteins are found in all types of organisms from prokaryotes to humans. They utilise energy from ATP binding and hydrolysis to transport a variety of substrates across the biological lipid bilayer (Wilkens 2015). ABC transporters can either be importers for the uptake of nutrients or exporters that can transport cell signalling molecules, drugs and toxins out of the cell. In many species of bacteria, ABC transporters have been linked to the rise in antibiotic resistance. In humans, which have 48 different ABC transporters, mutations have been linked to a number of disease states such as immune deficiency liver diseases, cystic fibrosis and cancers (Dean 2005, Sun, Patel et al. 2012). The 48 different ABC transporters found in human can be separated into seven subfamilies ABCA-ABCG (Dean, Rzhetsky et al. 2001). The human ABC transporter focused on in this study ABCC4/MRP4 is in the C subfamily

1.4.1 Structure of ABC transporters

Human ABC transporters are made up of four core domains: two transmembrane domains (TMDs) and two nucleotide binding domains (NBD). Each of the two TMDs comprises of 6 transmembrane alpha helices and the two NBDs have binding sites for ATP which are homologous throughout the super family unlike the TMDs (Linton 2007). The Walker A and Walker B motifs are two sequence motifs that are also conserved between all ABC transporter superfamily member (Leslie, Deeley et al. 2005). Separated by between 100 and 200 amino acids these two motifs are contained in each

of the NBDs and perform different functions. The Walker A motif contains a lysine residue that participates in binding of the β-phosphate of ATP. An aspartic acid residue in the Walker B motif can interact with Mg^{2+} making both of these motifs important for the functionality of ABC transporters. Between these two highly conserved motifs there is a third conserved amino acid sequence, the ABC signature motif or C motif (ALSGGQ). Evidence has shown this ABC signature motif is involved in the binding and hydrolysis of ATP and is located so that the signature motif of one NBD sits adjacent to the Walker A sequence of the opposite NBD. There is also evidence that the serine in this ABC signature motif can interact with the Walker A motif and possible interact with γ-phosphate of ATP making it another important part of the ABC transporter structure and function (Leslie, Deeley et al. 2005).

1.4.2 ABC transporter function

All human ABC transports are exporters and are capable of transporting a wide variety of ligands or substrates across the lipid bilayer of cell membranes. The TMDs are able to bind the substrate and transport it across the membrane. The NBD binds and hydrolyses ATP to drive the transport of the substrate. The protein undergoes significant conformation changes during the transport cycle. When ATP binds it is thought that the two NBDs dimerise, and this transmits conformational changes throughout the TMDs. The classic model of ABC transport takes four steps: 1) substrates bind to the TMDs in the open dimer conformation which increases the affinity for ATP leading to step 2) the binding of ATP closing the dimer which is able to produce a large enough conformational change to translocate the substrate across the membrane and secrete it. Step 3) allows for the hydrolysis of ATP to ADP and Pi with the ABC transporter still in the closed

state until step 4) where the ADP and Pi are released and the ABC transporter is restored to the open conformation as shown in figure 1.4.2.1 (Linton 2007).

Figure 1.4.2.1: Diagram of the mechanism of ABC transporters. *The open dimer configuration allows for ligand binding. After ATP binding the ABC transporter is in closed dimer conformation secreting the ligand. ATP hydrolysed and released as the ABC transported returns to the open dimer configuration. (Linton 2007)*

There has been much debate whether or not there are other intermediate conformational states. Various models have been proposed including the one shown in figure 1.4.2.2 by Shintre et al which has these four classical states along with other intermediate states (Shintre, Pike et al. 2013). This model shows that there can be an inward facing step where there is no substrate bound but two molecules of ATP are bound and an outward facing step where two Pi molecules are released, with ADP still bound.

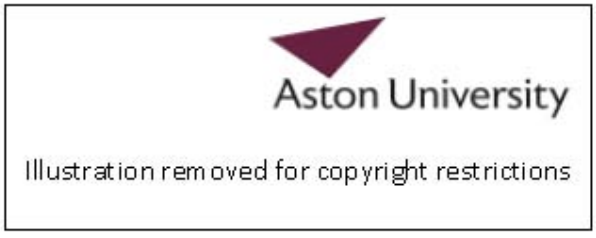

Figure 1.4.2.2: Proposed model of the steps taken in the transport cycle of ABC transporters*. The TMD are blue and orange and the NDM are purple and red. ATP is green, the substrate yellow and ADP in grey. The asterisk shows nucleotide bound state and the pound symbol show nucleotide-free state. This model was based on the work done on ABCB10. (Shintre, Pike et al. 2013)*

1.4.3 ABCC4/MRP4

The ABC transporter used in this study was ABCC4/MRP4 (multidrug resistance protein 4).

MRP4 was first found in human T-lymphoid cell lines and when overexpressed was linked to the efflux of antiviral nucleoside based drugs which impaired the efficacy of the anti-virals. MRP4 is in the C subfamily of human ABC transporters, whose other members include MRP1, 2, 3 & 5, as well as the chloride channel CFTR responsible for cystic fibrosis, ABCC6 which is responsible for pseudoxanthoma elasticum (Dean, Rzhetsky et al. 2001), and SUR1 and SUR2 which are modulators of the K_{ATP} channel (Lefer, Nichols et al. 2009).

The members of the C subfamily are split into two groups, the 'short MRPs' which have typical structure of two TMDs each consisting of six transmembrane helices and two cytosolic NBDs, and the 'long MRPs' which have an additional 5 transmembrane helices at the N-terminus, termed TMD_0 (Figure 1.4.3.1). MRP4 is one of the short MRPs, in fact it is the shortest member of the ABCC family and consists of 1325 amino acids (Russel, Koenderink et al. 2008).

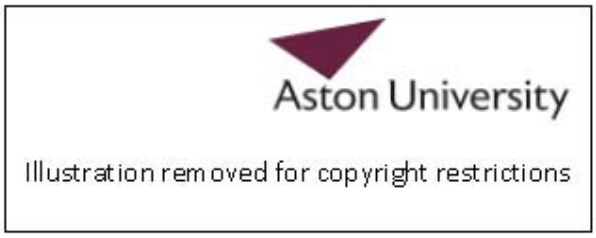

Figure 1.4.3.1: MRPs and MRP4*: A and B are diagrams of the short and long MRP4 respectively showing the transmembrane domains and ATP-bind domains. (Gottesman, Fojo et al. 2002)*

To date there is no known structure of human MRP4, only a homology models exist. The first model was based on the structure of the ABC transporter Sav 1866 form *S.aureus* with the amino acid sequence homology of these two proteins being only 24% (Ravna and Sager 2008). Another model with an outward facing state was based on the crystal structure of Sav 1866 and the crystal

structure of the ATP binding domains of human P-gp (Russel, Koenderink et al. 2008) as shown in figure 1.4.3.2. A more recent model has been made based upon X-ray crystal structures of P-gp and is an inward facing conformation. This model was embedded in different lipid bilayers to allow for molecular dynamic simulations. The positions of three previously unresolved domains were investigated and a p.Gly187Trp mutant was also simulated and helped rationalise known dysfunctions associated with this polymorphism (Chantemargue, Di Meo et al. 2018).

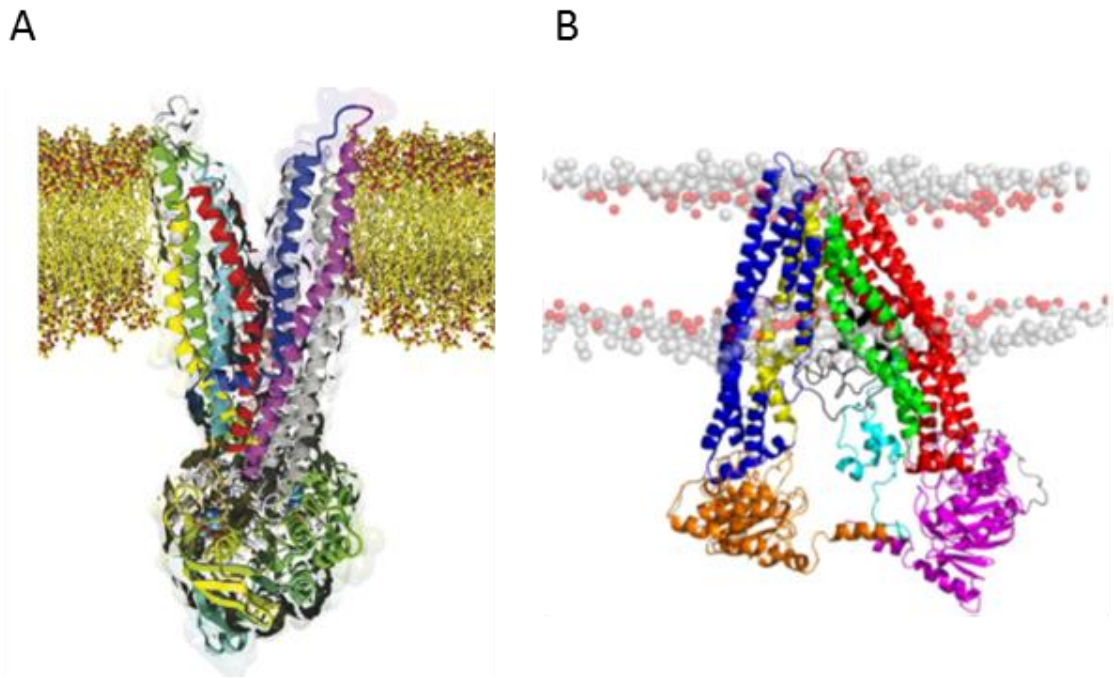

Figure 1.4.3.2: Molecular modelling of MRP4 structure*. Model A is the outward facing state of MRP4 and was based on the crystal structure of Sav 1866 and crystal structure of the ATP binding domains of human P-gp (Russel, Koenderink et al. 2008). Model B is the inward facing state of MRP4 and is based on the crystal structure of P-gp (Chantemargue, Di Meo et al. 2018).*

This membrane protein can be found in a wide range of cells all over the human body including blood cells, neurons, testis, ovaries, adrenal glands, prostate tubuloacinar cells and renal proximal tubule cells (Ravna and Sager 2008). One rather unique characteristic of MRP4 is its ability in polarised cells to have dual membrane localisation. It can be localised to the basolateral membrane of hepatocytes and the apical membrane in renal proximal tubule cells (Russel, Koenderink et al. 2008). MRP4 has also been shown to be localised on both the basolateral and apical membranes of a colonic epithelial cell line (Li, Krishnamurthy et al. 2007). MRP4 is able to

transport a wide variety of endogenous and xenobiotic anionic compounds including cyclic nucleotides, eicosanoids, folate, bile acids antibiotics, antivirals and chemotherapy drugs (Wittgen, van den Heuvel et al. 2012).

Although it was first discovered for its abilities to export exogenous drugs it also has endogenous roles in inflammation and cell signalling. Its role in inflammation comes through its ability to transport prostaglandins and leukotrienes (Sauna, Nandigama et al. 2004). MRP4 also has the ability to bind cyclic nucleotides such as cyclic AMP (cAMP) and cyclic GMP (cGMP) (Sinha, Ren et al. 2013). These molecules are second messengers enabling a wide range of cellular responses but whether or not MRP4 regulates the intracellular level of cAMP and cGMP is still up for debate. This is due to the relatively low affinities that MRP4 has with nucleotides and the fact that only modest decreases in cAMP and cGMP were found on cellular levels. However some evidence suggests it could regulate local microdomain levels (Li, Krishnamurthy et al. 2007). More recent evidence suggest MRP4 can regulate the intracellular cAMP level which was found in HT-29 gut epithelial cells with treatment of a MRP4 inhibitor and stimulation with adenosine. Down regulation of MRP4 in human coronary artery smooth muscle cells showed an increase in intracellular cAMP (Schymeinsky, Mayer et al. 2013). MRP4 is also involved in the transport of GSH in the sinusoidal membrane of hepatocytes. Here it is able to cotransport glutathione (GSH) and cholytaurine (C-tau) a conjugated bile acid (Rius, Nies et al. 2003).This cotransport of GSH and C-tau could be a regulator of intrahepatocyte bile acid concentrations and as well as acting a reservoir of GSH for other tissues. (Rius, Hummel-Eisenbeiss et al. 2006).

How MRP4 is able to transport such a wide variety of substrates is not well known. In particular how it can recognise, bind and transport both relatively hydrophilic molecules like cAMP and hydrophobic molecules such as bile salts or drugs like methotrexate is unclear. This could be due to the lack of structural knowledge about the TMDs of MRP4 which are responsible for transporting substrates. The Km values of many substrates are high indicating a large amount of non-specific binding which may contribute to its ability to transport a wide variety of substrates

(Russel, Koenderink et al. 2008). MRP4 also has regulatory binding sites that can affect the transport of substrates in an allosteric manner. This allosteric influence can either be positive or negative, for example in insect cells that have MRP4 overexpressed urate can stimulate cGMP transport but inhibits methotrexate however the location of the regulatory binding sites is not clear (Van Aubel, Smeets et al. 2005).

2 Aims and Objectives

The aim of this project was to express, purify and stabilise MRP4 for structural and functional studies.

Specifically the objectives were:

1) Evaluate overexpression of MRP4 in both *Pichia pastoris* yeast, *Sf* 9 insect cells and HEK mammalian cells to find the best system for producing the highest yields of functional MRP4.
2) Develop a fluorescent vesicular transport assay to measure the function of MRP4
3) Compare conventional detergents to novel approaches using calixarene-based detergents or SMA (styrene maleic acid co-polymers) for the solubilisation and stabilisation of MRP4
4) Optimise purification of MRP4
5) Investigate the structure and function of purified MRP4

3 Materials and methods

3.1 Materials

Insect cell media Insect Xpress (SLS), pOPINE plasmid (OPPF), his_6-MRP4 (Susan Cole), restriction enzymes and phosphatase (NEB), anti-his antibody (R&D Sytems), anti-MRP4 antibody (Abcam), anti-mouse/rat HRP antibody (Cell Signalling), Instant blue (Expedeon), fluo-cAMP (Biolog), DDM (VWR), DC protein assay kit (BioRad), ABT Ni-NTA resin (Web Scientific), SMA polymers (Cray Valley or Polyscope)

Lysogeny broth (LB), mini prep and gel extraction kit GeneJet, PVDF, Silver stain Pierce kit, molecule weight markers, DH 10 Bac *E.coli,* BCA assay kit, enhanced chemiluminescence (ECL) Pierce kit, HisPure nickel NTA resin, zeocin and bovine serum albumin (BSA) were all purchased from Thermofisher.

All other chemicals were purchased from Sigma

3.2 Gels

3.2.1 SDS PAGE

All SDS PAGE analysis was performed using 8% polyacrylamide gels unless specified. SDS PAGE was always carried out in SDS running buffer (25 mM Tris, 192 mM glycine, 0.1% (w/v) SDS). Gels were typically run at 120 volts through the stacking gel before increasing the voltage to 180 volts.

5x Laemmli Sample Buffer (LSB) (60 mM Tris-Cl pH 6.8, 2% (w/v) SDS, 10% (v/v) glycerol, 5% (v/v) β-mercaptoethanol, 0.01% (w/v) bromophenol blue) was used for sample preparation.

For non-specific detection of proteins the gels were stained with either Instant Blue or using the Pierce Silver staining kit. The precast gels (Mini-PROTEAN TGX Stain-Free Precast Gels, Bio Rad)

used during the studies at Calixar were stain free gels allowing them to be visualised under UV. For specific detection of MRP4, gels were used for Western blot transfer.

3.2.2 Native PAGE

Native PAGE, for SMA analysis, were prepared using the same procedure at SDS PAGE without SDS and no stacking gel. For calixarene analysis, pre-cast gels (4-16%) were purchased from Bio-Rad. Native gel running buffer was a Tris Glycine buffer (25mM Tris, 190mM glycine) pH 8. Native gels were run on ice with no reverse electrode. Native gels were stained using the same procedure as SDS gels or used for Western blot transfer.

3.2.3 Western Blot

Western transfer from acrylamide gels to PVDF membrane (activated by washing in methanol) was performed for 1 hour at 100V in Western Blotting buffer (25mM Tris, 190mM glycine and 20% (v/v) methanol). The PVDF membrane was then blocked using 5% (w/v) BSA solution in Tris-Buffered Saline with Tween (TBSt) (20mM Tris, 150mM NaCl and 0.001% (v/v) Tween) + 0.01% (w/v) sodium azide for 1 hour at room temperature or overnight at 4^{o}C. The block was removed and primary antibody applied (mouse anti-His antibody (R+D Systems) at 1:500 concentration in 5% (w/v) BSA TBSt solution or rat anti-MRP4 antibody (Enzo) at 1:100) for 1 hour or overnight at 4^{o}C. PVDF membrane was then washed three times in TBSt and secondary antibody applied (anti-mouse horse radish peroxidase (HRP) antibody (Cell Signalling) 1:3000 in TBSt or anti-rat horse radish peroxidase (HRP) antibody (Sigma) 1:3000) for 1 hour. After 5 washes in TBSt the membrane was developed using Pierce Enhanced Chemiluminescence kit for HRP, and imaged using X-ray film or C-Digit Western Blot scanner.

3.2.4 Agarose Gel

All DNA was separated on 0.8% agarose gels in TAE buffer (40 mM Tris, 20 mM acetic acid, 1 mM EDTA) containing ethidium bromide and run at 100 volts until sufficient separation occurred. Gels were visualised using a UV light box.

3.3 Molecular Biology

3.3.1 Chemically Competent E.coli transformation

50µL of chemically competent DH5α *E.coli* were defrosted on ice. 1-5 µl containing 1 pg-100 ng of plasmid DNA was added to the *E.coli* and incubated on ice for 30 minutes. The sample was subjected to a heat shock for 30-45s at 42^{o}C and then placed back on ice for 2-5 minutes. 900µL of LB (Luria Broth) was added and incubated at 37^{o}C for 1 hour. 100µl was spread on LB agar plates containing the appropriate selection antibiotic (either 100µg/ml ampicillin or 25µg/ml zeocin).

3.3.2 Rapid Screen of Transformants

Lysis buffer (10% (w/v) Sucrose, 100mM NaOH, 60mM KCl, 5mM EDTA, 0.25% (w/v) SDS, 0.05% (w/v) Bromophenol Blue) was prewarmed to 37^{o}C. Colonies were picked and placed in 30µl warmed lysis buffer and incubated at 37 – 45^{o}C for 5 minutes. Samples were then placed on ice for 5 minutes, then centrifuged at 14,000g for 1 minute. Supernatant was loaded onto a 0.8% agarose gel and run at 100 volts.

3.3.3 Amplification and purification of plasmids

Small (5ml) overnight cultures were established by picking transformed colonies and placing them into 5ml LB supplemented with appropriate selection agent, then grown at 37°C, 200rpm overnight.

DNA minipreps were carried out using the Genejet miniprep kit (Thermofisher). Briefly 1-5ml of overnight culture was centrifuged at 6800x g and resuspended in resuspension buffer with RNAase added. Cells were then lysed using Lysis buffer and neutralised with Neutralising solution and centrifuged at 5 minutes. Supernatant was loaded onto the supplied spin columns and centrifuged 1 minute, then washed twice using 500µl Wash solution and centrifuged for an additional 1 minute to remove excess wash solution. Elution was done using 20-50µl of Elution buffer.

3.3.4 Production of Bacmid DNA

Three recombinant DNA constructs were utilised for the expression of human MRP4 in *Sf 9* insect cells: his_6-MRP4, MRP4-his_6 and MRP4-3C-GFP-his_8. MRP4-his_6 and his_6-MRP4 were both in pFastBac plasmids. To generate recombinant baculoviruses these plasmids were transformed into specialised DH10 *E.coli* competent cells for the production of recombinant bacmid DNA used in the Bac-to-Bac Baculovirus Expression System by Life Technologies. Briefly MAX Efficiency® DH10Bac™ competent cells were thawed on ice and 1µL of pFastBac his6-MRP4 was added to the competent cells left on ice for 30 minutes. Heat shock was done for 30-45 seconds at 42^{o}C and then on ice for 2-5 minutes. 900µL of SOC medium was added and incubated at 37^{o}C for 1 hour shaking at 225 rpm. This was then plated on LB agar plates containing 50 µg/mL kanamycin, 7 µg/mL gentamicin, 10 µg/mL tetracycline, 100 µg/mL Bluo-gal, and 40 µg/mL IPTG to select for DH10Bac™ transformants.

The MRP4-3C-GFP-his_8 construct was within the pOPINE plasmid. Both the plasmid and the recombinant baculovirus generated from it were provided by the Oxford Protein Production Facility (OPPF).

3.3.5 Isolation of recombinant bacmid DNA

Isolation of recombinant bacmid DNA was carried out following the Life Technologies manual. Briefly singular colonies of DH10 Bac *E.coli* were incubated overnight shaking at 37^{o}C in LB containing 50 µg/mL kanamycin, 7 µg/mL gentamicin and 10 µg/mL tetracycline. 1.5mL of bacterial culture was centrifuged at 14,000 x g for 1 minute. The pellet was resuspened in 0.3 mL solution 1 (15mM Tris-HCl, pH 8.0, 10mM EDTA, 100µg/mL RNase A; filter-sterilized) and then 0.3 mL solution 2 (0.2 N NaOH, 1% (w/v) SDS; filter-sterilized) was added and incubated for 5 minutes at room temperature. 0.3 mL of 3M potassium acetate, pH 5.5 was slowly added and then placed on ice for 5 to 10 minutes. This was then centrifuged at 14,000 g for 10 minutes and the supernatant transferred to tube containing 0.8mL isopropanol and placed back on ice for 5 to 10 minutes. This was then centrifuged at 14,000 g for 15 minutes and the supernatant removed. 0.5 mL of 70% ethanol was added to the supernatant and centrifuged at 14,000 g for 5 minutes. The supernatant was removed and the pellet was air dried for 5 to 10 minutes then dissolved in 40 µL of 1X TE buffer, pH 8.0

3.3.6 *Pichia pastoris* molecular biology

3.3.6.1 Digestion of pFastBac MRP4-his_6 and pPICZαC

The recombinant pPICZαC MRP4-his_6 construct was created using a double digest of the pFastBac MRP4-his_6 plasmid and pPICZαC, using EcoRI, followed by re-ligation of the MRP4-his_6 into the pPICZαC plasmid.

pFastBac MRP4-his6 and pPICZαC were restriction digested in Cutsmart buffer using EcoRI for 1 hour at 37°C. pPICZαC was then subjected to an Antarctic Phosphatase treatment using 1µl Antarctic Phosphatase, 5µl of 10x Antarctic Phosphatase Buffer and incubated at 37°C for 30 minutes. The digested plasmid DNA was then separated on a 0.8% agarose gel and MRP4-his_6 and pPICZαC were excised from the gel and purified using a Gene Jet Gel Extraction kit from Thermo Fisher and quantified using a nano drop.

3.3.6.2 Ligation of MRP4-his_6 and pPICZαC

Ligation of MRP4-his_6 and pPICZαC was performed using a vector (pPICZαC) to insert (MRP4-his_6) molar ratio of 1:3. Ligations were performed overnight at 16°C.

Once ligated, pPICZαA MRP4-his_6 was transformed into chemically competent DH5α cells using the heat shock method previously described. Cell were plated on low salt LB agar plates containing 25ug/mL Zeocin.

Following transformation, colonies were grown up, mini-prep DNA extracted and subjected to diagnostic digest using EcoRI, SacI or PmeI.

3.3.7 HEK cell molecular biology

3.3.7.1 Digestion of pcDNA 3.1

460ng of pcDNA 3.1 was digested with EcoRI in Buffer 2.1 for 1 hour 37°C. After running on a 0.8% agarose gel the digested pcDNA 3.1 was gel extracted using the GeneJet Gel Extraction Kit. pcDNA 3.1 was then subjected to an Antarctic Phosphatase treatment , incubated at 37°C for 30 minutes and then heat inactivated.

3.3.7.2 Ligation of pcDNA 3.1 and MRP4-his

Ligation of MRP4-his6 and pcDNA 3.1 was performed using a vector (pcDNA 3.1) to insert (MRP4-his6) molar ratio of 1:3 and 1:5. The ligation was incubated for either 1 hour or overnight at room temperature before transformation into XL-10 Gold, DH5α and Top10 E.coli.

Colonies were screened using the Rapid Screening Protocol. Screened colonies containing pcDNA 3.1 MRP4-his were subjected to a diagnostic digest using EcoRI and NdeI.

3.4 Expression of recombinant human MRP4 in *Spodoptera frugiperda (Sf 9)* cells

3.4.1 Maintaining *Sf* 9 cell cultures

Sf 9 cells were grown up from a -80^{o}C stock in T25 monolayer cultures. Once highly confluent *Sf* 9 cells were maintained in either T75 monolayers or 250mL shaker flasks in Insect Express medium supplemented with 10% (v/v) FBS, 100U/mL penicillin and 100 mg/mL streptomycin. These were kept at 27^{o}C with the 250mL shakers shaking at 115rpm. The densities of the shaker flasks were maintained between 0.5 x 10^{6} *Sf* 9 cells/mL and 4 x 10^{6} *Sf* 9 cells/mL.

3.4.2 Transfection of *Sf* 9 cells

Isolated recombinant bacmid DNA was then transfected into *Sf* 9 cells to produce a P1 viral stock. 9 x10^{5} *Sf* 9 cells were seeded in each well of a 6 well plate in 2mL of growth medium and allowed to attach for at least 1 hour at 27^{o}C. Bacmid DNA:Cellfectin reagent complexes were prepared by diluting 1µg of purified bacmid DNA in 100µL of unsupplemented Grace's Medium. 6µL of Cellfectin Reagent was diluted in 100µL of unsupplemented Grace's Medium and then mixed with the diluted bacmid DNA for 15 to 45 minutes at room temperature. Whilst DNA:lipid complexes were incubating the medium from the attached *Sf* 9 cell was removed and washed with 2mL

unsupplemented Grace's medium. 0.8mL of unsupplemented Grace's medium was added to the DNA:lipid mixture after incubation and then added to each well and left to incubate for 5 hours at 27^{o}C. The DNA:lipid mixture wash then removed and replaced with growth medium and incubated for at least 72 hours. The P1 viral stock was collected by centrifugation of the medium from each well at 500 g for 5 minutes and then transferred to a fresh 15mL tube and stored at 4^{o}C. A small 1mL sample was kept at -80°C for long term storage.

3.4.3 Baculovirus amplification

The P1 viral stock was then amplified to a P2 viral stock in a 20mL culture of *Sf* 9 cells at 1 x 10^{6} *Sf* 9 cells/mL. A virus to cell ratio of 450:1 was used to amplify the virus, for a 20mL culture 44µL of P1 was added. The 20mL culture was incubated, shaking at 115rpm for 5 days at 27^{o}C. The P2 viral stock was harvested by centrifugation at 500 g for 5 minutes to remove cells and then transferred into a fresh sterile 50mL tube and stored at 4^{o}C. This P2 viral stock could then be used for expression and further amplification using this method. The baculovirus titre was estimated according to the Bac-to-Bac manual.

3.4.4 Small scale trial expression in *Sf* 9 cells

Test expression of the recombinant human MRP4 within *Sf* 9 cells upon infection with recombinant baculovirus were carried out in 20mL volumes. Different expression conditions were tested to optimise the expression. The volume of baculovirus and cell density upon infection along with the cell media and infection time were all varied and outline in the table 3.4.4.

Condition	
Multiplicities of Infection (MOI)	2 and 4
Cell density	1 and 2 x 10^6 cells/mL
Cell media	Insect Xpress
Infection Time	24, 48 and 72 hours

Table 3.4.4: Conditions for optimising MRP4 expression in Sf 9 cells. *1 or 2 x 106 cells/mL Sf 9 cells were infected at an MOI of 2 or 4 for 24 -72 hours and grown in Insect Xpress media for optimising expression of MRP4.*

3.4.5 *Sf* 9 Membrane Preparations

After the designated time points the culture was transferred to a 50mL Falcon tube and centrifuged at 6000 g for 10 minutes at 4°C. The cell pellet was resuspended in 20mL homogenisation buffer (50mM Tris-HCl pH 7.4, 250mM Sucrose, 0.25mM $CaCl_2$ and protease inhibitors (benzamidine, leupeptin and pepstatin), then placed into a nitrogen cavitation chamber. 500 psi of nitrogen pressure was applied to the chamber and left on ice for 15 minutes. The cell lysate was collected and centrifuged at 750 g for 10 minutes at 4°C, then the supernatant was centrifuged at 100,000 g for 20 minutes at 4°C to form a membrane pellet. This pellet was resuspended in TSB buffer (50mM Tris-HCl pH 7.4, 250mM Sucrose), aliquoted and stored at -80°C.

The total protein content was quantified using a Pierce BCA Protein Assay kit or DC Protein Assay kit. For both protein assay kits membranes were diluted 1/3, 1/10, 1/30 1/100 in H_2O. For BCA protein assay kit 10µl was added to 200µl of BCA reagents A and B (50:1 ratio) and for DC Protein Assay kit 25µl was added to 200µl of DC reagents A and B (50:1 ratio) in a 96 well plate. After a 1 hour incubation at 37°C the 96 well plate was read at 560nm on a microplate reader.

3.4.6 *Sf* 9 whole cell lysate

Initial trial expressions were performed using a variety of different conditions over a 72 hour period in 20mL cultures. Every 24 hours a 1mL sample was taken and centrifuged at 6000 g for 10 minutes. The sample were stored at -20^{o}C until all samples were collected. The Sf 9 cells were then lysed in a 400µL lysis buffer (150mM NaCl, 50mM Tris pH 8 and 1% Triton X100) and incubated on ice for 30 minutes. The lysed cells were centrifuged at 14000 g at 4^{o}C for 15 minutes, supernatant removed and analysed with Western Blot.

3.5 Expression of MRP4-his$_6$ in *Pichia pastoris*

3.5.1 Agar plates

YPDS (yeast extract, peptone, dextrose an sorbitol) plates were made from autoclaving 5 g yeast extract, 10g peptone, 91.1 g sorbitol and 10g agar in 450 mL of water. After autoclaving and once cooled, 50mL of sterile filtered 20% dextrose was added. Zeocin was added to a final concentration of 25ug/mL to 500ug/mL.

3.5.2 Growth Media

BMGY (Buffered Glycerol-complex Medium) and BMMY (Buffered Methanol-complex Medium) was made using 10 g of yeast extract and 20 g peptone was dissolved in 700 mL water and autoclaved. To which: 100 mL 1 M potassium phosphate buffer, pH 6.0, (13.2 mL of 1M K2HPO4 and 86.8 mL of 1M K2HPO4), 100 mL 10X YNB (13.4% Yeast Nitrogen Base with Ammonium Sulfate without amino acids), 2 mL 0.02% Biotin, 100 mL 10% Glycerol for BMGY or 100 mL 5% Methanol for BMMY was added after filter sterilisation.

3.5.3 Transformation of X33 *Pichia pastoris*

pPICZαC MRP4-his_6 was linearized using a PmeI restriction digest at 37^{o}C for 3 hours before heat inactivation at 65^{o}C for 20 minutes. PCR purification kit was used to purify pPICZαC MRP4-his_6.

Linearized pPICZαC MRP4-his_6 was transformed into *P.pastoris* X33 using electroporation. 2.7µg of linearized pPICZαC MRP4-his_6 was added to 80µl X33 and incubated on ice for 20 minutes before pulsing at 1800V. 1mL of ice cold 1M sorbitol was added and the sample was transferred to an Eppendorf and incubated at 30^{o}C for 1 hour. 100µl of transformed X33 was plated on YPDS plates containing between 0 – 500 µg/mL and incubated at 30^{o}C.

3.5.4 Colony expression screen

Colonies were grown in 25 mL BMGY in sterile 250 mL flasks at 30°C in a shaking incubator (250-300 rpm) until the culture reached an OD600 of 2-6. The cells were harvested by centrifugation at 3000g for 5 minutes and all BMGY removed. The cell pellet was washed with BMMY and then resuspended in BMMY at an OD600 of 1.0 and returned to the shaking incubator at 30°C. Sterilized pure methanol was added every 24 hours to a final concentration of 0.5% (v/v) methanol. Samples were taken every 24 hours over a 72h period.

3.5.5 *P. pastoris* membrane preparation

Cells were pelleted via centrifugation at 25000 g for 30 minutes and then resuspened in breaking buffer containing protease inhibitors (5.5 % w/v glycerol, 2 mm EDTA, 100 mM NaCl, 50 mM NaH2PO4, 50 mM Na2HPO4, x2 EDTA free protease inhibitor tablets (Complete EDTA free protease inhibitor tablets, Roche)). Cells were resuspened at a breaking buffer (mL) to cell pellet weight (g) of 3 : 1.

For small scale expression the resuspended pellet was placed in breaking tubes containing glass beads. This was placed in a cell homogenizer shaking at 50 Hertz for 10 minutes. For larger scale expression the resuspened cell pellets were broken by passing them through the C3 machine at least three times.

The homogenized cells were then centrifuged at 5000 g for 5 minutes, the supernatant was harvested and centrifuged at 13,000 g for 15 minutes then finally the supernatant was centrifuged for 1 hour at 100,000 g. Membrane pellets were resuspended in Buffer A (20 mM HEPES, 50 mM NaCl, 10 % w/v glycerol, x 1 EDTA free protease inhibitor tablets (Complete EDTA free protease inhibitor tablets, Roche)) or TSB at stored at -80^{o}C

3.6 HEK cell expression of MRP4-his$_6$

24 hours prior to transfection 300,000 HEK cells/well in a 6 well plate were seeded in DMEM containing 10% FBS and 1% Penicillin/Streptomycin. 3 hours prior to transfection the media was replaced with low serum DMEM containing 2.5% FBS and 1% Penicillin/Streptomycin. For transfection 4ug of pcDNA3.1 MRP4-his$_6$ was combined with 18uL of 10mM linear polyethylenimine (PEI) and 100uL reduced serum media (OPTIMEM) then was added to each well. 24 hours after transfection the media was replaced with DMEM containing 10% FBS. Every 24 hours over a 72 hour period samples were taken.

3.7 Vesicular Transport Assay (VTA)

VTAs were performed using *Sf* 9 cell membrane preparations. 10 – 100 µg of total protein in the *Sf* 9 cell membranes were defrosted on ice and had a final concentration of 10mM $MgCl_2$ and 10mM ATP or AMP added. The membranes subjected to ATP had an ATP regenerating system added

which consisted of a final concentration of 100µg/mL creatine kinase and 10mM creatine phosphate. The substrate used to measure transport activity was 8- (2-[Fluoresceinyl]aminoethylthio) adenosine- 3', 5'- cyclic monophosphate (fluo-cAMP) (Biolog) at varying concentrations of 5- 100 µM. Tris Sucrose Burffer (TSB) (50mM Tris pH 7.4 and 250mM Sucrose) was used to make up to a final volume of 50µL before incubating at 37^{o}C for 10 - 30 minutes.

3.7.1 Filtration Method

After incubation transport was stopped by the addition of 900µL of ice cold TSB. Samples were filtered using a glass fibre or PVDF filter and a vacuum conical flask. The filter was washed with 5mL of ice cold TSB and then the trapped vesicle solubilised by soaking the filter in 1mL of SDS/HEPES buffer (1% (w/v) SDS and 7.5mM HEPES) for 10-15 minutes. The amount of fluo-cAMP transported was measured by the fluorescence signal (RFU) of the solubilised sample measured on a Perkin Elmer LS 55 Fluorescence Spectrometer (excitation 480 ± 5nm, emissions 500-600 ±20nm). Samples were run in triplicate and an average of 5 scans was taken for each sample.

3.7.2 Spin Method

After incubation the transport was stopped by centrifugation at 14,000g for 5 minutes. The remaining supernatant was removed and the pelleted vesicles were washed with 1mL ice cold TSB and centrifuged for 5 minutes at 14,000g. TSB was removed and 1mL SDS/HEPES buffer to solubilise the vesicles for 10-15 minutes before measuring fluorescence using the parameters described above.

Data fitting for concentration curves in the VTA was performed by fitting a Michaelis-Menten and for MK571 inhibition was performed by fitting [inhibition] vs normalised response curve.

Statistical analysis was performed using an un-paired two-tailed t-test or two-way ANOVA. Data fitting and statistical analysis was done on GraphPad prism.

3.8 Solubilisation

3.8.1 SMA polymer solubilisation

SMA polymers were obtained from the suppliers as styrene-maleic anhydride polymers and had been hydrolysed in NaOH to form the styrene-maleic acid form as described previously (Rothnie 2016). Solubilisation of *Sf* 9 MRP4-his using SMA was carried out according to the protocol from (Rothnie 2016). Briefly, SMA at 5% (w/v) in SMA buffer (20 mM Tris–HCl pH 8, 150 mM NaCl) was mixed with an equal volume of MRP4-his membranes at 60 mg/mL wet pellet weight or around 5mg/mL total protein for 1 hour at room temperature before centrifugation at 100,000g for 30 minutes. The soluble supernatant was removed and the pellet resuspened in an equal volume of 1% (w/v) SDS.

3.8.2 Detergent Solubilisation

3.8.2.1 Dot Blot

Dot Blot analysis was used to examine the solubility of MRP4 of conventional, novel, detergent mixtures and polymers. MRP4 membranes were solubilised at 4^{o}C for 2 hours at 10x critical micelle concentration (cmc) of each detergent or 2.5% for SMA polymers and at 5 mg/mL total protein. This was then loaded into the Dot blot apparatus from Bio Rad, filtered and washed. Anti-his HRP antibody was used to detect the solubilised MRP4-his and imaged on a ChemDoc imaging system.

3.8.2.2 Solubilisation Efficiency

Western Blot analysis was performed to assess the solubilisation efficiency. MRP4-his was solubilised at 10x CMC at 4^{o}C for 2 hours then centrifuged at 100,000 g to pellet the insoluble fraction. The insoluble pellet fraction was resuspended in 1% (w/v) SDS. Equal volumes of total, soluble and insoluble MRP4-his was evaluated via Western Blot. Solubility efficiency was calculated by subtracting the density of the insoluble MRP4 band from the density of soluble MRP4 band. The total protein band was used as a reference to make sure the combined density of the soluble and insoluble fractions equal that of the total. The density was calculated by either using ImageJ or Image Studio analysis software.

3.9 Thermostability

3.9.1 Thermostability of soluble MRP4

Thermostability of MRP4 was measured using a simple Western Blot analysis based on (Ashok, Nanekar et al. 2013). 50µL samples of MRP4, solubilised at 30 mg/mL WPW with 2.5% SMA or 10 X CMC of detergent, was heated in a PCR machine for 30 minutes at varying temperatures and centrifuged at 100,000 x g for 30 minutes to pellet all aggregated protein. The supernatant was removed and analysed by Western Blot.

3.9.2 Thermostability of purified MRP4

Thermostability of purified MRP4 was measured in the same way except 25µL of purified MRP4, at 2 – 8 µg/mL, was heated for 10 minutes at 37, 50, 60, 70, 80, 90 and 100 °C. The samples were then centrifuged at 14, 000g for 10 minutes and the supernatant removed and analysed by SDS PAGE and Western Blot.

Data fitting for thermostability assays was performed by fitting a [inhibitor] vs normalised response curve using GraphPad Prism.

3.10 Purification

3.10.1 Affinity Purification using Calixarenes

Small scale purifications were carried out using micro affinity spin columns. 50µL of cobalt Talon resin was equilibrated with 2 cmc detergent. Once solubilised MRP4 was passed through the column then was washed with 3 x 10 column volumes wash buffer (2 cmc detergent, 5mM Imidazole in PBS) and eluted in 5 x 1 column volumes using elution buffer (2 cmc detergent, 200 mM Imidazole in PBS). Large scale purification was performed using the same protocol except using 2.5mL Talon resin in a gravity flow column and washed with 3 x 5 column volumes of wash buffer. MRP4 was concentrated using a 50kDa MWCO spin concentrator.

3.10.2 Affinity Purification using SMA

Affinity purification using SMA polymer was performed using an adapted protocol from (Rothnie 2016).

The optimised purification procedure involved binding SMA 2000 solubilised *Sf* 9 MRP4-his$_6$ with Ni-NTA resin overnight at 4^{o}C a volumetric ratio of 20:1 (soluble MRP4:resin). Ni-NTA resin had previously been washed with water and equilibrated with SMA buffer. Using a gravity flow column MRP4-his$_6$ was washed with 5 x 10 column volumes of SMA buffer supplemented with 20mM imidazole. MRP4 was then eluted from the column with 5 x 1 column volumes of SMA buffer supplemented with 200mM imidazole. Equal volume samples were taken from each

fraction and analysed by Western Blots and SDS-PAGE. Elution fraction were pooled together and concentrated using a 30 MWCO spin column.

Purification of DDM solubilised MRP4 was carried out in essentially the same manner except all buffers were supplemented with 0.1% (w/v) DDM.

3.10.3 Quantification of Purified Protein

Quantification of purified MRP4-his was carried out using BSA standards on an SDS PAGE. BSA standards ranging from 0.1 µg – 2 µg were run alongside 1 – 20µL purified MRP4-his. The gels were either stain free or stained with Instant Blue. The densities of the bands were analysed using ImageJ software, BSA standards were used to make a standard curve and concentration of MRP4-his quantified using this standard curve.

3.10.4 Size Exclusion Chromatography (SEC)

SEC was performed on an AKTA pure chromatography system using Unicorn software. A Superdex 200 30/10 column was used for SMA and a Superdex 200 5/150 column for calixarenes. The column was either equilibrated with 1 cmc C4C7 or 5 cmc DDM in PBS for MRP4-his_6 purified with Calixarenes. For MRP4-his_6 purified with SMA the Superdex column was equilibrated with SMA buffer. Purified MRP4 was injected and a flow rate of 0.1 – 0.3 mL/minute used. All fractions were collected and analysed via Western Blot.

3.11 Binding Studies

Tryptophan fluorescence quenching was used to assess the ability of purified SMALP encapsulated MRP4 to bind to known substrate fluo-cAMP. The substrates were diluted to 6, 24, 30, 60, 240,

300, 600 and 2400uM. 80uL of the purified SMALPed MRP4 was loaded into a Perkin Fluorimeter (excitation wavelength – 280nm, excitation slit width – 5nm, emission wavelength – 300 – 500nm, emission slit width – 20nm, scan speed – 50-500) to measure the fluorescence intensity of the purified SMALPed MRP4.

1uL of each substrate dilution was added one after the other and the fluorescence intensity measured at 340nm.

A tryptophanamide control was used to assess non specific binding. For 80uL of 4uM tryptophanamide was loaded and 1uL of each substrate dilution added one after the other and the fluorescent intensity measure at 360nm.

To calculate the percentage of tryptophan quenching of the substrates to the purified SMALPed MRP4 the fluorescence intensities of the tryptophanamide control were subtracted from the fluorescent intensities of the purified SMALPed MRP4.

Data fitting for tryptophan quenching assay was performed by fitting a Michaelis-Menten curve using GraphPad Prism.

3.12 Structural Studies

3.12.1 EM

First the grids were glow discharged. Then 4µl sample was added to the grid for 30s-1min, blotted, washed twice with water, then stained with 2% (w/v) uranyl acetate or 2% (w/v) gadolinium acetate, blotted and washed. Then imaged using a Jeol 2100 electron microscope.

4 Results

In order to study the structure or function of MRP4 a large quantity of highly stable and homogenous protein is needed. To accomplish this the protein must be functionally overexpressed and then solubilised and stabilised for purification. It is important that human MRP4 be maintained in its native conformation in order for it to be used in functional and structural studies.

This section contains the results from the overexpression of MRP4 for functional and structural studies. In this study three different expression systems were investigated: baculovirus-infected *Spodoptera frugiperda* (*Sf* 9) insect cells, *Pichia pastoris* yeast cells and human embryonic kidney (HEK) cells. The goal was to produce the highest amount of MRP4 as possible. Not only do large quantities of MRP4 need to be expressed but it also has to be functional. A vesicular transport assay was used to confirm if MRP4 was functional. After this confirmation, conventional and novel solubilizing techniques were used in order to extract the most amount of MRP4 possible from the membrane. Once solubilized, MRP4 can be purified to gain a homogenous sample. The stability and functionality of the purified sample is tested to make sure MRP4 is still in its native conformation and stable. The most stable and functional MRP4 sample can then be used for structural techniques.

The first step is to overexpress the protein. As these recombinant MRP4 proteins are human they need to be expressed in a eukaryotic expression system. Expression in *Sf* 9 insect cells was chosen as the main expression host as MRP4 had previously been expressed in this way.

4.1 Strategies for expression of recombinant human MRP4 in Sf 9

This study took advantage of the insect cell baculovirus expression system using three different recombinant baculovirus including human MRP4 constructs (his_6-MRP4, MRP4-his_6 and MRP4-GFP-his_8). Each of these constructs contains a histidine tag (his_6 or his_8) which will allow for the affinity purification. The MRP4-GFP-his_8 also contains a green fluorescent protein (GFP) tag and a cleavage site. The system works by producing a baculovirus that contains one of the recombinant human MRP4 genes which is then used to infect *Sf* 9 insect cells that will express the recombinant MRP4. By changing the expression conditions such as cell to virus ratio or multiplicity of infection (MOI), cell density and infection time the optimal conditions for protein expression were investigated.

Recombinant human MRP4 constructs

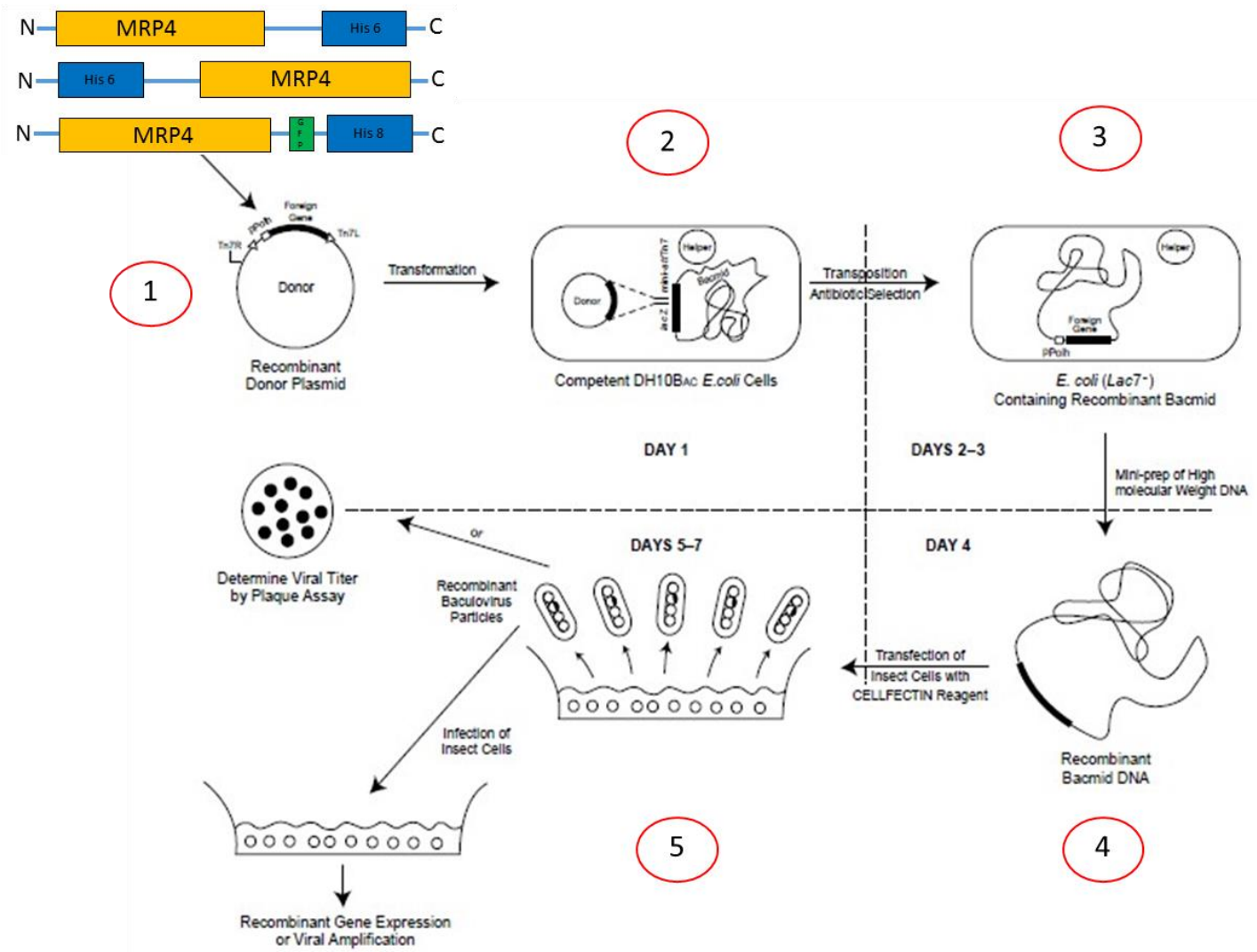

Figure 4.1.1: Outline of the production of baculovirus using the Bac-to-Bac Baculovirus expression system. *To express proteins using the Bac-to-Bac Baculovirus expression system a baculovirus containing the recombinant gene must first be produced. The Bac-to-Bac Baculovirus system has 5 main stages in the production of recombinant baculovirus. The first stage is cloning the genes of interest (his_6-MRP4, MRP4-his_6 and MRP4-GFP-his_8) into the pFastBac or pOPINE donor plasmid. Specialised DH10 Bac E.coli are then transformed with the plasmid (stage 2) where recombination between the donor plasmid and bacmid DNA occurs to transfer the gene of interest to form recombinant bacmid DNA. Through antibiotic selection the DH10 E.coli containing the recombinant bacmid DNA was selected (stage 3). The recombinant bacmid DNA was then isolated (stage 4). Sf 9 cells were transfected with the isolated recombinant bacmid DNA and recombinant baculovirus particles produced (stage 5). This recombinant baculovirus was amplified by infection of fresh Sf 9 cells and/or used for protein expression.*

The results in this section show how the his_6-MRP4 construct has been attempted to be made into recombinant bacmid DNA, how the MRP4-his_6 construct has gone through initial expression tests and the optimal expression conditions have been found, and how the MRP4-GFP-his_8 construct that was provided by the Oxford Protein Production Facility (OPPF) as a P1 recombinant viral stock has gone through viral amplification and optimal expression conditions where found as shown in the table 4.1.1.

Construct	pFastBac/ pOPINE	Recombinant Bacmid DNA	Recombinant Baculovirus P1 stock	Rounds of viral amplification	Initial expression trials	Optimisation of expression
his_6-MRP4	pFastBac	✓ *				
MRP4-his_6	pFastBac	✓	✓	✓	✓	✓
MRP4-GFP-his_8	pOPINE		✓ **	✓	✓	✓

Table 4.1.1: The different stages of protein expression in Sf 9 cell. *Each of the three MRP4 constructs were at different stages of expression at the beginning of this study. Attempts were made to generate recombinant bacmid DNA from the his_6-MRP4. The production of the recombinant his_6-MRP4 bacmid was unsuccessful and stopped at this stage (*). The MRP4-his_6 construct was successfully taken through the process and the optimal expression conditions were determined. The MRP4-GFP-his_8 construct was a P1 viral stock from the OPPF (**) and optimal expression conditions were also found. Only the MRP4-his_6 construct was taken onto large scale expression.*

4.2 Expression of his_6-MRP4 in *Sf* 9 cells

4.2.1 Bacmid DNA Production of the his_6-MRP4 construct

The pFastBac his_6-MRP4 vector was a kind gift from Professor Susan Cole (Queen's Cancer Institute, Canada). In order to produce a baculovirus containing the his_6-MRP4 construct, recombinant bacmid DNA must be produced. This was through the transformation of specialised DH10Bac *E.coli* containing a helper plasmid, stage 2 in figure 4.1, with pFastBac his_6-MRP4. The results below show the amplification and production of pFastBac his_6-MRP4 bacmid DNA.

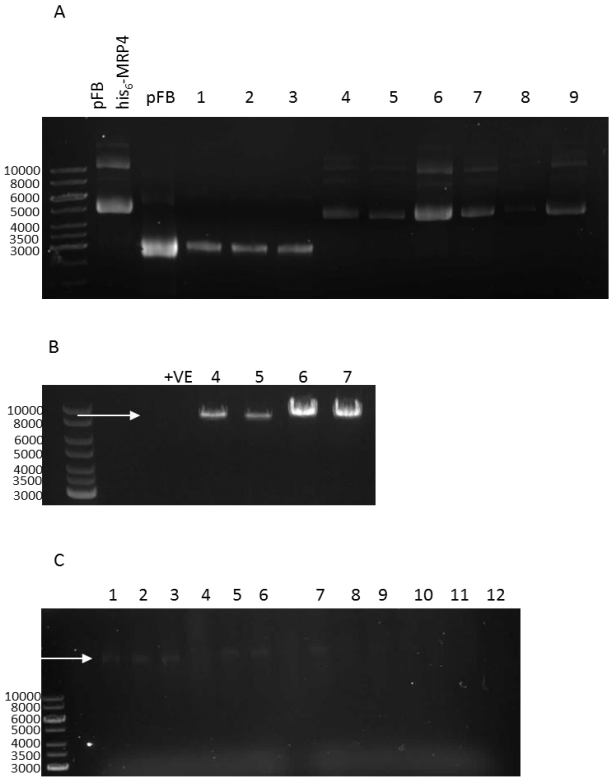

Figure 4.2.1: Amplification of his_6-MRP4 pFastBac and production of his_6-MRP4 bacmid DNA. *A) Agarose gel showing the DNA isolation after miniprep from 9 DH5α colonies (lanes 1-9) transformed with pFastBac his_6-MRP4 (pFB his_6-MRP4) construct (8700 bp) with pFastBac (pFB) as a control. B) Agarose gel of pFastBac his_6-MRP4 plasmids for colonies 4, 5, 6 and 7 digested with XhoI showing a single band at 8700bp (white arrow). C) Agarose gel of bacmid DNA isolation from 6 DH10Bac E.coli colonies after transformation with pFastBac his_6-MRP4 isolated from colony 7(4.2 A). Lanes 1-6 were bacmid DNA isolated from colonies on the original agar plate and lanes 7-12 were colonies from the re-streaked agar plate with the white arrow indicated level of potential his6-MRP4 bacmid DNA.*

Figure 4.2.1 shows the production of his$_6$-MRP4 bacmid DNA which is used to create his$_6$-MRP4 Baculovirus. The pFastBac his$_6$-MRP4 plasmid was propagated in DH5α *E.coli* and the results of 9 minipreps to isolate pFastBac his$_6$-MRP4 are shown in figure 4.2.1 A. Out of the nine colonies screened six appeared to contain the pFastBac his$_6$-MRP4 plasmid; the banding pattern in these six colonies was the same as the positive control (pFB his$_6$-MRP4). Colony number six showed the most intense bands containing 347ng/µL of plasmid DNA and colony seven has 147ng/uL plasmid DNA.

Purified pFastBac his$_6$-MRP4 plasmid was digested with XhoI to confirm the presence of the plasmid as the previous results were from undigested samples and can contain supercoiling. Figure 4.2.1 B shows the digestion of plasmid DNA from colonies 4, 5, 6 and 7. All plasmids ran at the correct molecular weight of 8700bp confirming the presences of pFastBac his$_6$-MRP4 (indicated by the white arrow). The positive control was very dilute so would not be visible on this gel.

After transformation in DH10Bac *E.coli* with recombinant pFastBac his$_6$-MRP4 plasmid DNA purified form colony 7; 100µL of undiluted and serial diluted (1/10, 1/100 and 1/1000) DH10Bac *E.coli* cells were plated on agar plates and incubated at 37^{o}C. No colonies formed after 24 or 48 hours with any dilution and it was only after 72 hours on the undiluted plate 6 that white colonies were formed. These six colonies were re-streaked on a separate agar plates and grown at 37^{o}C. The agar plates contain three antibiotics (Kanamycin, Gentamycin and Tetracycline) along with 5-bromo-4-chloro-3-indolyl-β-D-galactopyranoside (X-gal) and isopropyl β-D-1-thiogalactopyranoside (IPTG). The use of so many different antibiotics could have contributed to the lengthy time to produced colonies. Blue-white screening with X-gal can also take up to 48 hours to have distinguishable results.

After overnight cultures were grown from the six colonies in the original and re-streaked agar plates the bacmid DNA was isolated as shown in figure 4.2.1 C. The DH10 Bac *E.coli* contains a baculovirus shuttle vector (bacmid) that is 136 kb and with the transposition of his$_6$-MRP4 (4 kb)

into the bacmid the total molecular weight is 140 kb. The singular band at the top of the agarose gel in most colonies could indicate the presence of bacmid DNA that contains his_6-MRP4. Unfortunately, no shuttle vector control was available as a comparison but even if it had been, finding the difference between 136kb and 140kb would be challenging, as at these high molecular weights a 4kb difference would be hard to see. A 1% agarose gel was used in figure 4.2.1 C which is normally used for lower molecular weight DNA so a lower percentage agarose gel could be used to better identify these higher molecular weight bands. The DH10Bac *E.coli* cells used in figure 4.2.1 were old potentially reducing their competency and viability and may not have yielded the desirable results.

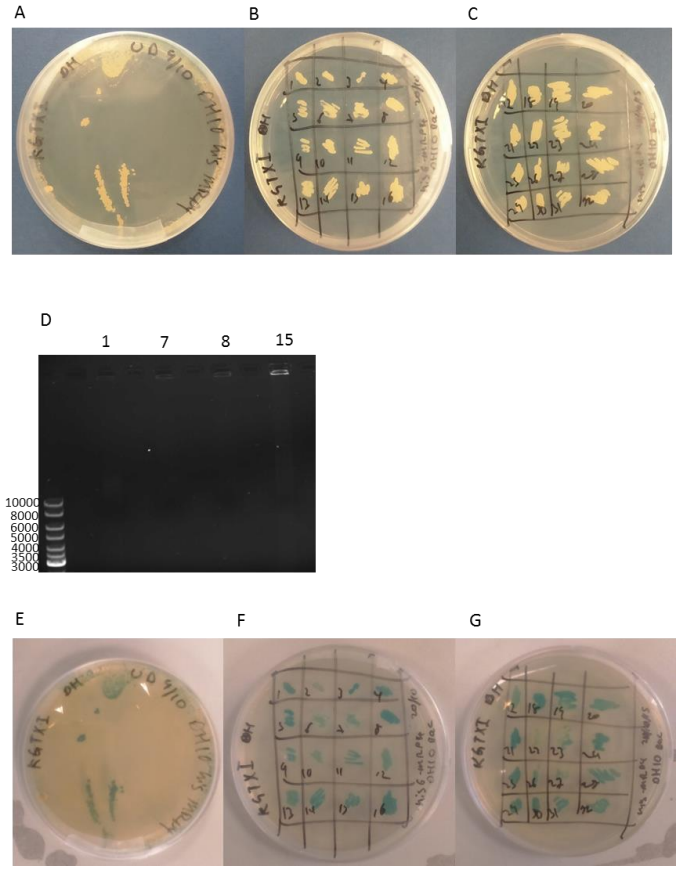

Figure 4.2.2: Transformation of DH1Bac E.coli with pFastBac his_6-MRP4 and isolation of his_6-MRP4 bacmid DNA. *A) Agar plate of 100µl undiluted DH10Bac E.coli transformed with pFastBac his_6-MRP4 showing white colonies after 72 hours incubation at 37°C. Re-streaked agar plates (B) colonies 1-15 and (C) colonies 16-32 form agar plate (A). C) shows agarose gel of four overnight cultures from colonies 1, 7, 8 and 15 form agar plate (B). Agar plates E, F and G are agar plate A, B and C after two months at 4°C showing blue colonies.*

A second transformation was attempted using pFastBac his_6-MRP4 plasmid DNA isolated from colony 6 (Figure 4.2.1 A) and newly procured DH10 Bac *E.coli* (Figure 4.2.2). Again 100ul of transformed DH10Bac *E.coli* at undiluted and serial diluted (1/10, 1/100 and 1/1000) was plated and incubated overnight at 37^{o}C. All plates showed no growth so were incubated for a further 48 hours, again showing the slow growth of DH10Bac *E.coli* cells even when using fresh cells. Colonies only formed on the undiluted plate as shown in figure 4.2.2 A and all appeared white. 32 colonies were chosen and re-streaked on another plate and incubated overnight at 37^{o}C (Figure 4.2.2 B and C) and again all appeared white. Overnight cultures were made from 15 colonies (Figure 4.2.2 B) but unfortunately little or no growth appeared in any culture. These were left for a further 24 hour at 37^{o}C and after 48 hours in total only 4 colonies showed growth. Bacmid DNA was extracted from these four colonies and ran on a 0.6% agarose gel (Figure 4.2.2 D) but no bands appeared at any molecular weight. The remaining colonies (colonies 17-32) were not taken forward as all the previous colonies showed no bands on the agarose gel. The plates were kept at 4^{o}C and it was noticed after about 2 months all of the colonies were blue showing the his_6-MRP4 construct was not potentially introduced into the bacmid DNA (Figure 4.2.2 E, F and G). However, it would have been expected that Bacmid DNA should still have been isolated from the DH10Bac *E.coli* regardless if the recombination had been successful.

The production of his_6-MRP4 bacmid DNA was unsuccessful after two attempts. Old DH10Bac *E.coli* were used in the first attempt (Figure 4.2.1) but even using fresh DH10 Bac *E.coli* in the second attempt (Figure 4.2.2) no bacmid DNA was isolated. The first attempt did show high molecular weight bands (Figure 4.2.1 C) but was unclear if it was recombinant bacmid DNA that contained his-MRP4. Untransformed DH10 Bac *E.coli* could have plated out on agar plates and used a screening control and for bacmid DNA isolation. This isolated bacmid DNA could have been used as a control to compare against potential recombinant his_6-MRP4 bacmid DNA on the agarose gel. Because these results shows the recombinant his_6-MRP4 bacmid DNA production was unsuccessful this recombinant MRP4 construct was not taken any further.

4.3 Expression of MRP4-his$_6$ in *Sf* 9 cells

Sf 9 insect cells were used to overexpress recombinant human MRP4 containing a C-terminal hexa histidine tag (MRP4-his$_6$). The Bac-to Bac baculovirus system was the method used to overexpress MRP4-his$_6$. The pFastBac MRP4-his$_6$ construct and subsequent bacmid DNA were generated by Dr Ian Kerr (University of Nottingham) and Dr A Rothnie (Aston University) respectively (Gulati et al 2014). The pFastBac MRP4-his$_6$ construct was sequenced and had 100% sequence identity to human MRP4. MRP4-his$_6$ bacmid DNA had previously been transfected into *Sf* 9 insect cell to produce the MRP4-his$_6$ baculovirus used in this study. Expression of MRP4-his$_6$ had also previously been accomplished but not optimised (Gulati et al 2014). This section shows the optimisation of MRP4-his$_6$ expression in *Sf* 9 cells by changing the infection period, cell density and the multiplicity of infection (MOI). According to the Bac-to-Bac baculovirus manual (Invitrogen) the recommended expression parameters were: 24-96 hours infection period, 1-2 million *Sf* 9 cells per millilitre and an MOI of 1-5.

The concentration or plaque forming units (PFU) of baculovirus can contribute to the level of expression of proteins. There are numerous methods for calculating the PFU of baculovirus such as plaque assay, antibody based assay, real time PCR and the use of a novel Sf 9 easy titre cell line. Each has its advantages and limitations, and can give quite differing results (Kost, Condreay et al. 2005, Hopkins and Esposito 2009). In this study PFU was estimated according to the Bac-to-Bac manual (Invitrogen). As the baculovirus is a virus it will have detrimental effects on the *Sf* 9 insect cell and over time due to the nature of viruses it will cause cell lysis. If the MOI of the baculovirus is too high it will cause the cells to lyse potentially before the protein can be expressed. Even if the protein is able to be expressed the cells may still be lysed due to the high level of virus present causing reduced protein expression. Similarly, if the MOI is too low protein expression will be reduced, as only small amounts of virus will be able to enter the cell.

4.3.1 Whole cell lysate of MRP4-his$_6$ expression in *Sf* 9 cells

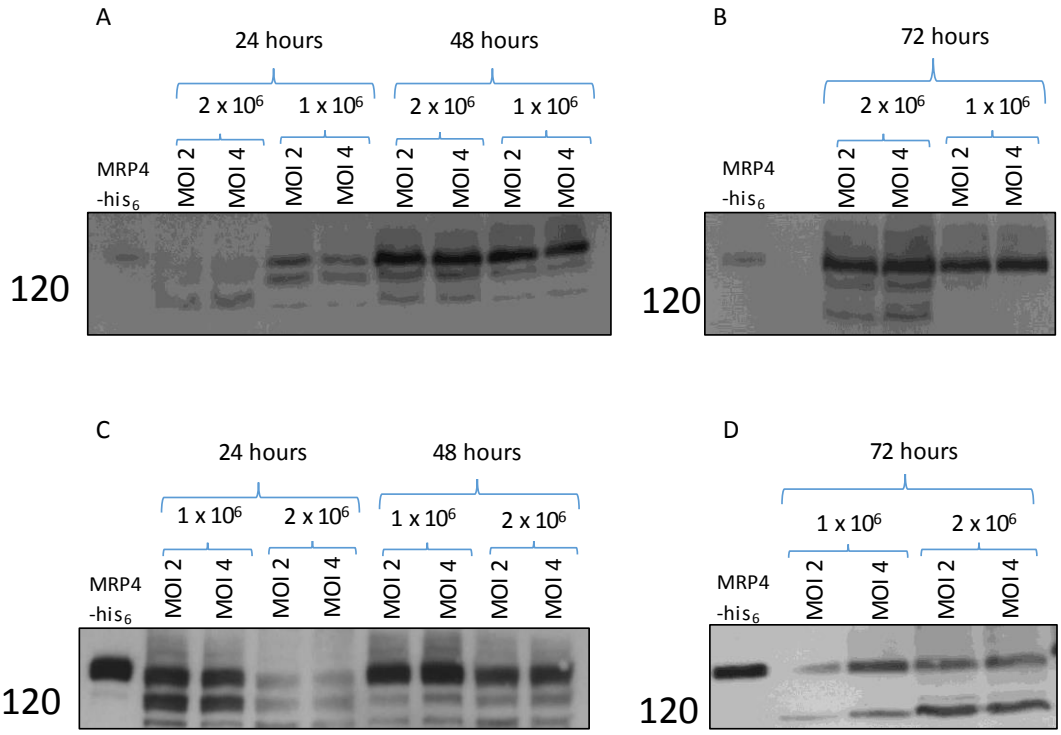

Figure 4.3.1: Whole cell lysate of MRP4-his$_6$ trial expressions in Sf 9 insect cells. *Western blots A and B show the first trial expression and western blots C and D are from the second trial expression of MRP4-his$_6$. A primary anti-his antibody and anti-mouse HRP secondary antibody was used to detect MRP4 expression. These whole cell lysates show the expression levels after 24, 48, and 72 hours using either 1 x 10^6 or 2 x 10^6 Sf 9 cells at a multiplicity of infection (MOI) of 2 or 4 from two trial expressions. A stock of MRP4-his$_6$ membranes from a previous expression (Gulati et al 2014) was used as a positive control on all Western blots*

Whole cell lysates are a fast and simple method of detecting the expression levels compared to membrane preparations, which are a much longer procedure. However the whole cell lysate does not show if MRP4-his$_6$ resides in the membranes of *Sf* 9 insect cells, it simply shows whether MRP4-his$_6$ is being expressed. The positive control used was a stock membrane preparation from a previous expression (Gulati et al 2014) and was used to make sure MRP4-his$_6$ expressed was the correct molecular weight; it also functioned as a control for the antibodies used on the western blots, and allowed for comparison between different blots. Two different cell densities, 1x10^6 and

2 x 10^6 cell per millilitre (1 x 10^6/mL and 2 x 10^6/mL) were used as these cell densities were recommended in the Bac-to-Bac baculovirus manual. These cell densities are commonly used during expression using the baculovirus system allowing the cells to go through roughly one doubling procedure, as these cell densities are found during log growth phase of *Sf* 9 insect cells (Invitrogen). Densities can reach between 2 x 10^6 /mL and 4 x 10^6 /mL, but should be kept below 6 million per millilitre making 1 and 2 million per millilitre optimal conditions for expression.

The western blots from two separate experiments in figure 4.3.1 show the expression levels of MRP4-his_6 over a 72 hour infection period with cell densities of 1 x 10^6 and 2 x 10^6/mL and an MOI of 2 and 4. After 24 hours, the expression levels are dependent on the cell densities with 1 x 10^6/mL having visibly higher expression level than 2 x 10^6/mL. This shows that after 24 hours even at an MOI of 4, where more baculovirus is added, this is not enough to induce expression at the higher cell density after such a short infection period. After 48 hours, there is higher expression levels compared to 24 hours. There appears to be very little difference in expression level for either cell density or MOI after 48 hours. The 72 hour expression levels cannot be compared to 24 and 48 hour expression levels as they are on a separate western blot. Expression levels at this time point do not vary with cell density or MOI. Because the expression levels were so low after 24 hours this time point was not taken forward for membrane expression tests.

4.3.2 Membrane expression of MRP4-his$_6$ in *Sf* 9 cells

As MRP4 is a membrane protein the expression levels in the membranes of the *Sf* 9 insect cells must be assessed. MRP4 is naturally expressed in the outer membrane of cells in the human body so this should also occur in *Sf* 9 insect cell. Membrane preparations used in this study would include all membranes of the *Sf* 9 insect cell including Golgi, endoplasmic reticulum and outer membrane so even with these membrane preparations it is unknown if the MRP4 is expressed on the outer membrane. Regardless of which particular membrane MRP4 is being expressed in, as long as it in folded properly and functional, purification can still take place. *Sf* 9 cells will carry out some glycosylation but not the same level as in mammalian cells. Again if the MRP4 being expressed is functional the level of glycosylation is not as issue but glycosylation level of MRP4 has been known to effect the transport of certain molecules. Positive control expression parameters are 72 hour expression period at an MOI of 5 and are found in the Gulati et al 2014 study.

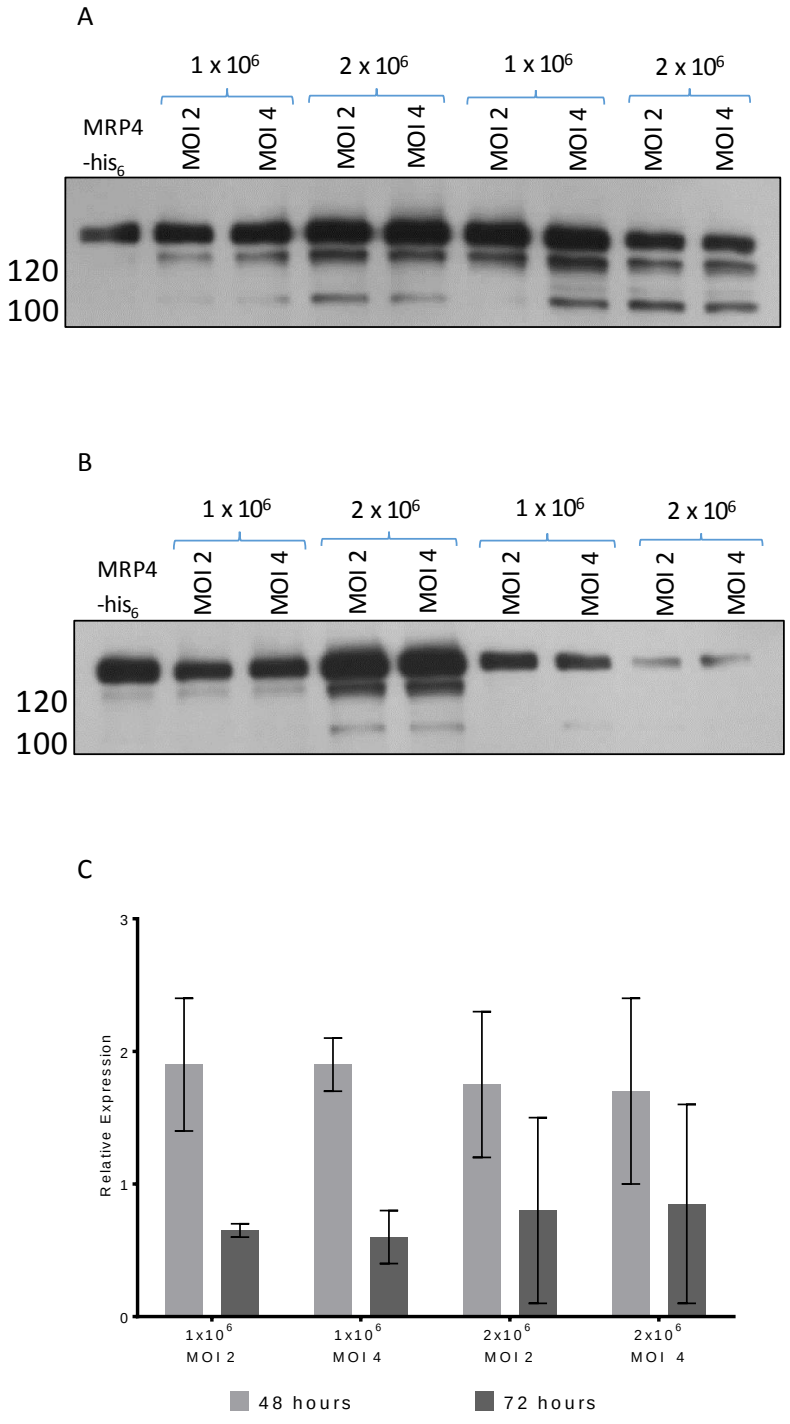

Figure 4.3.2: Membrane expression of MRP4-his$_6$ in Sf 9 insect cells. *Western blots A and B show typical examples of the expression levels after 48 and 72 hours with either 1 or 2 x 10^6 Sf 9 insect cells. An MOI of 2 or 4 of the MRP4-his$_6$ baculovirus was used. A primary anti-his antibody and anti-mouse HRP secondary antibody was used to detect MRP4. A stock of a previous membrane preparation for MRP4-his expressing Sf9 cells was used is a positive control (MRP4-his$_6$) and used to quantify the relative expression. The relative expression based on the density of the MRP4-his$_6$ band under the different expression conditions compared to the positive control is shown in graph C. Data are mean ± sem, n≥2.*

Figure 4.3.2 shows the expression of MRP4-his_6 after 48 and 72 hours using 1 and 2 x 10^6/mL at an MOI of 2 and 4. Western blots A and B show that MRP4-his_6 expressed is the correct molecular weight as it runs at the same level as the as the positive control. All 48 hour samples show a double band with the upper larger band at the same molecular weight as positive control and a smaller band just below. This lower band could be due to incomplete MRP4 expression or breakdown of the MRP4 protein. Visibly the western blots shows an increased expression level after 48 hours compared to 72 hours.

Quantification of expression levels was done by comparing the density of the MRP4-his_6 (upper band only) to the previous standard expression level (Gulati et al 2014) (MRP4-his_6). Graph C shows these densities plotted as relative expression levels with 1 being the previous expression level. It clearly shows the 48 hours expression period increases the expression to on average around double that previously achieved level regardless of cell density or MOI. 72 hour expression levels were on average less than 1 and also have a huge variability. Reduced expression after 72 hours could be due to the lytic action of the baculovirus and this increases over time. By lysing the cells MRP4-his_6 expression could be degraded by proteases released by lysed cells and the membrane integrity of the *Sf* 9 would be compromised leading to denaturation of MRP4. These results show 48 hours is the optimal infection period but there is no difference between and MOI of 2 and 4 at either cell density.

4.4 MRP4-GFP expression in *Sf* 9 cells

The other recombinant MRP4 construct expressed in this study was MRP4 conjugated to green fluorescent protein and an octa-his tag (MRP4-GFP-his_8). The MRP4-GFP-his_8 (MRP4-GFP) construct was provided as P1 viral stock form the Oxford Protein Production Facility (OPPF). Viral amplification and initial trial expressions were carried out. The initial trial expressions were performed in 6 well plates which showed the viral amplification was successful, the MRP4-GFP baculovirus was not quantified before moving onto trial expression using different expression conditions.

4.4.1 Whole cell lysate of MRP4-GFP expression in *Sf* 9 cells

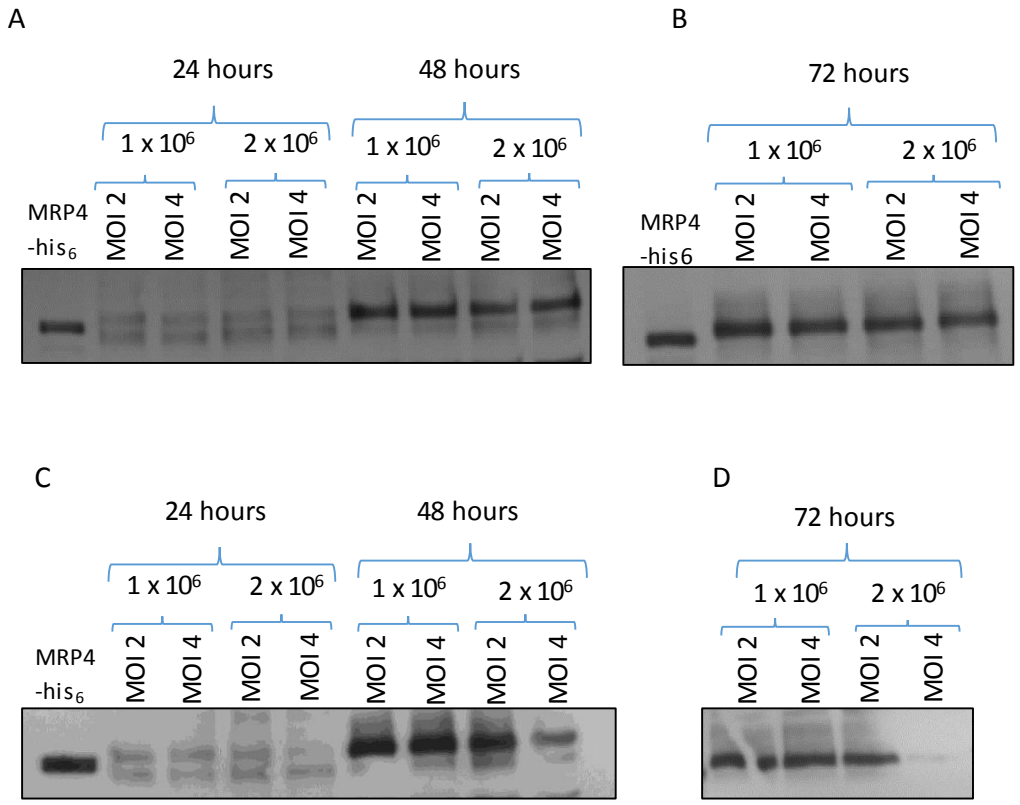

Figure 4.4.1: Whole cell lysate expression of MRP4-GFP trial expressions. *Western blots A and B shows examples of the expression levels of MRP4-GFP from the first trial and western blots C and D from the second trial. Whole cell lysate samples were taken after 24, 48 and 72 hours with 1 and 2 x 10^6 Sf 9 cells insect cells. An MOI of 2 and 4 of the MRP4-GFP baculovirus was used to infect and express MRP4-GFP. MRP4-his_6 was used as a positive control along with a primary anti-his antibody and an anti-mouse HRP secondary antibody.*

Whole cells lysates were performed to determine which conditions were worth taking forward for membrane preparations. The same expression conditions as MRP4-his_6 were tested with MRP4-GFP. MRP4-his_6 was used as a positive control in all the MRP4-GFP expression studies as MRP4-GFP had not previously been expressed. The MRP4-GFP will run at a higher molecular weight as it contains GFP a 26kDa protein.

Figure 4.4.1 shows the expression levels of MRP4-GFP over a 72 hour period from two separate experiments. After 24 hours the expression levels were low and did not vary with increased MOI or cell densities. The expression levels increased after 48 hours compared to 24 hours but showed little variability at different MOI and cell densities. The expression levels after 72 hours cannot be compared to 24 and 48 levels but shows MRP4-GFP is being expressed after 72 hours and again little variability with increased MOI and cell densities. These whole cell lysates show MRP4-GFP ran at higher molecular weight compared to MRP4-his_6 which was expected indicating MPR4-GFP was being expressed. As the expression levels were so low after 24 hours only the 48 and 72 hour time points were taken to measure the expression level in membranes of *Sf* 9 insect cells.

4.4.2 Membrane expression of MRP4-GFP in *Sf* 9 cells

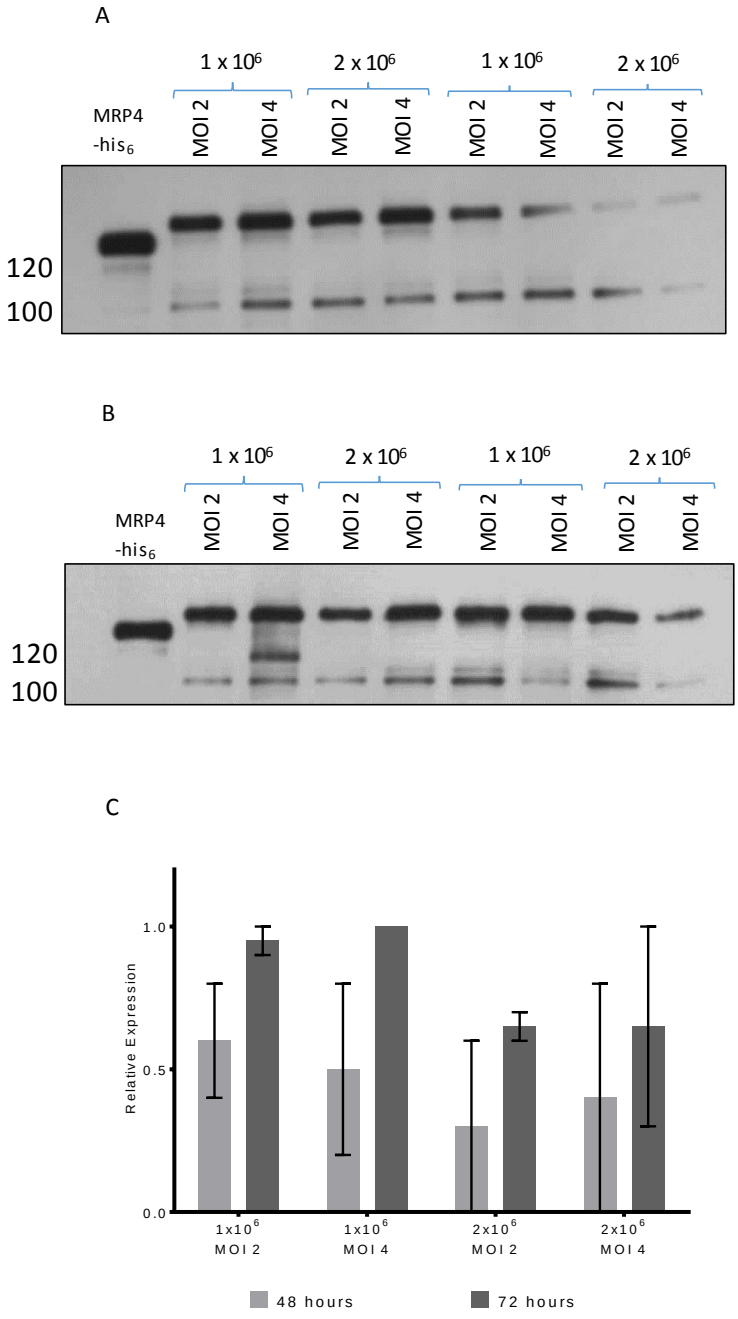

Figure 4.4.2: Membrane expression of MRP4-GFP in Sf 9 insect cells. *Western blots A and B show examples of the expression level of MRP4-GFP after 48 and 72 hours respectively. 1 and 2 x10⁶ Sf 9 insect cells were infected with MRP4-GFP baculovirus at an MOI of 2 and 4. A primary anti-his antibody and an anti-mouse HRP secondary antibody was used to detect MRP4. MRP4-his₆ was used as a positive control and used to quantify the expression level. The density of the MRP4-GFP expressed in Sf 9 membranes was compared to the MRP4-his₆ positive control band and average relative expression levels plotted on graph C. Data are mean± sem, n=2.*

Membranes were prepared from trial expressions of MRP4-GFP and analysed via densitometry of the bands on the western blot. Western blots A and B shows the expression levels from 48 and 72 hour infection periods over two separate experiments. MRP4-his_6 was used as a positive control and used as a comparison to measure expression levels. All membranes were quantified for total membrane protein and 5μg of total membrane protein was loaded for each sample as a way of normalising the samples. All the bands in the MRP4-GFP samples ran at higher molecular weight as expected compared to the MRP4-his_6 control indicating MRP4-GFP was being expressed in these membranes. Graph C shows the densitometry results from the two experiments with the relative expression of 1 being the level of expression from the MRP4-his_6 control. There was a large degree of variability observed for all conditions, and no statistically significant differences, however it appeared that the expression level was lower at 48 hour and increased after 72 hours and that the expression level was lower using 2 x 10^6/mL *Sf* 9 cells regardless of MOI and time. 72 hour infection period at an MOI of 2 or 4 and using 1 x 10^6/mL *Sf* 9 cells showed the highest expression levels. All expression levels were lower than the positive control, suggesting the addition of the GFP tag to an already large protein hindered the expression to some degree.

4.4.3 Fluorescent microscopy images of *Sf* 9 cells expressing MRP4-GFP

The MRP4-GFP construct allows for visualisation of MRP4 during expression in *Sf* 9 insect cells. Using fluorescent microscopy the GFP conjugated to MRP4 will be visible and indicate the expression of MRP4. The fluorescent microscopy images prove that the *Sf* 9 cell expressing MRP4-GFP were GFP positive (white arrows) as they were visible under fluorescent conditions. The native *Sf* 9 cell and *Sf* 9 cell expressing MRP4-his_6 are only visible under white light and with no GFP was visible under fluorescence. This result along with the western blot provides good evidence that MRP4-GFP was expressed in *Sf* 9 cells.

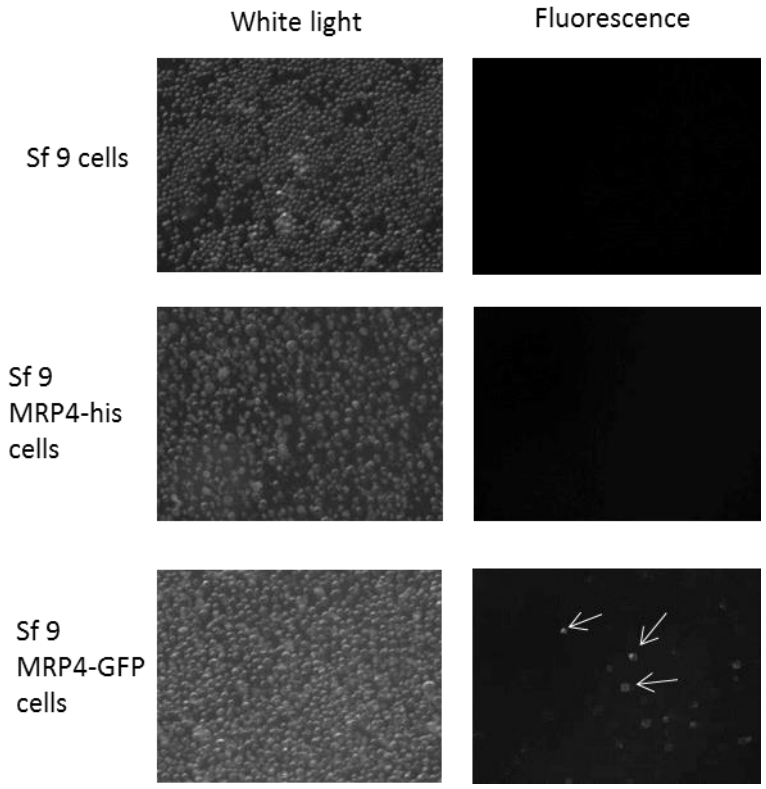

Figure 4.4.3: Fluorescence microscopy images Sf 9 MRP4-his and MRP4-GFP. *1 x 10^6 Sf 9 cell were infected with recombinant MRP4-his or MRP4-GFP baculovirus and imaged after 3 days under white and fluorescent light. Sf 9 cells expressing MRP4-GFP were visible under fluorescence as indicated by the white arrows. Sf 9 cell expressing MRP4-his and Sf 9 cell themselves showed no visible cells under fluorescence.*

Due to the fluorescent nature of GFP the MRP4-GFP construct could also be used to measure the level of expression by measuring the fluorescent intensity. The images in Figure 4.4.3 were simply used to confirm the expression of MRP4-GFP but if pictures were taken over the infection period the level of expression could be measured. Using more powerful fluorescent microscopes and advanced techniques the localisation of MRP4-GFP could be visualised.

4.4.4 Flow cytometry of *Sf* 9 cells expressing MRP4-GFP

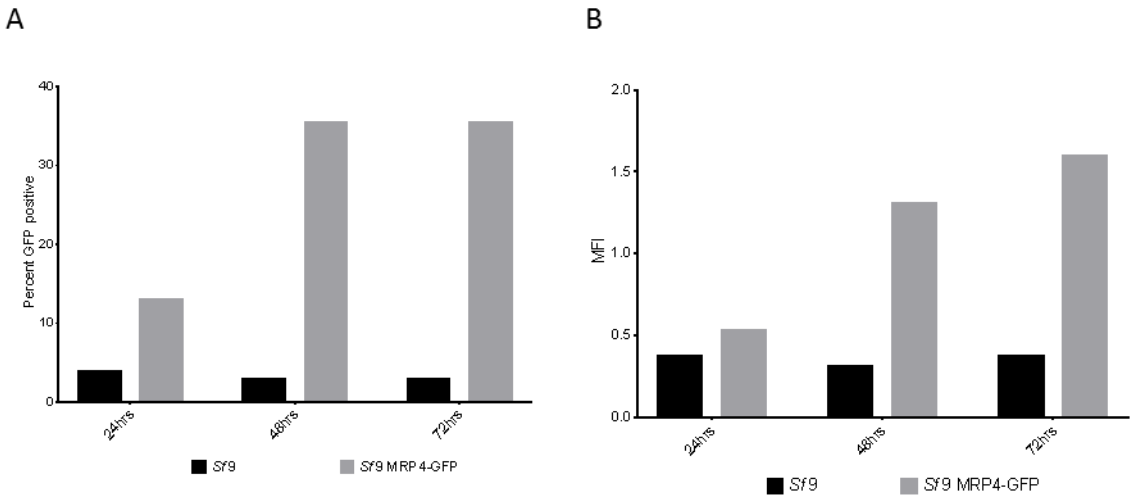

Figure 4.4.4: Flow cytometry analysis of Sf 9 MRP4-GFP*. Graphs A shows the percent of GFP positive cells from Sf 9 native cells (Sf 9) and Sf 9 cell expressing MRP4-GFP (Sf 9 MRP4-GFP) over a 72 hour period. Graph B shows the mean fluorescent intensities (MFI) of the Sf 9 and Sf 9 MRP4-GFP cells over 72 hours. (n=1)*

Flow cytometry was also used to measure the level of expression by measuring GFP fluorescence. Native *Sf* 9 cells were measure against *Sf* 9 cells expressing MRP4-GFP over a 72 hour period. The level of GFP would represent the level of expression of MRP4. There is a dramatic increase in the percent of GFP positive cells with *Sf* 9 cells expressing MRP4-GFP from 24 to 48 hours. The percent of GFP positive cell (*Sf* 9 MRP4-GFP) does not change from 48 to 72 hours. The percent of GFP positive cells for the native *Sf* 9 cells does not change over the 72 hours period. By measuring the mean fluorescent intensity the level of MRP4-GFP expression can be evaluated. This shows that again there is a large increase from 24 to 48 hours with *Sf* 9 MRP4-GFP. There was a further but far less noticeable change in the MFI from 48 to 72 hours. The MFI of native *Sf* 9 cells does not

change over the 72 hour period. These results show there is an increase in percent of MRP4-GFP expressed, mainly taking place in the first 48 hours. The MFI results show that although there are the same number of *Sf* 9 cells expressing GFP the MFI values is highest after 72 hours indicating more MRP4-GFP is being expressed per cell. This is in line with the western blot results which show that the expression level of MRP4-GFP was highest after 72 hours. The experiment performed was only an initial trial but does show that flow-cytometer can be used to measure the expression levels of MRP4 in *Sf* 9 cells.

4.5 Large scale expression of MRP4-his$_6$ in *Sf* 9 cells

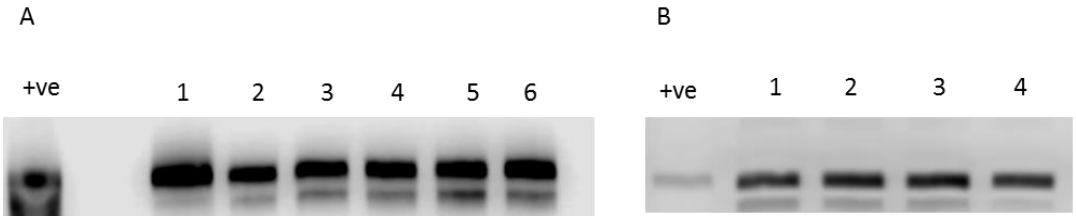

Figure 4.5: Large scale expression of MRP4-his$_6$ in Sf 9 cells*. Western blot A show the expression of six different 300mL cultures. Western Blot B show four different 300mL cultures using a lower passage baculovirus. All expression were performed with 1 x10^6 cells/mL at an MOI of 2 for 48 hours.*

Western blots in figure 4.5 show the large scale (300mL) expression of MRP4-his$_6$ in *Sf* 9 cells. The expression level in western blot A are around twice that of the control. Expression levels in B are around 10 times higher than the positive control. These results show that large scale expression is at least at the same level as the small scale trial and that using a baculovirus with a lower passage factor may increase the expression level.

Overall MRP4-his$_6$ and MRP4-GFP was expressed in *Sf* 9 insect cells. Whole cell lysates were a quick and simple technique to test for expression but was only qualitative. Membrane preparation were able to give a quantitative expression level. The membrane expression levels of MRP4-his$_6$ was able to be about doubled compared to previous expression levels. MRP4-GFP was

not previously expressed in *Sf* 9 cells and had to undergo viral amplification, these results show that virus amplification was success*f*ul along with expression although lower than MRP4-his_6 expression. The MRP4-GFP expression prove useful in finding other ways in quantifying the expression and location in membrane. Only MRP4-his_6 was taken forward for large scale expression using an MOI of 2 over 48 hours and 1 x 10^6/mL *Sf* 9 cells as these conditions showed the highest expression levels.

4.6 MRP4 expression in *Pichia pastoris*

Sf 9 insect cells are not the only way of expressing recombinant human membrane proteins. An alternative that was also investigated in this project was expression in yeast. Yeast cells are used for recombinant human membrane proteins, as they are able to grow to very high cell densities increasing the yield. These cells are very simple and cheap to culture and are easily scaled up. The recombinant membrane protein is integrated into the yeast genome reducing the prep-to-prep variability, whereas *Sf* 9 expression is dependent on different virus batches and the effectiveness of infection each time. *Pichia pastoris* was the specific type of yeast chosen during this study as it had previously been shown to be used in the successful overexpression of 25 different human ABC transporters (Chloupkova, Pickert et al. 2007). Specifically the X33 strain of *P. pastoris* was chosen as recombinant MRP4 was going to be cloned in the pPICZαC plasmid. This plasmid has a Zeocin resistance gene and X33 allows for the selection of Zeocin resistance expression plasmids and is recommended by the Invitrogen pPICZα manual (Invitrogen). This plasmid allows for the high level methanol inducible expression of the gene of interest.

For expression of MRP4-his_6 in *P.pastoris,* the MRP4-his_6 gene was first extracted from the pFastBac plasmid via double digestion and ligated into the *P.pastoris* expression plasmid pPICZαC. Once ligated *P.pastoris* was transformed and the gene integrated into the *P.pastoris* genome before optimisation of expression was performed, outlined in figure 4.6.

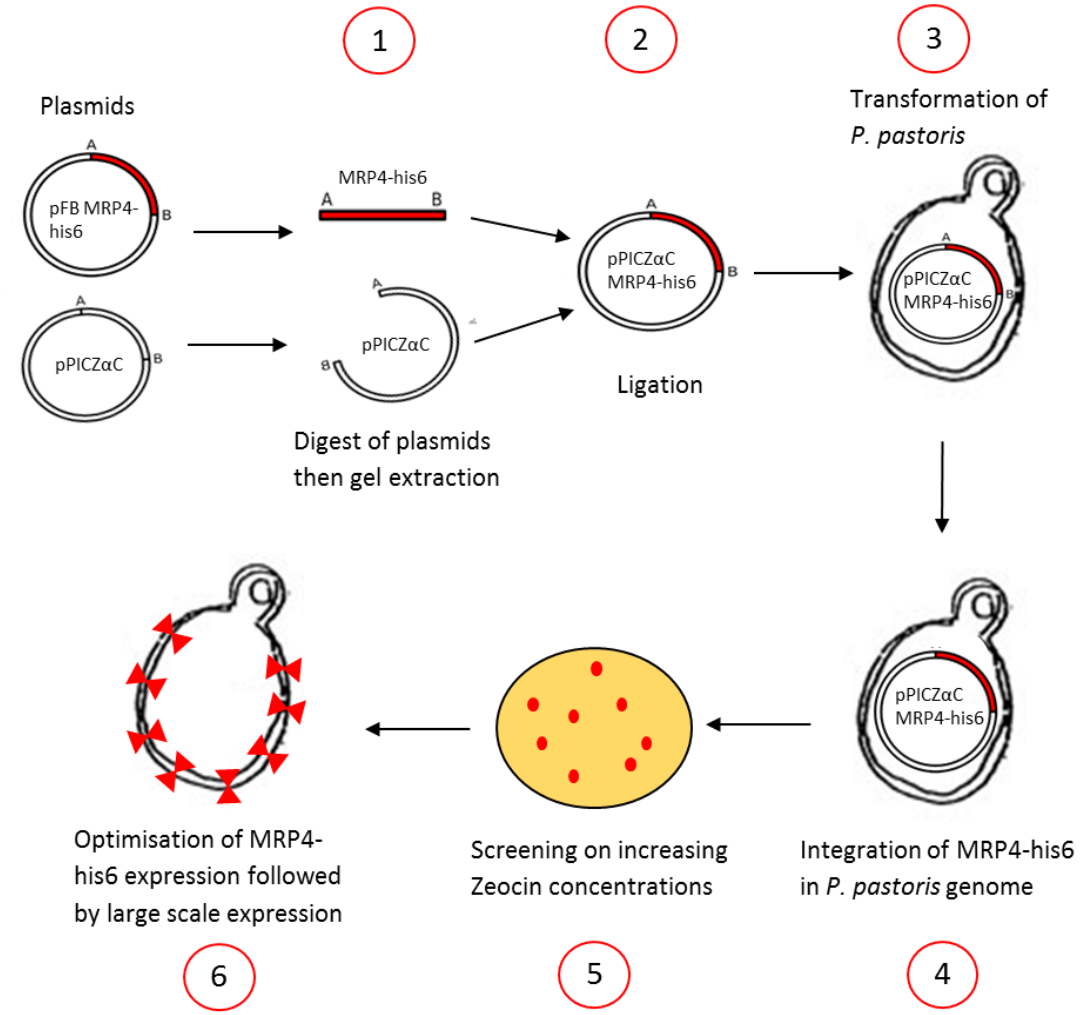

Figure 4.6: Schematic of Pichia pastoris work flow to expressed MRP4-his$_6$. *1) Extraction of the MRP4-his gene from the pFastBac MRP4-his$_6$ (pFB MRP4-his$_6$) plasmid and digestion of the pPICZαC plasmid using restriction enzymes followed by agarose gel separation and extraction. 2) Ligation of MRP4-his$_6$ into pPICZαC plasmid to create pPICZαC MRP4-his$_6$. 3) Transformation in electro competent Pichia pastoris X33 yeast cells. 4) Integration of MRP4-his$_6$ into the P. pastoris genome. 5)Screening of transformed P. pastoris X33 cells on YPD agar plates containing increasing concentrations of Zeocin and checking for successful integration of pPICZαC MRP4-his$_6$ with small scale expression and western blot analysis. 6) Optimisation of expression conditions with successful transformants and then large scale expression.*

4.6.1 Molecular Biology of production of pPICZαC MRP4-his

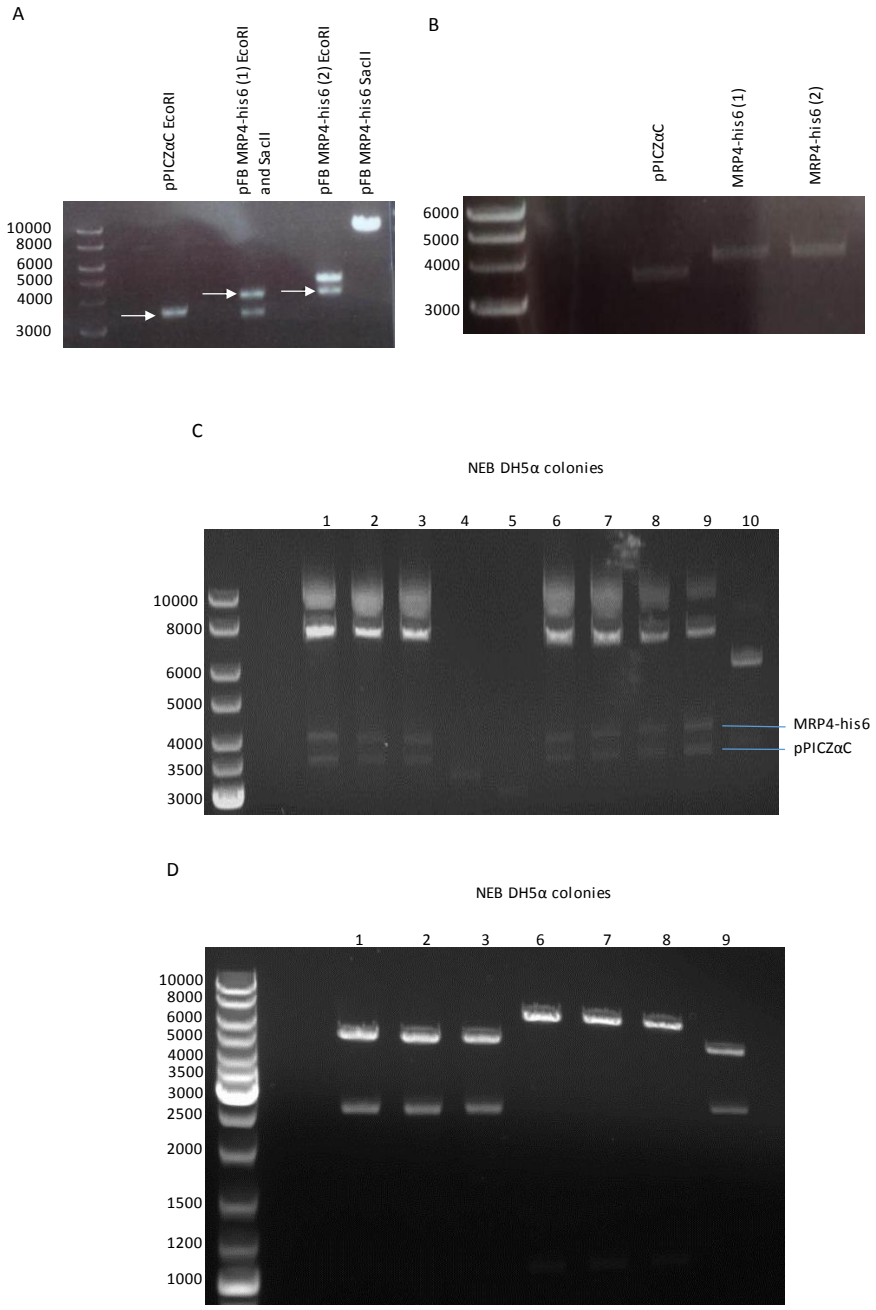

Figure 4.6.1: Molecular biology of cloning MRP4-his$_6$ from pFastBac MRP4-his$_6$ into pPICZαC. *Agarose gel A shows the digestion of pPICZαC with EcoRI, digestion of pFastBac MRP4-his$_6$ (pFB MRP4-his$_6$) with EcoRI and SacII (pFB MRP4-his$_6$ (1) EcoRI and SacII) and single digests with each of those restriction enzymes, pFB MRP4-his EcoRI (2) and pFB MRP4-his SacII. The white arrows indicate the bands extracted after which they were ran on agarose gel B for confirmation of successful gel extraction prior to ligation (stage 1 figure 4.6.1). Agarose gel C shows purified and digested pPICZαC MRP4-his$_6$ plasmid DNA with EcoRI of 10 NEB DH5α E.coli colonies after ligation (stage 2 figure 4.6). Agarose gel D shows the diagnostic digest of 7 DH5α colonies with SacI.*

The first step in the production of pPICZαC MRP4-his$_6$ was the digestion of pPICZαC and pFastBac MRP4-his$_6$. pPICZαC was single digested with EcoRI, pFastBac MRP4-his$_6$ (pFB MRP4-his$_6$) single digested with EcoRI or SacII and double digested with EcoRI and SacII. pPICZαC only has one EcoRI restriction site which would result in the linearization of the plasmid. The linearized pPICZαC plasmid ran at the correct molecular (3500bp) as shown in figure 4.6.1 A and demonstrated the digestion was successful. Digestion of pFastBac MRP4-his$_6$ with EcoRI resulted in two fragments. The higher band at 4700 bp corresponds to pFastBac plasmid and the lower band at 4101bp is the MRP4-his$_6$ insert (Figure 4.6.1 A). The pFastBac MRP4-his$_6$ was double digested with EcoRI and SacII resulting in three fragments. The higher band was the MRP4-his$_6$ insert again resulting from the digestion with EcoRI. The other fragment was the pFastBac plasmid, which had a SacII restriction site in it creating a larger fragment at 3414bp and a smaller fragment at 1286bp. The one SacII restriction site within the pFastBac MRP4-his$_6$ would result in the linearization of the plasmid and ran at the correct molecular weight of 8801bp showing digestion was successful. The three bands in figure 4.6.1 A indicated with black dots were then extracted and purified.

The agarose gel in figure 4.6.2 B shows that the bands extracted from the previous gel are the correct products as pPICZαC is around 3500 bp and the two MRP4-his$_6$ products are around 4000 bp. MRP4-his$_6$ (1) was the band extracted from pFB MRP4-his$_6$ EcoRI and SacII and MRP4-his$_6$ (2) was extracted from pFB MRP4-his$_6$ EcoRI from figure 4.6.2 A.

The two MRP4-his$_6$ products were then ligated into pPICZαC overnight at 16^{o}C. The ligations were transformed into competent DH5α cells (DH5α) produced by the Kerr lab in Nottingham and commercially bought highly competent DH5α cells from New England Biolabs (NEB DH5α). The table below shows the number of colonies of each agar plate form two different dilutions.

.

	DH5α		NEB DH5α	
Dilution	1/10	9/10	1/10	9/10
pPICZαC cut	0	1	0	2
pPICZαC MRP4-his$_6$ (1)	1	0	2	17
pPICZαC MRP4-his$_6$ (2)	0	0	4	15

Table 4.6.1 Number of colonies counted on each agar plate after transformation with pPICZαC MRP4-his$_6$. *Two different strains of chemically competent DH5α E.coli cells were used, laboratory made (DH5α) and commercially bought from New England Biolabs (NEB DH5α). Two different dilutions (1/10 and 9/10) of the total volume (1mL) of transformed E.coli cells were plated and incubated overnight at 37^{o}C*

The DH5α and NEB DH5α negative controls had no colonies showing that neither of the DH5α *E.coli* strains were Zeocin resistant. The DH5α and NEB DH5α positive controls, transformed with pPICZαC, had a lawn of colonies showing both these *E.coli* strains were competent and able to be transformed with the pPICZαC plasmid which contained the Zeocin resistant selective gene. The results from table 4.6.1 show the DH5α cells were poorly transformed with the pPICZαC MRP4-his$_6$ plasmid as only 1 colony was formed from the four different combinations of dilutions and plasmids. The NEB DH5α cells colonies produced many more colonies showing they are far more competent and allowed for screening of many colonies increasing the probability of finding a colony with MRP4 inserted in the correct orientation in the pPICZαC plasmid.

Ten colonies from the NEB DH5α pPICZαC MRP4-his$_6$ (1) 9/10 were selected, overnight cultures produced and the plasmid DNA isolated. The agarose gel in figure 4.6.1 C shows the digestion with EcoRI. As EcoRI was used to cut out the MRP4-his$_6$ gene from the pFastBac MRP4-his$_6$ plasmid and used to digest pPICZαC, the digestion of pPICZαC MRP4-his$_6$ should result in two bands. One band corresponding to pPICZαC (3500bp) and one for the MRP4-his$_6$ gene (4101bp). This gel shows that 7 of the 10 NEB DH5α colonies contained pPICZαC MRP4-his$_6$ as when digested with EcoRI two bands are present, pPICZαC is at 3500bp and MRP4-his$_6$ is at around 4000bp.

These 7 colonies where then diagnostically digested with SacI. As EcoRI cuts out the MRP4-his_6 insert and is used to digest the pPICZαC plasmid there is 50/50 possibility for the insert (MRP4-his_6) to be inserted the wrong way around. The diagnostic digest was used to determine if the MRP4-his_6 insert was ligated into pPICZαC the correct way around. If the insert was the correct way around a large band at 6667bp and a smaller band at 1031bp would appear. If it was the incorrect way around two bands of similar sizes would appear. As shown in figure 4.6.2 D three colonies (6, 7 and 8) had bands at 6667bp and 1031bp indicating the MRP4-his_6 insert was in the correct orientation whereas the other four colonies had the incorrect orientation of the MRP4-his_6 insert. This is in line with the 50/50 possibility for the insert to be ligated in the wrong way around. The three colonies with the correct orientation of the MRP4-his insert in the pPICZαC plasmid were amplified and purified resulting in 332ng/µL, 296ng/µL and 313ng/µL for colonies 6, 7 and 8 respectively.

4.6.2 Expression of MRP4-his$_6$ in Pichia pastoris

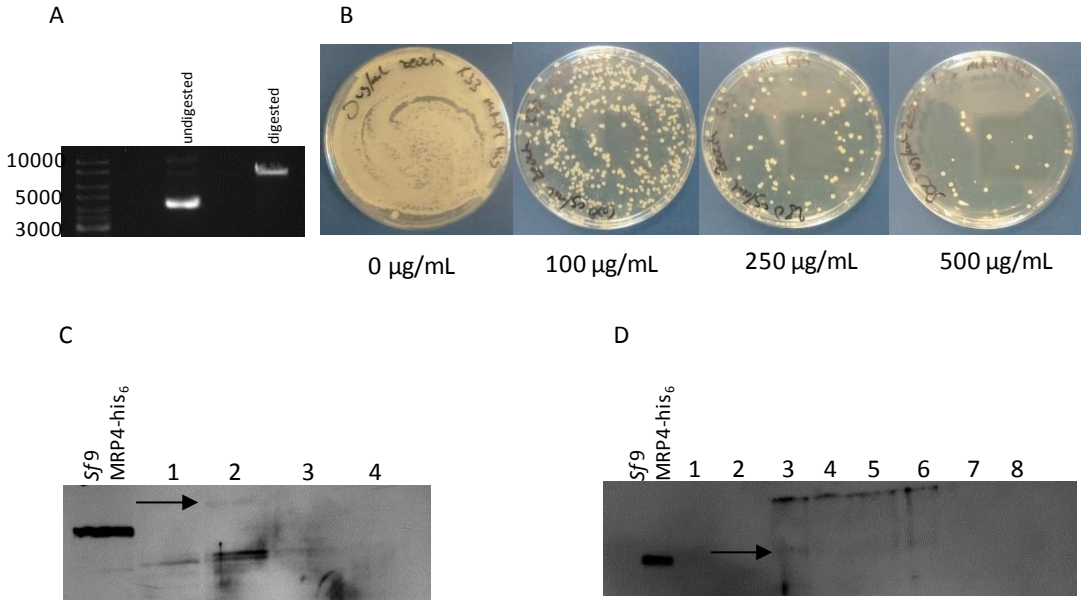

Figure 4.6.2: Transformation and trial expression of MRP4-his$_6$ in P.pastoris X33. *Agarose gel A shows the digestion of pPICZαC MRP4-his$_6$ with PmeI (digested) against an undigested control (undigested). YPD agar plates in B show colonies of transformed P.pastoris X33 with PmeI digested pPICZαC MRP4-his$_6$ (digested 4.6.3 A) on increasing concentrations of Zeocin (0, 100, 250 and 500 µg/mL). Western blot C shows the screening of four colonies from the 500µg/mL Zeocin YPD agar plate and western blot D the screening of eight colonies from the 250µg/mL Zeocin YPD agar plate. The arrows on each western blot indicate the expression of MRP4-his$_6$ with MRP4-his$_6$ expressed in Sf 9 cells (Sf 9 MRP4-his$_6$) used as a positive control. Anti his primary antibody and anti-mouse HRP secondary antibody were used to detect MRP4 in both western blots C and D.*

After confirming the MRP4-his insert was ligated into the pPICZαC in the correct orientation, a maxi prep was carried out to increase the amount of plasmid DNA as 5-10 µg is needed for transformation. 8.64 µg of pPICZαCMRP4-his$_6$ was produced and then digested with PmeI. Figure 4.6.2 A confirms that digest was successful as the linearized plasmid ran at the correct molecular weight of 7698bp.

Heat inactivated pPICZαCMRP4-his$_6$ was purified resulting in 2.7 ug of linearized pPICZαMRP4-his$_6$. This was transformed into X-33 strain of *P.pastoris* using electroporation and 100 µL plated on YPDS plates with increasing concentrations of Zeocin (0, 100, 250 and 500 µg/mL). After a 72 hours incubation period at 30°C colonies formed. Figure 4.6.2 B shows that with increasing concentrations of Zeocin less colonies were formed. The 0 µg/mL Zeocin plate contained a lawn of white X-33 but also lots of small pink colonies showing there was some contamination, but on the 100-500 µg/mL Zeocin mostly large white colonies were formed with some smaller white satellite colonies but no small pink colonies. This indicates there are no contaminants on any of the plates containing Zeocin. The satellite colonies were formed because the Zeocin surrounding the larger white colonies would have decreased allowing the satellite colonies to form and these colonies would not contain the plasmid so were not chosen for screening.

Four colonies from the plate containing 500µg/mL Zeocin and 8 colonies from the 250µg/mL were cultured in a 20mL shaker flask and screened for expression. The Western Blots in figure 4.6.2 C and D shows the results of membrane fractions from these colonies. Western blot C shows the trial expression of four colonies from the 500µg/mL Zeocin with no band present at the same molecular weight as the positive control of *Sf* 9 MRP4-his$_6$ but there is a band at an increased molecular weight, indicated by the arrow on colony 2. Western blot D shows the trial expression of eight different colonies taken from the 250µg/mL Zeocin plate. There are faint bands that appear at a slightly higher molecular weight as the *Sf* 9 MRP4-his$_6$ positive control in colonies 3, 4, 5 and 6.

The protein concentration from the trial expression was not quantified and the faint bands could be due to lower amounts of total protein loaded onto the Western blot. Alternatively since an anti his antibody was used for these Western blots this could explain the faint bands as the histidine tag might not be as accessible when MRP4-his is expressed in *P.pastoris*.

The positive MRP4-his_6 control expressed in *Sf* 9 cells will not be fully glycosylated due to the nature of expression in *Sf* 9 cells (Kost, Condreay et al. 2005). *P.pastoris* are able to glycosylate membrane proteins but only through the addition of core $(Man)_8$-$(GlcNAc)_2$ groups (Byme 2015). Although *P.pastoris* can hypermannosylate membrane proteins, mammalian cell glycosylation will produce a much more diverse glycan structure (Ahmad, Hirz et al. 2014). So MRP4-his_6 expressed in *P.pastoris* would undergo core glycosylation increasing the molecular weight but not to the same level seen in mammalian cells. There are seven glycosylation sites on MRP4 but it is unclear the level of glycosylation that occurs during expression in *P.pastoris*. However, if there were higher levels of glycosylation during expression in *P.pastoris* this would result in a MRP4 band at a higher molecular weight.

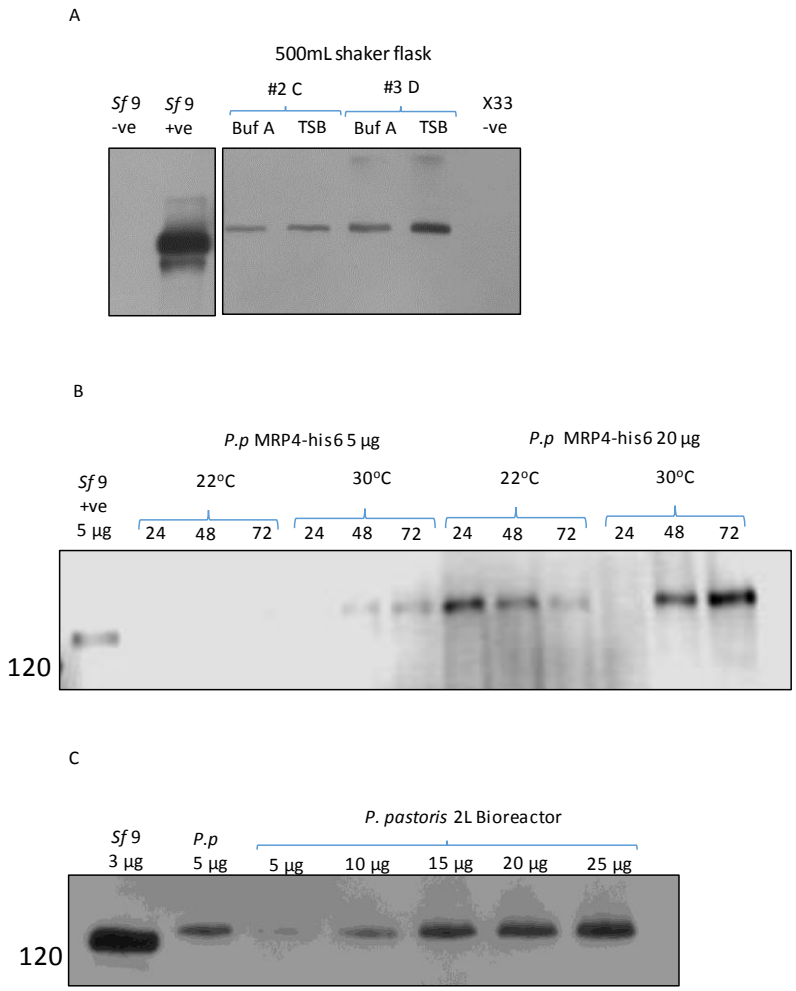

Figure 4.6.3: Large scale expression of MRP4-his$_6$ in P. pastoris. *Western blot A shows a comparison of expression of MRP4 in Sf 9 insect cell, and P.pastoris X33 yeast cells (anti MRP4 antibody). 5µg of total membrane protein previously expressed MRP4-his$_6$ in Sf 9 insect cells was used as a positive control (Sf 9 +ve) along with a Sf 9 negative control (Sf 9 –ve). 15µg of total membrane protein of the 500mL shaker flasks scale up of MRP4-his$_6$ expressed in P.pastoris X33 from either colony number 2 from 4.6.3 C (#2 C) or colony number 3 from 4.6.3 D (#3 D) was loaded on western blot A. Membranes were either resuspended in Buffer A (Buf A) or a Tris sucrose buffer (TSB). A P.pastoris X33 strain expressing no MRP4-his$_6$ (X33 –ve) was used a negative control. Western blot B shows the expression MRP4-his$_6$ in 500mL shaker flasks after 24, 48 and 72 hours at 22 and 30°C. Either 5 or 15µg of total membrane protein of P.pastoris MRP4-his$_6$ (P.p MRP4-his$_6$) was loaded onto the gel. 5µg of Sf 9 total membrane protein from previously expressed MRP4-his$_6$ was used a positive control (Sf 9 +ve 5µg).Anti his antibody. Western blot C shows the expression level of MRP4-his$_6$ from Sf 9 cells and P.pastoris yeast cells. 3µg of total membrane protein form Sf 9 MRP4-his$_6$ (Sf 9 3µg) was used a positive control. 5µg of total membrane protein form the 500mL shaker flask of P.pastoris MRP4-his$_6$ (P.p 5µg) was loaded and compared to 5, 10, 15 or 20µg from the 2 L bioreactors expression of P.pastoris MRP4-his$_6$ from colony #2 (4.6.3 C). Anti MRP4 antibody was used.*

Colony #2 from the 500µg/mL Zeocin plate and colony # 3 from the 250µg/mL Zeocin plate (which had the most intense band) were taken for a scaled up expression in a 500mL shaker flask at 30°C for 48 hours. Membranes were produced from these two colonies and either resuspended in Buffer A or TSB. Buffer A was used for resuspension of *P.pastoris* membranes whereas TSB was used for the resuspension of *Sf* 9 cell membranes. Western blot A shows the expression levels of these two colonies in these two buffers and *Sf* 9 cell expression.

5µg of total membrane protein for both the *Sf* 9 negative and positive MRP4-his control was loaded. 15µg of total membrane protein for both the *P.pastoris* in Buffer A and TSB was loaded as the expression level was thought to be lower than that of the *Sf* 9 cell expression. An anti MRP4 antibody was used for this Western blot to explore the possibility the anti-his antibody could not bind very well to the *P.pastoris* samples.

The western blot clearly shows that the expression level of both the *P.pastoris* colonies, regardless of which buffer the membranes were resuspened in, had far lower expression levels compared to *Sf* 9 expression levels. Colony 2 showed a 56 (Buffer A) and 40 (TSB) times reduction in expression level compared to *Sf* 9 cells. Colony 3 showed a slight increase compared to colony 2 but still a 25 (Buffer A) and 15 (TSB) times reduction compared to *Sf* 9 cells expression. Again the bands that appear in *P.pastoris* samples were at a slightly higher molecular weight indicating that the MRP4-his_6 expressed in *Pichia* could have undergone more extensive glycosylation than the *Sf* 9 cells. MRP4 is not natively expressed in *P.pastoris* but an X33 *P. pastoris* control was also loaded confirming there is no native expression of MRP4 in this *P.pastoris* strain.

A second larger scale expression was tested over a 72 hour period at 22°C and 30°C using shaker flasks to examine the effect of temperature and time. Western blot 4.6.3 B shows that expression levels were improved from the previous levels and now only slightly less compared to *Sf* 9 cells the expression levels. At 22°C the highest level of expression was after 24 hours and then decreased after 48 and further decreased after 72 hours. The highest level of expression at 22°C after 24 hours was only 1.13 times lower than *Sf* 9 cell expression. The opposite was true for

expression at 30°C with increasing expression level over the 72 hour period. The highest expression level at 30°C in *P.pastoris* was after 72 hours and was 1.17 times lower than *Sf* 9 cell expression.

Large-scale expression was carried out in 2 litre bioreactors. Bioreactors are able to produce large volumes of increased cell density and expression conditions can be kept under tighter control. Western blot 4.6.3 C shows the expression level of colony #2 (Figure 4.6.2 C) expression in 2L bio reactors compared to the expression levels in the 500mL shaker flask and a *Sf* 9 positive control. Again, it is clear the expression levels in the bio reactor are far lower than in *Sf* 9 cells and lower than the same colony expressed in 500mL shaker flasks. Compared with the *Sf* 9 cell expression the 2L bioreactor expression is 13 times lower. Compared to the 500mL shaker flasks the 2L bioreactor expression is around 3 times lower.

MRP4-his_6 was successfully expressed in *P.pastoris* yeast cells but at a level less than achieved with *Sf* 9 cell expression. At first the expression level in shaker flasks and in 2L bioreactors (Figure 4.6.3 C) was far lower than *Sf* 9 cell expression and it was not until much later on in this study that the expression levels were improved. By this time, MRP4 has successful been expressed in large volumes in *Sf* 9 cells and shown to be functional. The MRP4 expressed in *Sf* 9 cells had also already been used in solubilisation and purification trials. For this reason, expression of MRP4-his_6 was not continued in P.pastoris. However, as the expression levels in *P. pastoris* have recently been improved, future investigation maybe beneficial given the higher quantity of *P.pastoris* cells produced and lower cost.

4.7 MRP4 expression in HEK cells

Recombinant MRP4 was also expressed in a human cell line human embryonic kidney (HEK) cells. HEK cell expression has a few advantages over *Sf* 9 and *P. pastoris* expression systems. Firstly, MRP4 is naturally expressed in HEK cells meaning this system has all the capabilities of naturally expressing MRP4. The MRP4 expressed in HEK cells will be fully glycosylated compared to *Sf* 9 cells (Kost, Condreay et al. 2005). Other expression systems such as *Sf* 9 insect cells and *P. pastoris* yeast cells do not naturally express MRP4 so introducing a foreign protein in their systems may have detrimental effects. The lipid environment is more native in HEK cells compared to other expression systems, potentially allowing for a more native conformation. HEK cells expression can occur via transient and stable transfections. The disadvantage of transient expression is that there can be a fair amount of batch-to-batch variability as the quality of plasmid DNA can change and the transfection efficiency can vary. In addition, many transfection reagents are expensive and toxic to cells and finding the optimal expression conditions can be time consuming. Creating stable cells lines can remove the batch to batch variability but in doing so many reduce the expression yield. Stable cells line are very time consuming to make but once produced all that is needed is growth of the cell line to express the proteins. The growth of HEK cells is mostly in monolayers making scale up a rather laborious task where as other expression systems can grow to higher cell densities in much larger volumes. New methods that allow for HEK cell suspension cultures have been developed improving the volumes in which HEK cells can be grown. If the expression levels are much higher than the *Sf 9* and *P. pastoris,* then producing even small volumes of HEK cells may be beneficial. This section shows the results from the production of a pcDNA3.1Zeo+ MRP4-his_6 plasmid and the transient trial expressions.

4.7.1 Production of pcDNA 3.1Zeo+ MRP4-his$_6$

To express MRP4-his$_6$ in HEK 293 cells the MRP4-his$_6$ gene had to be subcloned into the pcDNA3.1 Zeo+ (pcDNA 3.1) plasmid. This was done in a similar manner as previously described as MRP4 was subcloned into the yeast expression vector. MRP4-his$_6$ was digested out of the pFastBac MRP4-his$_6$ plasmid using EcoRI and then ligated into the pcDNA 3.1 plasmid to create a pcDNA3.1Zeo+ MRP4-his$_6$ (pcDNA 3.1 MRP4-his$_6$) plasmid. The pcDNA 3.1 plasmid used has a Zeocin resistant gene incorporated to allow for stable HEK cell expression if needed.

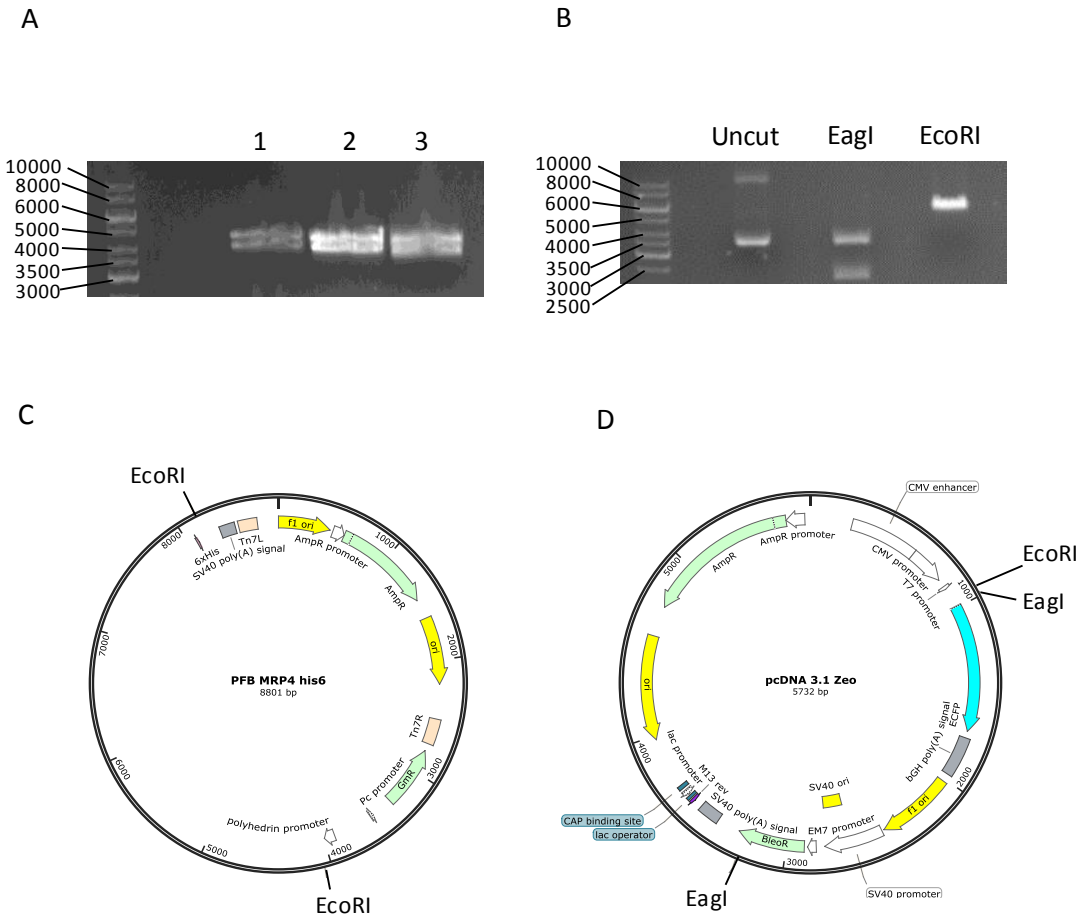

Figure 4.7.1: Digestion of pFastBac MRP4-his$_6$ and pcDNA 3.1. *Agarose gel A shows the digestion of pFastBac MRP4-his$_6$ (pFB MRP4-his$_6$) of three separate DNA isolations from DH5α E.coli cells (1, 2, 3) with EcoRI. Agarose gel B shows the digestion of pcDNA 3.1 plasmid with EagI and EcoRI along with an undigested (uncut) control. C) shows the plasmid map of pFastBac MRP4-his$_6$ with EcoRI restriction sites and D) shows the pcDNA 3.1 plasmid map with EagI and EcoRI restriction sites. Both plasmid maps were created by SnapGene.*

Figure 4.7.1 A shows the digestion of pFastBac MRP4-his$_6$ with EcoRI. *In silico* digestion of pFastBac MRP4-his$_6$ showed the plasmid should be digested into two bands as there are two EcoRI restriction sites (Figure 4.7.1 C), one at 4700bp corresponding to the pFastBac plasmid and a lower band at 4101bp corresponding to the MRP4-his6 insert. Three different digestions were set up to make sure the maximum amount of high quality MRP4-his$_6$ could be extracted. All three digestions were successful as two bands at the correct molecular weights appeared. After digestion and gel extraction #3 (Figure 4.7.1 A) had high quality DNA and contained 9ng.

Figure 4.7.1 B shows the digestion of pcDNA 3.1 with EagI or EcoRI. pcDNA 3.1 has two restriction sites for EagI and *in silico* digestion produces two bands, one at 3479bp and one at 2253bp (Figure 4.7.1 D). Figure 4.7.1 B demonstrations that digestion with EagI was successful as two bands appeared which coincided with the *in silico* digestion. EagI was used to make sure this stock solution did not contain any additional DNA ligated in, as previous digestion showed pcDNA 3.1 contained an insert (data not shown). EcoRI was used as this was the same restriction enzyme used to digest the pFastBac MRP4-his$_6$ plasmid and extract the MRP4-his$_6$ insert. The pcDNA 3.1 plasmid has one restriction site for EcoRI and figure 4.7.1 B shows the digestion was successful pcDNA 3.1 ran at the correct molecular weight of 5732 bp and after gel extraction pcDNA 3.1 was at 7.6 ng/µL

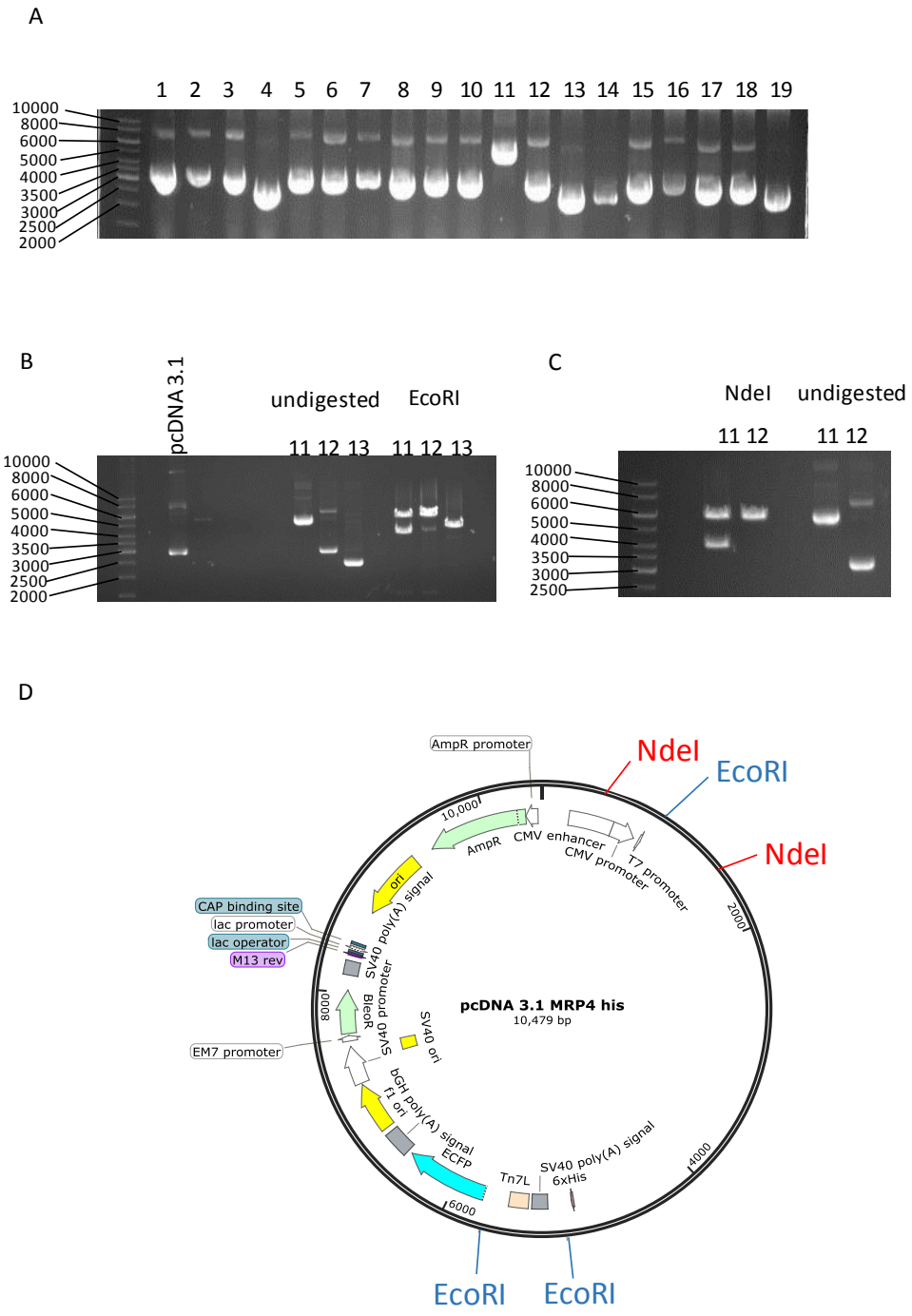

Figure 4.7.2: Colony screen 1 of DH5α E.coli transformed with pcDNA 3.1 MRP4-his$_6$ and restriction enzyme digest. *Agarose gel A shows the colony screen of 19 DH5α E.coli colonies transformed with pcDNA 3.1 MRP4-his$_6$. Agarose gel B is the digestion of three colonies from 4.7.2 A, colonies 11, 12 and 13, that were either undigested or digested with EcoRI. Undigested pcDNA 3.1 (pcDNA 3.1) and pcDNA 3.1 digested with EcoRI (EcoRI) were used as a control. Agarose gel C is the diagnostic digest with NdeI of colonies 11 and 12 along with undigested controls. Plasmid map D shows where the restriction sites of EcoRI and NdeI are in pcDNA 3.1 MRP4-his$_6$.*

Digested pcDNA 3.1 vector and MRP4-his_6 insert were ligated together using a vector : insert ratio of 1:3 either for 1 hour or overnight at room temperature. After transformation into DH5α cells and overnight incubation only colonies were formed using overnight ligation. Figure 4.7.2 A shows the rapid colony screen of 19 colonies from the overnight ligation. This method was used as it is a rapid way of screening a large quantity of colonies without need for purification. The downside of this method is that supercoiling of the plasmid DNA can occur and native DNA contaminants will be present. Because of this the pcDNA 3.1 MRP4-his_6 plasmid (10,479bp) may not be visible. For this reason differences in the banding pattern were investigated. The majority of the colonies showed the same banding pattern but #11 and #13 showed higher and lower bands respectively. Colony #12 showed the same banding pattern as all of the other colonies so colony 11, 12 and 13 were taken for purification and digestion.

Figure 4.7.2 B shows the purified plasmids from colonies 11, 12 and 13 as well as empty pcDNA3.1 with and without EcoRI digestion. This shows the EcoRI digested pcDNA 3.1 plasmid runs at the expected molecular weight (5732bp). The undigested plasmids from colonies 11, 12 and 13 show the same banding pattern as in the colony screen.

Digesting the plasmid from colonies 11, 12 and 13 with EcoRI should result in three bands, one at 5732bp corresponding to pcDNA 3.1, one at 4101bp corresponding to the MRP4-his_6 insert and a small fragment of 646bp according to the *in silico* digestion with Snapgene. The results in figure 4.7.2 B show that both colonies 11 and 12 had a higher band that is in line with pcDNA 3.1 at 5732bp and one just below at around 4000bp which could correspond to MRP4-his_6 (4101bp). The third and lowest band is at around 1500bp which is much higher than the in silico digest suggests. Colony 13 shows two bands, one around 5000bp and the other very faint band at around 4000bp. Although the lower band is at a similar molecular weight to that expected for the MRP4-his_6 insert (4101bp), the higher band is below the correct molecular weight of the pcDNA 3.1 plasmid. As this higher band in colony 13 didn't correspond to that expected for pcDNA 3.1 and the two larger molecular weight bands in colonies 11 and 12 appear to correspond to pcDNA 3.1 and MRP4-his_6,

but with an unknown band at around 1500bp, colonies 11 and 12 were taken for analysis via diagnostic digest.

In silico digestion of pcDNA 3.1 MRP4-his_6 with NdeI showed that if the MRP4-his_6 insert was in the correct orientation there would be two bands, a higher band at 9,466bp and a lower band at 1013bp. If MRP4-his_6 was in the incorrect orientation there would be two bands at similar molecular weights. Figure 4.7.2 C shows the digested, with NdeI, and undigested plasmids purified from colonies 11 and 12. The undigested plasmids have the same banding pattern as in figure 4.7.2 B. The digested plasmid from colony 11 shows the MRP4-his_6 insert was in the incorrect orientation as there are bands at around 6000bp and 4000bp, not the 9466bp and 1031bp as suggested by the in silico digest. Colony 12 showed only one band at around 6000bp that could suggest this band corresponds to the pcDNA 3.1 plasmid with no MRP4-his6 insert, as there is only one NdeI restriction site in the pcDNA 3.1 plasmid and NdeI would just linearize the plasmid. This would have been a result of the pcDNA 3.1 plasmid religating back to itself. Because the banding pattern of colony 12 in the first colony screen was the same as the majority of the other colonies in that screen it indicated the ligation was not successful and most of the pcDNA 3.1 had religated back to itself.

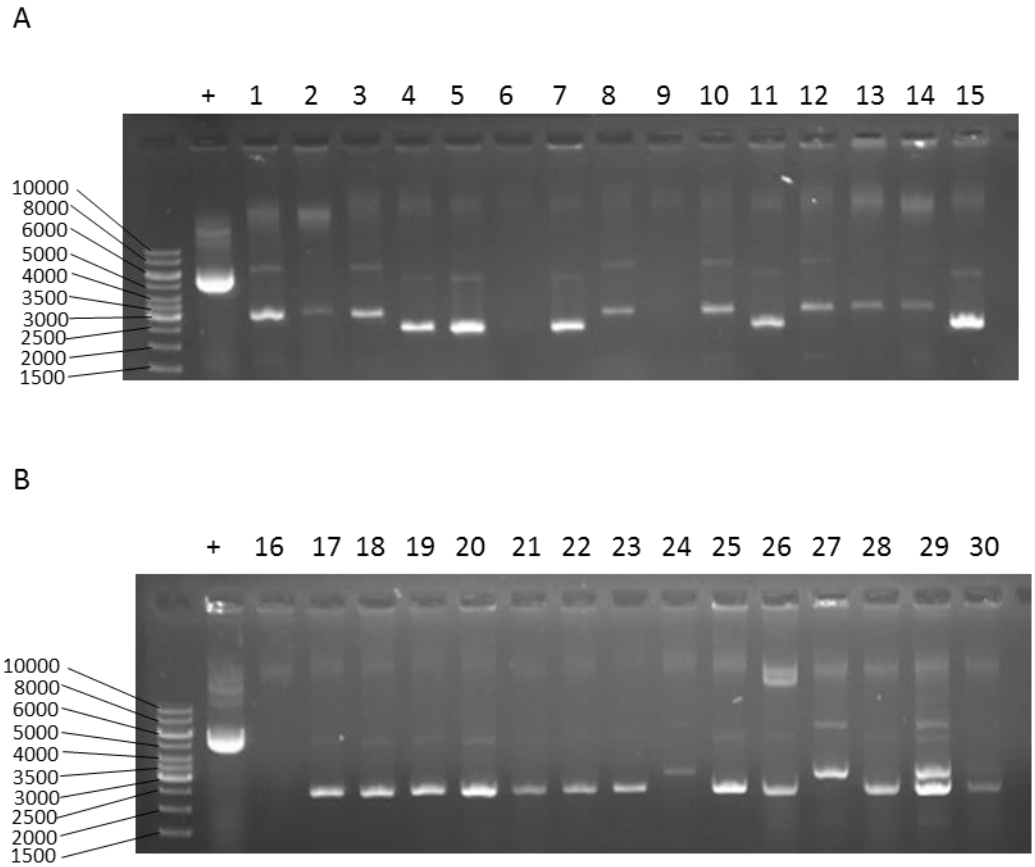

Figure 4.7.3: Second colony screen of 30 DH5α E.coli colonies from the first transformation of pcDNA 3.1 MRP4-his6. *Agarose gels A and B show the DNA from 30 DH5α E.coli colonies from the first transformation (4.7.2). The positive control (+) was colony 11 from 4.7.2 A which showed the MRP4-his6 insert was there, in the incorrect orientation, but should run at the correct molecular weight of pcDNA 3.1 MRP4-his6.*

Another colony screen was performed on an additional 30 colonies (Figure 4.7.3 A and B). Colony 11 from the previous colony screen was used as a make shift positive control (+) as that colony appeared to have the MRP4-his_6 insert ligated in albeit wrong way around. This second screen showed that none of the colonies had the same banding pattern as the positive control. Most of the colonies showed a similar banding pattern to that of colony 12 (4.7.2 A) indicating the pcDNA 3.1 plasmid religated back to itself. In order to prevent this from happening again dephosphorylation with alkaline phosphatase of the pcDNA 3.1 plasmid was conducted prior to ligation with the MRP4-his insert. Re-ligation is more likely to occur when only one restriction enzyme is used.

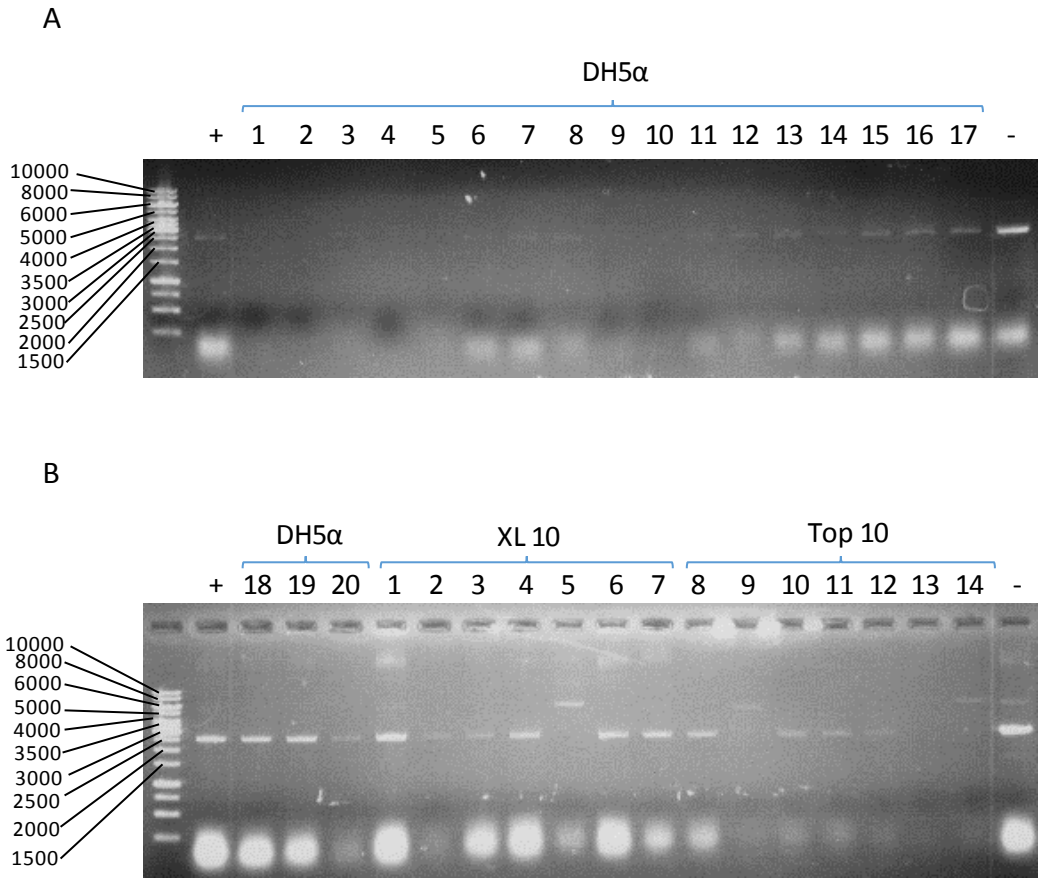

Figure 4.7.4: Third colony screen of E.coli colonies from a second transformation of pcDNA 3.1 MRP4-his6 after dephosphorylation of pcDNA 3.1. *The newly ligated pcDNA 3.1 and MRP4-his6 was transformed into DH5α, XL 10 and Top 10 E.coli. Agarose gel A shows the colony screen from 17 DH5α colonies (1 -17) and agarose gel B shows an additional three more DH5α colonies (18, 19 and 20) along with seven XL 10 colonies (1-7) and seven Top 10 colonies (8 -14). A positive control (+) colony 11 (Figure 4.7.2 A) and a negative control (-) colony 13 (Figure 4.7.2 A) was used.*

After dephosphorylation of the pcDNA 3.1 plasmid the MRP4-his_6 was ligated in at a vector : insert ratio of 1:3 and 1:5. The ligations were incubated for either 1 hour or overnight. These ligations were transformed into DH5α (both 1 hour and overnight ligations), XL10 (overnight ligation) and Top 10 (overnight ligation) chemically competent *E.coli*. The vector : insert ratio, ligation incubation period and type of chemically competent *E.coli* were varied to increase the chance of producing the correct condition for producing pcDNA 3.1 MRP4-his6 in the correct orientation.

The colony screen in figure 4.7.4 shows 20 DH5α, seven XL10 and seven Top 10 colonies. The positive (+) and negative (-) controls were colonies 11 and 13 from the first colony screen. It is unclear why both of these controls had the same banding pattern as each other. As these controls do not match what was expected they were not taken into consideration when deciding which colonies to pick for purification and digestion. The difference in the banding patterns was the deciding factor. All the DH5α colonies have the same banding pattern so only one of these colonies (4.7.4 B 18) was picked. Out of the seven XL10 and seven Top 10 colonies only colony 5 (XL10) (4.7.4 B 5) and colonies 9 and 14 (Top 10) (4.7.4 9 and 14) had a different banding pattern to that of all the other colonies. For this reason colony 5 (XL10) and colonies 9 and 14 (Top 10) where picked for purification and digestion.

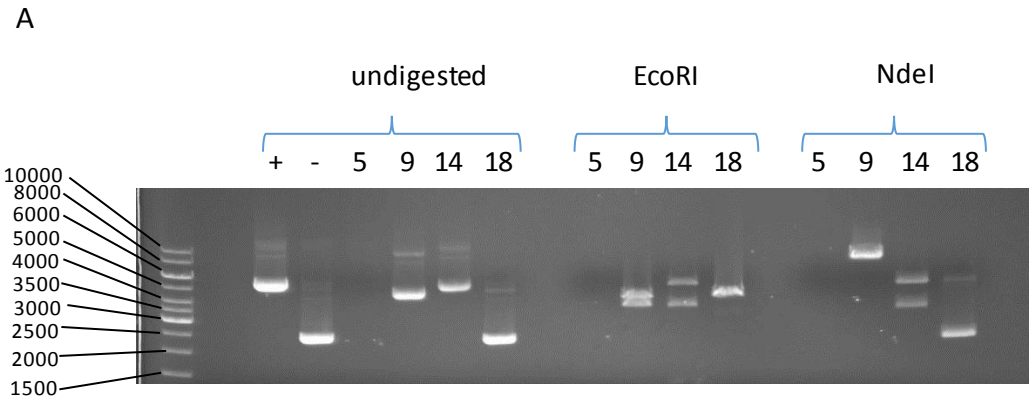

Figure 4.7.5: Restriction enzyme digestion of four colonies from third colony screen (4.7.4). *Agarose gel A shows the undigested and digested purified plasmid DNA with EcoRI and NdeI. Four E.coli colonies from 4.7.4 were chosen, colony 5 (XL10), colony 9 and 14 (Top 10) and colony 18 (DH5α). The positive (+) and negative (-) controls were colony 11 (+) and 13 (-) form 4.7.2 A.*

Figure 4.7.5 A shows the undigested and digested purified plasmid DNA with EcoRI and NdeI of the four colonies picked from the third colony screen along with colonies 11 and 13 (Figure 4.7.2 A) which were used as positive (+) and negative controls (-). This time the controls ran at the same molecular weights and the first colony screen indicating these can be used as controls. Either the

amplification or purification of colony 5 (XL10) did not work as no bands can be seen in either the undigested or digested samples. The undigested plasmid from colony 14 (Top 10) and 18 (DH5α) had the same banding pattern as the positive and negative control respectively. Colony 9 (Top 10) had a different banding pattern with the larger band running at a slightly lower molecular weight compared to the positive control.

All four colonies were digested with EcoRI and then diagnostically digested with NdeI. When colony 14 was digested with EcoRI two bands appeared, a higher band that is in line with pcDNA 3.1 at 5732bp and a lower one corresponding to MRP4-his_6 (4101bp) indicating the presences of MRP4-his_6 within the pcDNA 3.1 plasmid. When colony 14 was diagnostically digested with NdeI it showed that the MRP4-his_6 insert was ligated in the incorrect orientation as two bands of similar molecular weight (6000 and 4000bp) appeared. If it were in the correct orientation two bands at 9466bp and 1031bp should appeared as suggested by the in silico digest. The banding pattern when digested with either EcoRI or NdeI was the same as colony 11 (4.7.2 B)

Digestion of colony 9 (Top 10) with EcoRI shows two bands, the lower band is in line with the lower runs at around 4000bp indicating this could be the MRP4-his_6 insert (4101bp). The upper band is only at around 5000bp which does not correspond to the molecular weight of the pcDNA 3.1 plasmid (5732bp). When colony 9 (Top 10) was diagnostically digested with NdeI it resulted in one visible band around 9000bp. As stated previously if MRP4-his_6 is in the correct orientation digestion with NdeI would result in two bands at 9466bp and 1013bp. The absences of the lower band could be due to the low molecular weight and low quantity of DNA. Taking this into account and also the fact that colony 9 (Top 10) showed a different banding pattern when digest with EcoRI compared to colony 14 (Top 10), which had MRP4-his_6 inserted in the incorrected orientation; this result is consistent with the successful ligation of MRP4-his_6 into the pcDNA 3.1 plasmid in the correct orientation.

Colony 18 (DH5α) had a different banding pattern to colony 9 and 14 (Top 10) when digested with EcoRI or NdeI. If this colony had just the pcDNA 3.1 plasmid it should run at 5732bp when cut with

EcoRI or NdeI. The digestion with EcoRI does not suggest this and the digestion with NdeI does show a faint band around that molecular weight but also a lower one around 2500bp.

These results show that after digestion of pcDNA 3.1 with EcoRI and dephosphorylating ligation of MRP4-his insert was successful and resulted in the production of the pcDNA 3.1 MRP4-his6 plasmid which can be used for overexpression in HEK 293 cells. This plasmid must be sequenced to confirm that MRP4-his6 was ligated in the correct orientation.

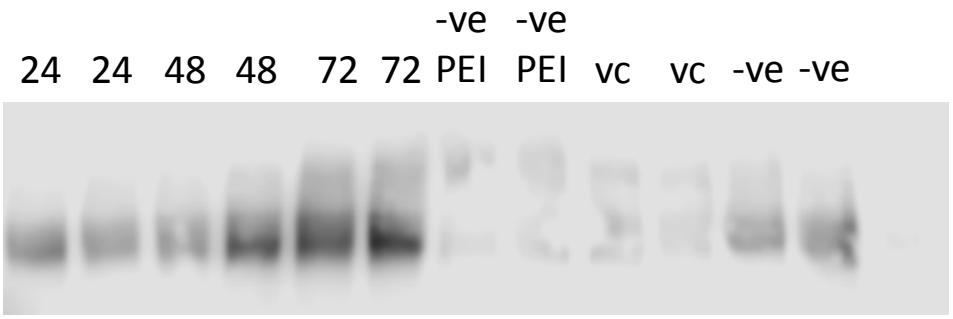

Figure 4.7.6: MRP4 expression in HEK cells. Western blot showing whole cell lysate expression levels after 24, 48 and 72 hours with transfection of pc DNA 3.1 MRP4-his_6 using PEI. Negative controls include: HEK with PEI (-ve PEI), HEK with pc DNA 3.1 only (vc) and HEK only (-ve). An anti MRP4 antibody was used.

Western blot in figure 4.7.6 shows the expression of MRP4 in whole cells lysates of HEK cells. The 24 and 48 hours samples showed on average equal to or less then the HEK only control. It was only 72 hours post transfection that there was an increase in expression. The expression level was 1.7 times higher than the HEK only control. The HEK with PEI and HEK with pc DNA 3.1 only, had reduced expression level of MRP4 compared to the HEK only control. This results shows that compared to native expression levels, HEK only control, MRP4 was overexpressed in HEK cells. The expression level was not compared against *Sf* 9 and *P. pastoris* expression levels.

4.8 Vesicular Transport Assays

“Vesicular transport assays are not an easy thing to do.” Professor Piet Borst (ABC meeting Innsbruck, 2016).

When membrane proteins such as MRP4 are overexpressed their functionality has to be tested as overexpression can lead to misfolded and non-functional protein that may still be present in the membrane. This is also coupled with the fact that if there are any tags attached to the membrane protein, which could interfere with the function. An assay for testing the functionality of MRP4 which has been overexpressed in *Sf* 9 insect cells was developed. Vesicular transport assays (VTA) are a technique for analysing the transport activity of proteins expressed in crude membrane vesicles. Historically in the literature VTA have utilised radiolabelled substrates and ATP was added to drive the transport of the radioactive substrate across the membrane into the vesicles (Rius, Hummel-Eisenbeiss et al. 2006, El-Sheikh, van den Heuvel et al. 2008). By measuring the amount of substrate transported into the vesicle when ATP is present compared to AMP the specific transport activity can be determined. However, we wished to develop an assay utilising a fluorescent substrate instead of using radioactivity. For our assay we utilise a fluorescent analogue of cAMP: 8- (2- [Fluoresceinyl]aminoethylthio)adenosine- 3', 5'- cyclic monophosphate (fluo-cAMP). cAMP is known to be a substrate for MRP4 (Borst, de Wolf et al. 2007), the fluorescent cAMP analogue has a fluorescein group attached to the adenosine (Figure 4.8 A).

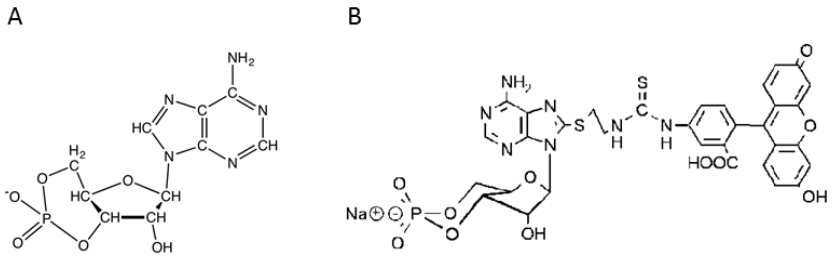

Figure 4.8 A: Structures of cAMP and fluo-cAMP. *A shows the molecular structure of cyclic-adenosine monophosphate (cAMP) (Information). B show the fluoresecent analogue of cAMP 8- (2- [Fluoresceinyl]aminoethylthio)adenosine- 3', 5'- cyclic monophosphate (fluo-cAMP) (Biolog)(Information) used in this study.*

The use of fluo-cAMP for measuring MRP4 function was first described in Reichel et al who showed fluo-cAMP uptake in killifish tubules and *Sf* 9 cell membranes containing MRP4 (Reichel, Masereeuw et al. 2007). The method works on the principle that when MRP4 is functional it is able to hydrolyse ATP driving the transport of the fluo-cAMP across the membrane into the vesicle. Figure 4.8.B shows the steps taken in the vesicular transport assay. Inhibitors of MRP4 can also be used in these assays to examine their efficacy with the theory being that less fluo-cAMP will enter the vesicle when MRP4 is inhibited. Only MRP4 that has the ATP binding domain facing outwards will be able to transport the ligand into the vesicle. ATP will not be able to reach the inward facing MRP4. One problem with this assay is there no way of knowing in which orientation the MRP4 is in the membrane and this can contribute to large variability.

To decrease this variability optimisation of the VTA has to be done. This involves finding the optimal set of parameters and their relative quantities. In this case the amount of total membrane protein (µg), concentration of fluo-cAMP (µM) and the time of incubation (minutes) was varied. When the total amount of protein is increased then so will be the amount of MRP4, thus speeding up the transport of fluo-cAMP. Increasing the concentration of fluo-cAMP will have a similar effect as more of the substrate is available for transport. The incubation time will have an effect on the level of transport as the longer incubation time will allow for a higher transport activity until a saturation level is reached. Too much protein with a concentrated amount of fluo-cAMP

for a long period will mean the saturation level will be reached too quickly. On the other hand too little protein and a low concentration of fluo-cAMP for a short time and the amount of fluo-cAMP transported will not be detectable. Finding the correct quantities of each parameter will allow the functionality of MRP4 expressed in *Sf* 9 cells to be tested. The traditional way of separating out the vesicles from the un-transported fluo-cAMP is through filtration. This method was used along with a centrifugation method to determine which method gave the best results.

Unfortunately the level of MRP4-his_6 expressed in *Sf* 9 insect cells in Reichel et al is unknown compared to the expression level in this study. The amount of total membrane protein present in the vesicles used in the Reichel et al study is also unknown. Finding the correct amount total membrane protein in the *Sf* 9 vesicles to allow for optimal transport was a parameter that had to be explored. Two known parameters from the Reichel et al study were the incubation period (0-30 minutes) and the concentration of fluo-cAMP (0 – 25µM). Increasing any of these parameters should increase the level of transport until it reaches its maximum level.

Only *Sf* MRP4-his_6 (MRP4) was tested for its functionality because at this time the expression levels of MRP4-his_6 in *P.pastoris* had still not been optimised to their highest level and the pcDNA 3.1 MRP4-his_6 plasmid had not yet been produced. The results below show the optimisation of the VTA using MRP4-his_6 and fluorescent cAMP by varying amount of total membrane protein (µg), concentration of substrate (µM) and the time of incubation (minutes) from both the filtration and centrifugation method.

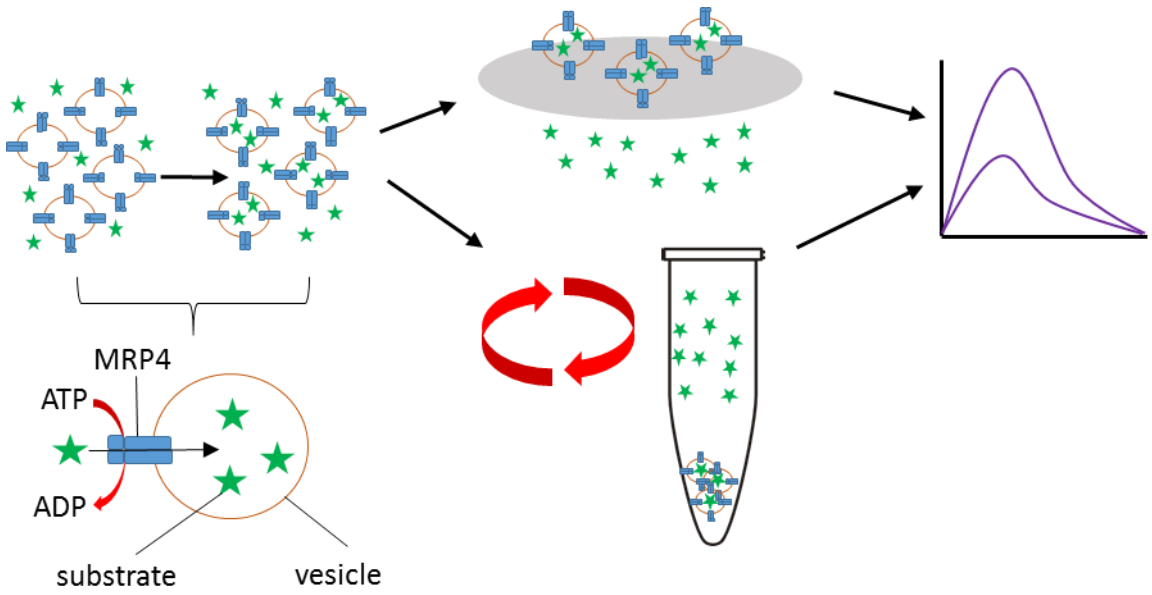

Figure 4.8 B: Diagram of the steps in the vesicular transport assay. *The first step is the incubation of the fluorescent cAMP substrate (green stars) with the membrane vesicles (orange circles) in the presence of AMP or ATP (along with an ATP regenerating system). The fluorescenent cAMP is transported into the membrane vesicles via ATP hydrolysis. The vesicles are then either filtered or centrifuged to remove all excess fluorescent cAMP not transported into the vesicle, step 2. The vesicles are then solubilised and the amount of fluorescent cAMP transported into the vesicles is measure on a fluorescent spectrometer, step 3. The difference between ATP and AMP is calculated giving the specific transport activity.*

4.8.1 VTA filtration method

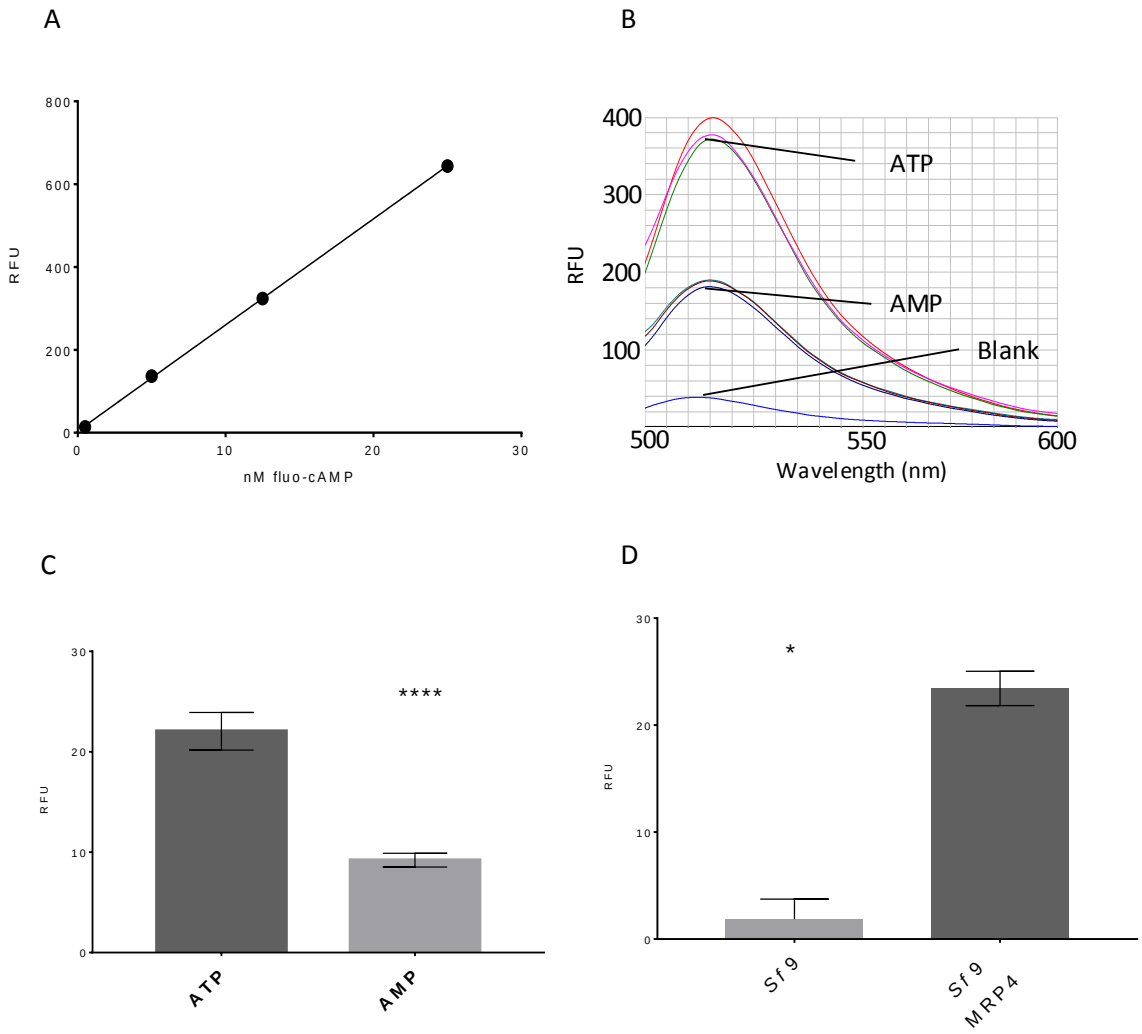

Figure 4.8.1.1: Optimisation of VTA using the filtration method. *Graph A shows the correlation between nM of fluorescent cAMP (fluo-cAMP) and the relative fluorescence units (RFU). B shows a typical read out of the fluorescence spectrum used to generate all graphs. Graph C shows the amount in relative fluorescent units (RFU) transported into membrane vesicles containing MRP4 when ATP or AMP is used during the incubations. 20µg of total membrane protein, with a 10 minute incubation period and 10µM fluo-cAMP. Data are mean ± sem (n=3) Un-paired two-tailed t-test **** P<0.001. Graph D is the evidence showing the specific transport activity between Sf 9 only vesicles (Sf 9) and Sf 9 vesicles containing MRP4 (Sf 9 MRP4). 30µg of total membrane protein was incubated for 20 minutes with 10µM fluo-cAMP Data are mean ± sem (n=2) Un-paired two-tailed t-test * P=0.0128.*

The results in figure 4.8.1.1 shows the optimisation of the vesicular transport assay that was used in this study to examine if the recombinant MRP4-his$_6$ (MRP4) is functional. To ensure the MRP4 is

functional it needs to meet specific requirements. Firstly, MRP4 needs to be able to transport a substrate in an ATP dependent manner as it is an ABC transporter. This means with the addition of ATP in the assays the level of transport must be higher than with AMP. Secondly the transport must be MRP4 specific so negative controls must be used.

Graph A shows there is a direct linear correlation between the concentration of fluo-cAMP and RFU. The fluorescent spectrum in figure 4.8.1.1 B shows a typical read out from the fluorimeter with the higher spectrum curves indicating the ATP transport level and the lower spectrum curves the AMP transport level. The lowest curve shows the fluorescent spectrum of the HEPES/SDS buffer or blank. Figure 4.8.1.1 C shows there is a significant increase in the amount of fluo-cAMP transported with the addition of ATP compared to AMP. This shows that the transport of fluo-cAMP was ATP dependent. It also shows that using 10µM fluo-cAMP and a 10 minute incubation period with 20ug total membrane protein show a good level of transport where there is a clear difference between ATP and AMP. To make sure that this ATP dependent transport of fluo-cAMP was MRP4 specific native *Sf* 9 membranes were used as a control. Figure 4.8.1.1 D shows a comparison of *Sf* 9 MRP4 membrane vesicles against native *Sf* 9 cell membranes vesicles. This shows that the ATP dependent uptake of fluo-cAMP is facilitated by MRP4 as there is a significant increase in the transport level compared to native *Sf* 9 membrane vesicles. The level of transport with *Sf* 9 MRP4 (AMP) or native *Sf* 9 cell membranes shows the amount of fluo-cAMP that can enter the vesicles without it being transported by ATP dependent MRP4. A small amount of fluo-cAMP is to be expected in *Sf* 9 MRP4 AMP or native *Sf* 9 membrane vesicles as they can be leaky by nature. Also due to the hydrophobicity of fluo-cAMP it would be able to either pass through the lipid bilayer, and into the vesicle, or bind to the lipids trapping it in the membrane.

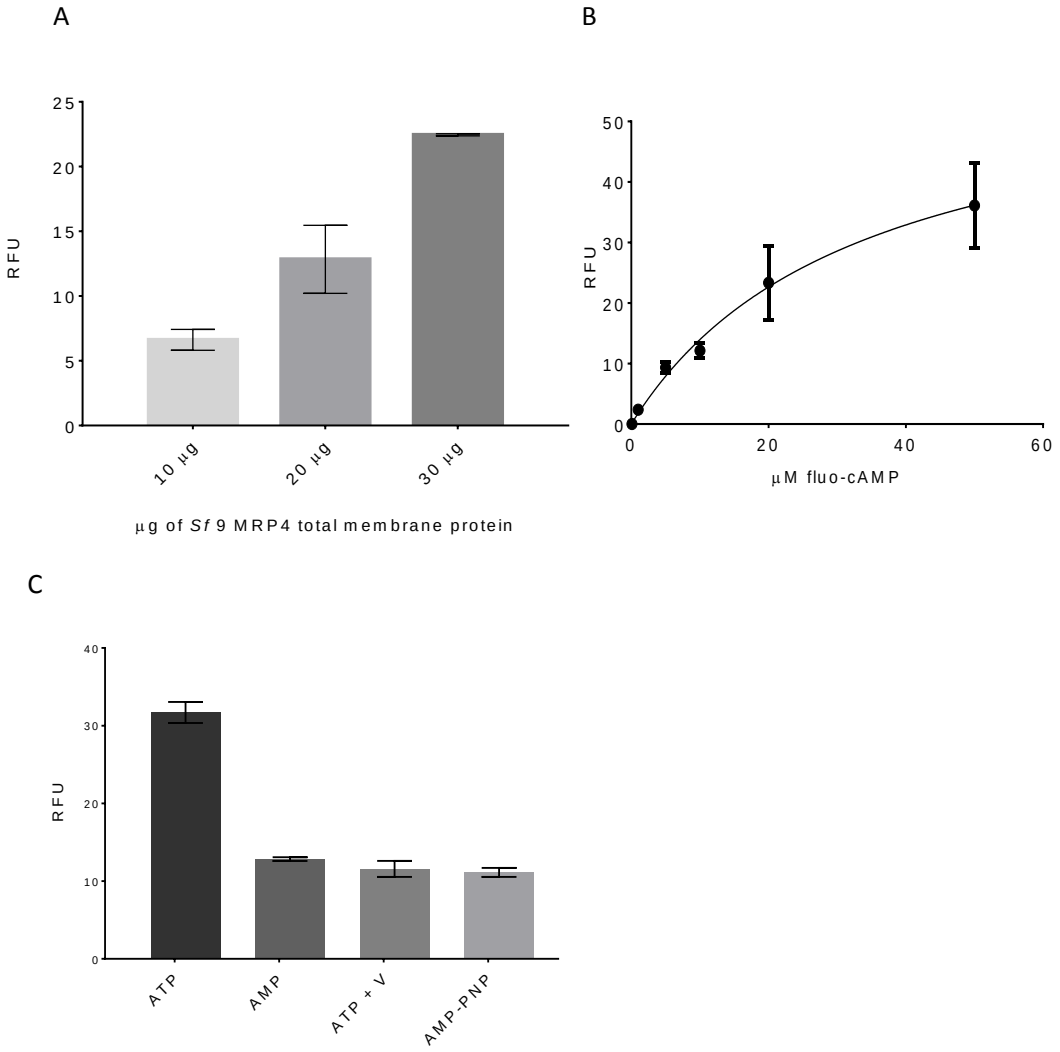

Figure 4.8.1.2: Further optimisation of VTA filtration method and inhibition studies. *Graph A is the specific transport activity (RFU) of 10, 20 and 30µg of total membrane protein (Sf 9 MRP4) with a 10 minute incubation and 10µM fluo-cAMP. Data are mean ± sem (n=3). Graph B shows the amount specific transport activity (RFU) over a concentration of 0 - 50µM fluo-cAMP using 10µg total membrane protein (Sf 9 MRP4) with a 5 minute incubation period. Data are mean ± sem (n=3)* V_{max} *60 RFU,* K_m *33 µM, Michaelis-Menten curve fitted. The inhibition of fluo-cAMP transport is graphed in C with known inhibitors of ABC transports. The amount of fluo-cAMP transported (RFU) is measure for ATP and AMP as controls along with two inhibitors Vanadate (ATP + V) and AMP-PNP. 30µg total membrane protein (Sf 9 MRP4) with an incubation period of 20 minutes and 10µM fluo-cAMP. Data are mean ± sem (n=3)*

To test what the optimal amount of total protein is in *Sf* 9 MRP4 membrane vesicles; 10, 20 and 30µg of total membrane protein was used with an incubation period of 10 minutes using 10µM fluo-cAMP. As the total amount of membrane protein increases so will the amount of MRP4 embedded in these vesicles and this will increase the amount of transport. The results shown in

figure 4.8.3 A are the ATP dependent transport of fluo-cAMP in *Sf* 9 MRP4 membranes and indicates that by increasing the amount total membrane protein the level of transport increases.

The ATP dependent transport of fluo-cAMP should be concentration dependent. As the concentration of fluo-cAMP increases, so should the level of transport as shown in the Reichel et al study. Figure 4.8.1.2 B shows the ATP dependent uptake of fluo-cAMP in *Sf* 9 MRP4 vesicles. This shows there is an increase in the level of transport as the concentration of fluo-cAMP increases from 0 – 50µM fluo-cAMP as the RFU increases with a V_{max} of 60 RFU (6 RFU/µg) and the K_m is 33 µM. There are larger error and degree of variability with higher concentrations of fluo-cAMP possibly because the fluo-cAMP could start binding to the filters.

ATP hydrolysis is needed for the transport of substrates with MRP4 and inhibiting ATP hydrolysis would therefore inhibit transport. AMP decreases the level of fluo-cAMP transport as AMP cannot be hydrolysed by the nucleotide binding domains of MRP4. However, as is evident from figure 4.8.1.2 C there is still a small level of transport with AMP. To make sure that AMP is a true negative control and any fluo-cAMP in the AMP controls comes from passive diffusion into the vesicles or nonspecific binding, two inhibitors of the ATP hydrolysis were used. ATP in combination with vanadate and AMP-PNP, a non-hydrolysable form of ATP, were used as inhibitors of MRP4. Although not specific to MRP4 vanadate traps the nucleotide binding of ABC transporters inhibiting the hydrolysis of ATP and therefore transport of fluo-cAMP. As AMP-PNP cannot be hydrolysed, the transport of fluo-cAMP will again be inhibited. As figure 4.8.1.2 C shows there is an increase of fluo-cAMP transport with ATP compared to AMP as expected. The level of transport for both ATP + Vanadate (ATP + V) and AMP-PNP are at the same level as AMP indicating that AMP was a true negative control. It also confirms that ATP hydrolysis was driving the transport of fluo-cAMP and any transport in *Sf* 9 MRP4 vesicles was ATP dependent.

These results show that the MRP4-his_6 expressed in *Sf* 9 cells is functional as it is able to transport fluo-cAMP in an ATP dependent manner. It also shows that this vesicular transport assay can be used to test the functionality of MRP4 expressed. However some problems with the filtration

method did occur. The filters used were thought to be causing some light scattering problems as small particulates from the filters would end up in the final solubilised sample loaded into the fluorimeter. By centrifuging instead of filtering out excess fluo-cAMP these small particulates from the filters would not be a problem. The filtration method was also very time consuming as each sample had to be filtered individually and all experiments were repeated three times in triplicate for each condition. The centrifuge used could hold up to 24 Eppendorfs allowing for a larger sample set to be pelleted, increasing the efficiency of these experiments.

4.8.2 VTA centrifugation method

Due to the problems with the VTA filtration method a different method was explored. To remove all the fluo-cAMP that was not transported the vesicles were pelleted through centrifugation. The fluo-cAMP that was not transported would be removed by removing the supernatant, the vesicle pellet washed to get rid of any excess fluo-cAMP and then solubilised. One concern with the centrifugation method is the speed which is needed to pellet the vesicles, the vesicle could collapse under the centrifugal force expelling all transported fluo-cAMP. If the centrifugal force was not strong enough some of vesicles might not be pelleted and removed when excess fluo-cAMP is removed increasing the error of these experiment.

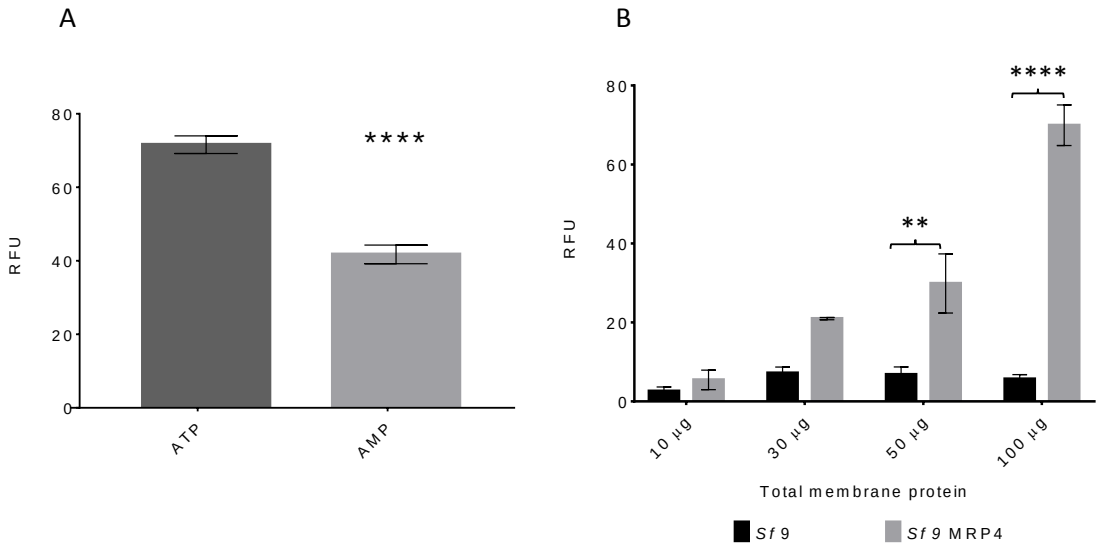

Figure 4.8.2.1: Centrifugation method of VTA showing ATP dependent uptake of fluo-cAMP facilitated by MRP4. *Graph A shows the difference between ATP and AMP fluo-cAMP uptake in Sf 9 MRP4 membrane vesicles. Data are mean ± sem (n=3) Un-paired two-tailed t-test ****P<0.001. B shows the specific transport activity between Sf 9 native (Sf 9) and Sf 9 MRP4 membrane vesicles using 10, 30, 50 and 100µg of total membrane protein. Data are mean ± sem (n=3) Two-way ANOVA** P=0.071 ****P<0.001.*

Graph 4.8.2.1 A shows the difference in transport levels between ATP and AMP with ATP having a significant increases in transport levels compared to AMP. This demonstrates that, not only does this method work, but the transport of fluo-cAMP is ATP dependent matching the results from the

filtration method. Graph 4.8.2.1 B shows the difference in ATP dependent transport between native *Sf* 9 vesicles (*Sf* 9) and *Sf* 9 MRP4 vesicles (*Sf* 9 MRP4) over an increasing amount of total membrane protein. Increasing the total membrane protein of the *Sf* 9 MRP4 vesicles increase the transport level showing a direct correlation. This is to be expected, as once again increasing the total membrane protein amount will increase the amount of MRP4 present therefore increasing the transport level and is consistent with the filtration method. There is only a significant difference between *Sf* 9 and *Sf* 9 MRP4 once there is 50µg or more of total membrane protein. There is no increase in transport levels when the total membrane amount is increased with native *Sf* 9 membranes (Figure 4.8.2.1 B). The level of passive diffusion or non-specific binding must therefore not increase with increasing amount of total membrane protein. This result shows again the ATP dependent uptake of fluo-cAMP was facilitated by MRP4.

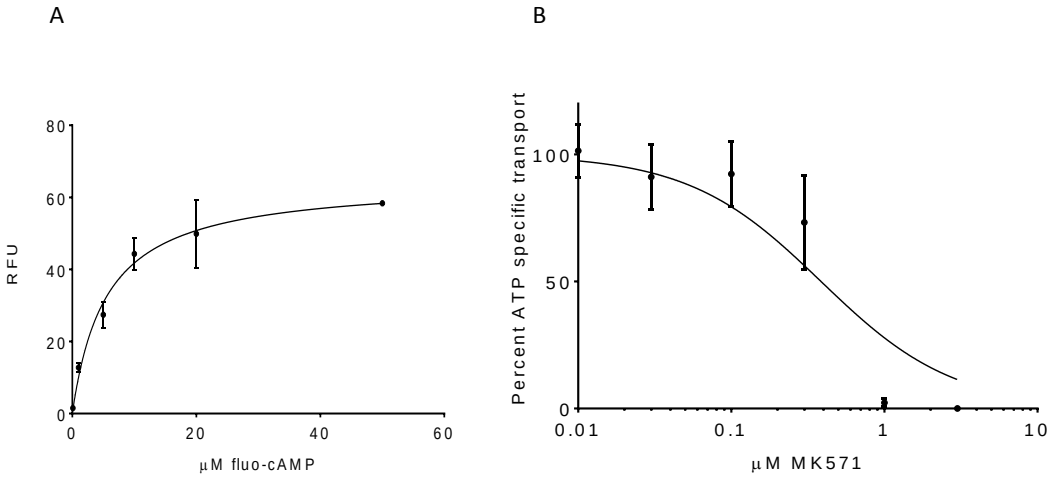

Figure 4.8.2.2: Centrifugation method of VTA showing a concentration curve of fluo-cAMP uptake and inhibition using MK571. *Graph A is the specific transport activity of Sf 9 MRP4 over 0 – 50 µM fluo-cAMP showing a concentration dependent increase. Data are mean ± sem, n=2, V_{max} 64 RFU, K_m 5.5 µM, Michaelis-Menten curve fitted. Graph B is the inhibition of MRP4 in Sf 9 membrane vesicles using a concentration of 0.01 - 5µM MK 571. The percent of ATP specific transport was measured using ATP as 100%. Data are mean ± sem, n=3, IC50=0.39µM MK571, [inhibitor] vs normalised response curve fitted.*

Graph 4.8.2.2 A shows the results from the concentration curve using the centrifugation method. Here 50µg of total membrane protein was used in comparison to the filtration method where only 10µg total membrane protein in *Sf* 9 MRP4 vesicles was used. In order for there to be a visible

pellet after centrifugation a larger amount of total membrane protein had to be used in the centrifugation method. Increasing ATP dependent transport levels were achieved with increasing concentrations of fluo-cAMP as to be expected with a V_{max} of 64 RFU (1.3 RFU/µg) and a K_m of 5.5 µM. The Vmax is very similar to the filtration method but when corrected for protein concentration the value is far lower. The K_m value of fluo-cAMP using the centrifugation method is much closer to previously reported values (Reichel, Masereeuw et al. 2007) and is 6 times lower than the filtration method.

In order to demonstrate the functionality of MRP4 a known inhibitor of MRP4 was used. MK571 was designed as a cysteinyl leukotriene receptor antagonist. The cyteinyl leukotrienes include LTC4 which is a substrate MRP4 and MK571 was found to inhibit MRP4. MK571 inhibits transport of substrates by having effect on the binding site rather than the nucleotide bind site (Wu, Klokouzas et al. 2005). Figure 4.8.2.2 B shows that MK571 inhibits the transport of fluo-cAMP in a concentration dependent manner. This shows that MRP4 is functional as MK571, a known inhibitor of MRP4, is able to inhibit the transport of fluo-cAMP with an IC 50 of 0.39µM. The exact IC50 value is not given for previous MK571 inhibition of fluo-cAMP but the value appear around 1µM (Reichel, Masereeuw et al. 2007).

All the centrifugation method results are comparable to the well-established filtration method confirming this approach is a viable method to measure transport activity. In some ways this method is superior to the filtration method as it is quicker, simpler and uses less consumable material. More samples can be run in parallel in the same time frame and no expensive filters need to be used. The down side to this method is larger amounts of total membrane have to be used to make the pellet of the vesicles visible. This may not be too much of a problem as even large amount of total membrane protein only equates to tens of microliters of membrane preparations, at least in this study, but this depends on the concentration of total membrane protein in the membrane preparation and expression level.

Both the filtration and centrifugation methods are viable ways of determining if MRP4 expressed in *Sf* 9 cells are functional. The fluo-cAMP was a substrate known to work in vesicular transport assays previously and this study also confirmed these findings. MRP4 expressed in *Sf* 9 cells was shown to be ATP dependent as well as being inhibited by known inhibitors of the ATP hydrolysis (vanadate and AMP-PNP) along with a known inhibitor of MRP4 (MK 571). *Sf* 9 native membrane vesicles showed greatly reduced specific transport activity compare to *Sf* 9 MRP4 membrane vesicles proving MRP4 was facilitating the transport of fluo-cAMP into the vesicles. Increasing the concentration of fluo-cAMP increased the RFU showing transport was in a concentration dependent manner as to be expected. All these results together verify MRP4 expressed in *Sf* 9 vesicles was functional and could be used for purification purposes.

4.9 SMA Solubilisation

Membrane proteins naturally reside in the membranes of cells surrounded by hydrophobic lipids making them insoluble in aqueous solution. Therefore, they need to be extracted from the membrane making them soluble in aqueous solution through a process called solubilisation. Solubilisation traditionally is done with detergents that are amphiphilic molecules. Detergents are able to surround the membrane protein, forming a micelle and making it soluble. The major problem is many detergents are able to solubilise membrane proteins but they also destabilise them causing the protein to become denatured or aggregate. The membrane protein needs to be kept stable but also soluble throughout the downstream processing. Novel Calixar detergents and SMA polymers have recently been shown to not only have high solubilisation efficiency but also maintain the stability of membrane protein. This section shows how these novel Calixar detergents and SMA polymers compare to conventional detergents in terms of solubility and stability with the aim of finding the most suitable conditions for downstream processing.

Figure 4.9: Schematic of detergent vs SMA solubilisation. *A shows a diagram of a solubilised membrane protein surrounded by a detergent micelle. B show a diagram of a SMA solubilised membrane protein with the SMA polymer encompassing a disc of phospholipids in which the membrane protein resides.*

4.9.1 Styrene maleic acid (SMA) solubilisation

Styrene maleic acid (SMA) is a co polymer comprised of alternating units of styrene and maleic acid. This polymer is able to solubilise membrane proteins by producing a disc of lipid surrounding the membrane protein, creating a SMA lipid particle (SMALP). There are two main advantages of this polymer over conventional detergents; the native lipids are kept surrounding the membrane protein and once soluble no additional SMA is needed to be added to any downstream buffers. Some disadvantages are the sensitivity to divalent cations and the fixed disc size, only allowing a certain amount of lipids or a maximum size of membrane protein within the disc. There are a variety of different SMA polymers and SMA like polymers that have tried to alleviate these problems. The ratio of styrene to maleic acid can be varied altering the size of the disc. Typical conditions for solubilisation with SMA is described in(Lee, Knowles et al. 2016, Rothnie 2016). These conditions are one hour at room temperature using 2.5% (w/v) SMA at 30mg/mL wet pellet weight. These conditions were tested to make sure they were the most optimal for MRP4-his expressed in *Sf* 9 insect cells.

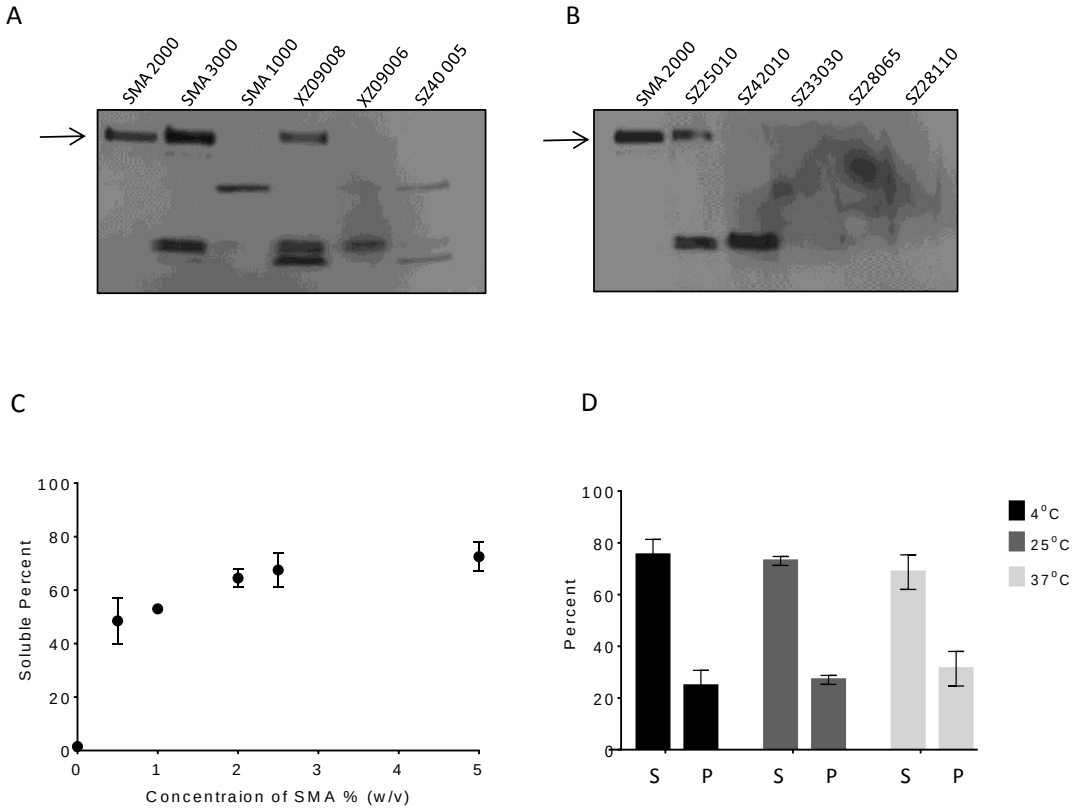

Figure 4.9.1 Solubilisation of Sf 9 MRP4 with SMA polymers*. Western blots A and B show the solubilisation screen of 11 SMA polymers with SMA 2000 as the control. Only the solubilised fraction from each of the polymers was ran on these western blot. Anti his primary antibody used. Graph C represents the soluble percent of Sf 9 MRP4 with 0 – 5% SMA 2000 (w/v). Data are mean ±sem (n=2). D shows the percent of soluble (S) and pellet (P) Sf 9 MRP4 at 4, 25, and 37°C. All solubilisations were conducted at 30mg/mL wet pellet weight for 1 hour. Data are mean ±sem (n=3).*

SMA can come in a variety of different styrene to maleic acid ratios and is manufactured by different companies. Western blots A and B in figure 4.9.1 show which SMA polymers were able to solubilise *Sf* 9 MRP4. SMA 2000 is the most commonly used polymer in our lab and has been shown to solubilise a wide variety of membrane proteins (Gulati, Jamshad et al. 2014). SMA 2000 has a 2:1 styrene to maleic acid ratio and was used as a positive control. The details of each SMA polymer can be found in the table 1.3.2.3.5. Only four of the 11 polymers were able to solubilise MRP4-his from *Sf* 9 membranes. SMA 2000, SMA 3000, XZ09008 and SZ25010 were all successful but interestingly only SMA 2000 showed one band on the western blot. The other three polymers

showed the MRP4 band, shown by the arrow, but also had a lower band indicating potential breakdown of MRP4. All of these polymers are between 7.5 and 10 kDa with a maleic acid content of either of 33 or 25%. XZ09006 and SZ42010 only showed the lower breakdown band and SMA 1000 and SZ4005 showed a middle band and the lower band. SZ33030, SZ28065 and SZ28110 all showed no clear bands on the western blot. The second trial showed similar results with the same four polymers being able to solubilise Sf 9 MRP4. Some of the breakdown products shown in the western blots (Figure 4.9.1 A and B) were not visible on the second blot indicating the membranes also play a role in the solubilisation as different membranes were used between the studies.

Compared to SMA 2000 over the two trials SMA 3000 increased the solubility to 135% but did show breakdown in both blots. XZ09008 and SZ25010 had 75 and 79% compared to SMA 2000 and both again had break down products in both the blots. The variability over the two blots was minimal for all polymers except SZ25010. Although SMA 3000 increased the solubility percent it did show some breakdown products so, based on a good level of solubility and absence of breakdown products SMA 2000 was chosen for further studies.

2.5% (w/v) SMA 2000 is the typical amount used to solubilise membrane proteins. Graph C (Figure 4.9.1) shows there is an increase in solubility of MRP4 with increased concentrations of SMA 2000 when solubilising *Sf* 9 MRP4 membranes at 30mg/mL WPW at room temperature. During this experiment the maximum amount of total MRP4 solubilised was 72.5% and this was achieved using 5%(w/v) SMA 2000, where as with 2.5% (w/v) SMA2000 67.5% of the total MRP4 was extracted. However, the graph in figure 4.9.1 C does show that the degree of solubilisation does appear to plateau and the use of 2.5% (w/v) SMA 2000 solubilises close to the maximum amount of MRP4. This result is in line with previous experiments showing 2.5% (w/v) is the optimal amount need to solubilise MRP4. Furthermore, 5% (w/v) SMA2000 may lead to excess SMA that could interfere with downstream processes.

Normally room temperature (25^{o}C) is used in SMA 2000 solubilisations. It is known that keeping membrane proteins at a lower temperature helps keep their stability during solubilisation and

purification when using detergents. The rigidity of membranes changes with temperature and could affect the solubilisation efficiency with SMA 2000 due to the nature of the way SMA 2000 functions. Detergents replace the lipids surrounding the membrane protein whereas SMA surrounds the lipids. Lower temperatures can increase the rigidity of the lipids and could make it harder for SMA to solubilise membrane proteins. An increase in temperature would make the membrane more fluid allowing the styrene groups to get in between the fatty acyl tails of the lipids but could also lead to a less stable membrane proteins. As these factors are unknown a simple experiment was setup to evaluate the solubilisation efficiency at three different temperatures. Graph D shows there is little change in the solubilisation efficiency between temperatures with 73.8% at 4^{o}C, 68.8% at 25^{o}C, 70.8% at and 37^{o}C for *Sf* 9 MRP4. The solubilisation efficiency achieved at 25^{o}C was the same as in the previous experiment (Figure 4.9.1 C) showing consistency in the solubilisation efficiency at 25^{o}C. Because room temperature had previously been used for solubilisation with SMA 2000 and was also shown to be effective in this study room, it was used for all subsequent experiments.

4.9.2 Solubility of MRP4 with SMA 2000 over time

Normally SMA 2000 solubilisation is performed for one hour. It was observed that upon the addition of SMA to Sf 9 MRP4 membranes the solution becomes much clearer by eye very rapidly. Because of this observation, the length of time it takes to solubilise MRP4 was questioned. When solutions that contain fatty molecules such as lipids become transparent it is an indication of solubilisation just like adding washing up liquid to greasy frying pan. The transparency of the solution can be measured using a spectrometer but this does not show if the MRP4 is actually being solubilised so western blot analysis is also needed. To gain a greater understanding of the dynamics of the process, dynamic light scattering can be used to measure the particle size and distribution.

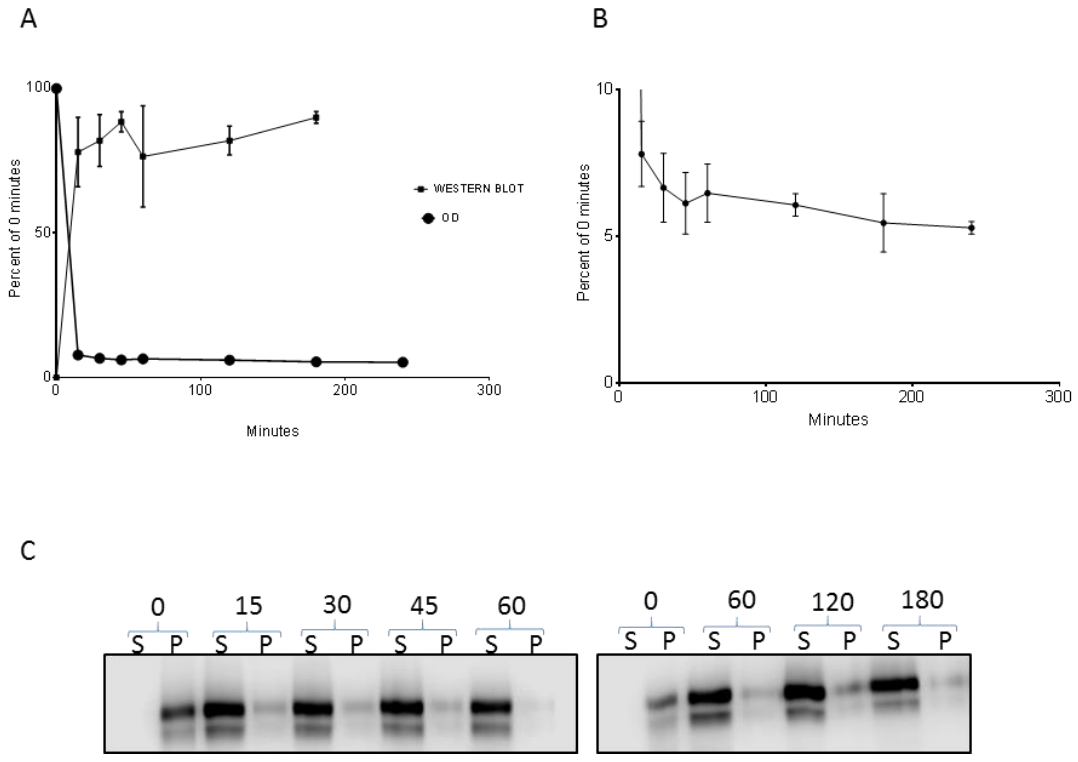

Figure 4.9.2: Solubilisation of Sf 9 MRP4 over time. *Graph A shows the percent soluble over 240 minutes based on OD 600 readings and western blot analysis, compared to 0 minutes. Graph B shows the same OD 600 readings as A but zoomed in to show the change after 15 minutes. Western blots C shows soluble (S) and pellet (P) of MRP4 solubilised from Sf 9 cell membranes, densitometry analysis plotted in graph A. Data are mean ± SEM (n =2) over 180 minutes.*

Graph A (4.9.2) shows optical density readings at 600nm over two hours. This shows that after 15 minutes the OD drops dramatically to around 10% of the control, where no SMA was added (0 minutes). At the same time point (15 minutes) the western blot analysis shows the 76% of MRP4 was solubilised. Both the OD readings (Figure 4.9.2 B) and western blot results remained relatively stable over the remaining time. This shows there is a correlation between the optical density and solubility of MRP4 with the vast majority happening within the first 15 minutes.

Western blots (C) and related graph (A) (Figure 4.9.2) shows the solubilisation of *Sf* 9 MRP4 using SMA 2000 over two hours. The western blot clearly shows that after 15 minutes there is an intense MRP4 band in the soluble fraction and only a small amount of MRP4 remaining in the pellet (insoluble) fraction. This does not visibly change over the following 3 hour period. Using densitometry analysis of the soluble and pellet fractions, the percent soluble was calculated. The majority of the solubilisation takes place within the first fifteen minutes as shown in figure 4.9.2 A. There is a not significant increase in percent soluble over the next three hours showing that an hour solubilisation is not necessarily needed. No time points shorter than 15 minutes could be analysed, as the minimum centrifugation time was 15 minutes to pellet all insoluble material.

4.9.3 Dynamic Light Scattering

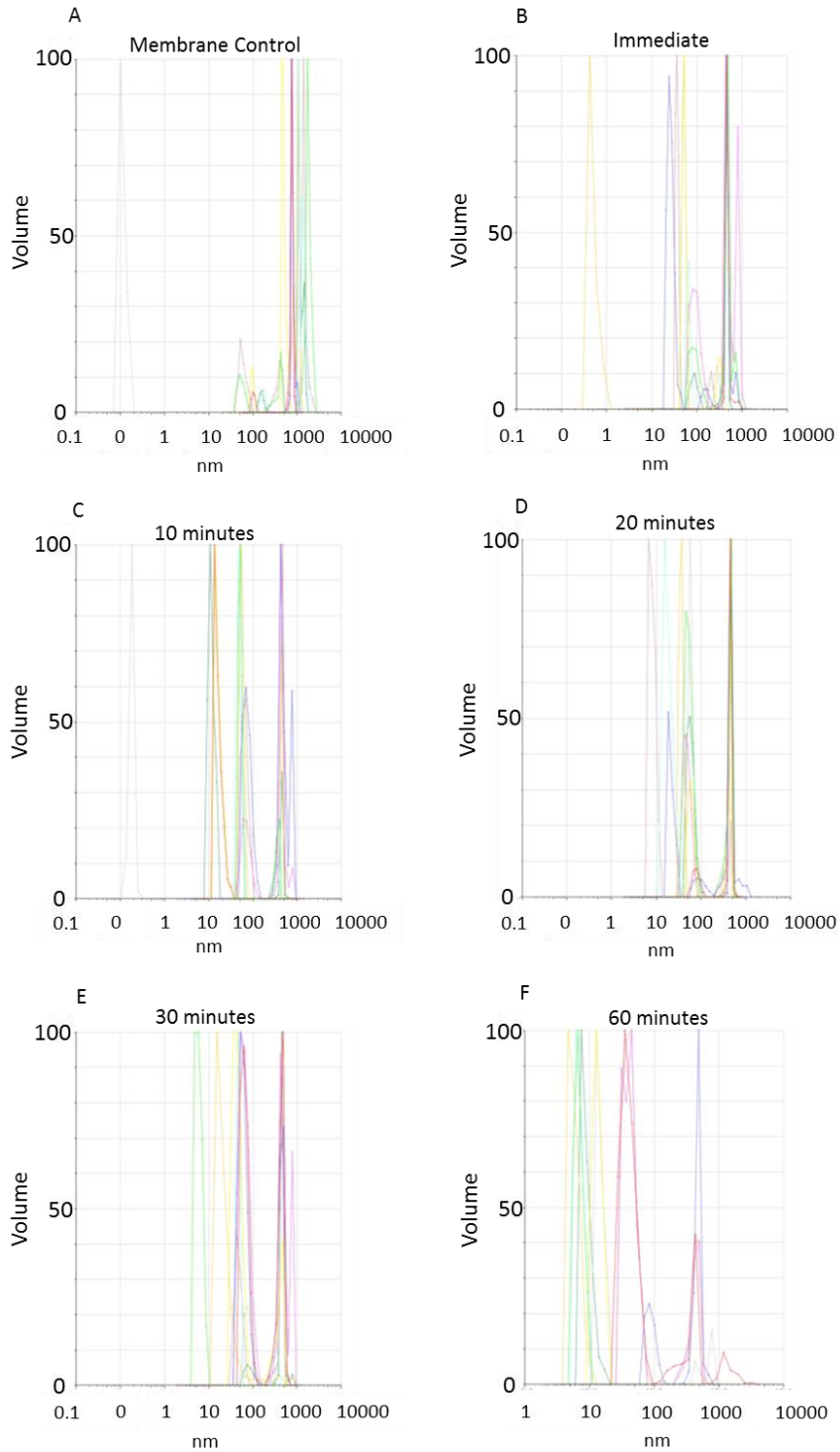

Figure 4.9.3: Dynamic light scattering (DLS) of Sf 9 MRP4 membranes with SMA 2000. *DLS scans A-F shows the particle size (nm) and the volume of these particles found during a 60 minute solubilisation. Read out A shows the particles found in the Sf 9 MRP4 membrane before solubilisation. B shows the particles found immediately after the addition of SMA 2000. Read outs C – F are the results taken 10, 20, 30 and 60 minutes during solubilisation. 10 scans (each a different colour) were performed on each samples and solubilisation was conducted at room temperature with 2.5% (w/v) SMA 2000. A Brookhaven, nanobrook 90 plus zeta was used.*

The DLS results in figure 4.9.3 show the particles size during the solubilisation of *Sf* 9 MRP4 membranes over 60 minutes. The OD 600 reading in figure 4.9.2 only gives an indication of how turbid the *Sf* 9 MRP4 membrane became when SMA 2000 was added. Although the turbidity during solubilisation can be linked to solubilisation, it does not show what the particle size is. DLS allows for a more in depth analysis of the particle size and the length of time it takes to reach a particle size of 10nm, which is the SMALP disc size of SMA 2000. The membrane control shows the majority of the particles are around 1000nm. Upon addition of SMA 2000 there is an immediate shift in the particle size with some particles appearing between 10 and 100nm although a large amount still remains at 1000nm. After 10 minutes (Figure 4.9.3 C) more particles around 10 and 100nm are found with some still at 1000nm. The results after 20 and 30 minutes are do not show much change compared to 10 minutes. After 60 minutes (Figure 4.9.3 F) there is a clear shift in particle size with the majority between 10 and 100nm and only a few at 1000nm showing it could take up to 60 minutes for the solubilisation of Sf 9 MRP4 to be completed. A 60 minute time period was chosen as this was the recommended time period for solubilisation with SMA 2000 and results in figure 4.9.2 shows the majority of MRP4 was solubilised after 60 minutes.

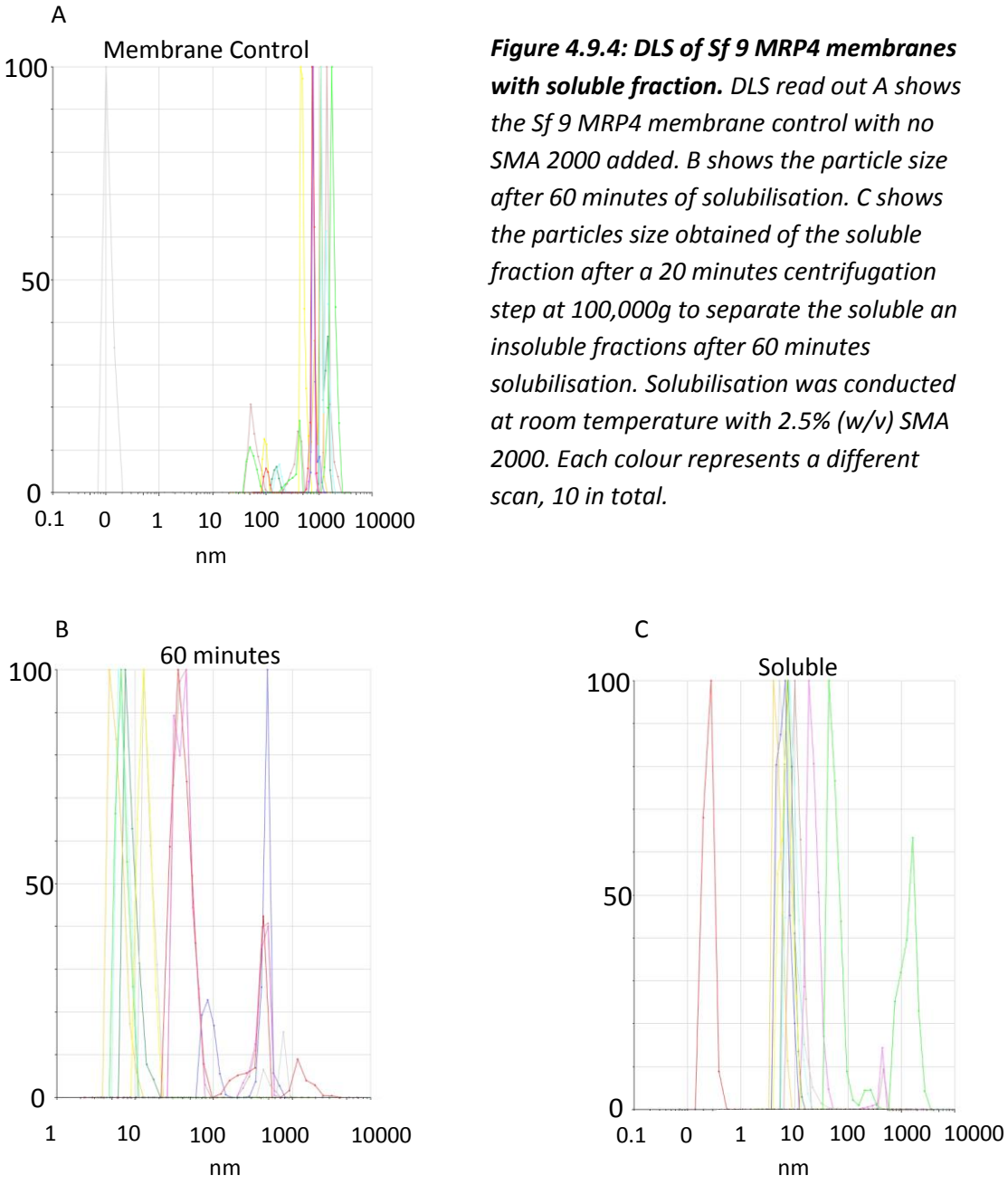

Figure 4.9.4: DLS of Sf 9 MRP4 membranes with soluble fraction. *DLS read out A shows the Sf 9 MRP4 membrane control with no SMA 2000 added. B shows the particle size after 60 minutes of solubilisation. C shows the particles size obtained of the soluble fraction after a 20 minutes centrifugation step at 100,000g to separate the soluble an insoluble fractions after 60 minutes solubilisation. Solubilisation was conducted at room temperature with 2.5% (w/v) SMA 2000. Each colour represents a different scan, 10 in total.*

Figure 4.9.4 shows the particle size of Sf 9 MRP4 membranes solubilised with SMA2000 after 60 minutes before and after a centrifugation step. The membrane control (Figure 4.9.4 A) shows the particles are all around 1000nm and after 60 minutes (Figure 4.9.4 B) there is a clear shift to particles sizes between 10 and 100nm. There are still some particles around 1000nm and it was thought these particles were un-solubilised fragments of the membrane. To examine this theory the sample was centrifuged at 100,000g for 20 minutes to separate the soluble and insoluble fractions. The soluble fraction was analysed (Figure 4.9.4 C) and this shows the majority of the

particles are around 10 nm. This is in line with previous studies that show the particle size of SMALP discs are around 10nm (Dorr, Scheidelaar et al. 2016). The results from previous studies, performed with lipids only, found a very uniform disc size. The DLS experiments in this study were carried out with Sf 9 MRP4 membranes, which would not only contain MRP4 but a vast array of other membrane proteins that would be solubilised. Membrane proteins are known to protrude into both the intra and extracellular sides of the membrane giving the disc more of an oval shape overall. As there are many different membrane proteins in the *Sf* 9 membrane, many of which are unknown in size and shape, this would give a reason why the particle size is dispersed but still mostly around 10nm.

4.10 Calixar Solubilisation

4.10.1 Calixar solubilisation dot blot screen

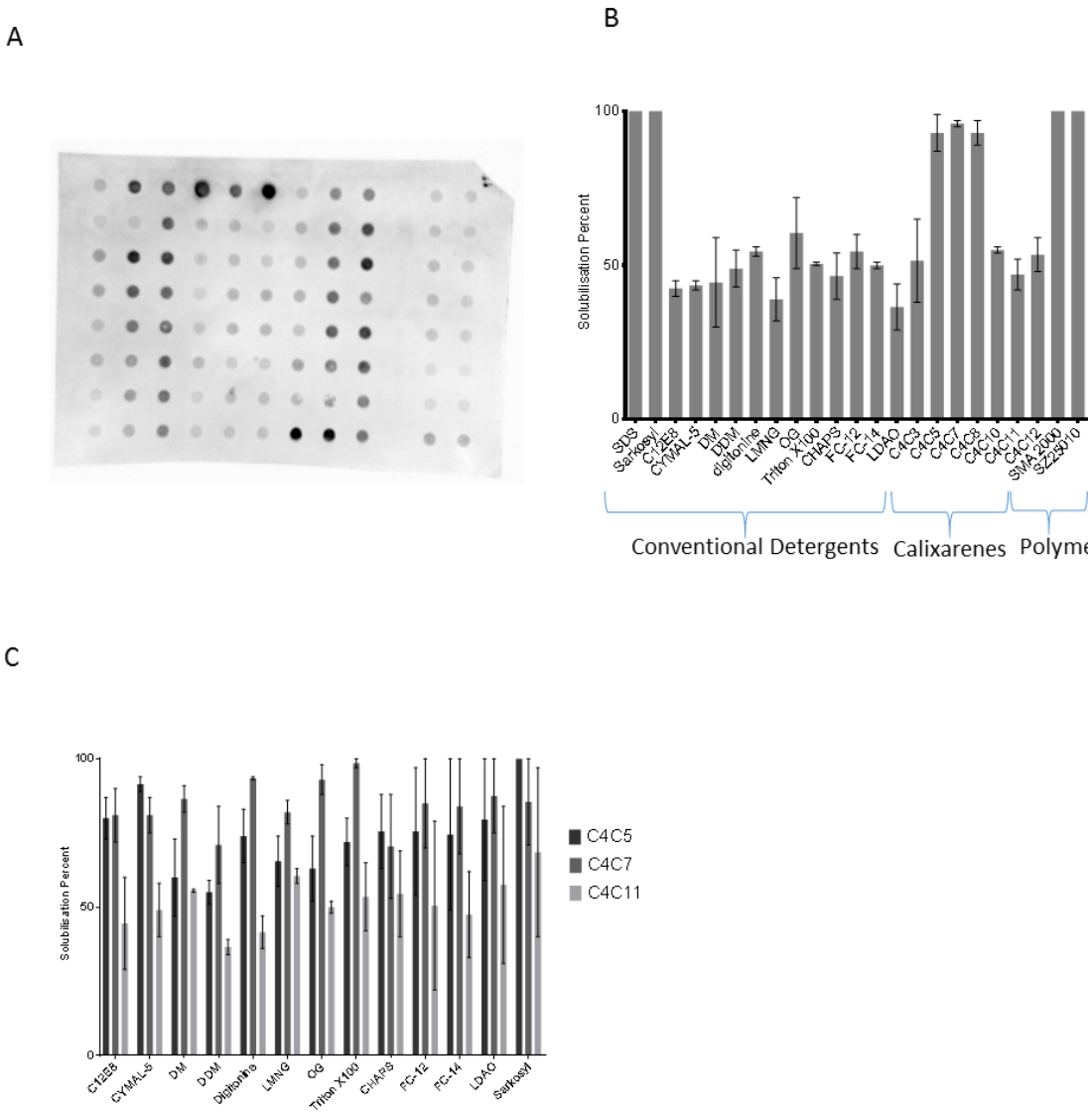

Figure 4.10.1: Dot blot solubilisation. *(A) show an example of the dot blot. Graph (B) shows the comparison of conventional detergents to novel detergents (Calixarenes) and SMA polymers from dot bot analysis. The density of each dot was compared to the density of SDS which was taken as 100%. Data are mean ± sem (n=2). Graph C shows the soluble percent of conventional detergents mixed with either C4C5, C4C7 or C4C11. Data are mean mean ± sem (n=2).*

In order to find out which detergents or polymers were best at solubilising MRP4 we carried out a screen with the largest variety of different detergents and polymers possible. Dot blot analysis was used to screen 85 different types of detergent, SMA co-polymers and detergent mixtures and determine which conditions had the highest solubilisation capabilities. Each dot in the dot blot (4.10.1 A) shows a different detergent, detergent mixture or SMA polymer and the qualitative result from this experiment showed clear differences in the density of the dots. The darker the dot the more soluble material was able to bind to the PVDF membrane, therefore showing increased solubility. The harsh detergent SDS was used as a positive control. 4.10.1 B shows the quantitative results from two of these dot blots. All conventional detergents screened, regardless of their ionic strength, were able to solubilise around 50% of MRP4 from *Sf* 9 cells membranes with the exception of the harsh anionic detergent Sarkosyl that was equal to SDS. The novel solubilisation agents (SMA co-polymers and calixarene detergents) had a range of 42 to 100% solubility. It has previously been shown that the length of the acyl tail of calixarene based detergents plays a key role in their ability to solubilise (Matar-Merheb, Rhimi et al. 2011). This was again the case in this study where having a short (3) carbon length showed decreased solubilisation efficiency. Once the carbon length was increased to 5 the solubilisation percentage dramatically increased and stayed high when increased again to 7 or 8 carbons. Calixarene detergents with an acyl tail length of 5, 7 and 8 carbons (C4C5, C4C7 and C4C8) were able to have a solubilisation efficiency of over 90%. However, unlike in the Matar-Merheb study where the percentage that was soluble stayed high with increasing carbon length, up to 12 carbons, we found that the solubility percentage decreased once the carbon length reached 10 carbons. The solubilisation efficiency stayed decreased, compared to carbon lengths of 5, 7 and 8, when the carbon length was increased to 11 and 12 carbons. This shows that Calixarenes with short (3) or long (10, 11 or 12) carbons only had the same solubilisation efficiency as conventional detergents.

Conventional and novel (calixarene) detergent mixtures showed a solubilisation efficiency increased when compared to conventional detergents but lower than the novel detergents. This can been seen in two ways; either the addition of conventional detergent decreases the

solubilisation efficiency of calixarene based detergent with an acyl tail of 5 (C4C5) or 7 carbons (C4C7), or C4C5 and C4C7 increases the solubilisation efficiency of conventional detergent. When the acyl tail of the calixarene was increased to 11 carbons the solubilisation efficiency decreases when compared to the addition of C4C5 and C4C7 to conventional detergents. These results are expected as the solubilisation efficiency of C4C5 and C4C7 is high, around 90%, and the solubilisation efficiency of conventional detergents is around 50%. Therefore, the combination of these two types of detergents show the expected results. The solubilisation efficiency of C4C11 has the same solubilisation efficiency as the conventional detergents so the mixture of C4C11 and conventional detergents would be expected to show no change.

These results show that the length of the acyl tail plays a key role in the solubilisation of membrane proteins for calixarene based detergents. The SMA co-polymers had high solubilisation efficiency with SMA and SZ25010 both at 100%. These results show that novel solubilising agents are capable of greatly increasing the solubilisation efficiency of MRP4 when compared to conventional detergents. The detergent mixtures showed expected results with an increase in the solubilisation efficiency of the conventional detergents with the addition of C4C5 or C4C7. These results allowed the number of detergents, detergent mixtures and SMA polymers to be narrowed down to the top 16 solubilisation agents.

4.10.2 Solubilisation Efficiency

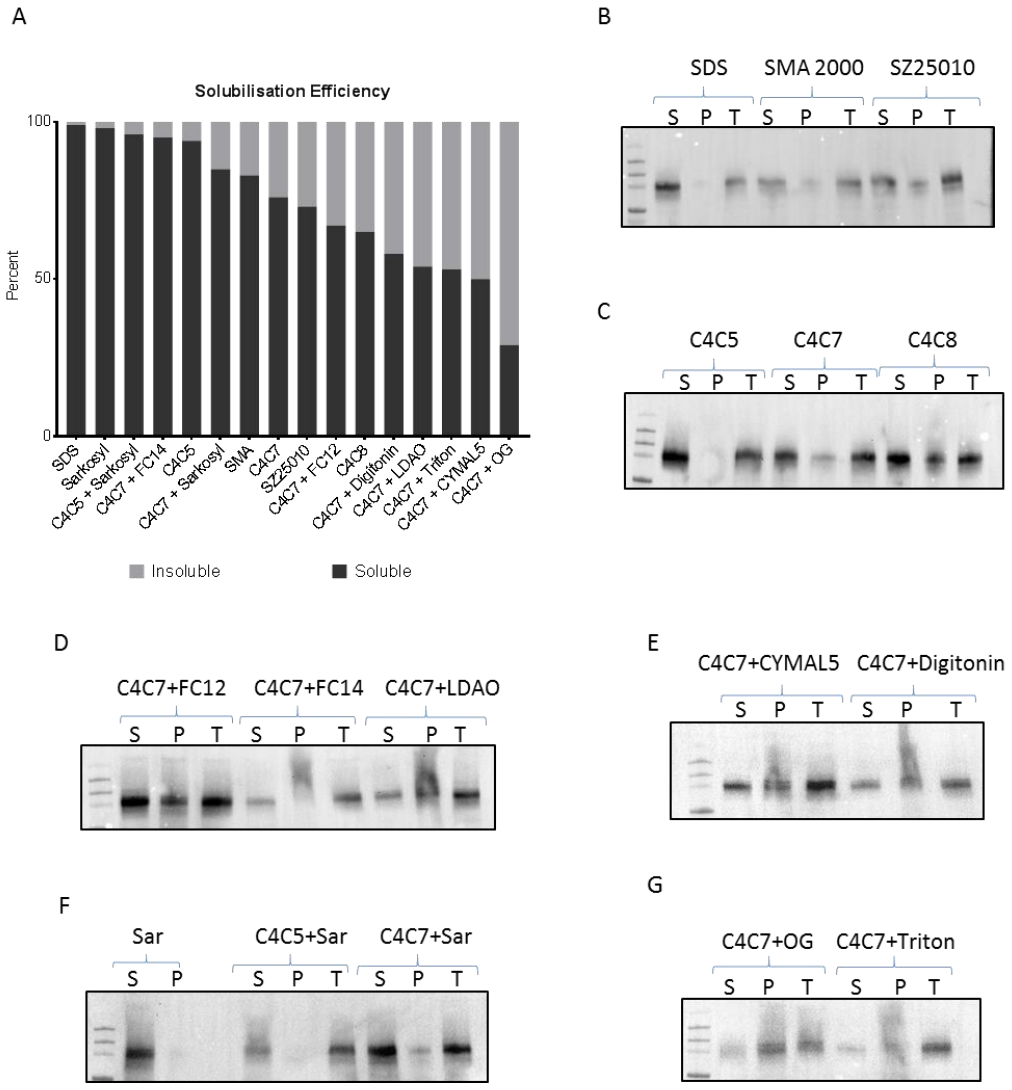

Figure 4.10.2: Solubilisation efficiency western blot*. The top 16 agents from dot blot analysis were chosen for solubilisation efficiency examination. The total (T), pellet (P) and soluble fractions from each condition analysed with western blot. Graph (A) shows the percent that was soluble and insoluble from the western Blots (B - G) from each condition based on the density of the soluble and pellet fractions. Primary anti-MRP4 antibody.*

The dot blot approach is a quick and easy way to carry out a large scale initial screen, however it can show higher solubility efficiency than expected results. For example using this technique the proteins are not separated first so all proteins that are detected by the primary antibody will be detected. If the primary antibody is not highly specific or it there is different oligomeric states of the proteins or if the detergent breaks the protein down this can result in increased signal that is

not directly related to the protein of interest. Therefore the results need to be confirmed by a more traditional Western blot approach allowing for separating and direct detection of the specific protein. From the Dot Blot results, the top 16 conditions were chosen to be measured and confirm the solubility efficiency using western blot analysis. It is interesting to note that DDM did not fall within the top 16 conditions even though it has been extensity used in the solubilisation of ABC transporters. Detergents such as SDS and Sarkosyl were in the same solubility range as measured by the dot blot, (fig 4.10.1) but this is not surprising as these are two very harsh detergents. Only C4C5 managed to maintain a very high solubility efficiency whereas C4C7 dropped to 76% soluble and C4C8 reduced to 65% solubility again showing the length of the acyl tail can affect solubility efficiency. The two co-polymers SMA and SZ25010 also dropped to 83 and 73% respectively, which agrees well with the results reported in section 4.9.1.

The majority of detergent mixtures involving C4C7 and conventional detergents, which were all highly soluble in dot blot analysis, dropped by almost half the amount in this western blot analysis. Only high solubility efficiency was shown with the addition of either Sarkosyl or FC-14 with C4C7. The solubilisation efficiency of C4C5 was high with the addition of Sarkosyl but the high solubilisation efficiency was likely mostly contributed by Sarkosyl. Although SDS and Sarkosyl have very high solubilisation efficiency these were not chosen for further study as these two conventional detergents are very harsh and likely to denature the protein fully.

The amount of different detergents was whittled down from an initial 85 to just two (C4C5 and C4C7) which show the highest solubility efficiency. The SMA polymers have also shown very high solubility efficiency. Nevertheless, solubility efficiency is only one aspect and MRP4 must also be kept stable. This means the measuring the stability of MRP4 in these solubilising agent to determine which one is not only the most efficient at solubilisation but also stabilisation.

4.11 Thermostability of Soluble MRP4

A common method for measuring the stability of proteins is through their ability to withstand high temperatures. The higher the thermostability of a protein the more stable it is. Y. Ashok et al. developed a simple method for measuring the thermostability of un-purified soluble membrane proteins. This method allows quick screening of the stability of membrane protein in different detergents, without the need for purification, allowing the assessment of which detergent is most likely to keep the membrane protein stable throughout the purification process. The method was used to test the stability of MRP4 in the present of different detergents based on aggregation. As proteins are heated they become denatured, losing their native structure and forming aggregates. By measuring the percent of soluble MRP4 remaining through western blotting after heating and centrifuging, the ability for the detergent or polymer to maintain the native structure of MRP4 can be assessed. The denaturing mid-point/transition or melting temperature can be calculated by finding the temperature at which 50% of MRP4 remains soluble. One problem with this method is that other proteins within the membrane maybe less stable than the protein of interest, these will form aggregates and may interact with your protein causing it to aggregate.

Although calixarene detergent and SMA co-polymers had high solubilisation efficiency their ability to stabilise MRP4 needed to be examined. Other conventional detergents (C12E8, CYMAL, DDM and FC-12) were used for thermostability testing as a comparison to the novel detergents and co-polymers. These conventional detergents were chosen as they have been used in studies involving the solubilisation of ABC transporters, all have a similar solubilisation percentage and offer a variety of different properties e.g. non-ionic and zwitterionic detergents, as shown in table 5.2.1.

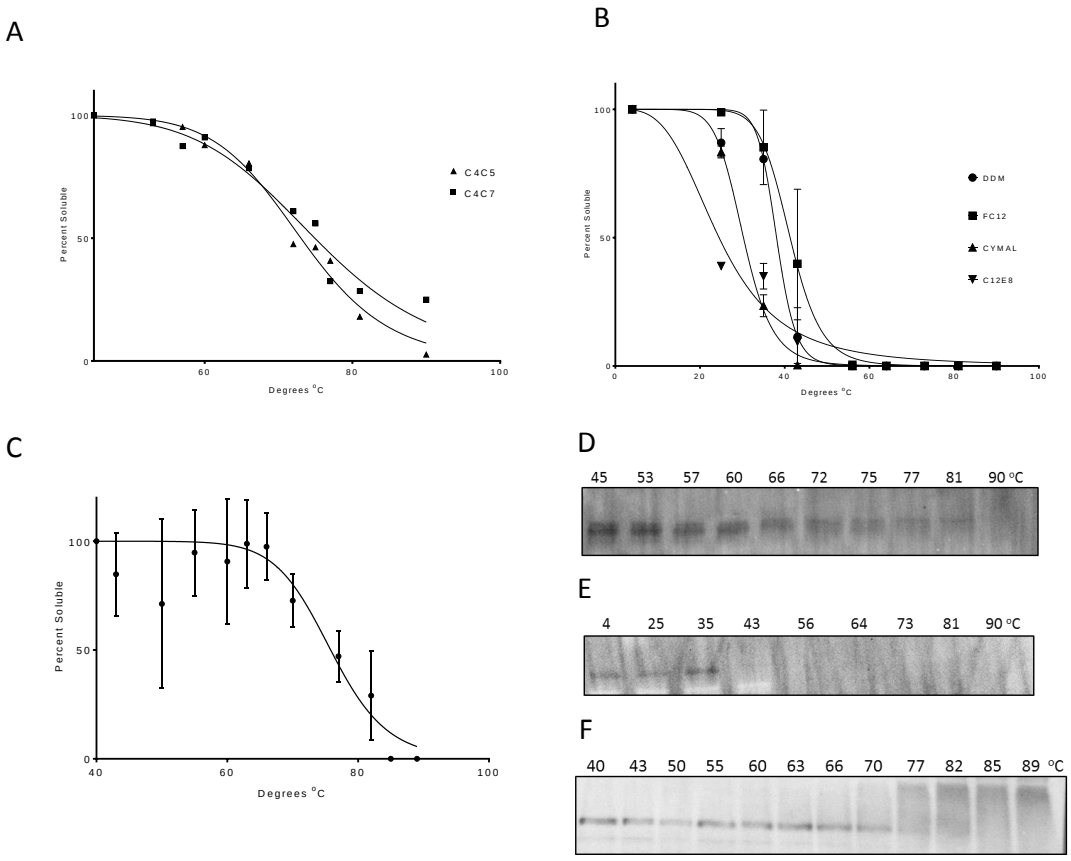

Figure 4.11: Thermostability of MRP4*. Thermostability was measured by the percent of soluble ABCC4 present after heating. Graph (A) shows the thermostability of ABCC4 solubilised with calixarenes C4C5 and C4C7 from 45 to 95°C (n=2). Graph (B) is showing conventional detergent thermostability from 4 to 90°C (n=2). Graph (C) is the thermostability results for SMA from 40 to 89°C (n=2). The Tm was calculated as the temperature at which 50% remained soluble. [inhibitor] vs normalised response curve fitted for all graphs. Western Blots (D), (E) and (F) shows the results from C4C7, DDM and SMA respectively and the visual decrease in the MRP4 band.*

C4C5 and C4C7 both showed a very high Tm of around 73°C when compared to conventional detergents. The conventional detergents ranged from 28 to 40°C with FC 12 being the highest and C12E8 the lowest. The western blots show a clear difference in the amount of MRP4 still soluble at each temperature. C4C7 western blot shows a clear and steady decrease in the band intensity whereas with DDM after 35°C there is an almost complete lack of MRP4. The DDM temperatures had to be lowered because the first trial that was conducted at the same temperatures at C4C7 showed no MRP4.

SMA also showed a very high Tm of around 75°C which is very similar to the Calixar detergents and again much higher than conventional detergents. The western blot of SMA shows interesting results because there isn't a constant decrease in the density of the MRP4 band as the temperature increase, like C4C7 shows, but instead the band intensity if fairly constant until around 66-70°C. After that, the MRP4 band disappears showing that there is more of a cut off temperature with SMA rather than a gradual decrease.

The Tm of the calixarene detergents (C4C5 and C4C5) and SMA tested was much higher compared to conventional detergents demonstrating that these detergent are not only capable of high solubility efficiency but are also more stable.

These results show that the solubilisation conditions outlined in (Lee, Knowles et al. 2016, Rothnie 2016) were also optimal for the solubilisation of MRP4 from *Sf* 9 cell membrane with SMA. SMA 2000 was chosen as the best SMA polymer and was used for further solubilisations. 2.5% (w/v) SMA 2000 at room temperature with the membranes at 30mg/mL wet pellet weight were the most optimal conditions. Solubilisation at lower temperatures could help keep MRP4 more stable but solubilisation at room temperature was more convenient. Figure 4.9.2 does show that solubilisation only takes about 15 minutes to reach maximum solubilisation percent but 1 hour was chosen as the DLS results showed the particle size was in line with previous findings.

The dot blot showed that conventional detergents were only able to solubilise around 50% of MRP4 whereas some Calixar detergents (C4C5, C4C7 and C4C8) were able to solubilise over 90% of MRP4. The SMA polymers also showed very high solubilisation efficiencies in the dot blot. The western blot analysis showed that C4C5 managed to maintain a very high solubility efficiency whereas C4C7, C4C8 and the two polymers SMA 2000 and SZ25010 had a reduced solubility efficiency but still no lower than 65% and were the best performing solubilisation agents. Through the combination of a dot blot and western blot the most efficient detergent was found in a very short space of time. The thermostability of MRP4 was investigated with C4C5 and C4C7 along with

SMA 2000 and compared to conventional detergent. This showed that not only do these Calixar detergents and SMA polymers have increased solubility efficiency but they also have a dramatically increased thermostability. It was for these reasons that C4C7 and SMA 2000 were used in the purification of MRP4.

4.12 Calixar Purifications

Structural and functional studies of any protein requires the protein of interest to be purified, so that it can be examined in isolation. MRP4 expressed in this study contains a hexa-his tag at the C terminal allowing for affinity chromatography. It has previously been shown that both calixarene detergents and SMA co-polymers can be used with an affinity chromatography purification process (Matar-Merheb, Rhimi et al. 2011, Gulati, Jamshad et al. 2014, Rothnie 2016). Small scale trial purifications were performed to give an indication of which detergents and polymers were able to purify MRP4 and to what extent. The novel detergents chosen were the calixarene detergents, C4C5 and C4C7, as they had the highest solubility efficiency and the greatest enhancement of thermostability. Two SMA-polymers (SMA 2000 and SZ25010) were also chosen because of their high solubilisation efficiency. Four conventional detergents were chosen: DDM, C12E8, CYMAL and FC12 and although these detergents had low solubilisation efficiencies and poor thermostability their use in purification was still evaluated in case they yielded good results and as a comparison. These four conventional detergents were chosen as they represented different ionic strengths of detergents and have previously been used with other ABC transporters. DDM is a very popular detergent used for membrane protein solubilisation and purification and is a mild non-ionic detergent. CYMAL is another non-ionic detergent and has been used to solubilise and purify ABCB11 in the past (Ellinger, Kluth et al. 2013). C12E8 has previously been used in conjunction with DDM for studies of Sav 1886 (Galian, Manon et al. 2011). FC12 is a zwitterionic detergent that has been used to study BmrC/BmrD (Galian, Manon et al. 2011).

Calixar is a biotechnology company that specialised in used calixarene based detergents for the stabilisation of membrane proteins. During my PhD I spent four months, spread over two trips, at Calixar in Lyon using calixarenes for solubilisation and purification of MRP4.

4.12.1 Conventional, novel detergent and SMA polymer small scale purification trial

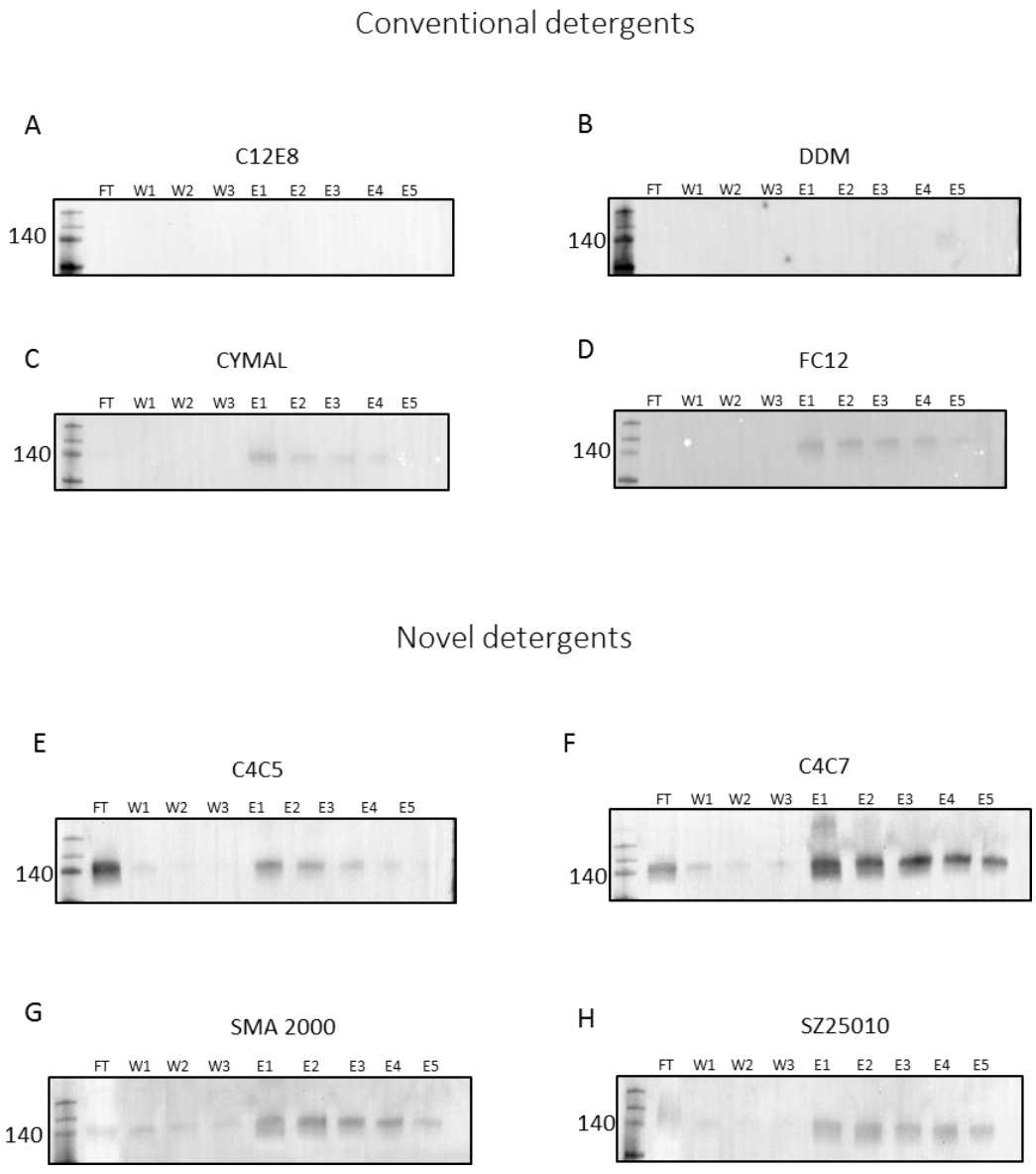

Figure 4.12.1: Small scale purification trials with conventional, novel Calixar detergents and SMA polymers. *Western blots A-D show the purification profiles of Sf 9 MRP4 in the presence of C12E8, DDM, CYMAL and FC12. Western blots E and F are the purification profiles of C4C5 and C4C7 respectively. Western blots G and H are the purification profiles of SMA 2000 and SZ25010 respectively. Each of the western blots show the flow through (FT), the wash fractions (W1, W2 and W3) and five elution fractions (E1 – E5). 500µL of soluble Sf 9 MRP4 was bound to 50µL cobalt resin and washed 3 x 10 column volumes (CV) with PBS then eluted with 5 x 1 CV of 200mM imidazole in PBS. When detergents are used 1xCMC of that detergent was used in all the purification buffers. An anti MRP4 primary antibody (1:100) and an anti-rat HRP secondary antibody (1:5000) was used on all western blots (n=1).*

The results from the trial purifications (Figure 4.12.1) show visible difference between the conventional and novel detergents. Out of the four conventional detergents only two, CYMAL and FC12 showed bands of MRP4 on the western blot. These bands were only in the elution fractions and this was most likely due to the small elution volumes used, one column volume. This is compared to the 10 column volumes used in the wash steps and although no imidazole was used in the wash steps MRP4 could have been diluted to an undetectable level. Surprisingly no MRP4 was present in the FT with the conventional detergents. This could have been because either MRP4 had fully bound to the resin or due to the poor solubility efficiency of the conventional detergents only small amounts were solubilised and were undetectable. These novel detergents all showed small amounts of MRP4 in the wash steps and all elution fractions, with a general trend of decreasing amount eluted off from fraction one to five. Unfortunately, the soluble fraction was not loaded on the western blot so the binding efficiency could not be measured so another trial purification was attempted. Conventional detergents were not included in this second trial because of their poor solubilisation efficiency.

4.12.2 Second small scale purification trial with novel Calixar detergents and SMA polymers

A

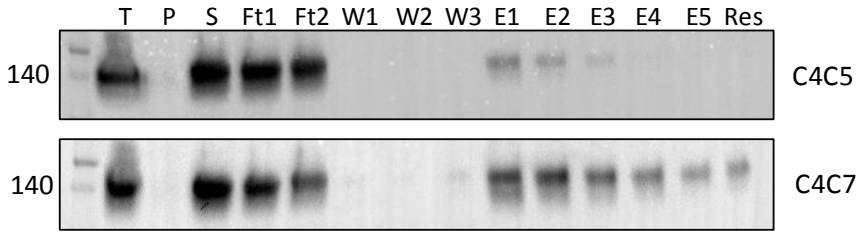

B

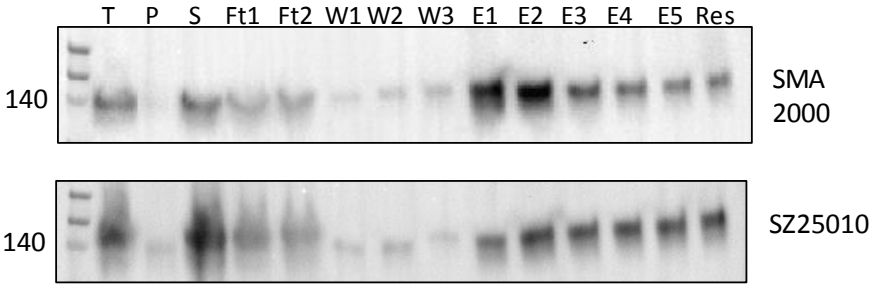

C

Fraction	C4C5	C4C7	SMA 2000	SZ25010
Soluble	100	100	100	100
FT 1	95	73	60	53
FT 2	72	59	56	37
W1	0	1	11	9
W2	0	0	14	11
W3	0	2	22	8
E1	1.5	5.2	20.2	5.1
E2	0.7	5.1	21.3	8.6
E3	0.3	3.4	11.3	6.3
E4	0	2.4	7.7	5.7
E5	0	1.3	5.6	5.8

Figure 4.12.2: Second small scale purifications using novel Calixar detergents and SMA polymers. *Western blots in A show the purification profiles form C4C5 and C4C7 and western blots in B are SMA 2000 and SZ25010. The tables in C shows the densitometry results from the western blots in A and B as a percent compare to the density of the soluble fraction. The western blots include the total (T), pellet (P), soluble (S), two flow through (Ft1 and Ft2), three PBS washes (W1, W2 and W3), 5 200mM imidazole elution fractions (E1 – E5) and one resin fraction (Res) (n=1). The same purification protocol and antibodies as in figure 4.12.1 was used.*

These second small scale purifications once again show that all conditions that had a high solubilisation efficiency (Calixar detergents and SMA polymers) and were able to purify MRP4. The two calixarene based detergents show differences with C4C7 out performing C4C5. The first flow though (Ft 1) was passed over the resin again and the binding efficiency was measured by the percent in the second flow through (Ft 2). Ft 2 fractions of C4C7 showed that 41% of the solubilised MRP4 was bound by the resin. Although this seems like poor binding efficiency, it was higher than C4C5 for which only 28% of the solubilised MRP4 bound to the resin. C4C7 had visible bands in the wash steps but these only equated to small amounts. The concentration of MRP4 was not measured directly but the elution pattern using C4C5 is different to that using C4C7. Only the first three elution fractions contained MRP4 with C4C5 whereas all elution fractions contained MRP4 using C4C7.If the density of the bands is compared to the total solubilised MRP4 then elution fractions 1, 2 and 3 of C4C5 contained 1.5, 0.7 and 0.3% of the MRP4 respectively. Whereas with C4C7 elution fractions 1 – 5 contained 5.2, 5.1, 3.4, 2.4 and 1.3% of the MRP4. This shows that both qualitatively and quantitatively C4C7 out performs C4C5.

Out of the two SMA polymers SMA 2000 solubilised MRP4 had a lower binding efficiency to the resin than SZ25010. Both the SMA polymers showed small amounts of MRP4 in the wash steps. Again the concentration of MRP4 was not quantified after purification but there were differences between the amounts contained in the elution fractions between SMA 2000 and SZ25010. With SMA 2000 the majority of MRP4 is eluted in the first three fractions with them containing 20.2, 21.3 and 11.3% and the last two containing 7.7 and 5.6%. Interestingly the amount eluted using SZ25010 is fairly consistent across all the elution fractions, however the amount overall is less than that observed using SMA 2000, especially in the last two elution fractions.

The yield of purified protein using both SMA polymers was higher than C4C5 or C4C7. It appears the full binding capacity of the resin was not reached as in each case the amount of MRP4 present in the first flow through was higher than the second flow through (Ft2), the flow though after the

first flow through (Ft 1) was passed over the resin again. This could also means a longer binding time is need or there is some level aggregation allowing some MRP4 to not bind. With the exception of C4C5 not all MRP4 was eluted as MRP4 is still present in the resin (Res) fraction. C4C7 and SMA 2000 were chosen for larger scale purification as they both showed the highest yield within their classes. Further experiments using C4C7 are detailed in this chapter. Purification using SMA 2000 is detailed in chapter 4.13.

4.12.3 Scaled up purifications with C4C7.

Using the same membranes as the small scale trial purifications a scaled up purification was performed. The small scale purifications also contained no imidazole in the wash steps so during the scaled up purification 5mM imidazole was added to the wash buffer to help increase purity. The scaled up purification was 18 times larger than the small scale containing 9mL of Sf 9 MRP4-his membranes at 9.7mg/mL total protein and solubilised with 10X CMC C4C7.

4.12.3.1 Scaled up purification of Sf 9 MRP4 with C4C7.

A

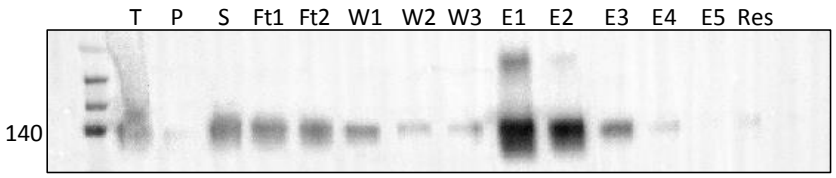

B

Fraction	%
Soluble	100
Ft1	87
Ft2	80
W1	52
W2	17
W3	24
E1	27.7
E2	22.7
E3	6.7
E4	0.9
E5	0.1

C

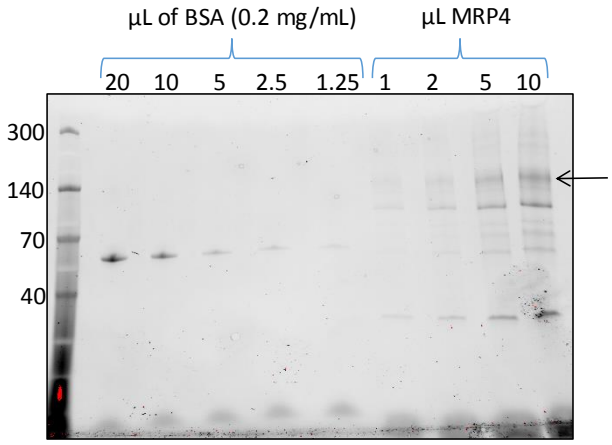

D

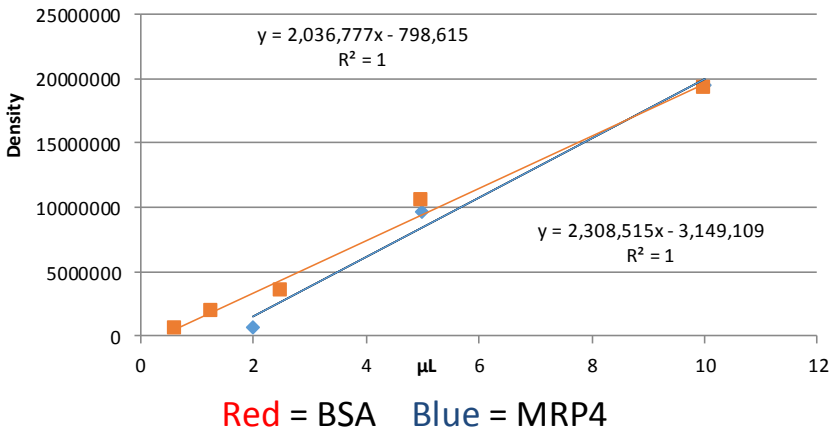

Red = BSA Blue = MRP4

Figure 4.12.3.1: Scaled up purification of Sf 9 MRP4 with C4C7. *Western blot A shows the purification profile and table B is the densitometry results from the western blot as a percent of the soluble fraction. Once concentrated, using a 50 kDa MWCO spin concentrator, MRP4 was quantified using the BSA gel in C (MRP4 indicated by the arrow), stain free imagining. The gradients of both BSA and MPR4 slopes plotted in graph D. Total (T), pellet (P), soluble (S), two flow through (Ft1 and Ft2), three wash (W1, W2 and W3) 5mM imidazole, 5 elution fractions (E1 – E5) and one resin fraction (Res) were loaded onto the western blot. An anti MRP4 primary antibody (1:100) and an anti-rat HRP secondary antibody (1:5000) was used.*

Western blot 4.12.3.1 A shows the purification profile of MRP4 using C4C7. Compared to the small scale trials only 20% of the solubilised MRP4 was bound to the resin halving the binding efficiency in this large scale purification. The addition of the 5mM imidazole increased the amount present in the wash steps by a considerable amount with 52% contained in the first wash step and 17% and 24% contained in the second and third step wash steps. Despite this increase in the wash steps the amount contained within the elution fractions was increased with the first two having 27.7 and 22.7% and the third 6.7%. Elution fractions 1-4 were pooled together equalling 8mL and concentrated to 250µL. Commercial protein assay kit will detected all protein in the sample, MRP4 and impurities. For this reason, the concentration was determined by SDS-PAGE as this way the purity of the sample can be assed and the actual amount of MRP4 calculated. The concentration was calculated by using the gradient of the two slopes in graph D (Figure 4.12.3 D) and the equation (Sample slope/BSA slope) x (BSA standard mg/ml). For the C4C7 sample the BSA slope = 2,036,777 and the MRP4 slope = 2,308,515 and plugging this into the equation: (2,308,515/2,036,777) x (0.2) = 0.22 mg/mL. This equated to 50 µg of MRP4 being produced. The purity was calculated by adding up the density of all the bands present in the 10µl lane (Figure 4.12.3.1 C) and then calculating the percentage the MRP4 band makes up out of the total. This makes the purity of MRP4 purified in C4C7 about 40%. There were two major contaminating bands a higher one at 120kDa and lower one at around 30kDa. It is unknown what these bands are; if they are breakdown products, proteins associated with MRP4 or contaminating proteins.

4.12.3.2 Native western blot aggregation analysis of C4C7 MRP4

Purified MRP4 was run on Native polyacrylamide gel to examine the aggregation and oligomeric states. SDS polyacrylamide gels are denaturing and reducing meaning that unless the protein is resistant to the reducing agents only monomers will be seen on gels or western blot. Due to the harsh nature of SDS, aggregated protein will become soluble and will show up as a band on the gel or western blot. Therefore, it would be difficult to determine if the membrane protein was initially aggregated. Native polyacrylamide contains no reducing agents and no SDS so aggregates will not enter the gel and collect in the wells.

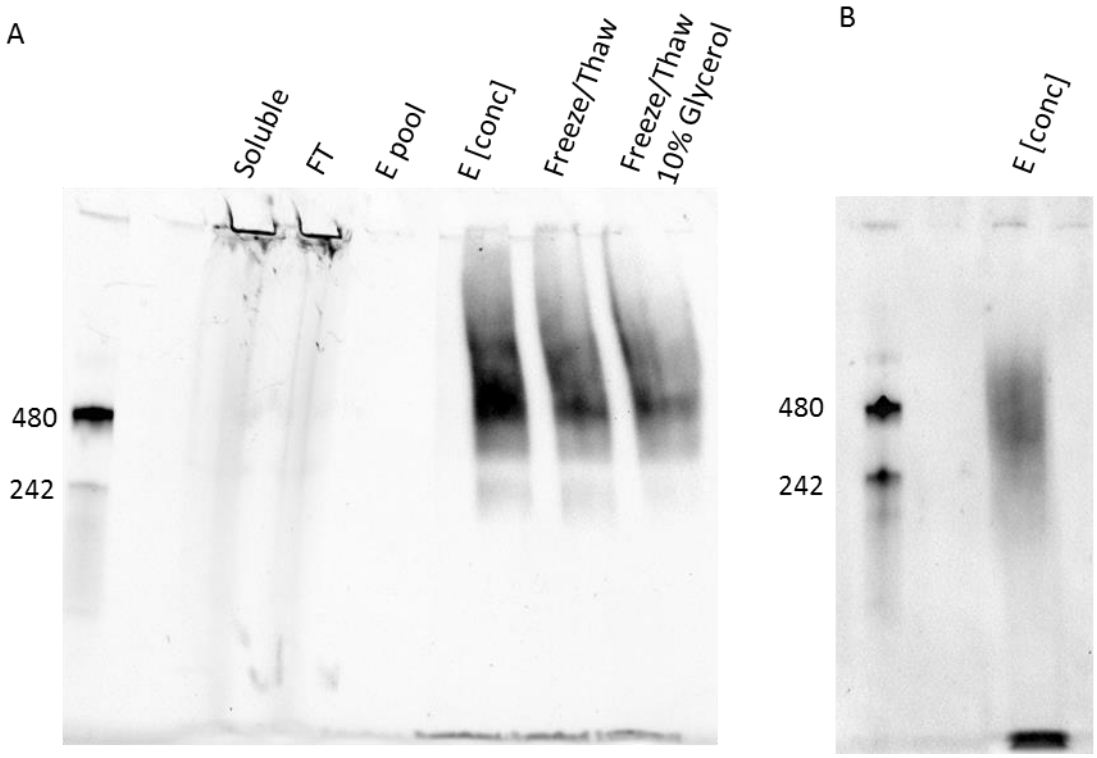

Figure 4.12.3.2: Aggregation checks of purified MRP4 with C4C7 using Native western blot. *Native western blot A shows the stability of the soluble, flow through (FT), pooled elution fractions (E pool), concentrated elution fractions (E [conc]) and two freeze thaw samples (using the concentrated elution fraction) with one containing 10% glycerol (Freeze/Thaw 10% glycerol). Native western blot B shows the stability of the concentrated elution sample (E [conc]) after 7 days at 4°C. An anti-his primary antibody with a HRP secondary antibody was used for both western blots.*

The stability of MRP4 was assessed using native western blots in figure 4.12.2.3. The soluble and FT fractions from the large scale purifications were run alongside purified MRP4, freeze thaw and time stability checks. Small amounts of aggregation were present in the wells of both the soluble and FT fractions but no distinct bands appeared in these two lanes. This was most likely due the low amounts of MRP4 in these two fractions. Although MRP4 is visible on SDS polyacrylamide western blots in these two fractions (Figure 4.12.2.3 A), native western blots generally require more protein than was present in these samples to be visible. The pooled purified elution fractions (E pool) showed no signs of aggregation showing that after purification MRP4 was still stable, but no bands appeared in the lane. This would have been again because not enough protein was contained in the sample to be visible. After concentrating (E conc) MRP4 was still stable and a large band appeared at around 480kDa with potentially a lighter band at a higher molecular weight and also one at a lower molecular weight around 242kDa. After one freeze thaw cycle MRP4 did not aggregate and the same bands appeared as in the concentrated sample. A freeze thaw cycle was also tried with the addition of 10% glycerol and MRP4 was not aggregated and showed the same banding pattern as the previous two lanes. After leaving MRP4 for 7 days at 4^{o}C the stability was checked on a separate Native western blot and showed no signs of aggregation and contained one large smeared band at around 480 kDa.

These results show that during the purification and concentration, MRP4 did not aggregate but was only detectable after concentrating. MRP4 was able to withstand freeze thaw cycles regardless of the addition of 10% glycerol. The reason for testing the freeze thaw is to determine if MRP4 can withstand this so it can be frozen, stored, and not aggregate allowing it to be used in functional and structural studies later. The 7 days stability test again shows MRP4 can be left at 4^{o}C for a week and not aggregate indicating it is still stable so if needed MRP4 can be stored at 4^{o}C and later used for functional and structural studies.

The most prominent band on the native western blot was at 480 kDa. The molecular weight of MRP4 is 150 kDa and is not known to form dimers or trimers. There are a handful of proteins that

can bind to MRP4 in humans but whether or not these are also expressed in *Sf* 9 insect cells is unknown or if the binding affinity is high enough to be co-purified along with is also unknown. These reasons then cannot explain why the most prominent band on this native gel is around 480kDa. The addition of the detergent micelle around MRP4 will add to the molecular weight but not enough to increase the weight to 480kda. What this one most prominent band does show is that there is one main species of MRP4 after purification which can remain stable.

4.12.3.3 Size Exclusion Chromatography (SEC) aggregation analysis of C4C7 MRP4.

The MRP4 purified with C4C7 was examined using size exclusion chromatography to investigate if there is any aggregation, therefore checking the stability, and the oligomeric state. Larger particles elute from the column first and typically aggregates will elute during the void volume. If MRP4 has multiple oligomeric states these will elute off at different retention times with higher oligomeric states, trimers and dimers, eluting first followed by monomers. This will result in multiple peaks on the elution profile of SEC but can only be confirmed if the eluate of these peaks are run on Native polyacrylamide gels. SDS polyacrylamide gels are reducing and they will only result in one monomeric band on the gel or western blot unless the protein is resistant to SDS and reducing agents.

SEC was performed under two different conditions, the purification buffer either contained 1xCMC C4C7 or 5xCMC DDM. The Calixar detergents are known to interact with the proteins forming salt bridges and creating a more stable protein as previously shown (Matar-Merheb, Rhimi et al. 2011). Normally during SEC using detergents 1 CMC of that detergent has to be kept in the purification buffer to keep the membrane protein stable. However, because of the ability of C4C7 to bind with MRP4 it was thought that the purification buffer could contain a different detergent such as DDM and it would maintain its stability as the C4C7 would stay bound to MRP4. The Calixar detergents are very expensive and although only 1 CMC is needed in the SEC buffer,

large volumes are required making it very costly. C4C7 absorbs at 280nm, which is the same wavelength used to detect proteins during SEC, making it very hard to produce a good base line. Not only is this an issue, but because of its spectral properties C4C7 can interfere in some functional studies such at tryptophan assays and ATPase assays. So if the detergent used in the SEC purification buffer could be switched to a conventional detergent such as DDM it would help counteract these problems and keep costs down.

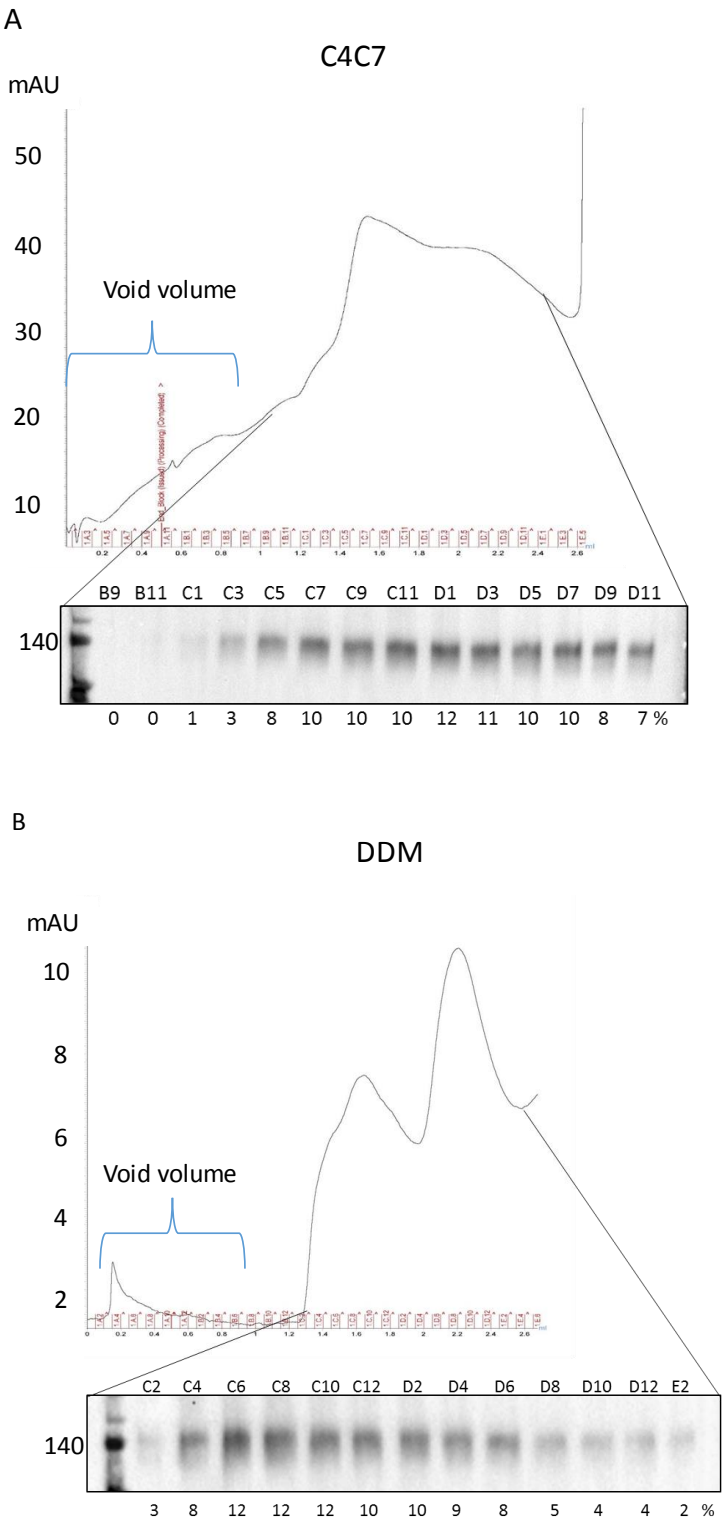

Figure 4.12.3.3: SEC of C4C7 purified MRP4. *SEC profiles A and B show the mAu at 280nm results from 6µg of Sf 9 MRP4 which was solubilised and purified in C4C7 and injected into a Superdex 200 1/150 column. A 1 CMC C4C7 buffer was used in A and a 5 CMC DDM buffer used in B. The western blots in A and B show the presence of MRP4 in each of the fractions with the percent of the whole amount below. An anti-MRP4 primary antibody (1:100) and an anti-rat HRP secondary antibody (1:5000) was used.*

The SEC profile A in figure 4.12.3.3 contained 6µg of purified MRP4 and shows a single broad peak which the western blot confirms is MRP4. The base line was not level at the beginning of the run due to the afore-mentioned spectral interference from C4C7 making the height of the peak hard to determine. But if the base line is taken as the bottom of the peak, around 2.6 mL, it would be around 22mAu and the top of the peak is around 43mAu making the height around 21mAu. MRP4 started to elute at 1.2mL, fraction C1, where there is a slight increase in the steepness of the peak. The peak continues until fraction D11 with the majority of MRP4 contained between fractions C7 and D7. No fractions were analysed after D11 but more MRP4 could still be eluting as D11 still contains about 7% of the total amount of MRP4 eluted. The sharp increase in the absorbance seen after 2.6ml was due to C4C7 eluting from the column as these are small molecules and are eluting off at the end of the column. The void volume contains no peaks showing the MRP4 was still stable after purification.

The SEC profile B in figure 4.12.3.3 shows two peaks when using 5 CMC DDM in the purification buffer. The first peak contains the majority of MRP4 as shown in the western blot. This first peak starts at fraction C2 where MRP4 starts to elute at ≈1.3mL, which is comparable to using C4C7 in panel A, and continues to D4. The second peak contains small amounts of MRP4 from fraction D6 to E2 even though the peak has a higher absorbance value. The end of the peak does coincide with that of the one in the C4C7 profile. The large trough between these two peaks matches a much smaller dip happening with C4C7 at around fraction D2. The trough is more prominent in the DDM profile as the background absorbance is reduced because C4C7 is not in the SEC purification buffer. DDM also allows for having a more stable base line due to the reduced background. No peaks are present in the void volume showing DDM can be used in the SEC purification buffer without causing MRP4 to aggregate. Again 6ug of MRP4 was loaded onto the column and the highest point of the second peak is around 10.8mAU making it half the height as with C4C7.

4.12.4 Further purification with C4C7 (work carried out on second trip to Calixar)

During the first trip to Calixar we were able to show that C4C7 was able to solubilise and purify MRP4 at both a small and larger scale but was not fully optimised. After producing a large amount of *Sf* 9 MRP4 membranes a second trip was undertaken to improve the purity and concentration of MRP4 using C4C7.

4.12.4.1 Reproduction of previous purification conditions

A trial purification was performed to make sure the new membrane preparation could be purified comparably to the previous membranes. 40mL of soluble MRP4 was bound to 5mL cobalt resin (8:1 soluble MRP4:resin ratio) for 2 hours and then purified using 3 x 5 CV 5mM imidazole wash and eluted with 5 x 1 CV 200mM imidazole.

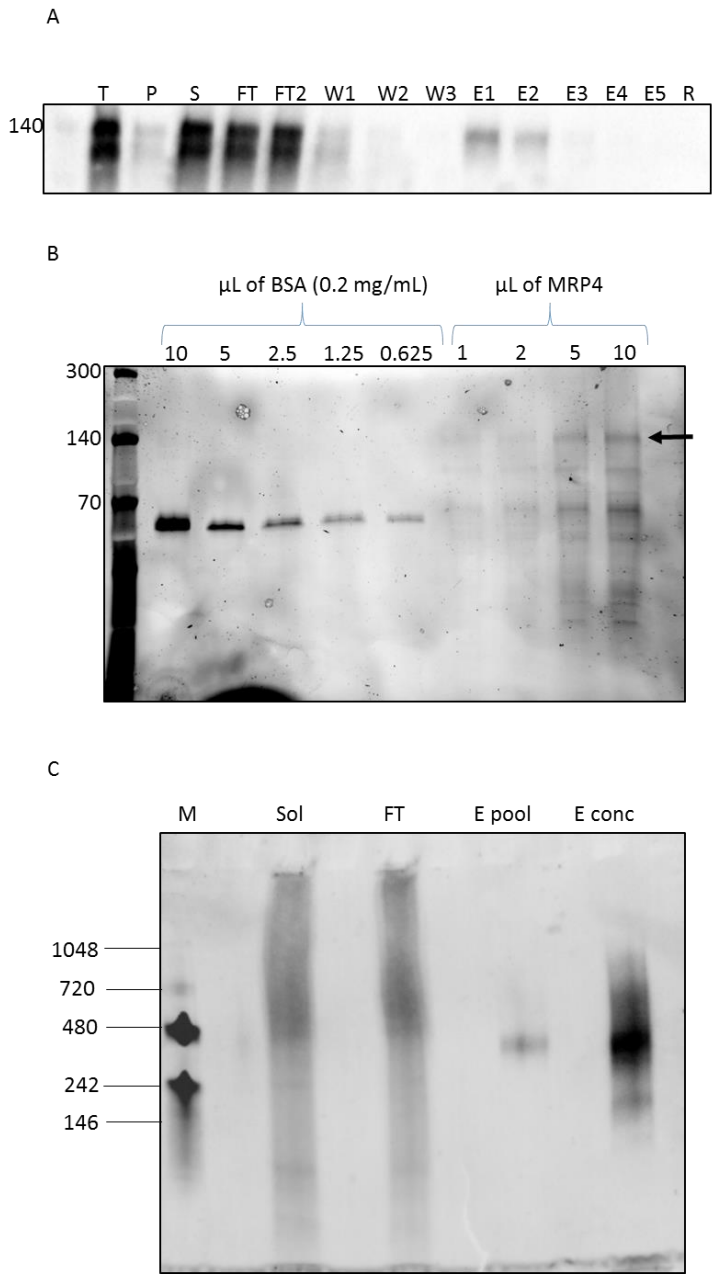

Figure 4.12.4.1: Reproduction of previous purification conditions. *Western blot A shows the purification profile of MRP4 purified with C4C7 using a cobalt resin. Total (T), pellet (P), soluble (S), two flow through (Ft1 and Ft2), three wash (W1, W2 and W3) 5mM imidazole, 5 elution fractions (E1 – E5) 200mM imidazole and one resin fraction (Res) were loaded onto the western blot. 1, 2, 5 and 10 µL of purified and concentrated MRP4 (indicated by the arrow) loaded on to the SDS gel B against BSA standards, which were used for quantification, stain free imaging. Native western blot C shows the aggregation and oligomeric state of MRP4 purified in C4C7. The soluble (Sol), flow through (Ft), pooled elution (E pool) and concentrated elution (E conc) fractions was loaded onto the native western blot. An anti MRP4 primary antibody (1:100) and an anti-rat HRP secondary antibody (1:5000) was used on blot the western and native blot.*

Western blot (A) in figure 4.12.4.1 shows the purification profile of this trial purification that was performed under the same conditions as the previous large scale Calixar purifications. One clear difference between this and the previous purifications is the presences of a double band in the total (T) lane, where as previously only one band was present (Figure 4.12.3.1). This could show that there are two species of MRP4 in these membranes compared to the one in previous purifications and could have an impact on the purifications. This double band is also present in the pellet (P), soluble protein (S), both of the flow-throughs (FT 1 and FT2) and the first 5mM imidazole wash step (W1). It is clear that C4C7 was still solubilising MRP4 as the majority of MRP4 appeared in the soluble band compared to the pellet. Large amounts of MRP4 were visible in both of the flow-through fractions indicating reduced binding. There was a faint MRP4 band in the first wash step but this was not uncommon when compared to the previous C4C7 purifications. Interestingly only the upper of the two bands that appear in the T, P, S, FT 1, FT 2 and W1 fractions is visible in the first two elution fractions. This could indicate that only the upper of the two bands was able to bind to the cobalt resin with enough affinity to be eluted.

The SDS polyacrylamide gel in figure 4.12.4.1 B shows the quantification of MRP4. MRP4 concentrated to 28µg/mL. There is a very dense band around 70kDa which is the major impurity on the sample. As mentioned before this could be breakdown of MRP4 and it is at the correct molecular weight to be half of MRP4. A number of other bands appear below this 70kDa impurity and one between it and MRP4. Although different membranes were used in this experiment compared to the previous Calixar purifications the expression levels were the same. The concentration of MRP4 was much lower than expected compared to the previous large scale Calixar purification, where the same volume of soluble MRP4 was purified and concentrated to the same volume (250µL), but the concentration was around 10x higher at 220µg/mL. These results shows under these conditions the new membranes were not purifying to the same concentration as previously. As there was a large amount of MRP4 present in the flow-through fractions it was thought MRP4 was not binding to the cobalt resin as efficiently as previously.

The native western blot in figure 4.12.4.1 C shows the aggregation and oligomeric state of MRP4 purified using C4C7.The soluble protein and flow through fractions show one main species, indicated by the darker patch between 480 and 720 kDa. These two fractions would contain other proteins and large amounts of C4C7 which could contribute to the smearing of the bands. There is no aggregation as indicated by the lack of MRP4 in the wells of the gel unlike in the previous large scale attempt (Figure 4.12.3.2 A). No aggregation is present in the pooled elution and concentrated elution fractions indicating MRP4 was stable throughout the purification process. The pooled elution fractions show a single, well defined band between 242 and 480kDa. After concentration (E conc) there are two bands with the most prominent at the same level as the pooled elution fractions and a fainter one at around 146kDa. The lower band in the concentrated sample is very close to the molecular weight of MRP4 (150kDa) and the upper band is potentially around 300kDa which would be the molecular weight of a MRP4 dimer. Two bands are also present in the concentrated fraction from the previous large scale attempt (Figure 4.12.3.2 A) but these both run at a slightly higher molecular weight to that shown in figure 4.12.4.1 C. The bands in figure 4.12.4.1 C show a close resemblance to how MRP4 would behave if there were monomers and dimers present. So although MRP4 is not known to form dimers and the one native western (Figure 4.12.3.2 A) shows two bands but not at the correct molecular weight for monomer and dimers the other in figure 4.12.4.1 C does show the two bands at the correct molecular weights indicating there could be dimer formations.

4.12.4.2 Optimisation of the purification, cobalt vs nickel resin

The first trial purification showed these new membranes did not bind with a great affinity to the cobalt resin. Nickel resin was the only other resin that was available at the time at Calixar so an experiment comparing the two resins was set up. As large amount of MRP4 was present in the second flow though from the previous experiment (Figure 4.12.4.1) it was used and bound to fresh cobalt or nickel resin. To also improve the concentration and purity the resin volume was change to a 15:1 soluble MRP4 to resin ratio, benzonase was added to the flow-through as the solution was very viscous and could have had DNA contaminants reducing binding efficiency and a 20mM wash step was added to reduce the amount of impurities.

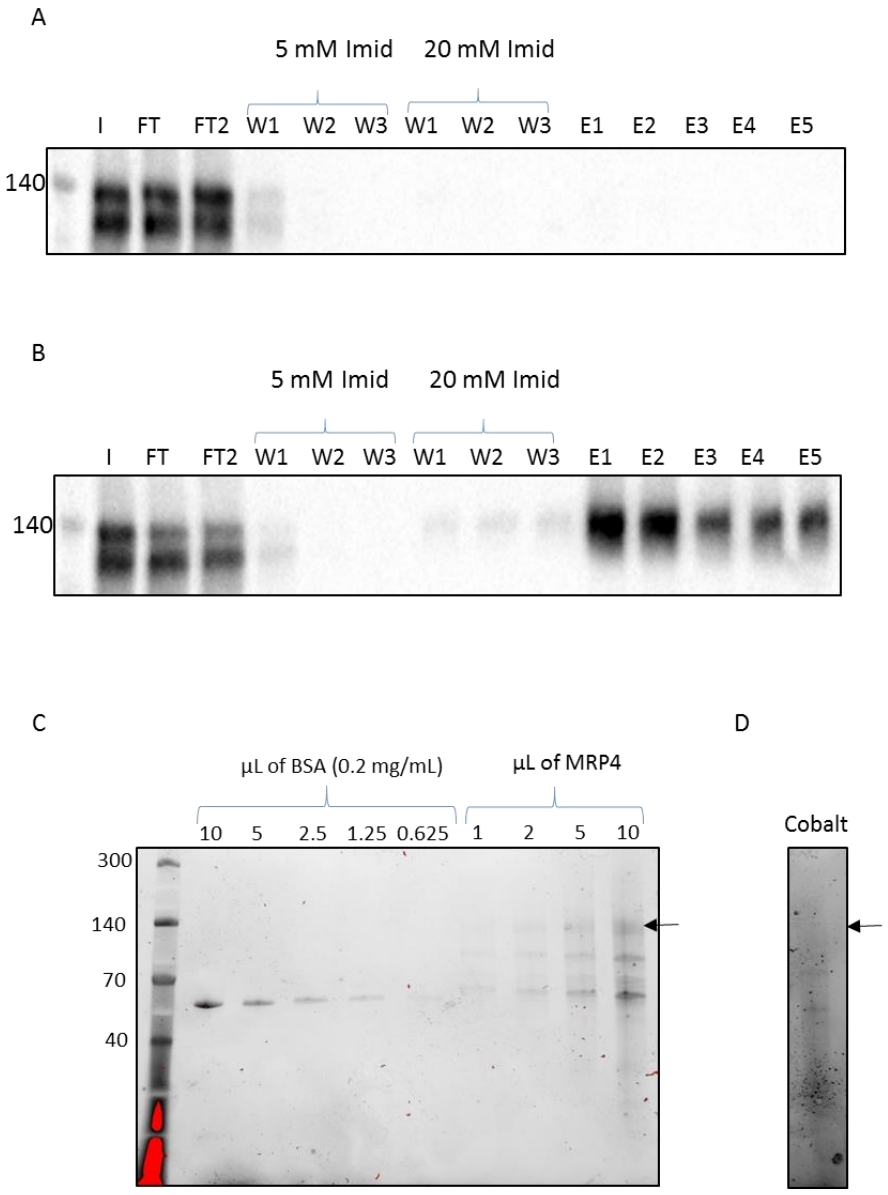

Figure 4.12.4.2: Purification of MRP4 in C4C7 with nickel and cobalt resin. *The flow-through of the previous experiment (4.12.4.1) was used in a test to determine if nickel resin was better than the previously used cobalt resin. Western blots A and B shows the purification profiles of the cobalt and nickel resins respectively. On the western blots the input (I) is the flow-thought form previous experiment. They also show two flow-through (FT1 and FT2), three wash steps (W1 –W3) from 5mM and 20mM imidazole and five elution fractions (E1-E5) 200mM imidazole. SDS gel C shows the quantification of MRP4 from the nickel resin, with 1, 2, 5 and 10µL of concentrated MRP4 loaded against a BSA standard. D shows the 10µL lane from the SDS quantification gel of MRP4 from the cobalt resin. The arrows on both quantification gels C and D indicate MRP4. An anti MRP4 primary antibody (1:100) and an anti-rat HRP secondary antibody (1:5000) was used on the westerns blots.*

Western blots A and B show the purification profiles of the cobalt and nickel resins with the input (I) being the second flow-through from the previous purification. There are clear visible differences between the cobalt and nickel resins purification profiles; with the cobalt resin only having bands in the input (I), flow-through (FT 1 and FT 2) and first 5mM imidazole wash step (W1). There is no decrease in the MRP4 band over the two flow-through fractions and no bands present in the elution fractions indicating no binding or elution of MRP4. The nickel resin shows a much more typical purification for MRP4, similar to what has been observed in this study previously with cobalt (Figure 4.12.3.1), although the double band is still present. There is a decrease in the top band in the two flow-through fractions showing binding to the nickel resin. Small amounts of the double band appear in the first 5mM imidazole fraction (W1) and small amounts of only the top band appear in the all of the 20mM imidazole fractions. The elution fractions show only the top band with the majority eluting off in the first two fractions (E1 and E2). This shows that the top band most likely is full length expressed MRP4-his containing the hexa-histidine tag as it is the only band that is eluted off and the lower band could be a truncated version of MRP4-his as the antibody used was an anti-MRP4 antibody.

Elution fractions 1-4 from both the cobalt and nickel were concentrated to 75 and 100µl respectively. Only the concentrated elution fractions from the nickel resin could be quantified and gave a concentration of 119µg/mL. There are two main impurity bands around 70kDa and 100kDa. These were also seen in the previous purification experiment (Figure 4.12.4.1) but unlike the previous attempts there are not significant contaminant bands below 70kDa in size this time. The addition of the 20mM wash step was most likely the cause of this increase in purity as the higher imidazole concentration would have washed off these impurities which the previous 5mM imidazole would not have.

These results clearly show the nickel resin out performs the cobalt resin using these new membranes. It is unknown why these membranes appear to bind with much higher affinity to the nickel resin compared to cobalt and why the cobalt resin preformed so poorly this time. This

double band that appears in these membranes may have an effect on the binding. Nickel resin was used for further experiments.

4.12.4.3 Purification optimisation – varying the concentration of NaCl

The previous results showed that using a nickel resin in combination with a 20mM imidazole wash step both improved the purity and concentration of MRP4. Sodium chloride (NaCl) concentrations in the purification buffer can also have an effect on the binding capabilities of affinity tags. To investigate this a normal PBS buffer containing 150mM NaCl and a high 300mM NaCl concentration were examined. The amount of Sf 9 MRP4 membranes used was increased to 100mL of soluble MRP4. Due to the large volume use and the cost of C4C7 only 5xCMC was used. The ratio of soluble MRP4 to resin was increased to 20:1 as this would keep the volume of resin down allowing for easier purification and it was thought at this point the resin was not getting saturated. Benzonase was also added after solubilisation to break down any DNA contaminants.

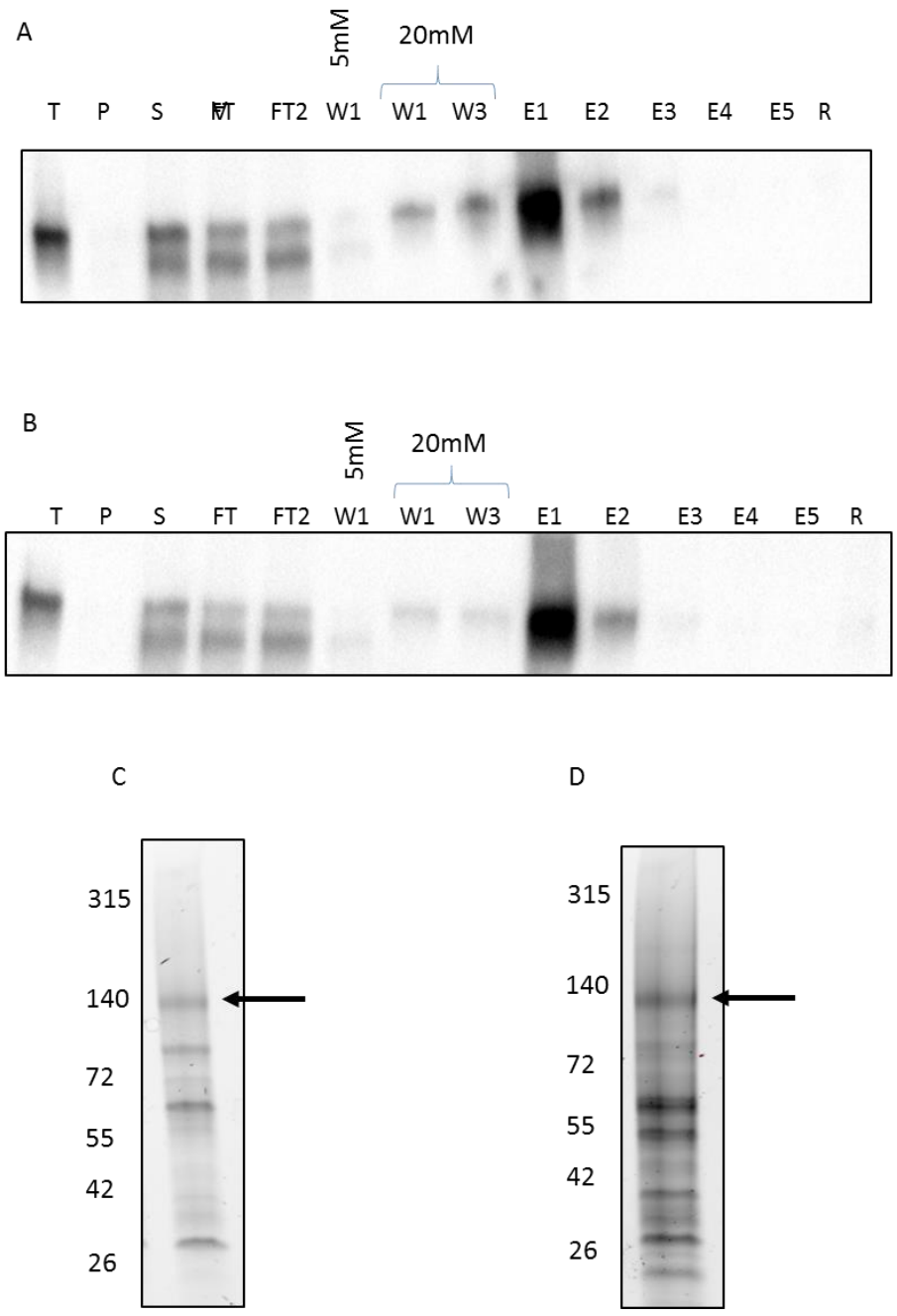

Figure 4.12.4.3: Varying the concentration of NaCl during purification. *Western blots A and B show the purification profile from the 150mM and 300mM NaCl PBS buffers respectively. The total (T), pellet (P), soluble (S), first and second flow-through (FT1 and FT2), first 5mM imidazole wash (W1 5mM), first and last 20mM wash (W1 and W3 20mM), five elution (E1 – E5) and a resin (R) fractions loaded on each western blot. An anti MRP4 primary antibody (1:100) and an anti-rat HRP secondary antibody (1:5000) was used on the westerns blots. SDS gels in C and D shows the concentrated elution fractions from the 150mM and 300mM NaCl PBS purifications respectively with MRP4 indicated by the arrow.*

Western blots A and B show the purification profiles from PBS purification buffer containing either 150mM NaCl or 300mM NaCl respectively. These results are very similar with both showing a single band in the total fraction and a double band in the soluble and two flow-through fractions. Previously the double band had also shown up in the total fraction, so it is unclear whether this lower band is a breakdown product, or MRP4 that is not fully expressed. However the MRP4 antibody is still able to detect it. Interestingly the lower band appears in the 5mM wash step in both conditions indicating reduced binding of the protein in this band. The upper band appears in both the 20mM wash steps and the first three elution fractions for both conditions. The majority of MRP4 is eluted in the first elution. No MRP4 is present in either of the resin fractions indicating it all has eluted off.

The SDS gels in figure 4.12.4.3 show the concentrated elution fraction from the 150mM and 300mM PBS purifications. The protein purified in 150mM NaCl was concentrated to 200µL at a concentration of 463 µg/mL (92.6 µg). Likewise the protein purified in 300mM NaCl was concentrated to 250µL and a concentration of 403µg/mL (88.6 µg) making the amount purified fairly similar. The purity on the other hand is vastly different between the two conditions. Using 150mM NaCl only three contaminating bands below the MRP4 band appear and the purity was at 23% compared to 300mM NaCl with at 12%. The 300mM NaCl concentrated sample appears to have many contaminating bands with two of them having a higher density than the MRP4 band. Because all the bands are lower than MRP4 this could indicate the NaCl does not contribute to increased binding but could interfere with the stability of MRP4 as the lower band could be break down products.

4.12.4.4 Stability of MRP4 purified with C4C7

The concentrated MRP4 from the 150mM and 300mM NaCl were examined used Native western blot to test for the aggregation and oligomeric state. They were tested straight off the column in the absence and presence of a reducing agent. The purified protein was concentrated and then diluted back to its original concentration for a more fair comparison and finally tested after a freeze thaw cycle.

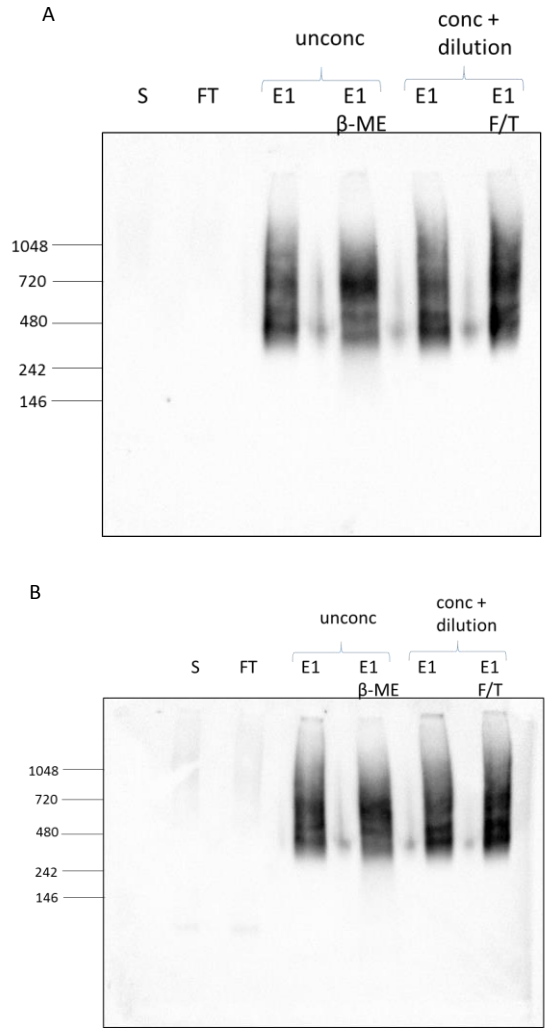

Figure 4.12.4.4.1: Native western blots of 150mM and 300mM NaCl purifications. *A and B are native western blots of the first elution fraction from the 150mM and 300mM NaCl purification respectively. Elution fraction 1 (E1) was loaded as an un-concentrated (unconc) sample and in the presences of a reducing agent 2-mercaptoethanol (E1 β-ME). E1 was concentrated and then a sample diluted back to the original concentration (conc + dilution) and also underwent a freeze-thaw cycle (F/T). An anti MRP4 primary antibody (1:100) and an anti-rat HRP secondary antibody (1:5000) was used on the westerns blots.*

The Native western blot shows (Figure 4.12.4.4.1) the stability of samples taken from the 150mM and 300mM NaCl purification. No bands were detected in the soluble and flow-through samples although they had previously appeared in the figure 4.12.4.1. Bands in the sample taken from the first elution fraction (E1) are not well defined in any of the conditions on either of the blots. The banding pattern is similar between all the conditions and both blots with two bands appearing at around 480kDa and just below and an upper band around 720kDa. No aggregation happens during purification as no aggregates appear in the well of the un-concentrated first elution fraction showing MRP4 is still stable after purifications. The addition of a reducing agents 2-mercaptoethanol was thought to stop MRP4 from creating potential dimers and produce a single band at 150kDa. This was not the outcome and the most prominent band in this sample was actually around 720kDa. After concentrating, and diluting back to the original concentration, the banding pattern did not change from the sample taken directly from the first elution fraction (E1). Even after a freeze/thaw cycle the banding pattern did not change indicating that even after concentrating and a freeze/thaw cycle no aggregation is present and MRP4 is still stable.

The elution fractions from both purifications were pooled together and then run through SEC. As both of the sample contained impurities it was thought that SEC might be able to eliminate of some of these impurities and increase the purity of the sample along with testing the stability.

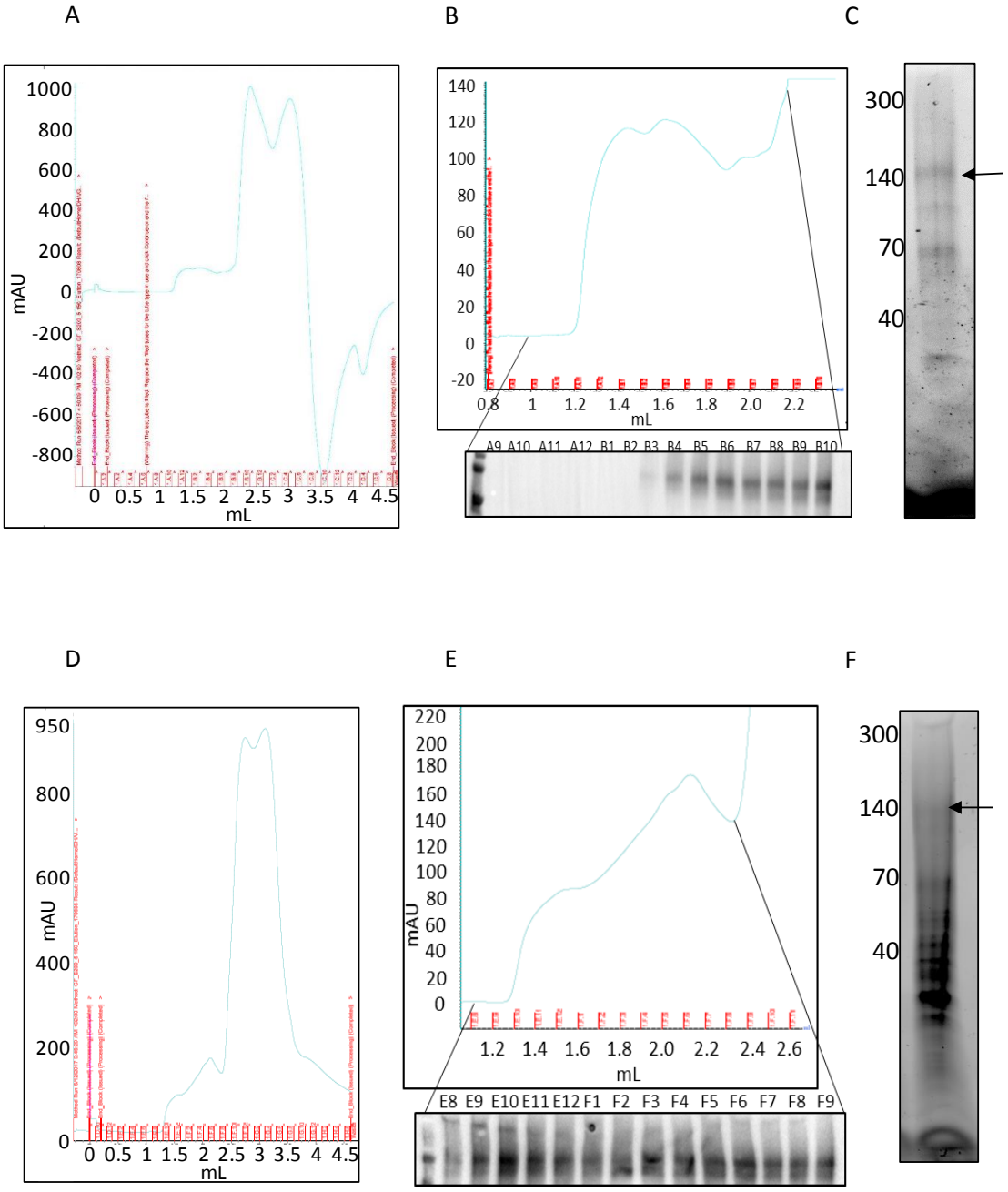

Figure 4.12.4.4.2: SEC of purified MRP4 with C4C7 using a C4C7 and DDM SEC buffer. *A, B and C are from the C4C7 SEC buffer and D, E and F show the results when a DDM buffer is used. A and D are the whole SEC readout measured in mAu. B and E are the zoomed in versions showing the first peak of the readout with the western blots from each fraction below. An anti MRP4 primary antibody (1:100) and an anti-rat HRP secondary antibody (1:5000) was used on the westerns blots. C and F are SDS gels showing MPR4 after SEC and concentration.*

The SEC shows that MRP4 is still stable when purified in the presences of either C4C7 or DDM in the buffer as no aggregation peaks appear in the void volume (Figure 4.12.4.4.2). Using C4C7 in

the SEC purification buffer shows and increase in 280nm trace around 1.2mL, the same as previous results (Figure 4.12.3.3 A). Unlike the previous results were MRP4 is eluted off after 1.3mL, this time MRP4 elutes off at 1.7mL and continues to 2.3mL. A large percentage is still being eluted off as the last fraction (B10) contains a high amount of MRP4. Whereas the previous results most of the MRP4 had been eluted off by 2.3mL. Because the elution fractions were combined from 150mM and 300mM NaCl purifications the level of purity cannot be directly compared to either one of these. The purity of MRP4 after SEC in C4C7 was around 25% and was at a concentration of 8 µg/mL. Using DDM in the SEC purification buffer shows similar results to the previous results (Figure 4.12.3.3 B) with MRP4 starting to elute off at 1.2mL until 2.5mL although the MRP4 band is not clearly defined on the western blot. The purity and concentration could not be easily assessed because of the low density of the MRP4 band and high amount of background. But visually the purity of MRP4 after SEC with C4C7 is clearly higher than with DDM as less contaminating or breakdown band appear.

4.12.4.5 Large scale purifications with C4C7

A final large scale purification was conducted using C4C7 with optimal purification conditions. These were using nickel resin with 150mM NaCl purification buffer with the addition of benzonase and the soluble to resin ratio at 20:1. This large scale purification was done using 200mL of MRP4 solubilised with C4C7 twice the amount as figure 4.12.4.3 and 5 x the amount as figure 4.12.4.1.

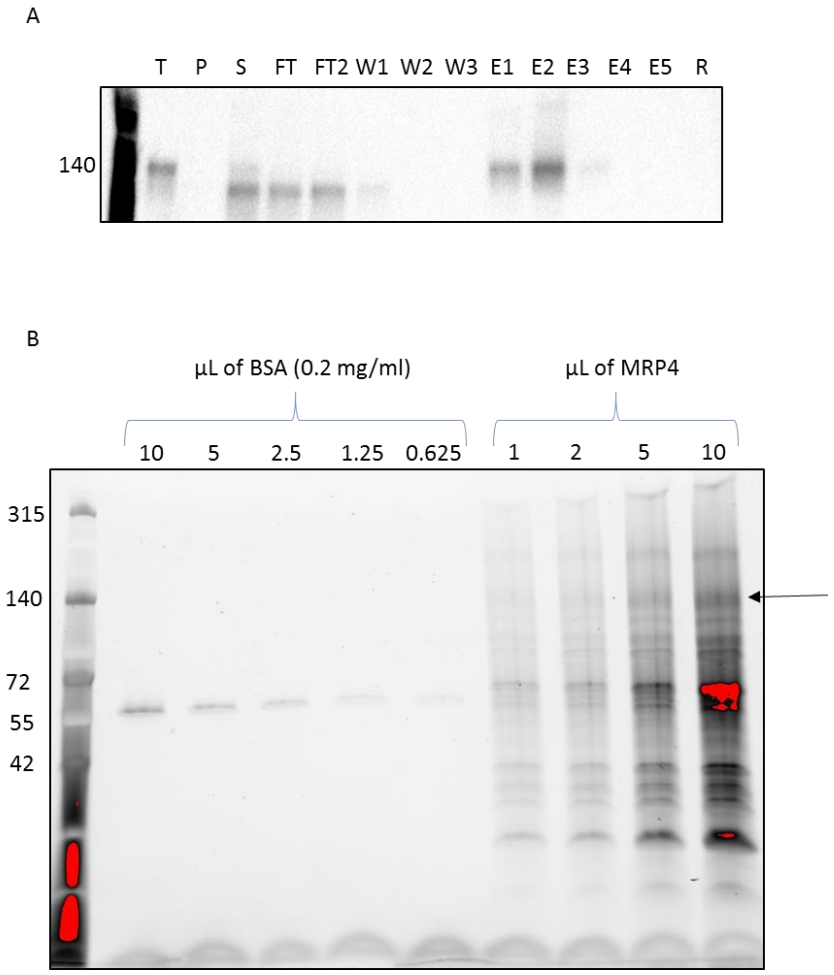

Figure 4.12.4.5: Large scale purification of MRP4 with C4C7. *Western blot A shows the purification profile of the large scale purification. An anti MRP4 primary antibody (1:100) and an anti-rat HRP secondary antibody (1:5000) was used on the westerns blot. SDS gel B is the quantification of purified and concentrated MRP4. 1, 2, 5 and 10µL of the concentrated sample were loaded against a set of BSA standard. MRP4 is indicated by the arrow.*

The western blot in figure 4.12.4.5 showed the soluble fraction mainly contains a band at a lower molecular weight compared to the total lane. This could show that increasing the volumes during solubilisation lead to some breakdown on MRP4. Interestingly this lower band also appear in the two flow through fractions and the first wash fraction showing that this was not binding to the resin and was easily washed off. The elution fractions on the other hand only contain bands at the same molecular weight as the total lane indicating that MRP4 at the correct molecular weight was being eluted off. After concentration to 550 µL MRP4 was quantified at 434 µg/mL. This shows that the quantity of this large scale is very similar to figure 4.12.4.3 as twice the amount of membrane was using in this large scale and it produced about twice the amount of MRP4 (238.7

µg) but the purity severely dropped. Previously the highest purity using C4C7, and these membranes during the second trip to Calixar, was 23% and during the large scale purification the purity was only at 3.75%. This shows that although this large scale purification produced large amount of MRRP4 the purity was at its lowest amount during these studies.

The Calixar purifications showed that calixar detergents C4C5 and C4C7 are able to purify MRP4 better than conventional detergents. Out of the two C4C7 appeared to be able to increase the percent eluted off in the elution fraction which lead to C4C7 being chosen for larger scale purification allowing for the purity and stability to be tested. In all stability tests MRP4 appeared to be stable; no aggregation peaks showed up during SEC, the Native gels and western blots contained no aggregation in the wells and only one main band of MRP4 was visible. Interestingly during the first trip the *Sf* 9 MRP4 membranes used were able to bind to cobalt resin and produce 50 µg of MRP4 at a 40% purity. The second trip using different Sf 9 MRP4 membranes were not able to bind to the cobalt resin and nickel resin was used. The highest purity using the nickel resin was 23% and the relative quantity of MRP4 produced was around half compared to the first set of Sf 9 MRP4 membranes and purifications. This shows that have good quality starting material can have a huge influence on the concentration and purity of the final sample.

4.13 SMA polymer purification

SMA polymers have been shown to have solubility efficiency and increased thermostability. SMA 2000 was used to solubilise MRP4-his_6 (MRP4) from *Sf* 9 membranes for purification as this solubilising agent had one of the highest solubilising efficiency and showed enhanced thermostability compared to conventional detergents. SMA2000 was shown in the small scale initial purification trials, in the previous chapter, to be better than conventional detergents and showed promise for effective purification. In order to produce the highest concentration and highest purity of MRP4 the purification condition were optimised. Purifications using the SMA polymer were described in (Gulati, Jamshad et al. 2014, Morrison, Akram et al. 2016) and used as a starting point for the optimisation. All solubilisations were performed using a wet pellet weight of 30mg/mL and 2.5% SMA 2000.

4.13.1 MRP4 elution profile.

After following the recommended conditions for solubilisation and binding to a nickel resin overnight at a ratio of 10:1 (solubilised protein : resin column volume), the first step was to investigate the optimal concentration of imidazole to elute MRP4. The resin with bound MRP4 was washed with 5 x 10 CV of 20mM imidazole and then with 2 x 10 CV 40mM imidazole. One CV of 60 – 400mM imidazole was used to determine the concentration at which MRP4 elutes off the nickel resin. By comparing the density of each band to the soluble fraction the percent contained within each fraction can be quantified.

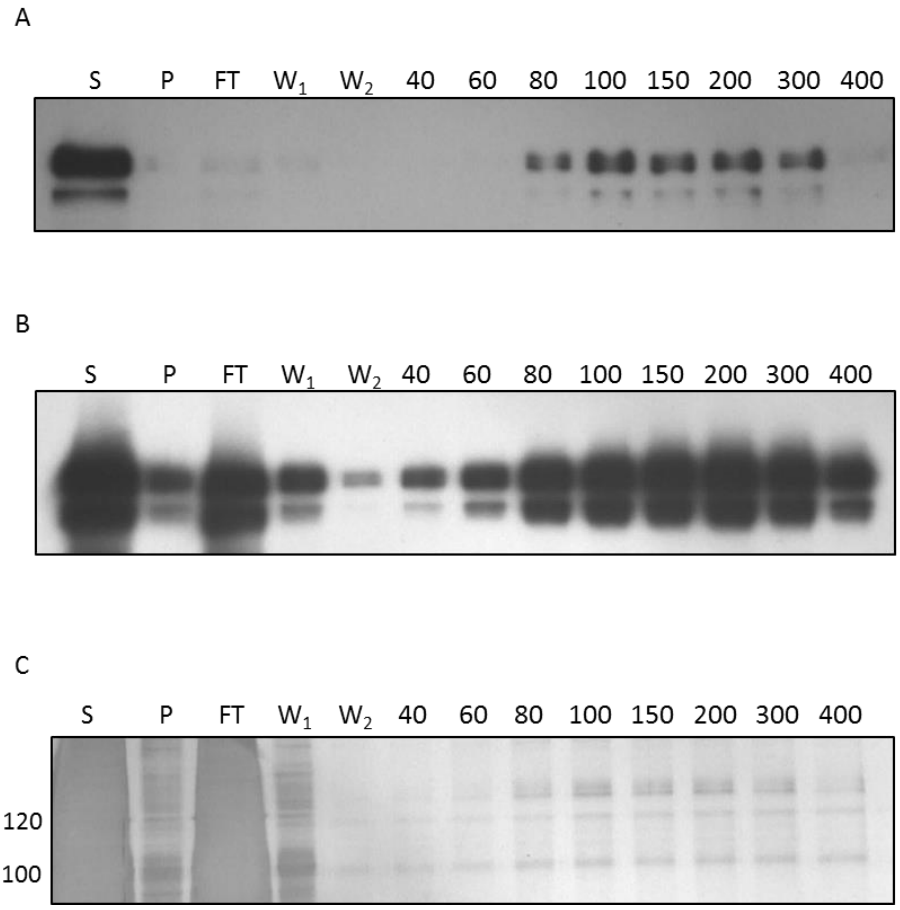

Figure 4.13.1: Elution profile of MRP4 with increasing concentrations of imidazole*. Western blot A and B shows the elution profile of MRP4 with increasing concentrations of imidazole with an anti-his and anti-MRP4 primary antibody respectively. C is a silver stain SDS gel showing the same profile. Soluble (S), pellet (P), flow-through (FT), the first two 20mM imidazole wash step (W_1 and W_2) and the first 40mM imidazole wash step (40) fractions were loaded on the western blots and silver stain gel alone with elution fraction from 60 - 400mM imidazole.*

Both blots show that the majority of the MRP4 was successfully solubilised by SMA 2000, with very little in the pellet. Most of the protein bound to the nickel resin as shown by the fainter bands in the flow through, although perhaps it seems there is more in the flow though using the anti-MRP4 antibody than there is when using the anti-his antibody, however this could just be related to the differing exposure levels. Both show little MRP4 in the 20mM imidazole washes, a small amount comes off with 40mM and 60mM imidazole, the MRP4 starts to elute largely using 80mM imidazole.

A silver stained SDS gel was used to detect all proteins in the elution profile as this technique shows total protein, not just MRP4. Large amounts of protein are detected in the soluble fraction but no MRP4 was visible because it was masked by all the other proteins present in the sample. On the whole much less protein is present in the pellet showing that SMA solubilisation was successful. The flow-through fraction contains a large amount of protein and this is expected as all proteins, other than the bound MRP4, would be visible in this fraction. The first 20mM wash steps show the largest amount of proteins of all the wash steps, indicating most of the weakly bound proteins are washed off during this first wash step. The second 20mM wash step and the 40mM wash only contained small amounts of protein with a faint MRP4 band indication some loss of MRP4 during these wash steps. The elution fractions show that small amounts of MRP4 are eluted off at 60mM imidazole with an increased amount at 80mM imidazole. Slightly higher levels of MRP4 are seen at 100mM -200mM imidazole with a decrease at 300mM and a considerably smaller amount in the 400mM imidazole fraction. Overall the profile for MRP4 is comparable to the Western blots. However the silver stain also shows the presence of contaminant bands which are present in all wash and elution fractions.

These results together show that SMA 2000 is able to solubilise MRP4 and bind to the nickel resin used, and MRP4 is eluted at significant levels using an imidazole concentration of 80-100mM.

4.13.2 Purification of MRP4 using nickel and cobalt resins.

Nickel resin has commonly been used in affinity purifications, but the hexa-histidine tag can also bind to cobalt resin. Although cobalt resin has a reduced binding capacity, it can lead to higher purity. The reduced binding capacity of the cobalt resin would not be a problem in the study as the amount of MRP4 being purified would never reach the binding capacity, but may lead to higher purity. The established protocol for purifying with SMA was employed here where after binding to the resin overnight at a soluble MRP4 to resin ratio of 10: 1, the resin was washed with 5 x 10 CV of 20mM imidazole, then with 2 x 10 CV 40mM imidazole and finally with 1 CV 60mM imidazole, followed by 5 x 1 CV 200mM imidazole for elution.

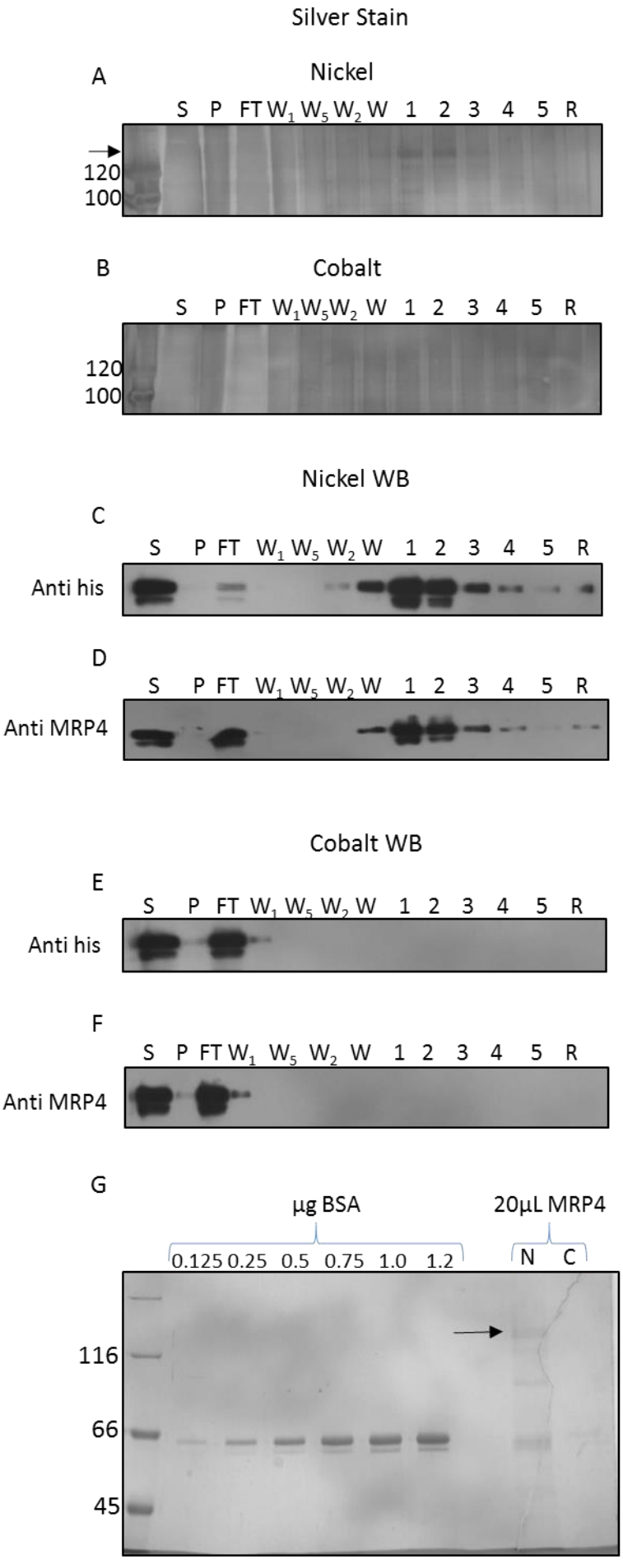

Figure 4.13.2: Purification of MRP4 with SMA 2000 using nickel and cobalt resin. *Silver stain gels A and B along with western blots C – F show the purification profile of MRP4 using either a nickel or cobalt resin. An anti his or anti MRP4 antibody was used on the western blots. Soluble (S), pellet (P), flow-through (FT), first (W_1) and last (W_5) 20mM imidazole wash step, second 40mM imidazole step (W2), 60mM wash step (W), five elution fractions (1-5) at 200mM imidazole and a resin fraction were loaded onto the silver stain gels and western blots. SDS gel G shows the quantification of concentrated MRP4 from the nickel (N) and cobalt (C) resin using BSA standards, stained with Instant blue.*

Figure 4.13.2 shows the results from the purification of MRP4 using either a nickel or a cobalt resin. These results clearly show the purifications with nickel resin were successful and the cobalt resin was not. Both the sliver stain gels and Western blots show a clear difference between the purifications with the nickel resin giving a small amount of MRP4 present in the 60mM imidazole wash step and large amounts in the first two elution fractions. In contrast, no MRP4 was present in any of the fractions beyond the flow through and first wash when using the cobalt resin.

Again, it can be seen that there are differences between the two antibodies used regarding the amount of MRP4 in the flow-through sample, however this time the exposure of the two blots are much more comparable. Using an anti-his antibody it appears that very little MRP4 is present in the flow through, however with the anti-MRP4 antibody the intensity of the flow through band is much higher. This may relate to the accessibility of the his-tag on some of the protein. It has been found by others that sometimes SMA interferes with binding to his-tags. Poor binding to Ni-NTA resin has also been reported (Pollock review BBA), and it has even been found to interfere with his-tag antibodies using Western blots (Dr. Ian Kerr, personal communication). So if a subset of the proteins had the his-tag obscured in some way, they would not bind to the resin or be detected on the Western blot. In contrast, the anti-MRP4 antibody would detect all MRP4 molecules.

After concentrating all elution fractions from the nickel and cobalt resins a 20µL sample was run on an SDS-PAGE gel alongside BSA standards (Figure 4.13.2 G) and an MRP4 band was only found in the sample using nickel resin. Using the nickel resin MRP4 was purified to a concentration of 6.5 µg/mL. The purity of MRP4 was about 25% with a large contaminating band at around 66kDa and which made up 63% of the total density. This showed that using nickel resin it was possible to purify MRP4 within SMALPs, whereas with cobalt resin it was not. However the current protocol with nickel resin only gave about a 25% purity which needed to be improved for the use of MRP4 in functional and structural studies.

4.13.3 Purification of MRP4 with varied NaCl concentrations in the purification buffer.

Varying the NaCl concentrations in the purification buffer has been suggested to improve the binding of SMALP-encapsulated proteins to affinity resins (Rothnie Methods in Mol Biol, Pollock BBA). Over time and after regenerating (old) nickel resin the binding affinity can also be affected. Typically the SMA purification buffer contains 150mM NaCl, this was increased to 500mM and 1M NaCl using old resin (resin that had been regenerated) and compared to new resin with the standard 150mM NaCl.

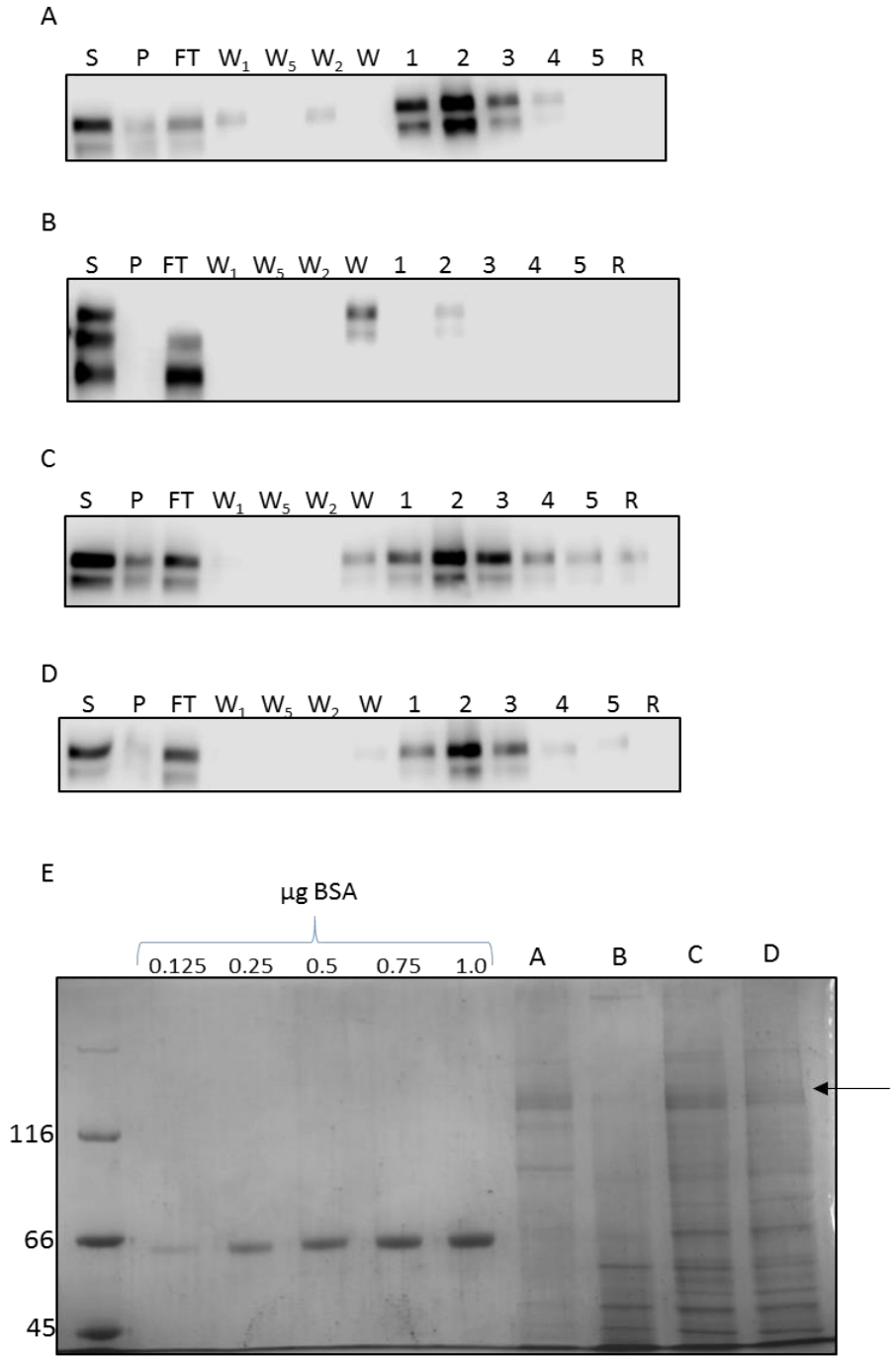

Figure 4.13.3: Purification of MRP4 with varied NaCl concentrations in the purification buffer. *Western blots A show the purification profile from using new nickel resin with a 150mM NaCl purification buffer. Western blot B, C and D show the purification profile using a 150mM, 500mM and 1M NaCl purification buffer with old nickel resin respectively. The Western blot shows the soluble (S), pellet (P), flow-through (FT), first (W_1) and last (W_5) 20mM imidazole wash step, second 40mM imidazole step (W2), 60mM wash step (W), five elution fractions (1-5) and a resin fraction. A 10:1 soluble MRP4 to resin ratio was used. A primary anti MRP4 antibody was used on all western blots. SDS gel E shows the quantification of MRP4 from pooled and concentration elution fractions from A, B, C and D. The quantification of MRP4 indicated by the arrow was measured against BSA standards, stained with Instant blue.*

The western blots in figure 4.13.3 show clear differences in their purification profiles. All western blots show MRP4 was solubilised although there are slight differences in the solubility efficiency with A, C and D showing an 83%, 80% and 90% solubilisation efficiency respectively and B having a 100% solubilisation efficiency. All show a double band in the soluble fraction with the exception of the soluble fraction in B showing three bands, with the top one being full-length MRP4, indicating potential breakdown. Using the new nickel resin and 150mM NaCl the binding efficiency was at approximately 48%. The binding efficiency of MRP4 with the old resin and 150mM NaCl could not be calculated as only the lower band is present in the flow through showing MRP4 was bound and the breakdown product did not bind. Increasing the NaCl concentration to 500mM with the old resin has the same binding efficiency as new resin and 150mM NaCl, whereas increasing the NaCl concentration further to 1M caused the binding efficiency to drop to 24%.

The SDS gel in figure 4.13.3 shows the clear differences in the final concentrations and purity between the different samples. All purifications with the old resin show an increased level of impurities compared to the new resin especially at lower molecular weights. MRP4 was at a concentration of 27µg/mL with new resin and 150mM NaCl. No MRP4 is present when the old resin and 150mM NaCl was used, but increasing the NaCl to 500mM gave a concentration of MRP4 equal to that of the new resin. This shows increasing the NaCl concentrations can improve the concentration of MRP4 when using old resin. However, increasing the NaCl concentration to 1M shows a reduced concentration of MRP4 (10µg/mL) indicating there is an optimal concentration of NaCl. The quality of the resin clearly has a considerable influence the purification as A shows a concentration same to C without increasing the NaCl concentration.

4.13.4 Purification of MRP4 with SMA 2000 varying NaCl concentration with new resin.

As increasing the NaCl concentration in the SMA purification buffer helped increase the concentration of MRP4 with old resin but the purity was reduced compared to new resin. Increasing the NaCl concentration was investigated using new nickel resin.

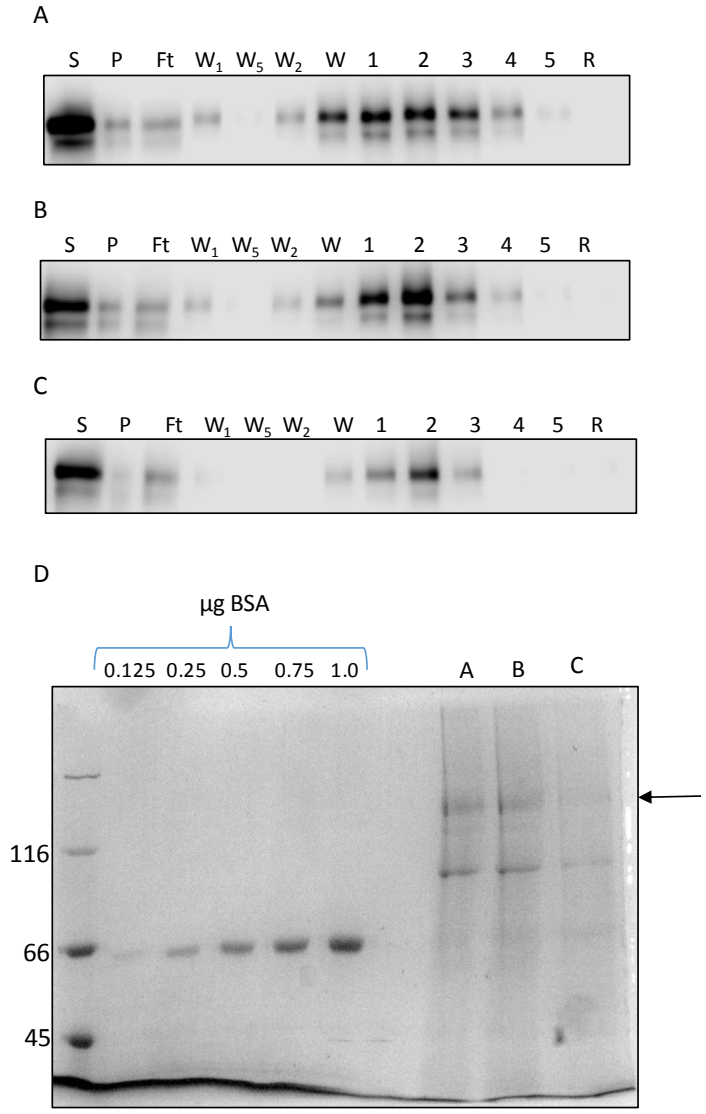

Figure 4.13.4: Purification of MRP4 with new nickel resin and varied NaCl concentrations in the purification buffer. *Western blots A, B and C show the purification profile of 150, 500 and 1M NaCl used in the purification buffer respectively. They show the soluble (S), pellet (P), flow-through (FT), first (W_1) and last (W_5) 20mM imidazole wash step, second 40mM imidazole step (W2), 60mM wash step (W), five elution fractions (1-5) and a resin fraction. A 10:1 soluble MRP4 to resin ratio was used. A primary anti MRP4 antibody was used on all western blots. SDS gel D shows the quantification of MRP4 from pooled and concentration elution fractions from A, B and C. The quantification of MRP4 indicated by the arrow was measured against BSA standards, stained with Instant blue.*

Using 150mM NaCl 90% of the soluble MRP4 was bound to the new nickel resin. There was an apparent decrease in binding efficiency when using higher concentrations of NaCl with 75% and 83% of the total solubilised MRP4 binding in the presence of 500mM and 1M NaCl. The amount of MRP4 that washed off during the wash step also varied with NaCl concentration. During the first wash step (20mM imidazole) approximately 6% was of the MRP4 was lost when using 150mM NaCl, 12% was lost with 500mM NaCl and only 2% with 1M NaCl. The losses of MRP4 during the second 40mM imidazole wash step were very similar with 6% washing off with 150mM NaCl, 11% with 500mM NaCl and 0% with 1M NaCl. Larger amounts were lost with the 60mM imidazole wash with 19% washing off using 150mM, 30% with 500mM NaCl and 8% with 1M NaCl. Overall, a NaCl concentration of 500mM has the worst binding efficiency which is also accompanied by the largest loss during the wash steps. Increasing the NaCl to 1M does increase the binding efficiency when compared to 500mM NaCl but it is still lower compared to 150mM NaCl as the least amount was lost during the wash steps. This shows that increasing the NaCl does not increase the binding efficiency but, when raised to 1M NaCl the MRP4 that does bind appears to be bound more tightly as the least amount is lost during the wash steps.

The elution profiles between the different conditions are similar with the majority of MRP4 being eluted in the first three elution fractions. After pooling all elution fractions and concentrating, MRP4 was quantified (Figure 4.13.4). In the presence of 150mM NaCl a total of 0.47µg MRP4 was purified at a concentration of 11.8µg/ml. With 500mM NaCl 0.52µg of MRP4 was purified at 13 µg/ml. In contrast with 1M NaCl only 0.006µg was produced at a concentration of 0.9µg/ml. The purity of MRP4 in the 150mM and 500mM samples were 42% and 45% respectively. There was a faint band just below MRP4 and a more intense lower band around 80kDa which made up around 50% of the total density for both of these samples. This lower band could be breakdown of MRP4 as ABC transporters are known to be prone to hydrolysis of the loop linking the two halves. Breakdown of this kind with MRP4 would result in a band at approximately 75kDa, as this equals half of MRP4 (150kDa), and would be more intense as the amount of protein present would be double. These results shows that increasing the NaCl concentration whilst using new nickel resin

does not increase the purity or the amount of MRP4. For this reason the NaCl was kept at 150mM during further purifications.

4.13.5 Larger scale purification of MRP4.

At this stage the results have shown that the recommended conditions for solubilising and purifying proteins within SMALPs were working and were better when using new resin. A larger scale purification was attempted to determine the amount that could be purified for use in functional and structural studies, as large amounts are needed for these techniques. For this 100mL of Sf 9 MRP4 membranes at 5mg/ml (total protein concentration) was solubilised with 20% SMA (w/v), in order to try to keep the total volume of solubilised MRP4 down. The solubilised protein was then mixed with new nickel resin at a column ratio of 10:1.

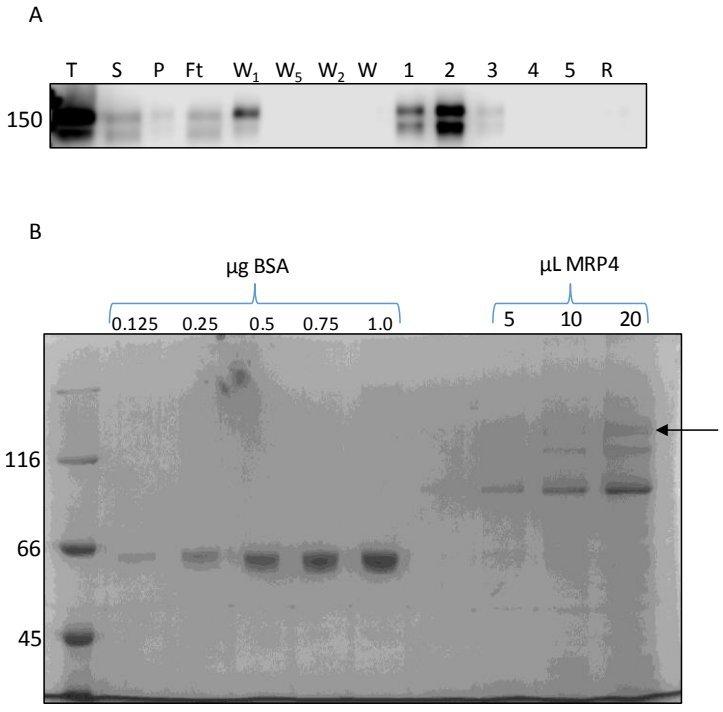

Figure 4.13.5: Larger scale purification of MRP4. *Western blot A show the purification profile of MRP4 with the soluble (S), pellet (P), flow-through (FT), first (W_1) and last (W_5) 20mM imidazole wash step, second 40mM imidazole step (W2), 60mM wash step (W), five elution fractions (1-5) and a resin fractions loaded. A 10:1 volume ratio of soluble MRP4 to resin was used with 100mL soluble MRP4 and 10mL nickel resin. A primary anti MRP4 antibody was used on the western blot. SDS gel B shows the quantification of MRP4 indicated by the arrow from pooled and concentration elution fraction, stained with Instant blue.*

Similar amounts of MRP4 are present in both the soluble and FT whereas during the previous smaller scale conditions (Figure 4.13.4) only a small fraction was present in the FT sample. This shows in this larger scale experiment there is reduced binding to the resin. This is further exemplified by the large amount of MRP4 present in the first 20mM imidazole wash fraction. As usual MRP4 that had bound to the resin eluted in the first three elution fractions .After concentrating to 750µL MRP4 was at a concentration of 3µg/ml making the total amount of MRP4 purified 2.25µg. This large scale experiment used 10 times more soluble MRP4 than the previous experiment (Figure4.13.4) where 0.47ug MRP4 was purified. If the scale up had worked at 100% efficiency, meaning 10 times more MRP4 should be produced, making it 4.7ug. By this calculation, the scale up only worked at 48% efficiency. Similar impurities are present in this large scale purification compared to the small scale (Figure 4.13.4) but the purity of MRP4 dropped to 17% with the lower most dense band making up 70% of the total density.

4.13.6 Size exclusion chromatography of large scale purification of MRP4.

Size exclusion chromatography (SEC) was performed on the MRP4 purified on the large scale purification to examine the stability and oligomeric state. The column used was a Superdex 200 10/300 GL with a column volume of 30ml and a void volume of 8mL.

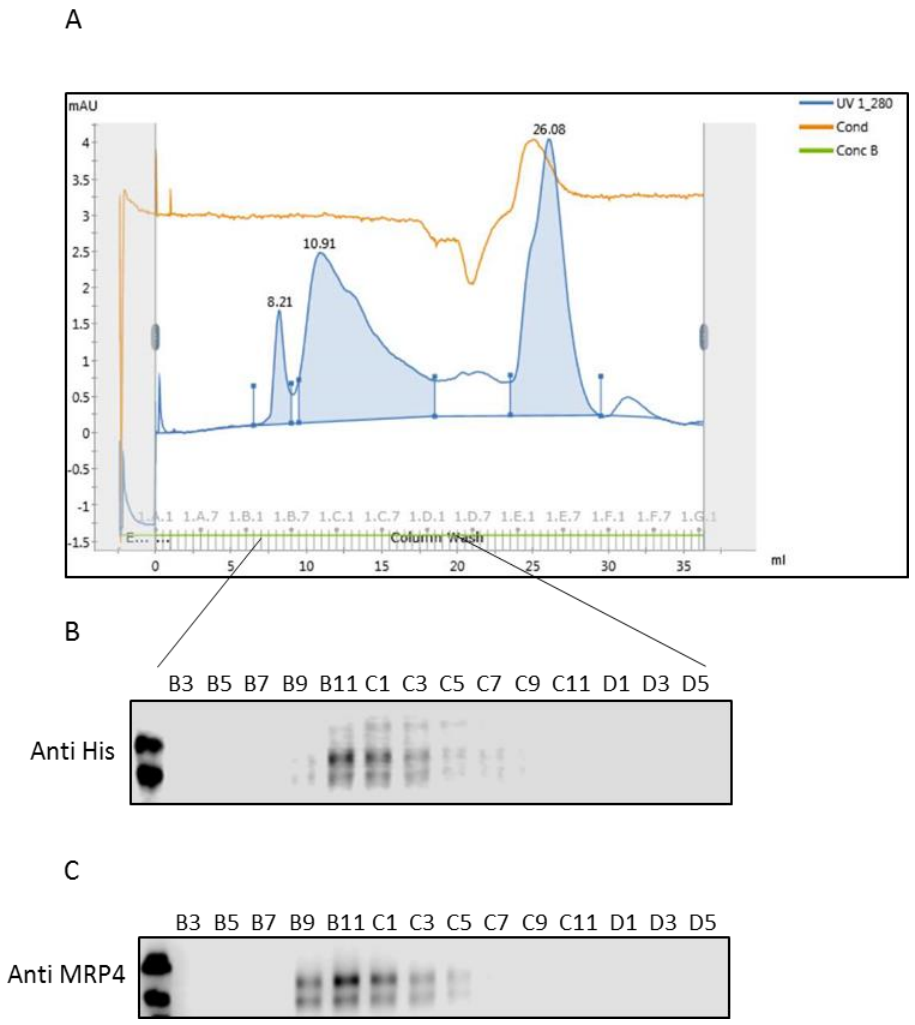

Figure 4.13.6: SEC of large scale purification of MRP4. *The SEC readout A shows the UV trace at 280nm and the conductivity of buffer A, SMA buffer, (20mM Tris pH 8 and 150mM NaCl). Western blots B and C show fractions B3 to D5 using either an anti-his antibody or an anti-MRP4 antibody respectively.*

The SEC readout shows three main peaks at 8.21, 10.91 and 26.08 mL. The first peak (8.21mL) with in the void volume and indicates this could be aggregates. Both of the western blots show that within this first peak, the B3 fraction, no MRP4 was detected, suggesting this peak did not contain MRP4. This peak could be aggregates of impurities during the purification. The western blot analysis shows MRP4 is contained within the second peak, peaking at 10.91 mL, and is eluted off between fractions B9 and C5. This second peak is rather broad and has a clear shoulder on it, however the MRP4 appears to be mainly contained within the first part of this peak. The last peak at 26.08mL is at the end of column volume and is likely to be excess free SMA polymer.

4.13.7 Removal of excess SMA 2000 prior to purification.

The scale up purification was not as successful as predicted so further optimisation was needed. Other parameters that could be altered were: type of resin, resin to soluble MRP4 ratio, removal of excess SMA, wash step imidazole concentrations and membrane quality. It has been previously reported that free excess SMA following initial solubilisation can be problematic for binding to purification resins (Pollock, Lee et al. 2018). The exact reason for this is unclear although SMA is sensitive to divalent cations and therefore could interact with the nickel attached to the resin. A study using a FLAG tag found it beneficial to remove the free SMA prior to bindings to the resin (Bersch, Dorr et al. 2017). Therefore, a simple experiment was performed to assess if the excess SMA was having an effect on binding. *Sf* 9 MRP4 membranes were solubilised with SMA and passed through a spin concentrator with a molecular weight cut off of 30kDa allowing the excess SMA to pass through and retain the MRP4. The spin concentrator was then topped up with SMA buffer and centrifuged, this was done three times and the flow through of each spin was examined along with the amount of MRP4 present after the fifth round (Figure 4.13.7).

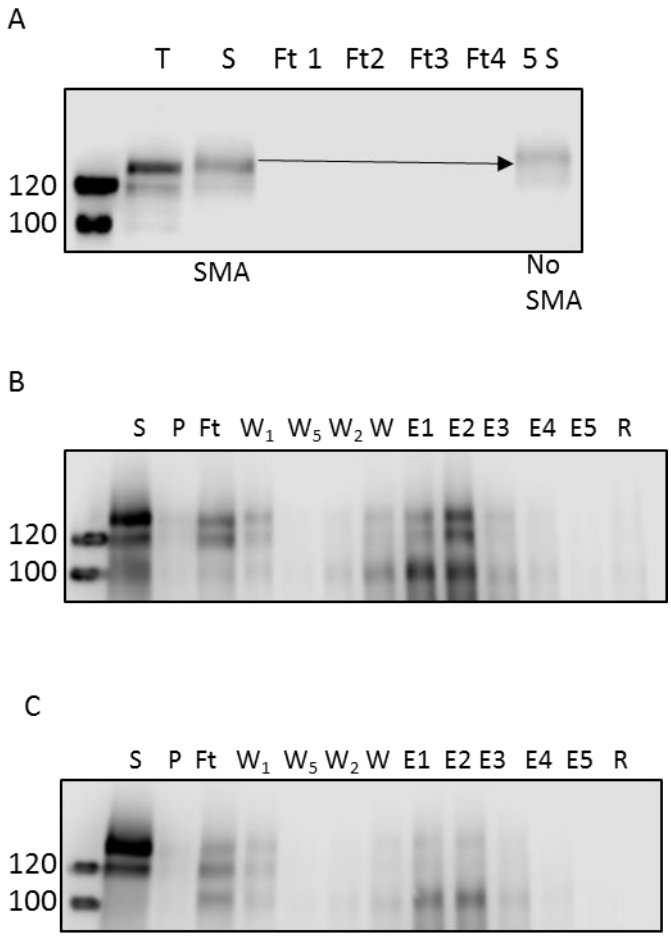

Figure 4.13.7: Removal of excess SMA 2000 prior to purification. *After solubilisation with SMA 2000 MRP4 was passed through a spin concentrator with a 30kDa molecular weight cut off. The spin concentrator was then topped up with buffer and concentrated again. This was repeated three more times and samples from each of the flow through were taken along with the final sample with SMA removed. Western blot A shows the amount of MRP4 present in the total (T), soluble (S), the four flow through (Ft 1 -4) and the final SMA removed sample (5S). Western blots B and C show the purification profiles of MRP4 before and after excess SMA was removed respectively. They show the soluble (S), pellet (P), flow-through (FT), first (W_1) and last (W_5) 20mM imidazole wash step, second 40mM imidazole step (W2), 60mM wash step (W), five elution fractions (1-5) and a resin fraction. A primary anti MRP4 antibody was used on the western blots.*

Western blot A in figure 4.13.7 shows the amount of MRP4 present after solubilisation (S), how much is in each flow through (Ft 1 – Ft 4) and the amount present after the final round (5S). It is clear that no MRP4 is present in any of the flow through samples. 80% of the MRP4 is present in the final sample (5S) compared to the soluble fraction indicating small, undetectable amounts of

MRP4 were lost during the removal of excess SMA, possibly binding to the filter since none was detected in the flow through. Western blots B and C show the side-by-side purification profiles of when excess SMA was not removed and when it was, respectively. Without removing the excess SMA a fairly typical purification profile is seen, although there appears to be more breakdown bands than usual. In contrast, when the excess SMA was removed much lower levels of MRP4 were present in the elution fractions. Thus, it appears that having the excess SMA present improves the purification. Alternatively, it is possible the repeated use of a filter concentrator was detrimental to the protein.

It also appears that during both of these purifications there is a large amount of degradation indicated by the appearance of the lower band at 100kDa and this cannot be from the removal of excess SMA as it appears in both of the western blots. Unfortunately, neither of the samples were able to be concentrated enough to evaluate concentration or purity of MRP4.

4.13.8 MRP4 purifications with varying resin volumes

Different volumes of resin can have an effect on the purification. To investigate this different volume ratios of soluble MRP4 to resin were investigated. Using 20mL of soluble MRP4 three different volumes of nickel resin were used; 0.5, 2 and 8mL. This would make soluble MRP4 to resin ratios of 40:1, 10:1 and 2.5:1 respectively. The 60mM wash was also taken out as previous results showed MRP4 was eluting off at this concentration.

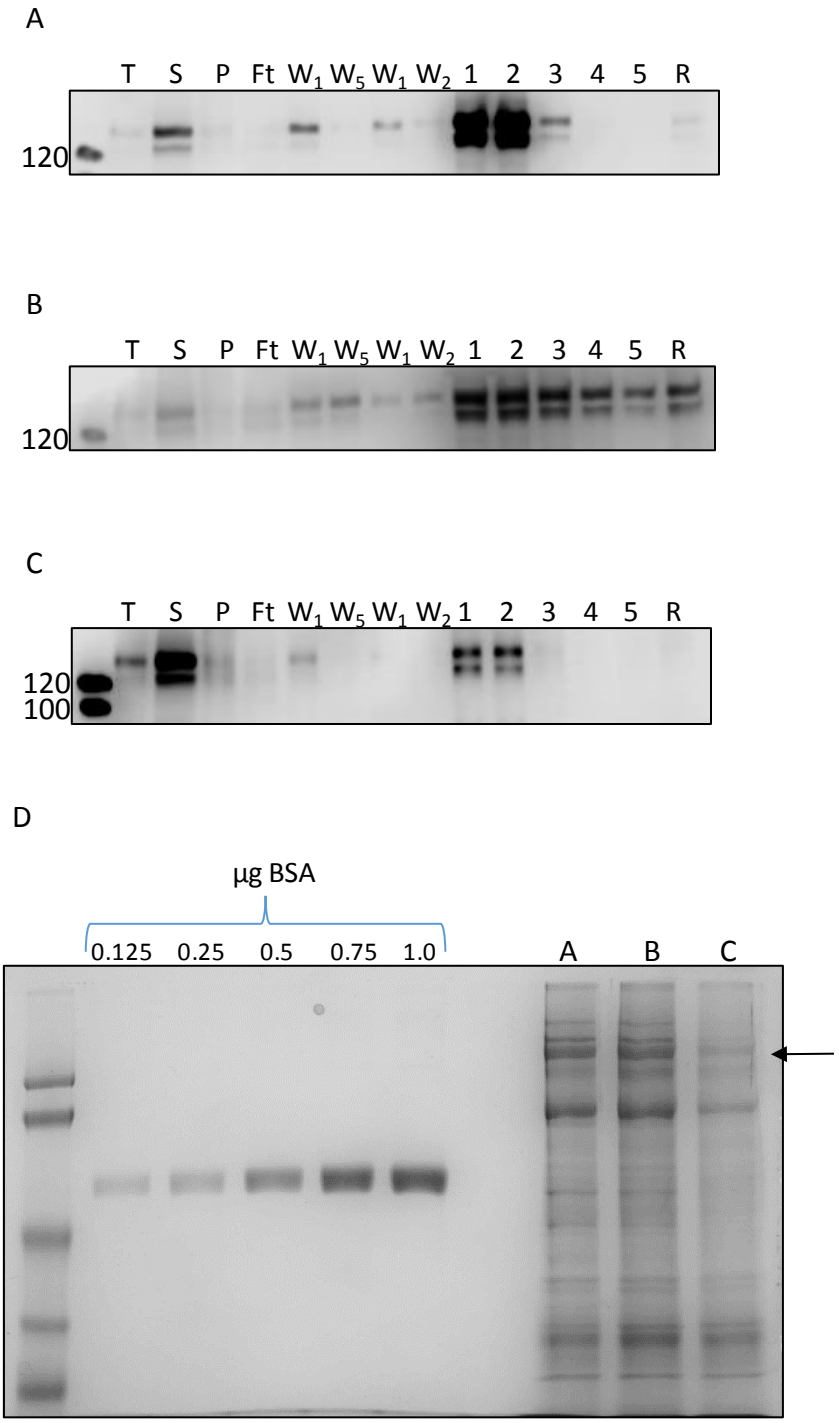

Figure 4.13.8: Purification of MRP4 using different soluble MRP4 to nickel resin ratios. *Western blot A, B and C show the purification profiles from side-by-side purifications using soluble MRP4 to nickel resin ratios of 40:1, 10:1 and 2.5:1 respectively. They show the soluble (S), pellet (P), flow-through (FT), first (W_1) and last (W_5) 20mM imidazole wash step, two 40mM imidazole steps (W_1 and W_2), five elution fractions (1-5) and a resin fraction (R). A primary anti his antibody was used on the western blots. SDS gel D shows the quantification of MRP4 from pooled and concentration elution fractions from the three purifications A, B and C, stained with Instant blue.*

The purification profiles show that regardless of the ratio the binding efficiency did not change as little to no MRP4 could be detected in the flow through fractions even with the smallest volume of resin. This shows that using the typical 10:1 ratio the maximum binding capacity is not reached. All elution fractions from each purification were concentrated to the same volume. Figure 4.13.8 D shows the quantification and purity of each purification. There was an increase in MRP4 concentration achieved with an increased ratio of soluble MRP4 to resin, with the 40:1 ratio giving an MRP4 concentration of 8µg/ml, the 10:1 ratio giving 5.7µg/ml and 2.5:1 ratio only producing MRP4 at 1.8µg/ml. This shows that using a smaller amount of resin could improve the yield of MRP4. By visual examination alone the purity of MRP4 didn't change when the soluble MRP4 to resin ratio was changed. It does appear that removing the 60mM imidazole wash step lead to decreased purity in this case. When compared to figure 4.14.4 D lane A where the same conditions as in figure 4.13.8 B there is considerably more contaminating proteins especially at lower molecular weights.

4.13.9 MRP4 purification with different types of nickel resin.

Nickel affinity resins are made at different qualities and with differing physical properties, which can effect purification. Up until this point ABT Nickel-NTA agarose resin had been used. Nickel resins from three different companies were tested: ABT, Thermofisher (HisPur) and Generon (Super Ni-NTA). As shown before old, regenerated resin compared to new resin can also change the purification and so old and new ABT resin were both included in this side-by-side test. The wash steps were also changed to decrease the concentration of imidazole in the initial wash steps to 10mM as previous results showed MRP4 washing off with 20mM imidazole. The 40mM imidazole wash step was also removed as this also showed MRP4 washing off at this concentrations. These wash steps were 10 CV and MRP4 was still showing up indicating large

amounts were being lost. However, it was noted that these wash steps might be critical for the purity of MRP4. The volume ratio of soluble MRP4 to nickel resin was at 20:1 for this experiment.

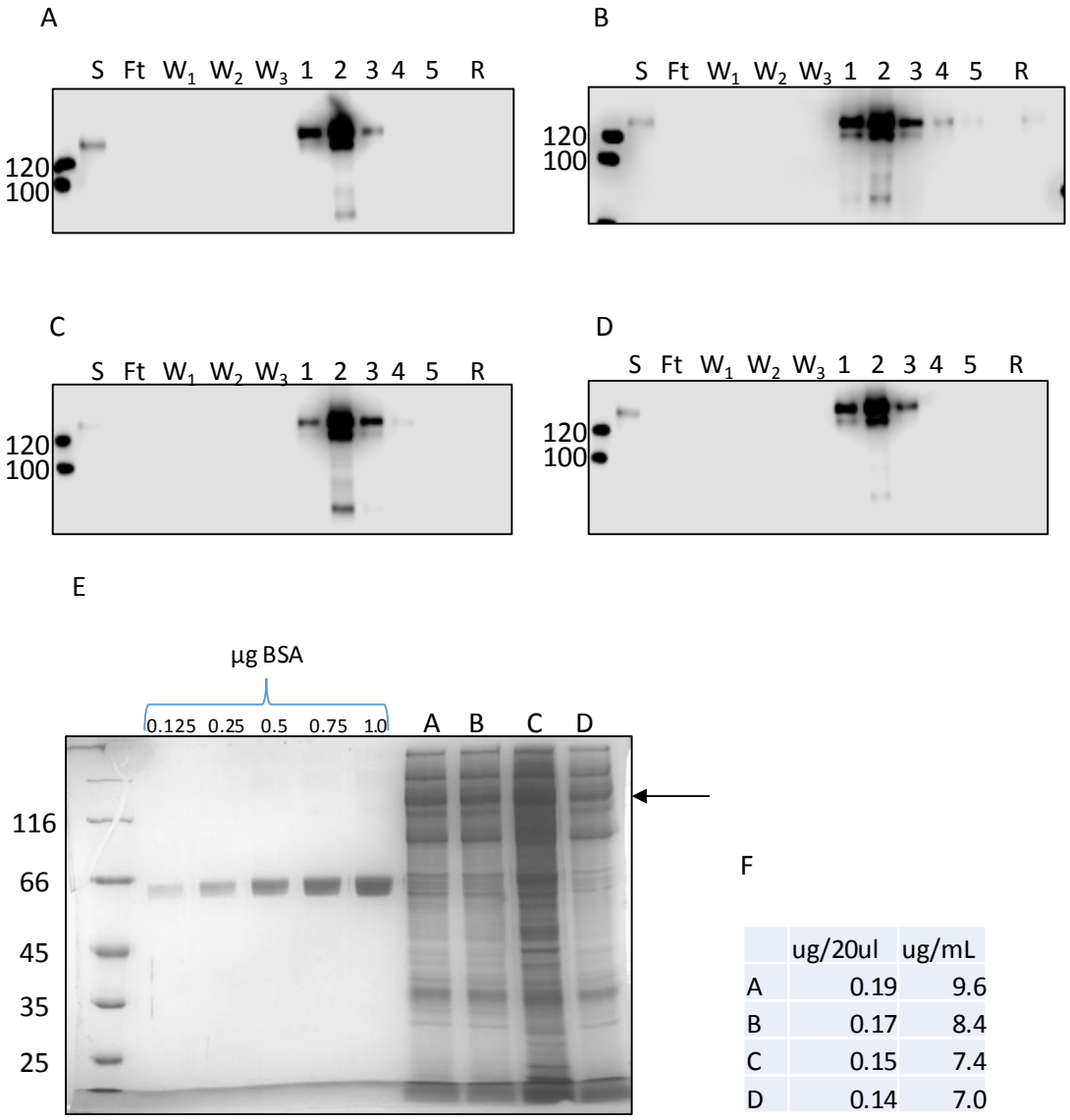

F

	ug/20ul	ug/mL
A	0.19	9.6
B	0.17	8.4
C	0.15	7.4
D	0.14	7.0

Figure 4.13.9: Purification of MRP4 using different nickel resin types. *Western blots A and B show the purification profiles from old (regenerated) and new nickel resin respectively from ABT. C and D are the purification profiles of nickel resin from Thermofisher (HisPur) and Generon respectively. They show the soluble (S), flow-through (FT), three 10mM imidazole wash step (W1, W2 and W3), five elution fractions (1-5) with 100mM imidazole and a resin fraction (R). A primary anti his antibody was used on the western blots. SDS gel D shows the quantification of MRP4 from pooled and concentration elution fractions from the four purifications A, B, C and D with the arrow indicating the MRP4 band, stained with Instant blue. Table F shows the amount (µg) present in the 20µL loaded onto the SDS gel and the corresponding concentration (µg/mL).*

The western blots in figure 4.13.9 show that regardless of the resin used there was no MRP4 present in the FT or any of the wash steps indicating no loss of MRP4 using 10mM imidazole. MRP4 was eluted off using 100mM and appeared in the first three elution fraction of all resin types, with the second fraction containing the majority of MRP4. Only small amounts of MRP4 were present in the resin fraction of the new ABT resin. This could indicate this new ABT has increased binding affinity to MRP4 as not all MRP4 was eluted off. The SDS page in figure 4.13.9 E shows visually that all of these samples were far less pure than previous purifications with many more contaminating proteins. This demonstrates that although using 20mM imidazole during the wash steps some MRP4 maybe lost the purity is increased. The concentrations of MRP4 contained within each sample did not vary a great deal but this may be due to the inability to solely distinguish the MRP4 band from the background. This was especially prevalent in the Thermofisher resin where the whole lane was much darker than the other resins. This could indicate increased binding of both MRP4 and the contaminating proteins meaning increasing the wash steps back to 20mM imidazole may increase the purity of MRP4. Between all the other resin types there is very little difference between the purity and concentration although previous results indicated clear differences between old and new ABT resins.

4.13.10Purification of MRP4 from newly produced *Sf* 9 membranes.

It was thought that because the vast majority of the contaminating proteins had a lower molecular weight than MRP4 this could indicate either breakdown or MRP4 that wasn't fully expressed. The membranes used up until this time had been frozen for many months and shipped back and forth to France which could have led to breakdown. Therefore, new MRP4 was expressed and fresh membranes were produced. The new ABT resin at a ratio of 20:1 soluble MRP4 to nickel resin was chosen for this experiment. 3 x 10 CV of 10mM imidazole was used for the wash steps.

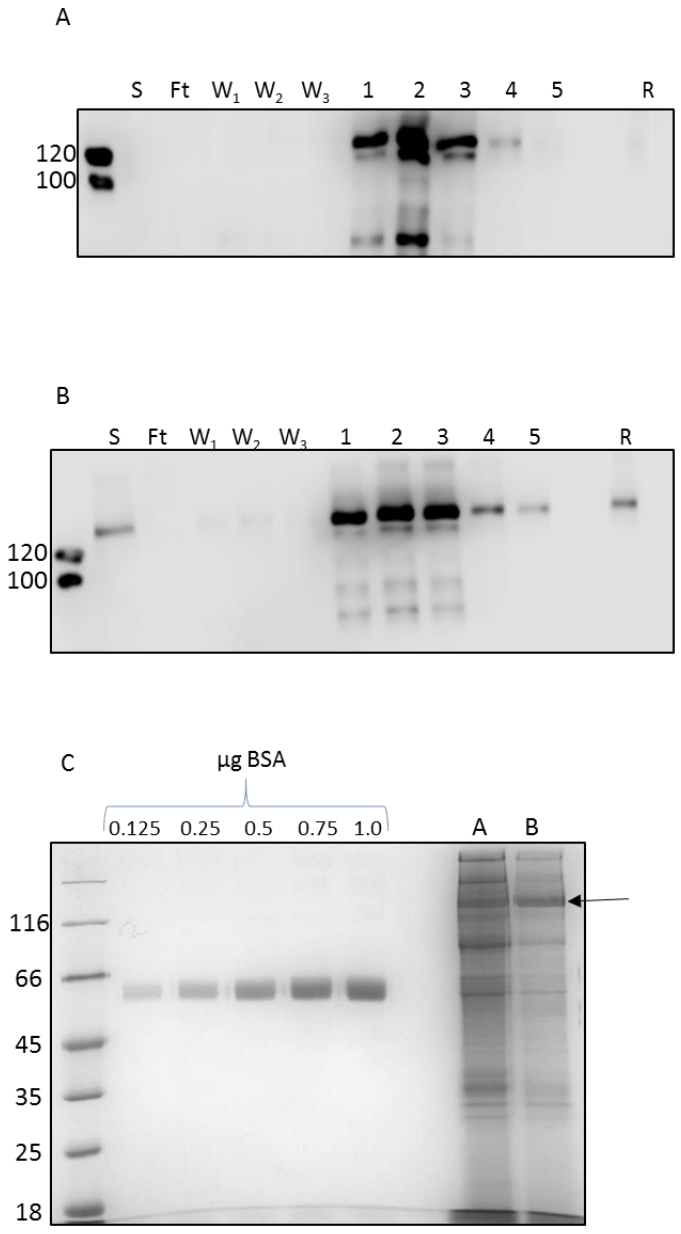

Figure 4.13.10: Purification of MRP4 form newly produced Sf 9 membranes. *Western blots A and B show the purification profiles form the old and new Sf 9 MRP4 membrane respectively. They show the soluble (S), flow-through (FT), three 10mM imidazole wash step (W1, W2 and W3), five elution fractions (1-5) with 100mM imidazole and a resin fraction (R). An anti-his antibody was used on both these western blots. SDS gel C shows the quantification of MRP4 from pooled and concentration elution fractions from the two purifications A, and B with the arrow indicating the MRP4 band, stained with Instant blue.*

The western blots in figure 3.13.10 show in both cases MRP4 was eluted again in the first three elution fractions. With the old MRP4 membranes (4.13.10 A) there is a band at a lower molecular weight with a high density in the second elution fraction that could equate to MRP4 breaking in half in the elution fractions.

The SDS PAGE in figure 4.13.10 shows visually clear differences in the purity and concentration. The purification using old membranes showed large amounts of contaminating proteins and although the purification using new membranes also contains contaminating proteins they are at a far lower concentration. The concentration of MRP4 purified from the old membranes was 1.7µg/ml (total amount 0.68 µg) whereas MRP4 purified from new membranes was at 7.6µg/ml (total amount 2.28 µg). This increase in MRP4 concentration was likely due to the increase in MRP4 expression achieved in the new membranes used. The expression level of MRP4 in these membranes was around twice that of the expression level in the old membranes. Large amounts of new MRP4-his was expressed in *Sf* 9 cells and used for further SMA purifications.

4.13.11SEC of MRP4 purified from old and new Sf 9 MRP4 membranes.

A

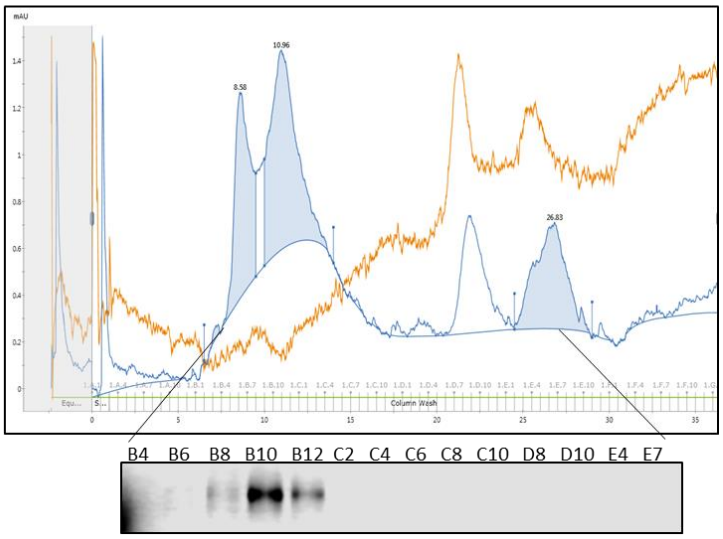

B

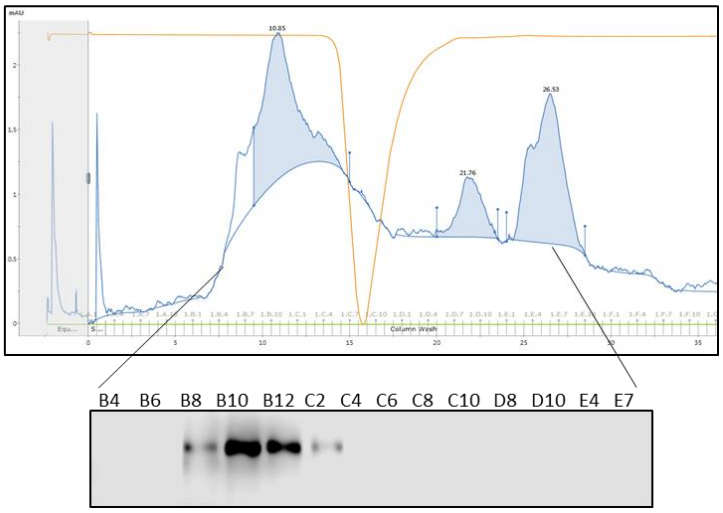

Figure 4.13.11: SEC of MRP4 purified from old and new Sf 9 MRP4 membranes. *A and B are the SEC readouts of MRP4 purified from old and new Sf 9 MRP4 membranes respectively. The readouts show the UV 280nm trace and have the western blot showing samples taken from fractions B4 to E7 below. An anti-his antibody was used on both of the western blots.*

SEC was performed on purified MRP4 from the old membranes and the new membranes to examine the purity and stability. Four major peaks appear in the SEC read out of MRP4 purified from the old membranes (4.13.11 A) and only three major peaks in MRP4 form the new membranes (4.13.11 B). The difference is the peak after 8mL, which only appears in the sample purified from the old membranes, showing a large amount of aggregation. Although this peak does not contain any MRP4 it does show there is considerably more aggregation during the purification showing the instability of proteins within the old membranes. The western blots

confirm MRP4 eluted off after 10mL in both A and B. This is in line with the previous results with SEC from figure 4.13.6. It is unknown what is contained in the last two peaks that are present in the same place on the elution profile in both A and B but they do not contain MRP4. The last peak, at 26mL was also contained in the SEC profiles in figure 4.13.6 and is thought to be excess SMA.

4.13.12 Purification of MRP4 from new *Sf* 9 MRP4 membranes using new ABT and Thermofisher resin.

It was now known that these new membranes had a higher expression level and appeared to have less breakdown. They were also able to be purified to a higher concentration and purity. The Thermofisher resin had increased binding although this also included non-specific binding of contaminating proteins but these could potentially be reduced though increased imidazole concentration and wash steps. Taking these parameters into account an experiment to test the Thermofisher against ABT resin with the new membranes and reverting to 5 x 10 CV of 20mM imidazole wash steps was carried out. The aim of this experiment was to increase the purity and concentration of MRP4.

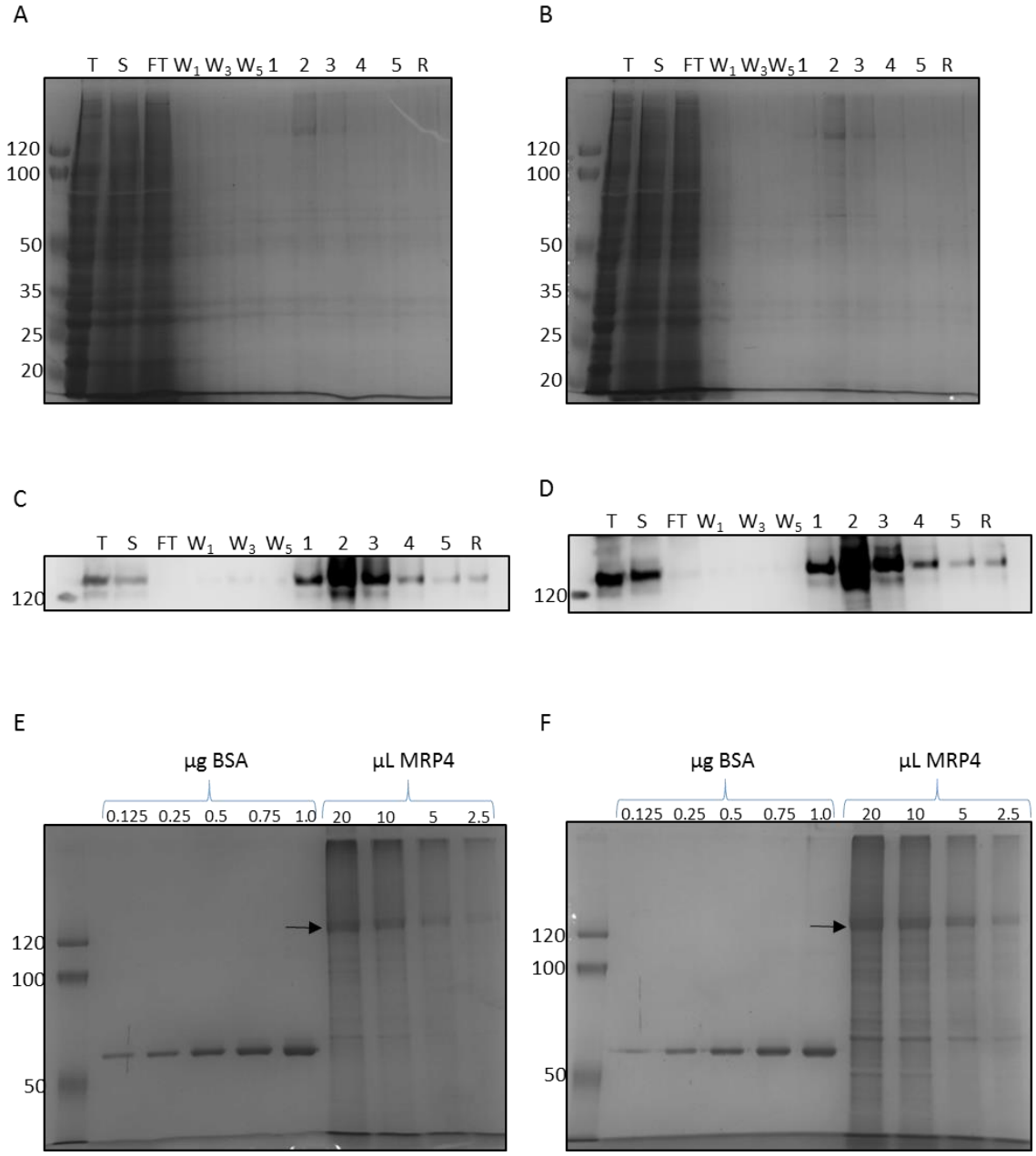

Figure 4.13.12: Purification of MRP4 from new Sf 9 MRP4 membranes using new ABT and Thermofisher resin. *SDS gel A, western blot C and SDS quantification gel E show the results from the purification of MRP4 with new ABT resin. SDS gel B, western blot D and SDS quantification gel F show the results from the purification of MRP4 with Thermofisher resin. The SDS gels A and B along with the western blots shows the purification profiles with the total (T), soluble (S), flow-through (FT), 20mM imidazole wash step (W_1, W_3 and W_5), five elution fractions (1-5) with 200mM imidazole and a resin (R) fractions. An anti-his antibody was used on both these western blots. SDS quantification gels E and F show 20, 10, 5 and 2.5µL of concentrated MRP4 from the two purifications with the arrow indicating the MRP4 band.*

The western blots and SDS-PAGE gels in figure 4.13.12 show the purification profiles of the two different resins. Both the resins showed similar elution profiles. Once concentrated the purified MRP4 was quantified and the purity examined (Figure 4.13.12 E and F). It appears that using the ABT resin the purity was higher at approximately 75% compared to the Thermofisher HisPur resin which was only 50% pure. Although there were the same contaminating proteins on both resins the contaminating proteins were more intense from the Thermofisher resin. Use of the Thermofisher resin however led to an increased concentration of MRP4 at 27.7µg/ml compared to 8.6µg/mL with ABT resin. Thus using the Thermofisher resin resulted in a decreased purity but an approximately 3-fold increase in yield.

4.13.13Purification of MRP4 using 2mM imidazole during binding.

Using the Thermofisher resin led to an increased yield of MRP4 but decreased the purity. Increasing the wash concentration of imidazole could lead to an increased purity but risked decreasing the concentration. Another way of increasing the purity is by adding small concentrations of imidazole during the binding. These small concentrations should reduce the non-specific binding but hopefully should not affect the ability of MRP4 to bind. 2mM imidazole was added during the binding of SMA solubilised MRP4 and compared to the most optimised version of SMA purification which is: washing with 5 x 10CV 20mM imidazole and eluting with 5 x 1CV 200mM.

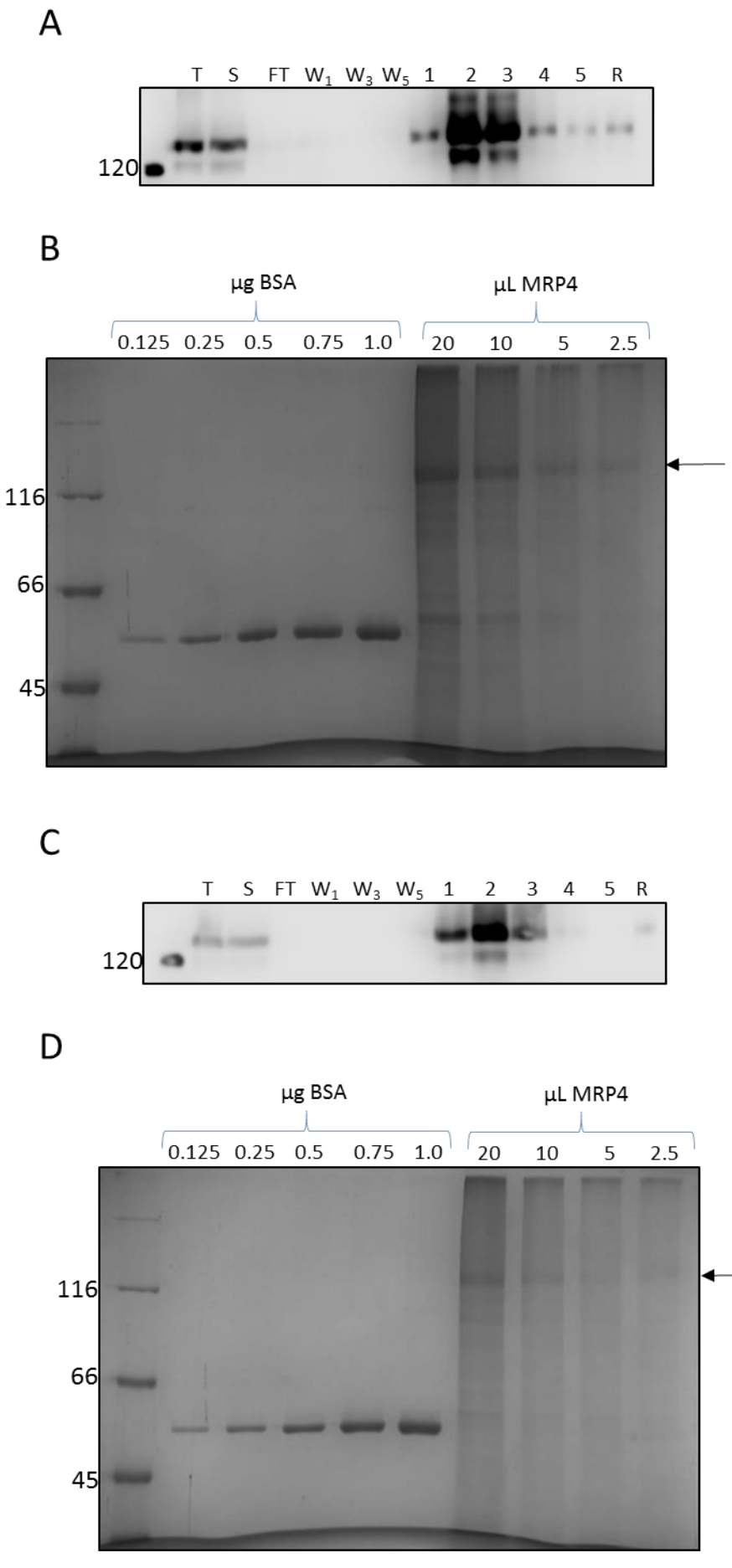

Figure 4.13.13: Purification of MRP4 with the adding of 2mM imidazole during binding to nickel resin. *Western blot A and C show the purification profiles of MRP4 under normal and with the addition of 2mM imidazole during binding respectively. These western blots show the total (T), soluble (S), flow-through (FT), 20mM imidazole wash step (W_1, W_3 and W_5), five elution fractions (1-5) with 200mM imidazole and a resin (R) fractions. SDS gels B and D show the quantification of MRP4 under the normal and 2mM binding conditions respectively.*

Figure 4.13.13 showed that adding 2mM imidazole during the binding did not seem to change the binding efficiency of MRP4 to the resin as no MRP4 was visible in either of the flow through fractions. However, the purification using 2mM imidazole during binding, MRP4 was only concentrated to 2.5µg/ml (total amount 0.625 µg) whereas the standard conditions, without imidazole during binding, MRP4 was concentrated to 8.5µg/ml (total amount 2 µg). The purity of MRP4 was very similar between the two conditions with the addition of 2mM imidazole giving a 66% purity and without imidazole a 62% purity. This showed that the addition of imidazole did not improve the purification of MRP4 and reduced yield.

4.13.14MRP4 purification with DDM detergent.

To allow a comparison between SMA and the conventional detergent DDM, side-by-side purifications were carried out where MRP4 was solubilised with either 2.5% SMA 2000 or 1% DDM. The optimised conditions for SMA were used in both cases, but this does not mean these are the most optimal conditions for purifications with DDM. DDM has previously been shown to solubilise MRP4 (Figure 4.10.1) but with a much lower solubilisation efficiency.

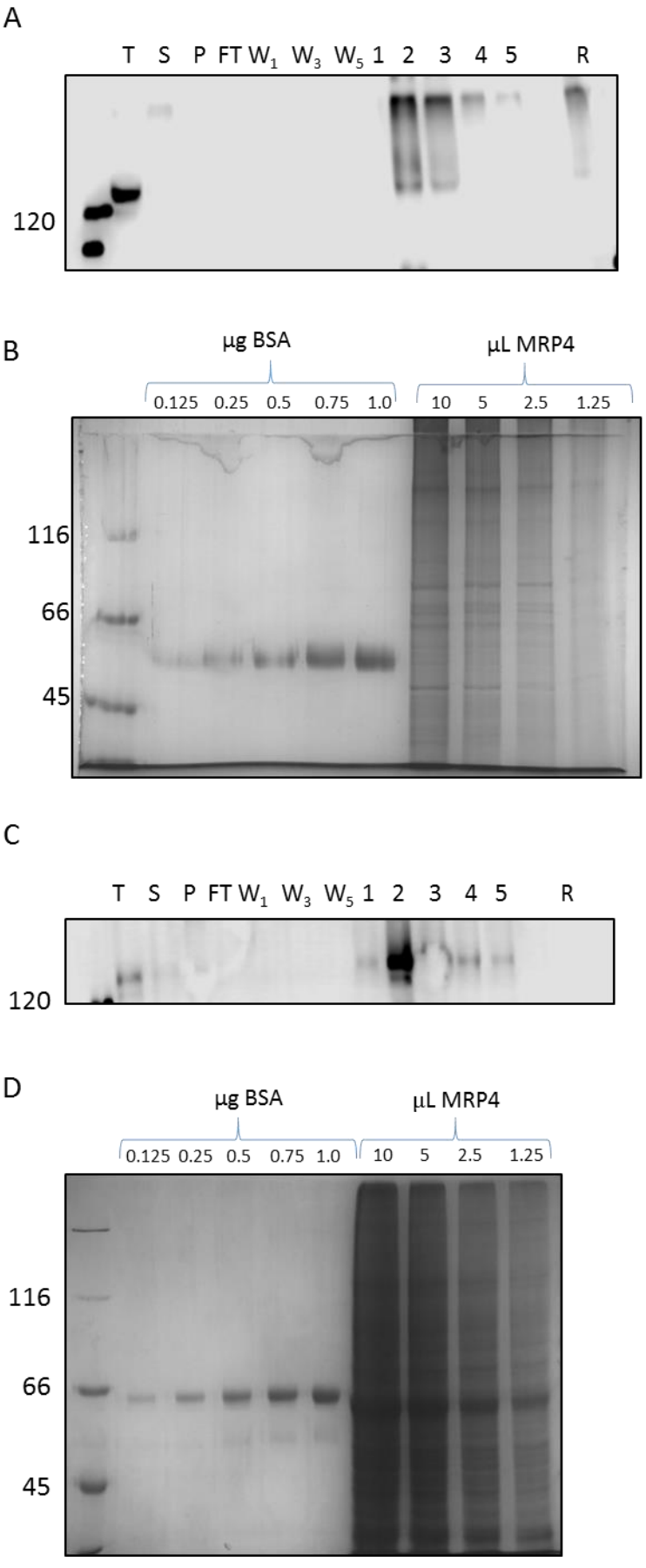

Figure 4.13.14: Purification of MRP4 using DDM detergent*. Western blot A and C show the purification profiles of MRP4 using 1% DDM or 2.5% SMA 2000 respectively. These western blots show the total (T), soluble (S), flow-through (FT), 20mM imidazole wash step (W_1, W_3 and W_5), five elution fractions (1-5) with 200mM imidazole and a resin (R) fractions. Primary anti-his antibody used. SDS gels B and D show the quantification of MRP4 using DDM or SMA 2000 respectively against a BSA standard.*

The western blot of the DDM purification figure (4.13.14 A) shows no MRP4 in the soluble faction and only MRP4 appearing in the total and elution fractions two and three. This does not mean that MRP4 was not solubilised with DDM but the amount loaded on the western blot may not have been detectable. The SMA western blot shows a typical elution profiles. When concentrated it is unclear if MRP4 is present in the DDM preparation as there is no prominent MRP4 band. There is a band indicated by the arrow (Figure 4.13.14 B) which is most likely to be MRP4 based on the molecular weight and the positioning of the band in comparison to SMA. It is also clear the purity of the concentrated DDM sample is a lot lower than the SMA purified MRP4. There is a clear MRP4 band when purified with SMA at a concentration of 22µg/mL and it has very few contaminating proteins with approximately 68% purity. This shows that compared to a conventional detergent such as DDM, SMA is able to purify MRP4 to a higher concentration and purity. As mentioned before the purification had not been optimise for DDM but the most likely limiting factor in the DDM purification is the solubilisation efficiency.

4.13.15Conclusion of SMA purifications

The purity and yield were both successfully improved through the optimisation of different purification parameters. The type of resin used, nickel or cobalt, showed drastic differences in the yield of MRP4 with nickel outperforming cobalt. The quality of the resin, how many times the resin had previously been used, was a huge impact on both purity and yield. New resin had a higher yield compared to older, more used, resin. Out of three different brands of nickel resin, Thermosfisher showed increased yields but less purity. By changing the concentration of imidazole and the volume of the wash step the purity was increased. One of the biggest increases to the purity and yield was the quality of the membranes. Newly produced *Sf* 9 MRP4 membranes showed increased yield and purity compared to older membranes. These increases may be attributed to the increased expression level in the newly produced membranes and the degradation occurring in the old membranes.

4.14 Analysis of Purified MRP4

Once membrane proteins have been purified their function and structure can be investigated. In order to gain useful functional and structural data the membrane protein must first be shown to be functional and stable.

The thermostability of purified MRP4 was assessed in a similar way to that of soluble un-purified MRP4. Purified MRP4 was heated at 37, 50, 60, 70, 80, 90 and 100 °C for 10 minutes before centrifuging. The principle behind this assay is that upon heating protein denaturing will occur causing it to aggregate. Centrifuging the sample will pellet all of the aggregated protein leaving only soluble protein. The amount of soluble protein left is then assessed by Western blotting. A control that remained at 4 degrees was used as a comparison for the amount of protein initially present. Taking the temperature at which 50% of the MRP4 is still soluble for each solubilising agent the transition/melting point (Tm) can be estimated.

To make sure the protein is still functional a tryptophan quenching binding assay was performed. Fluo-cAMP has been shown to be transported by MRP4 and its binding to MRP4 was measured here by tryptophan quenching. Unfortunately, this type of functional analysis could only be performed on SMA purified protein. Calixar detergents absorb at the same wavelength as tryptophan and would interfere with the signal. MRP4 solubilised in DDM was not purified to a high enough standard to be used in this assay.

The ability for MRP4 that had been solubilised and purified in SMA or calixarenes to be used in structural studies was also investigated. These solubilising agents would have to be compatible with structural techniques such as electron microscopy. Preliminary negative stain EM images were undertaken.

4.14.1 Thermostability of purified MRP with western blot analysis

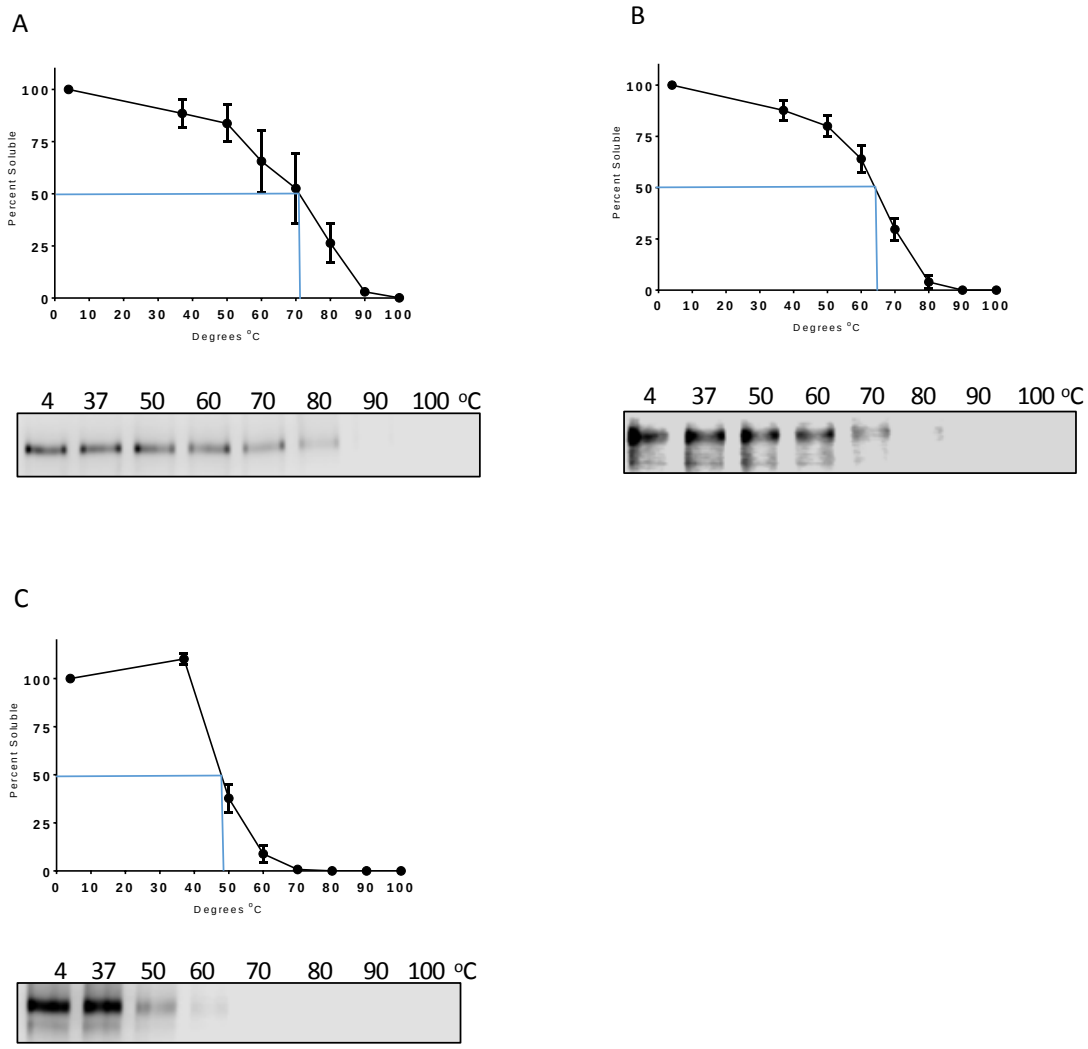

Figure 4.14.1: Thermostability of purified MRP4 using DDM, C4C7 and SMA 2000. *Graphs A, B and C show the thermostability of MRP4 purified in SMA 2000, C4C7 and DDM respectively, based on percent soluble after heating and centrifugation (n=3 ±SEM). The blue line represent the transition/melting point (Tm), the temperature at with 50% of MRP4 is still soluble. Western blots below graph A, B and C show examples of amounts of soluble MRP4 at each temperature in SMA 2000, C4C7 and DDM respectively. The density of each of the band was taken and compared to the 4°C control to calculate the percent soluble.*

Figure 4.14.1 shows the thermostability results from MRP4 that was purified in SMA 2000, C4C7 or DDM. Western blots of MRP4 in SMA or C4VC7 show a gradual decrease in the band intensities as the temperature increased and this is represented in the curvature of the graphs with a

broader curve. The DDM Western blot shows a dramatic drop in the band intensity from 37 to 50 degrees and the graph shows a sharp decline between those temperatures. The temperature at which 50% of MRP4 remained stable was 71^{o}C in SMA 2000, 65^{o}C in C4C7 and 49^{o}C in DDM. Within both SMA and C4C7 there is a clear increase in the stability compared to DDM.

The concentration of MRP4 purified in SMA varied between 2 and 8 µg/mL whereas the concentration of MRP4 in DDM and C4C7 was not varied. MRP4 that was purified with C4C7 was diluted 1/100 in SMA buffer containing 300mM NaCl to a concentration of 4.3 µg/mL. The concentration of MRP4 purified in DDM was not known, as after purification, concentrating MRP4 in DDM was not possible. The amount of MRP4 present could have an effect on the thermostability as more MRP4 present would lead to an increased possibility of interactions, potentially leading to more aggregation. It could also have an effect on the amount loaded onto the western blot and therefore the detection level. For this experiment the concentration of MRP4 in the SMA 2000 and C4C7 was not vastly different and therefore was most likely not a contributing factor to the thermostability.

These results show that as with the solubilised but un-purified samples in section 4.11, following purification the novel detergent C4C7 or SMA 2000 polymer were able to enhance the thermostability of purified MRP4 compared to the conventional detergent DDM. There was an increase of 22^{o}C and 16^{o}C in the Tm for SMA and C4C7 compared to DDM respectively. This enhanced thermostability may be advantageous for downstream structural studies.

4.14.2 Thermostability of purified MRP4 in SMA 2000 with native western blot analysis.

The thermostability of MRP4 solubilised and purified using SMA 2000 was assessed using Native western blots. These non-reducing gels would be able to show if there was any break down of MRP4 during heating, that did not lead to aggregation and any clear change in the oligomeric state of MRP4 during heating.

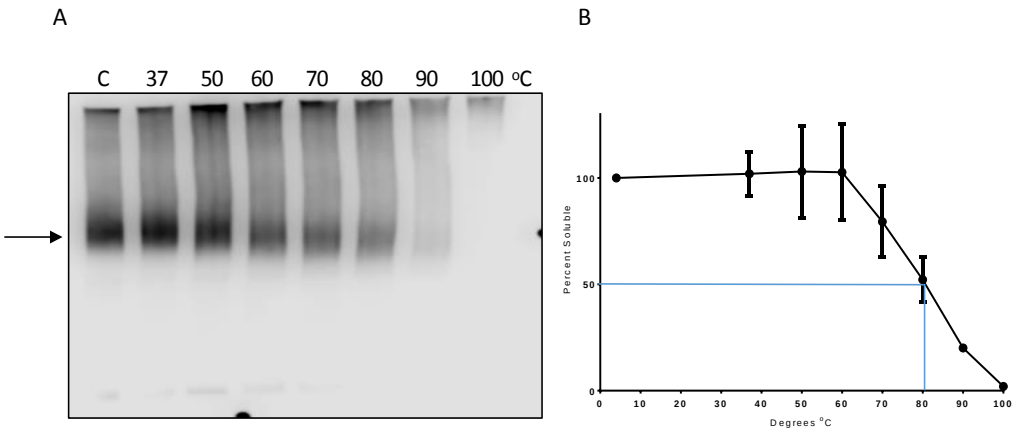

Figure 4.14.2: Thermostability of MRP4 in SMA 2000 using Native PAGE analysis. *A is an example of a native western blot that shows the level of soluble MRP4 (arrow) remaining at each temperature. The density of each MRP4 band was taken and compared to the control (C) sample that was kept at 4°C. The results are graphed in B with the blue line showing the Tm, the temperature at which 50% of MRP4 remained soluble.*

The native western blot in figure 4.14.2 shows one predominant band for purified MRP4. The intensity of this band decreases with increased temperature. There is no change in the molecular weight of MRP4 as the temperature increases, indicating there is no change in the oligomeric state. The decrease in the density of the MRP4 band shows that with increased temperature MRP4 becomes less stable and is denatured. Graph B shows the percent of soluble MRP4 at each temperature based on the density of the band. This shows that MRP4 solubilised and purified with SMA 2000 was 50% aggregated around 80°C, which is similar to the results in 4.14.1 A showing that both approaches produce similar results.

4.14.3 Binding assay for purified MRP4

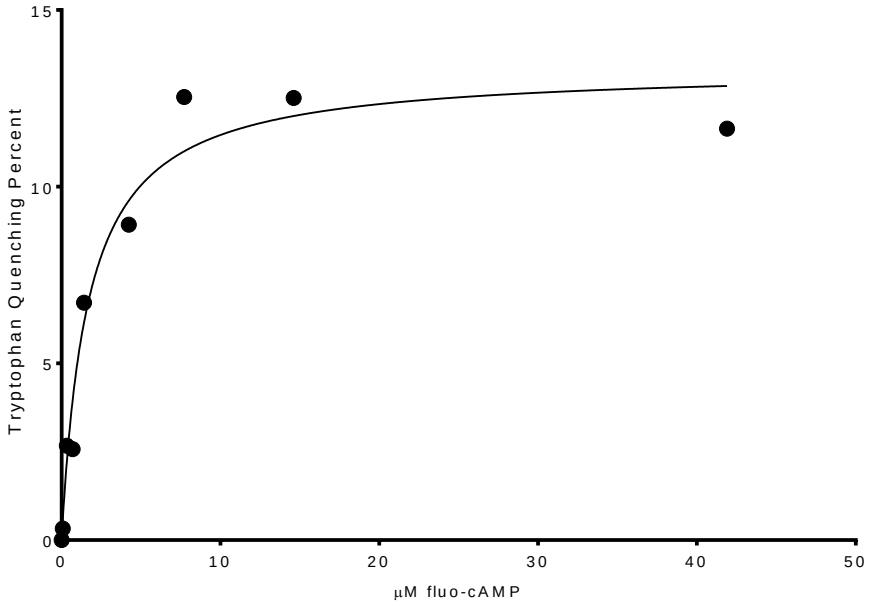

Figure 4.14.3: Fluo-cAMP binding with purified MRP4 in SMA 2000. *Graph shows the binding of fluo-cAMP to MRP4 that was solubilised and purified in SMA 2000. Binding is measured in the percent of tryptophan quenching using 0 - 30µM fluo-cAMP. Non specific binding was corrected using N-acteyl tryptophamide. Exctiation – 290nm, emmisions- 360nm.*

To assess if MRP4 that was purified in SMA 2000 was still functional a tryptophan fluorescence binding assay with fluo-cAMP was performed (Figure 4.14.3). This shows that there is a dramatic increase in tryptophan quenching between 0-10µM fluo-cAMP but it reaches the Bmax of 13.3 % quenching, and has a Kd of 1.65 µM fluo-cAMP. These results indicate that purified MRP4 within a SMALP is still able to bind fluo-cAMP.

4.14.4 Negative stain EM of MRP4 with C4C7

A

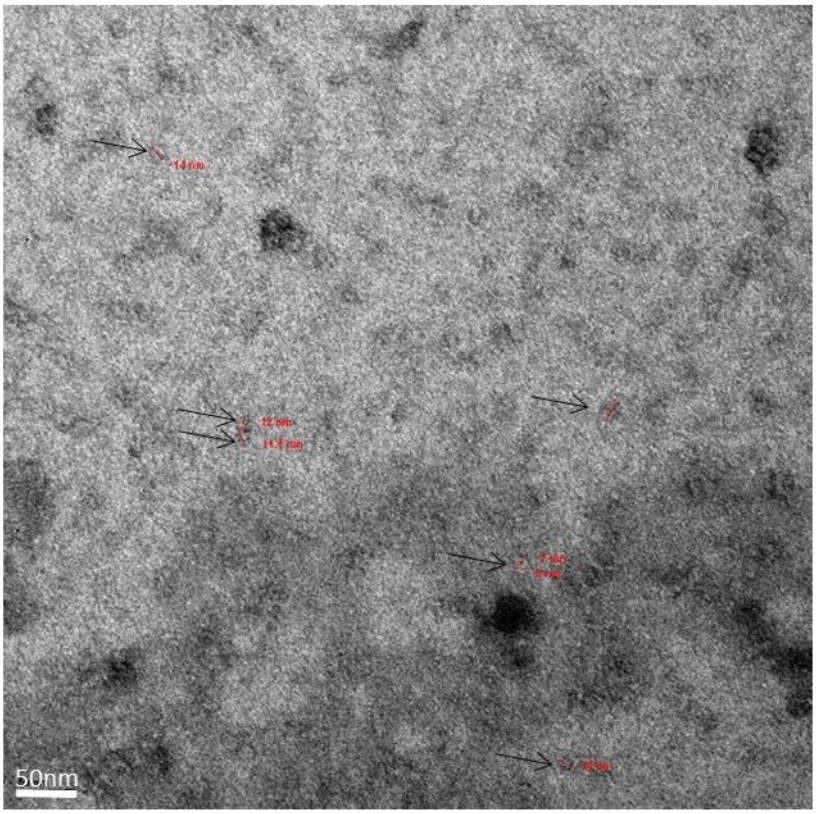

B

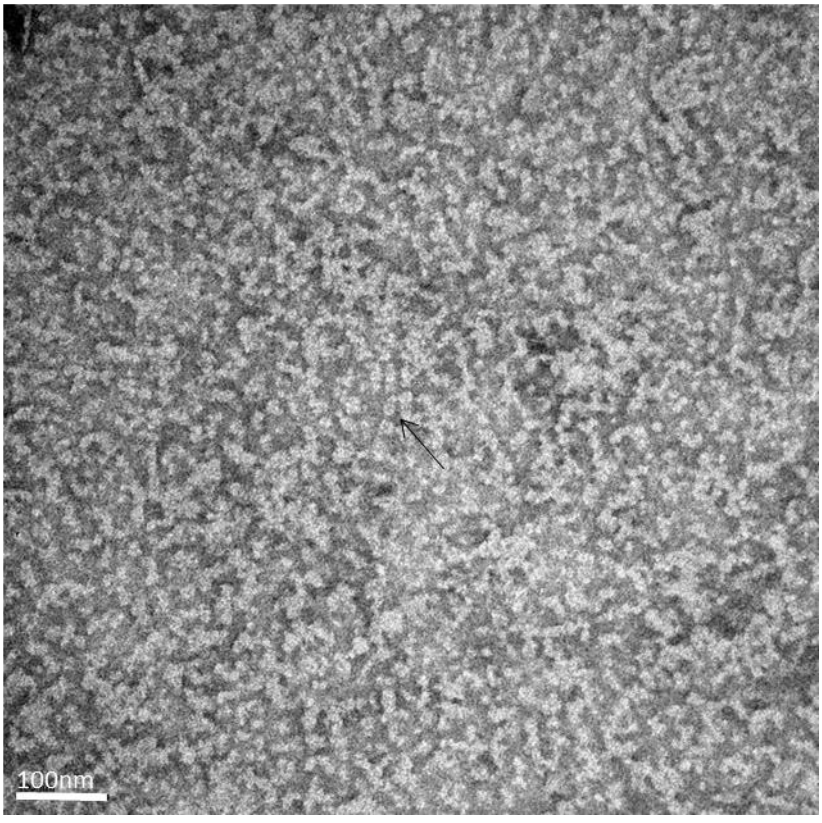

C

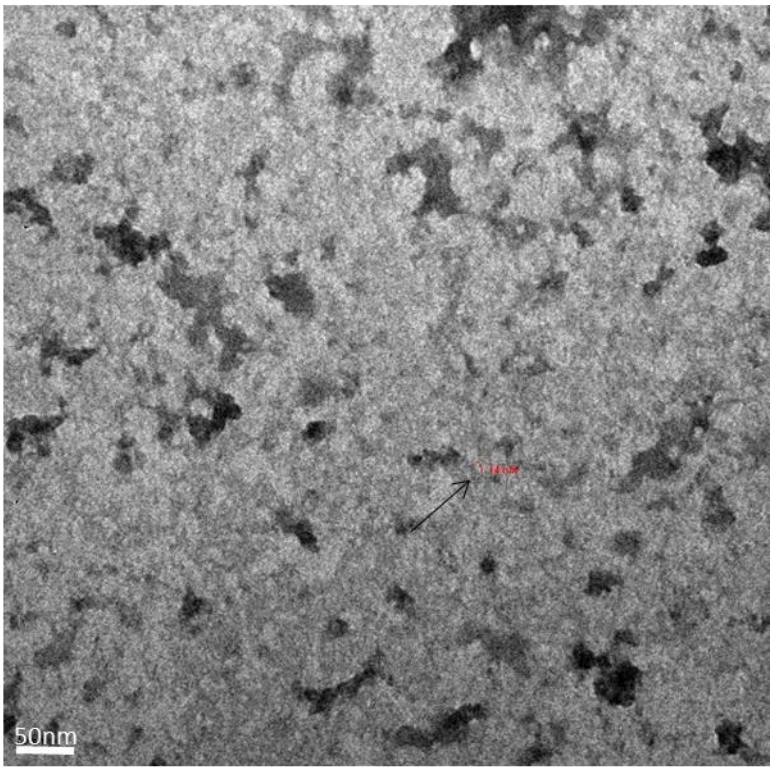

D

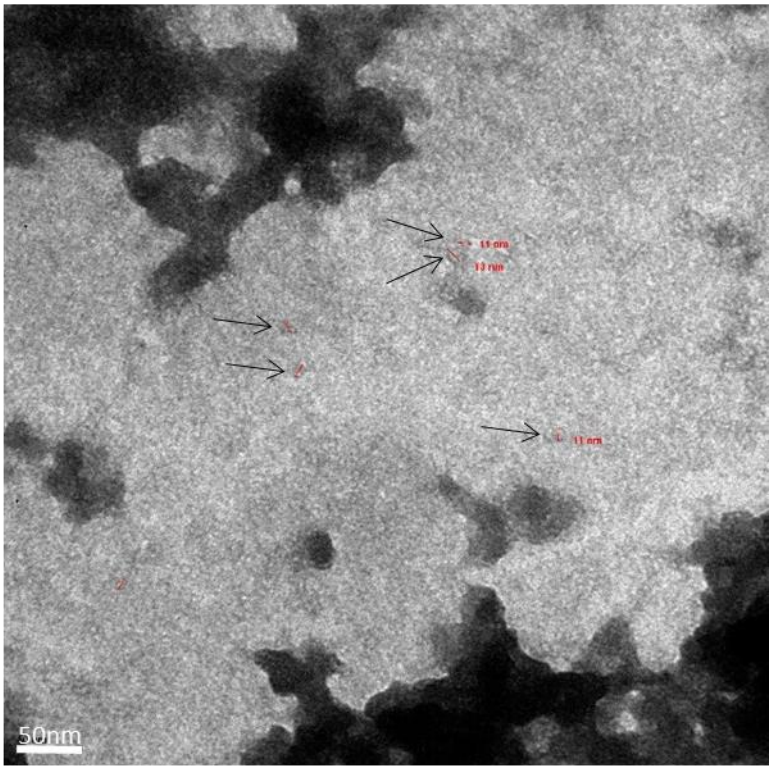

Figure 4.14.4: Negative stain EM with MRP4 in C4C7. *Images A and B are MRP4 in C4C7 at 10µg/mL and 50µg/mL respectively before freezing. Images C and D are MRP4 in C4C7 at 10µg/mL and 50ug/mL respectively after freezing. Images were taken at Lyon University. Arrows indicate potential MRP4 particles.*

Figure 4.14.4 shows preliminary negative stain images of MRP4 purified in C4C7 from *Sf* 9 membranes. The particles are not well defined. Panel A possibly shows some particles between 7 and 14nm in size, and are more defined than panel B suggesting that a lower concentration could help with the resolution. The higher concentration could have led to aggregation. Images C and D are after freezing and show that at a lower concentration the particles were less defined than before freezing.

4.14.5 Negative stain EM of MRP4 purified in SMA 2000

A

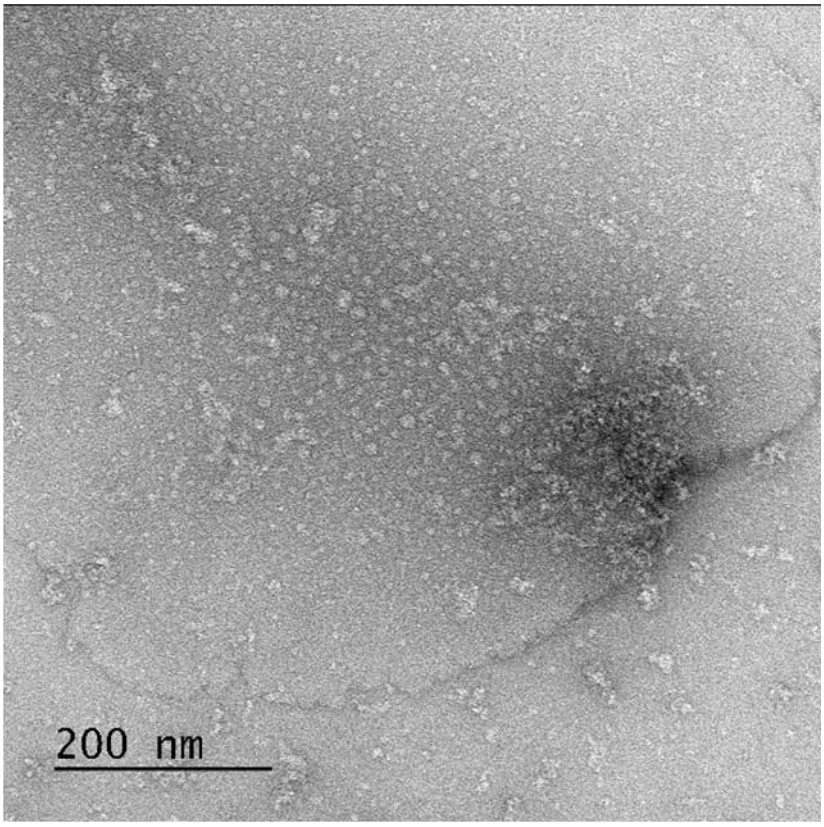

B

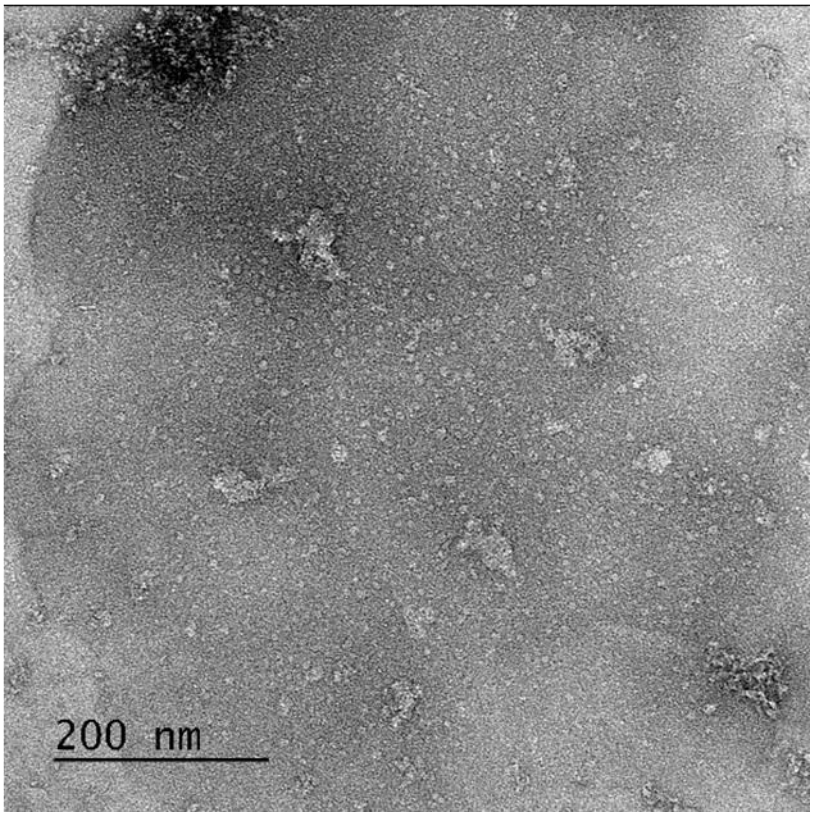

C

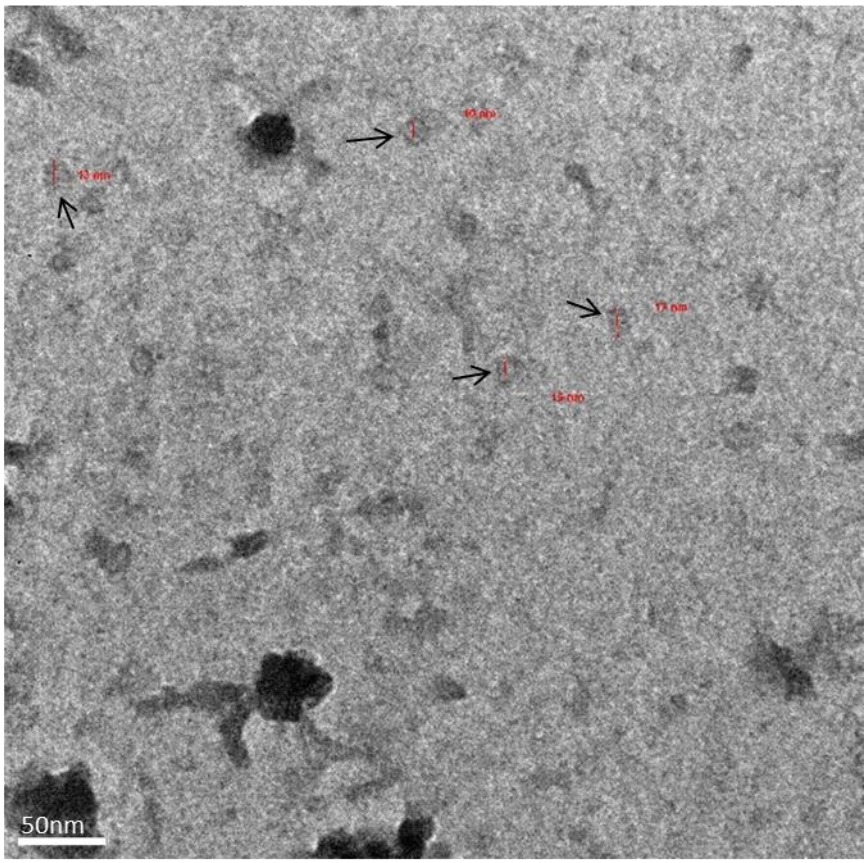

D

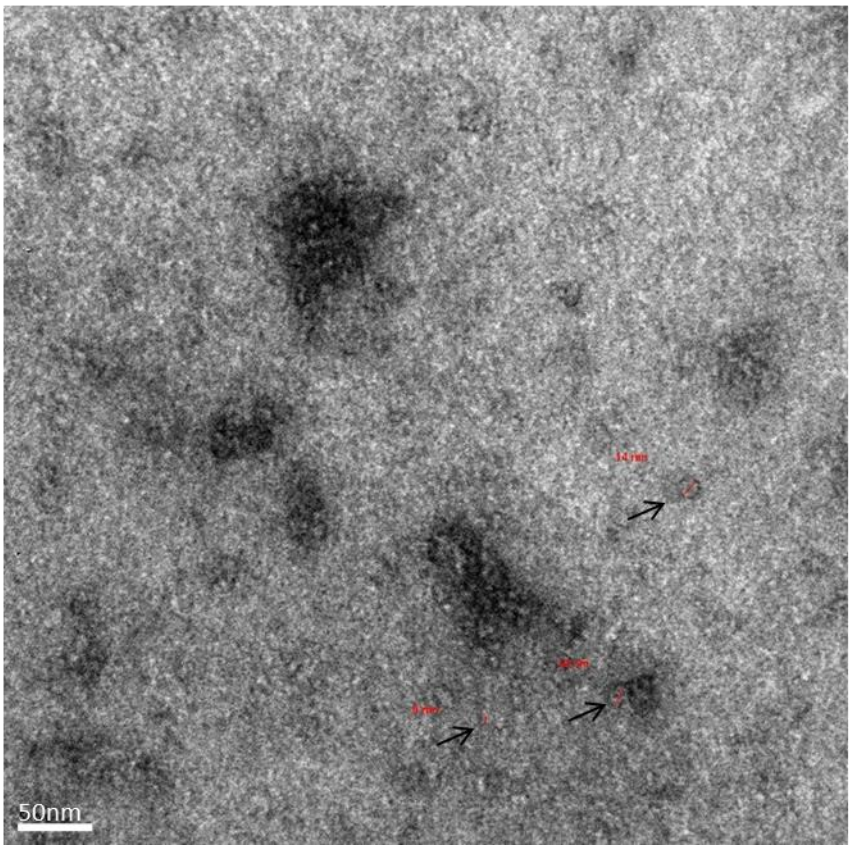

Figure 4.14.5: Negative stain EM with SMA MRP4. *Images A and B are negative stain EM of MRP4 purified in SMA 2000 at 9µg/mL. These images were taken at Warwick University with a Jeol 2100 EM and stained 2% (w/v) uranyl acetate with 60x magnification. Negative stain EM images C and D are MRP4 purified in SMA 2000 after freezing. Image C was at 10µg/mL and D at 50µg/mL. These images were taken at Lyon University using. Arrows indicate MRP4 particles.*

Images in figure 4.14.5 are of purified MRP4 in SMA 2000 from *Sf* 9 membranes. Images A and B show a large amount of circular particles of different sizes. MRP4 is 75% pure in these images meaning these particles are most likely MRP4 but some of them could also be contaminants. Images C and D show MRP4 purified in SMA 2000 after freezing. These particles appear with a darker outer ring with a lighter inner circle. The particles in C are between 10 and 17nm and the particles in D are between 8 and 14nm. These particles are in line with the average size of SMA particles that are normally around 10-12nm. The sizes may vary outside of this range, firstly depending on the angle of the particle and the fact that previous measurements of SMA particle were done with lipids only. Particles that contain MRP4 will have protein that protrudes from the top and bottom of the SMA particle increasing the size. It appears the lower concentration of 10µg/mL after freezing produced more defined particles. These particles appear with a thin outer dark ring with a thicker inner lighter ring and darker inner circle. The MRP4 purified in A and B are from a different purification to C and D.

4.14.6 Negative stain EM of MRP4 purified in XZ25010

A

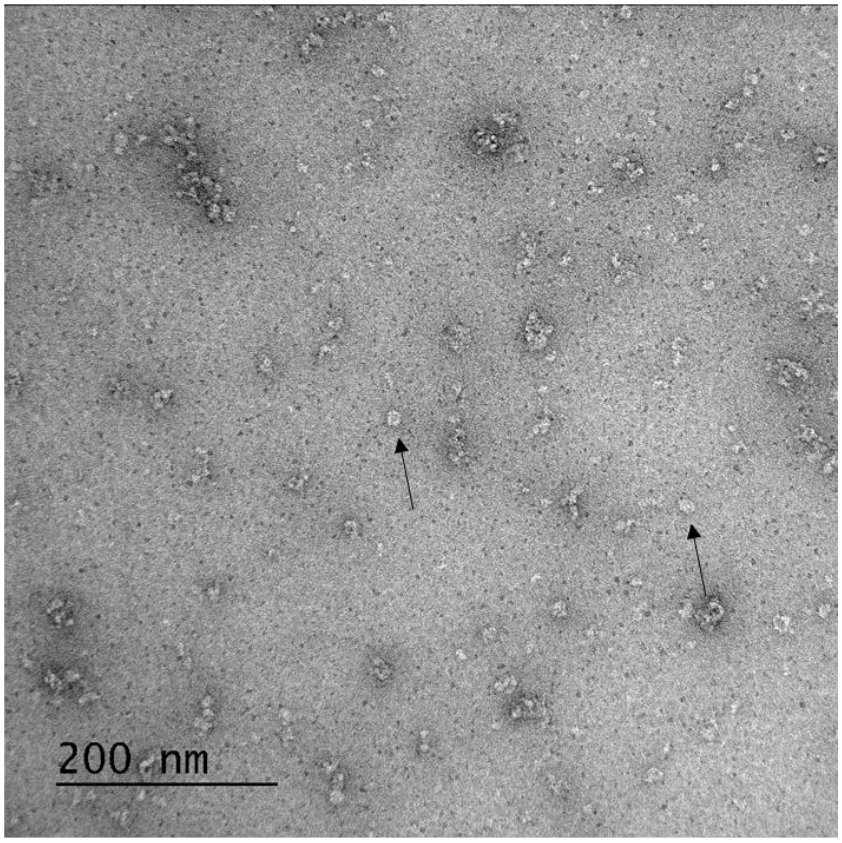

B

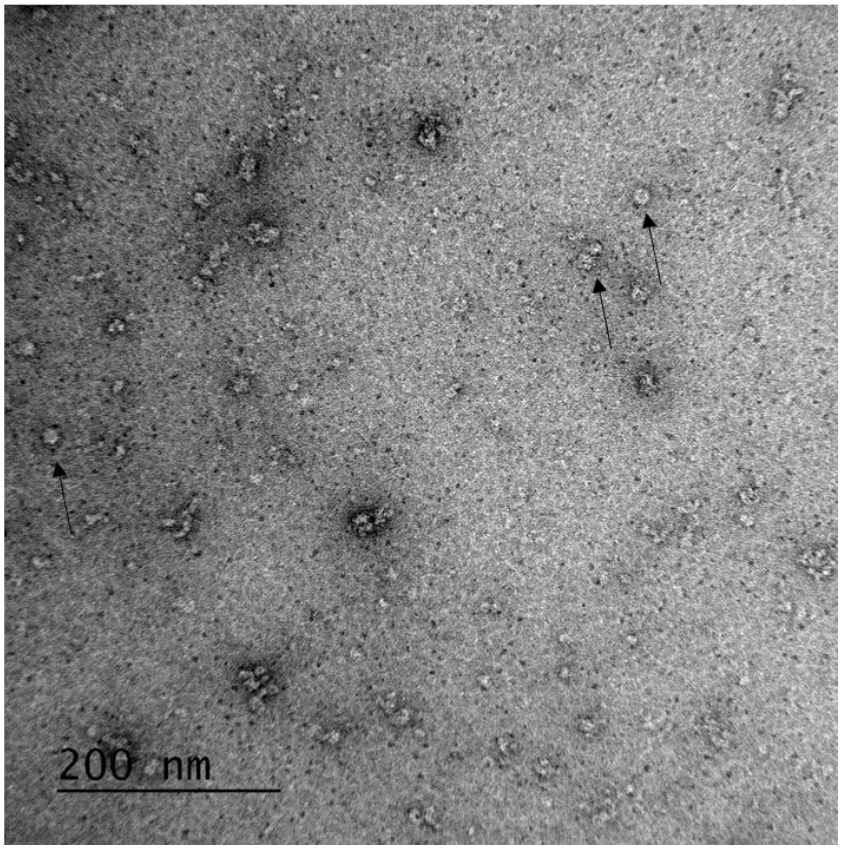

Figure 4.14.6: Negative stain EM with XZ25010 MRP4. *Images A and B are MRP4 purified in XZ25010 and either stained with 2% (w/v) uranyl acetate or 2% (w/v) gadolinium acetate respectively. MRP4 is at 48µg/mL and magnified at 60x (A) and 80x (B) with arrows indicating the MRP4 particles. Images were taken at Warwick University with a Jeol 2100 electron microscope EM.*

A high resolution protein structure within SMALPs was recently reported (Sun, Benlekbir et al. 2018) using a SMA polymer with a 3:1 ratio of styrene:maleic acid. Therefore, we also tried using MRP4 purified within the polymer SZ25010 from Polyscope, which has a 3:1 ratio. Negative stain images of this protein are shown in figure 4.12.6.

MRP4 is 71% pure in these images. When using uranyl acetate with SZ25010 there appears to be less aggregation than compared to SMA 2000 and the SMALP particles are more well defended.

Finally since SMA polymers are known to be sensitive to low pH which causes the SMALPs to precipitate, and a lot of aggregation had been observed, an alternative stain was trialled, gadolinium acetate (Figure 4.14.6 B). Some dark particles are observed, possibly with a lighter outer lighter ring. However, aggregation still appears to be an issue.

Use of these purified proteins for electron microscopy in the future will thus require some significant optimisation in terms of grid preparation, concentration and stain.

5 Discussion

The overall aim of this project was to develop methods and approaches to produce stable, purified MRP4 for use in functional and structural studies Producing membrane proteins for functional and structural studies requires a highly stable and homogenous sample at a high concentration. There are many bottlenecks in producing such a sample such as overexpression of functional membrane protein, solubilising and stabilising it for purification and compatibility of the solubilising agent with functional and structure techniques. This study shows demonstrates some ways in which each of these problems can be faced and how novel solubilising agents can aid in the production of a highly stable purified MRP4 sample.

5.1 Expression and Function

5.1.1 Overexpression of MRP4

One of the most important parts when investigating the function and structure of a protein is having good starting material to work with. This means having high level expression of functional protein.

As membrane proteins naturally have low expression levels overexpression of them is usually required to obtain a high enough yield. This can be done by increasing the level of expression in it native host through stimulus or by creating a recombinant membrane protein to be overexpressed. By creating a recombinant membrane protein modifications to improve stability and purification can also be undertaken, such as mutagenesis, addition of extra domains or use of orthologues. This has proven successful in the past for the determination of several structures (Johnson and Chen 2017, Alam, Kung et al. 2018); however, in this project the aim was to produce wildtype, stable human MRP4.

The three hosts chosen to overexpress the recombinant human MRP4: *Sf* 9 insect cells, *P.pastoris* yeast cells and HEK cells. *Sf* 9 insect cells were chosen as they have been shown previously to express functional human ABC transporters(Van Aubel, Smeets et al. 2002, Reichel, Masereeuw et al. 2007, Gulati, Jamshad et al. 2014).

Insect cells can grow to reasonably high cell densities and are easily infected with a baculovirus for protein expression. Baculovirus infected insect cells have previously been used for the successful expression of functional human ABC transporters such as P-glycoprotein/ABCB1 (Taylor, Storm et al. 2001) , ABCG2 (McDevitt, Collins et al. 2006) MRP1/ABCC1 (Gao, Loe et al. 1996) and MRP4 (Sauna, Nandigama et al. 2004). Although it should be noted that P-glycoprotein and ABCG2 both utilised High Five insect cells as opposed to *Sf* 9s. The making of the recombinant virus can be complex and time consuming and once the virus has been produced it repeatedly has to be amplified. This means there can be batch-to-batch variability in the baculovirus and unless the pfu/cell is calculated each time the expression level could vary. Also the media for growing insect cells can be very expensive.

P. pastoris offer a way around this batch to batch variability by integrating the MRP4 gene into its genome creating a stable cell line. *P.pastoris* has been used in the expression of many ABC transporters previously (Chloupkova, Pickert et al. 2007), including human MRP1 (Wu, Oleschuk et al. 2005). Pichia can be grown in either shake flasks or bioreactors to very high cell densities. It is relatively easy and cheap to culture. This means large quantities of an overexpressed membrane protein can be produced.

However, neither *Sf* 9 cells nor *P.pastoris* are native expression hosts for MRP4, HEK cells represent a more native human cellular environment. HEK cell expression has been used in producing numerous crystal structure of membrane proteins (Andrell and Tate 2013) including human ABCG2 (Taylor, Manolaridis et al. 2017). HEK cells can provide the correct post-translational machinery and a suitable lipid environment that could matter in producing a

functional membrane protein. Having the correct glycosylation can play a role in producing functional membrane proteins. Although *Sf* 9 cells can N-glycosylate (Kost, Condreay et al. 2005) and *P.pastoris* is able to hypermannosylate membrane proteins mammalian expression will produce a much more diverse glycan structure(Ahmad, Hirz et al. 2014). However, it can be more difficult to scale up HEK cell expression and for transient transfection this can become very expensive.

The results from this study show that in *Sf* 9 insect cells human MRP4 with a C-terminal his_6 tag gave the highest levels of expression. This MRP4-his_6 baculovirus had previously been shown to be overexpressed in *Sf* 9 cells (Gulati, Jamshad et al. 2014) using an MOI of 5 for 72 hours. This expression level was used as a control to determine if the yield could be increased by changing the MOI, time and cell density. This study showed that a shorter time period (48 hours) increased the yield of MRP4-his_6 to around twice the amount. However, the concentration of cells used and the MOI did not have an effect on the expression level. The increased level of expression was most likely attributed to the fact that after 48 hours the baculovirus started to lyse the insect cells causing the expression level to be reduced.

In contrast, the N-terminally tagged his_6-MRP4 construct within the pFastBac donor plasmid was unable to be made into a recombinant baculovirus so the expression of this construct could not be evaluated.

The expression of human MRP4 with a C-terminal GFP tag (MRP4-GFP) was also investigated. This construct showed a reduced expression level compared to MRP4-his_6. The level of expression was again mostly time dependent rather than the MOI and cell density. The highest expression level of MRP4-GFP was found after 72 hours using a cell density of 1×10^6 *Sf* 9 cells/mL. This could show that the addition of GFP to MRP4 takes longer to express and lowers the expression level or the viral concentration are different.

Even though the MRP4-GFP expression was lower than MRP4-his_6 adding GFP to a protein can also has its benefits. The GFP can allows the visual expression and localisation of MRP4 and can enable different quantitative measurements. The fluorescent images in figure 4.4.3 allowed a quick and easy way to determine if MRP4 was being expressed without the need of membrane preparations and western blotting. These results cannot show exactly where the MRP4-GFP is localised due to poor resolution but using a more advanced fluorescent microscope the location could be visualised. Flow cytometry could also be used to measure the level of expression by measuring GFP fluorescence. This technique shows how many cells out of the total population are expressing MRP4-GFP and to what level, it would also show how many cells are still viable. The viability of the cells is important, as mentioned before, the baculovirus has lytic effects on *Sf* 9 cells and if the MOI was too high causing cell lysis this would be shown using flow cytometry. GFP can also be used to track the monodispersity by SEC following solubilisation (Kawate and Gouaux 2006).

Sf 9 cell expression produced a higher yield of protein than *Pichia pastoris* yeast. Even when the much higher cell densities that could be achieved within a litre culture of yeast were accounted for, the total amount of MRP4 produced was still lower.

Only the MRP4-his_6 construct was cloned into other expression vectors for expression in *P.pastoris* and HEK cells as this construct showed the highest expression levels in *Sf* 9 cells. Expression levels in *P. pastoris* in shaker flasks were initially far lower than in *Sf* 9 cells (Figure 4.6.4 A), even when the much higher cell densities that could be achieved were accounted for, the total amount of MRP4 produced was still much lower. However later optimisation experiments showed the expression level cold be increased, nearly reaching the level of the *Sf* 9 cells (Figure 4.6.4 B). Using a 2L bioreactor in place of a shaker flask did not improve the expression level. This shows that although the 2L bioreactors are a more controlled environment, changing the

expression conditions in shaker flasks would be a more beneficial way of increasing expression yields.

Preliminary expression trials were carried out using transient transfection of HEK cells with PEI. This showed that overexpression in HEK cells is possible, whilst utilising one of the cheapest transfection agents. However, there was not time to test alternative transfection agents or to compare yields obtained with those obtained using *Sf* 9 cells or *Pichia pastoris*. Notably the MRP4 expressed in HEK cells ran at a higher molecular weight than *Sf* 9, presumably due to the extra glycosylation. Previous study showing MRP1 expression in insect cells running lower than in mammalian cells, due to less glycosylation (Gao, Loe et al. 1996). In the future, it would also be interesting to investigate the development of a stably expressing HEK cell line.

5.1.2 Functional assessment of MRP4

The membrane protein that is being over expressed should be tested for its function, proving that it is expressed in a native functional form. The means that it is known to be in it native conformation before solubilisation and purification and can be tested for its function after these processes.

One possible approach to this could have been to examine ATPase activity within the membrane fractions, as ATP hydrolysis is the driving force behind the transport mechanism of MRP4. This approach has been reported previously (Sauna, Nandigama et al. 2004) however this assay would have been conducted with crude membranes that contain other native membrane proteins from the expression host, some of which could be ATPases, and measuring MRP4-specific ATPase above the background activity would be very difficult. As the expression level of MRP4 was fairly low in *Sf* 9 cells and even lower in *P. pastoris* this would add to the challenges of this approach. In addition, although ATP hydrolysis may be the driving force it does not prove that the entire transport mechanism of MRP4 is functional.

Instead a vesicular transport assay was developed in this study as a way to prove MRP4 was being functionally overexpressed. This assay assesses the ability of MRP4 to transport a fluorescent derivative of cAMP (fluo-cAMP) into inside-out membrane vesicles when in the presence of ATP. Vesicular transport assays have been used for many years to assay ABC transporter activity within crude membrane preps, however they typically utilise radioactively labelled substrates. For reasons of cost, administration and technical ease this study aimed to develop a fluorescent based vesicular transport assay.

The premise behind using fluo-cAMP in testing the functionality of MRP4 expressed in *Sf* 9 cells was based on two studies carried out. One study showed that fluo-cAMP was a substrate for MRP4 in rat choroid plexus (Reichel, Klas et al. 2010), and another showed that MRP4 expressed in *Sf* 9 cell vesicle would uptake fluo-cAMP in an ATP dependent manner (Reichel, Masereeuw et al. 2007).

The results of the current study showed that MRP4 overexpressed in *Sf* 9 cells was able to transport fluo-cAMP in an ATP dependent manner (Figure 4.8.2). It also showed that MRP4 was facilitating the transport of fluo-cAMP as there was a significant increase in ATP dependent uptake in *Sf* 9 MRP4 membranes compared to *Sf* 9 native membrane (Figure 4.8.2).

One of the challenges encountered during the development of the assay was the method used for separation of free un-transported fluo-cAMP from the vesicles. Typically vesicular transport assays using radiolabelled substrates utilise rapid filtration through glass-fibre filters for this step. Initially this approach was used here, followed by soaking the filters in a buffer containing SDS to solubilise the vesicles and release the fluo-cAMP into solution for measurement by fluorescent spectroscopy. However this process led to particles/debris from the filters in the solution which caused a large amount of light scattering which interfered with the spectra obtained, especially as fluo-cAMP doesn't have a particularly large Stokes shift (λ_{ex} = 480nm, λ_{em} = 515nm). In addition, there was a concern that some of the vesicles were passing through the filters and not being trapped, and therefore not being measured. The filters used have a reported pore size of 0.7 µm

that may be larger than some vesicles. To overcome these issues centrifugation was instead used to separate the vesicles from the fluo-cAMP, followed by two rounds of washing of the pellet. This approach was much more suitable because as it allowed for more samples to be run in parallel, increasing the efficiency, and the vesicles are kept in the same container throughout the process reducing loss of vesicles.

Using this new modified approach *Sf* 9 MRP4 membranes showed a concentration dependent uptake of fluo-cAMP, with a K_m of 5.5 µM which is similar to previously reported values 5.3 ± 2 µM (Reichel, Masereeuw et al. 2007). The Km of cAMP itself is 45 µM which is closer to the Km of fluo-cAMP using the filtration method (33 µM) (Russel, Koenderink et al. 2008) . To test for the inhibition of MRP4 two types of inhibitor were used; one type inhibits the hydrolysis of ATP and the other binds to the transmembrane regions to compete with substrate binding. The inhibitors used to stop hydrolysis of ATP were the non-hydrolysable ATP analogue AMP-PNP, or orthovanadate, both of which showed transport levels at the same level as when AMP was present. MK571 is a well-established inhibitor of MRPs inhibited the uptake of fluo-cAMP with an IC_{50} of 0.39 µM . Although the exact IC50 value is not given for previous MK571 inhibition of fluo-cAMP but the value appear around 1µM (Reichel, Masereeuw et al. 2007). Showing the results obtained in this study are not far off the previous reported results. The IC_{50} values for MK571 inhibition of other molecules is between 2-10 µM (Reid, Wielinga et al. 2003, Rius, Nies et al. 2003).

As mentioned before having a large quantity of good quality membrane protein is a key first step in studying it. MRP4 was successfully expressed in *Sf* 9 cells, with increased expression levels compared to previous reports, and for the first time in *P.pastoris.* The expression levels overall were higher in *Sf* 9 cells but through improvement of the yeast cell culture the expression levels could be improved. This could greatly increase the amount of MRP4 produced as yeast cells can grow to higher cell densities than *Sf* 9 cells. MRP4 expressed in *Sf* 9 cells was found to be

functional through the use of vesicular transport assay. Instead of using the more tradition radioactively labelled substrate a fluorescent labelled substrate was used showing these too are effective way of measuring transport with great ease. Also by changing the step up of the VTA, using centrifugation instead of filtration, made this VTA more efficient.

5.2 Solubility and stability

5.2.1 Solubility

Traditionally detergents have to been used to solubilise membrane protein. The ability of detergents to solubilise membrane proteins is an important factor when studying their structure and function. It allows membrane proteins to become soluble in aqueous solution priming them for downstream processes such as purification. Nevertheless, solubilising the membrane protein is not the only factor that needs to be considered, making sure the protein is stable is an equally important factor. Finding detergents that have both the desired solubilising and stabilising properties are hard to come by and detergent screening can be a time consuming and costly procedure. In addition, what works for one membrane protein will not necessarily work for another. So finding a solubilising agent that can create a soluble but stable membrane protein would be highly beneficial.

Until recently conventional detergents such as DDM, OG and FC have been used in solubilisation and stabilisation of ABC transporters for functional and structural studies. DDM has been used in many studies involving the solubilisation of ABC transports including finding the structure of ABCB10 and Sav 1886 (Galian, Manon et al. 2011, Shintre, Pike et al. 2013). Table 1 shows that different detergents that have been using for the solubilisation of ABC transporters and it is clear how profound the use of DDM is.

Protein	Expression Host	Detergent
MRP4	*Sf 9*	DDM SMA (Gulati, Jamshad et al. 2014)
MRP4	*HEK*	SMA (Gulati, Jamshad et al. 2014)
ABCB10	*Insect cell*	DDM (Shintre, Pike et al. 2013)
ABCB11	*P.pastoris*	FC-16, DDM, Cymal-5 (Ellinger, Kluth et al. 2013)
ABCB4	*P.pastoris*	FC-16 (Ellinger, Kluth et al. 2013)
BmrC/BmrD	*E.coli*	FC-12, FC-16 (Galian, Manon et al. 2011)
ABCG2	*High Five*	FC-16 (McDevitt, Collins et al. 2006)
ABCG2	*P.pastoris*	DDM (Rosenberg, Bikadi et al. 2010)
ABCA4	*HEK23*	DDM (Tsybovsky and Palczewski 2014)
ABCC3	*P.pastoris*	DDM (Ellinger, Kluth et al. 2013)
ABCG5/G8	*P.pastoris*	DDM (Ellinger, Kluth et al. 2013)
MRD1	*P.pastoris*	DM, DDM, Lyso-PC, deoxycholic acid, Triton-X100 (Ellinger, Kluth et al. 2013)
Sav 1886	*S. aureus*	DDM + $C_{12}E_8$ (Galian, Manon et al. 2011)
TAP1/TAP1	*Sf 9*	DDM(Meyer, Vanendert et al. 1994)
BmrA	*E.coli*	DDM (Ravaud, Do Cao et al. 2006)
$MalFGK_2$	*E.coli*	DDM(Oldham and Chen 2011)

Table 5.2.1: Conventional detergents used for solubilisation of ABC transporters.

During this study a dot blot analysis was employed to screen 85 different detergents and SMA co-polymers and narrow it down to the top 16 most soluble conditions. This dot blot analysis cover the four classes of conventional detergents, calixarene based detergents, SMA co-polymers along with detergent mixtures of conventional and calixarene detergents. This showed a clear difference between the novel calixarene detergents, SMA co-polymers and conventional detergents. All conventional detergents were only able to solubilise around 50% of ABCC4

whereas some of the calixarenes and SMA co-polymers were able to solubilise 90 – 100%. In previous results OG was unable to solubilise MRP4 but DDM solubilised 78% from *Sf* 9 membranes(Gulati, Jamshad et al. 2014). SMA 2000 was able to solubilised 86% MRP4 from Sf 9 membranes in a previous study (Gulati, Jamshad et al. 2014). It has previously been shown that the length of the acyl tail of calixarene based detergents plays a key role in their ability to solubilise membrane proteins. There was dramatic change in solubility efficiency of both BmrA (from *E.coli*) and ABCG2 (from *Sf* 9 cells) when the length of acyl tail increased from 3 to 7 carbons (Matar-Merheb, Rhimi et al. 2011). This was again the case in this study where having a short (3) carbon length decrease the solubilisation efficiency. Once the carbon length was increased to 5 the solubilisation percentage dramatically increased and stayed high when increased again to 7 or 8 carbons. But unlike in the Matar-Merheb study the solubilisation percentage where the percentage that was soluble stayed high with increasing carbon length, up to 12 carbons, we found that the solubility percentage for MRP4 decreased once the carbon length reach 10 or 12.

Although using this technique allowed the screening of many detergents the solubilisation efficiency had to be confirmed by Western Blot. The top 16 most soluble conditions were examined for their solubility efficiency. It is interesting to note that DDM did not fall within the top 16 conditions even though it has been extensively used in the solubilisation of ABC transporters previously. Calixarene detergents with 5, 7 or 8 carbons along with SMA-copolymers and detergent mixtures mostly involving C4C7 were in the top 16 conditions. Interestingly it was either the calixarene detergents, by themselves, or the SMA co-polymers that had a higher solubilisation efficiency compare most detergent mixtures. Only detergent mixtures containing Sarkosyl had a high solubilisation efficiency which is not surprise as Sarkosyl is a very harsh detergent. Once again, just as it has been shown before these calixarene based detergents and SMA-copolymer have higher solubilisation efficiency compared to conventional detergents (Matar-Merheb, Rhimi et al. 2011, Gulati, Jamshad et al. 2014).

The solubilisation efficiency of SMA 2000 was investigated further. The standard starting conditions for SMA 2000 solubilisation of membrane proteins was set out in the Rothnie (2016) Methods in Mol Biol and Lee et al Nature protocols. This suggested that using a 2.5% (w/v) solution of SMA 2000 for 1 hour at room temperature with membranes at 30 mg/mL wet pellet weight would have the highest solubility efficiency. The results in this study showed that 2.5% (w/v) did give the highest solubilisation efficiency for MRP4 but the temperature at which it was conducted did not appear to change the solubilisation efficiency. The length of time required to solubilise MRP4 from Sf 9 membrane was also less than an hour. Optical density, western blot and DLS confirmed that most of the solubilisation happened within the first 15 minutes. Optical density reading dramatically dropped within 15 minutes indicating disruption of the membrane occurred very quickly. The size of the SMALPs is usually around 10 nm (Killian 2018) so DLS was performed on solubilised *Sf* 9 MRP4 to determine the particle size. This showed that most particles were around the 10nm indicating these were SMALPs but did not confirm if they contained MRP4. The western blot confirmed that the majority of solubilisation was occurring in the first 15 minutes and it was solubilising MRP4. This time frame may be true for solubilising MRP4 from *Sf* 9 membranes but other membrane proteins from different expression host may take a longer time due to the lipid environment.

Studies were taken to determine if other SMA polymers have a higher solubility efficiency than SMA 2000. A polymer screen showed that three other SMA polymers: SMA 3000, XZ09008 and SZ25010 were also able to solubilise MRP4. Interestingly these all had molecular weight between 7.5 – 10kDA and contained either 25% or 33% maleic acid. Any SMA polymer with a higher maleic acid content or molecular weight was unable to solubilise MRP4 showing that the SMA polymers must have certain properties for successful solubilisation (Morrison, Akram et al. 2016). It is unknown if any one polymer is able to solubilise all membrane proteins but SMA with a 2:1 styrene : maleic acid content has been used in many different membrane protein solubilisations(Gulati, Jamshad et al. 2014). It has previously been shown that SMA polymers with

a 3:1 and low molecular weights are more suitable for membrane protein solubilisation (Skaar, Korza et al. 2015).

5.2.2 Stability

Although calixarene detergents and SMA co-polymers had high solubilisation efficiencies, their ability to stabilise MRP4 needed to be examined. Other conventional detergents (C12E8, CYMAL, DDM and FC-12) were used for thermostability testing as a comparison to the novel detergents and co-polymers. These conventional detergents were chosen as they have been used in studies involving the solubilisation of ABC transporters, all have a similar solubilisation percentage and offer a variety of non-ionic and zwitterionic properties as shown in table 1.

A common method for measuring the stability of proteins is through their ability to withstand high temperatures. The higher the thermostability of a protein the more stable it is. A simple method for measuring the thermostability of un-purified membrane proteins was developed (Ashok, Nanekar et al. 2013). This method allows you to quickly screen the stability of membrane protein in different detergents, without the need for purification, allowing you to assess which detergent is most likely to keep the membrane protein stable throughout the purification process. Solubilised membrane proteins are heated and then all aggregated protein is separated through ultracentrifugation, revealing the percentage of soluble stable membrane protein that remains through western blotting. One problem with this method is that other proteins within the membrane may be less stable than your protein of interest, these will form aggregates and may interact with your protein causing it to aggregate.

During this study we examined the difference between conventional detergents that have been used to solubilise other ABC transports and novel solubilising agents in maintaining the stability of MRP4. The two calixarene based detergents, C4C5 and C4C7, displayed a considerable increase in the Tm compared to conventional detergents showing that MRP4 was more stable in these novel

detergents. This result shows that not only can these calixarene detergents solubilise MRP4 more efficiently but they are also able to make it more stable. SMA polymers have previously been shown to stabilise membrane protein more effectively compared to conventional detergents (Dorr, Koorengevel et al. 2014, Gulati, Jamshad et al. 2014, Jamshad, Charlton et al. 2015). The results in this study also showed a dramatic increase in the thermostability of MRP4 when solubilised with SMA 2000 compared to conventional detergents.

Extracting the highest amount of MRP4 from membrane in a stable form to allow for purification was one of the main goals of this study. These novel solubilising agent were able to extract around twice the amount of MRP4 from *Sf* 9 membranes. The novel detergents were able to stabilise MRP4 through interacting with the basic amino acids near the membrane domain by forming salt bridges. By interacting with the membrane protein these types of detergents stabilize the membrane protein rather than just surrounding it in detergent micelle. SMA polymers take a different approach by encapsulating the membrane protein in a lipid disc there for maintain its structure. The SMA polymer itself has a very high glass transition temperature of over 130^{o}C making it highly thermostable. The stability of the membrane protein is most likely to be influenced by the lipids surrounding them and is no wonder that membrane proteins in SMALP have a similar melting temperature to membranes(Rehan, Paavilainen et al. 2017). This study showed using novel solubilising agents such as calixarenes and SMA polymers have a higher solubility efficiency and more thermostable than conventional detergents.

5.3 Compatibility with functional and structural techniques

In order to investigate the function and structure of membrane proteins the membrane protein must first be purified to obtain a homogenous sample. Not only this, but the membrane protein must be kept stable throughout the purification process. This study has shown that novel

solubilising agents such as calixarenes and SMA polymers not only solubilise but stabilise MRP4 better than conventional detergents, but can they be purified and are these novel solubilising agents compatible with functional and structural techniques.

One of the main advantages SMA has over any class of detergent is its suitability for 'detergent free' purification. Once solubilised, the membrane protein is kept stable without the need for additional SMA, unlike detergents where at least 1 CMC has to be kept in all purification buffers. SMA polymers have been shown to increase the purity of membrane proteins (Morrison, Akram et al. 2016). This study also showed that compared to conventional detergents (DDM), SMA 2000 was able to produce a higher purity and yield. The low yield with DDM could have been due to the poor solubilisation of MRP4 making less soluble MRP4 available to start with. The purity maybe have been due to the poor stability of MRP4 in DDM causing the protein to breakdown or become aggregated. The calixarene detergent C4C7 was able to produce a much higher yield than SMA 2000. Using the same *Sf* 9 MRP4 membranes SMA 2000 was only able to produce 0.68ug of MRP4 where as C4C7 produced 46ug of MRP4, 68 times the amount. Even through optimisation of the SMA purification, and using *Sf* 9 membranes with an increased expression level, SMA was only able to produce at best 5 µg of MRP4. The purity of the optimised SMA sample was around 70% whereas with C4C7 the purity was only at best 40%. This shows that although C4C7 and SMA have very similar solubility efficiency and thermostability their ability to produce purified MRP4 is dramatically different. The binding affinity of SMALPed membrane proteins is low due to the interactions of SMA with the nickel resin (Dorr, Scheidelaar et al. 2016) and could be an explanation for the yield in SMA. Additionally the histidine tag attached to MRP4 may not have been as accessible when encapsulated within a SMALP leading to the poor binding affinity. A theory supported by the differences observed in the flow through fractions using an anti-his antibody in comparison to an anti-MRP4 antibody (4.13.1). It is particularly interesting that the brand of nickel resin used made a difference. Although they all utilised an NTA chemistry for the attachment of the Ni^{2+}, the beads themselves may explain the differences. Whereas ABT resin was made from 6% crosslinked agarose and had a bead size of 50-150µm, the Generon resin was

made from 7.5% agarose and had a bead size of approximately 40µm. Furthermore these beads are highly porous to maximise binding surface but the sizes of the pores may vary. The SMALPs are relatively large and highly negatively charged, both of which may affect the interaction with the beads. Introducing a longer histidine tag may improve the binding of MRP4 in SMA to the nickel resin. Alternatively a different type of affinity tag may offer improvements. To improve the purity of MRP4 solubilised with C4C7 the purification conditions such as binding time and concentration of imidazole in the wash step could be optimised in the future.

The stability of purified MRP4 was assessed after purification to establish if MRP4 was still stable. To assess the level of aggregation SEC and Native PAGE were used. For both MRP4 purified in C4C7 or SMA the SEC analysis showed that MRP4 was still stable as no peaks were found in the void volume and it was eluted off in a single peak. Similarly, the Native PAGE also revealed that no aggregation had occurred and MRP4 was found as a singular band in both cases. This shows that these two types of novel solubilising agent cause no aggregation of MRP4 during purification. Analysis of the thermostability following purification showed that MRP4 purified in C4C7 or within SMALPs also retained its increased thermostability compared to conventional detergents, as reported previously for other proteins (Gulati, Jamshad et al. 2014) making them good candidates for the use in functional and structural studies.

C4C7 and SMA may be able to efficiently solubilise and purify MRP4 in a stable state but can they be used in functional as structural studies? It is interesting from the large variety of detergents DDM has been the most used for x-ray crystallography (Stetsenko and Guskov 2017). Generally speaking detergents with shorter acyl tails that form smaller micelles are preferred during crystallography as they allow for more protein-protein interactions (Moraes, Evans et al. 2014). Calixarene based detergents come with a range of different length acyl tails, but the one that was most successful with MRP4 was C4C7 (7 carbon acyl tail). This does have a longer acyl tail than is considered optimal for crystallography, but it could potentially be exchanged for a detergent with

a shorter acyl tail to aid in the crystallisation. Alternatively, it could be exchanged for a shorter more conventional detergent for crystallization. In this study it was shown that exchanging into DDM post purification during SEC was possible. It is theorised that some of the calixarenes which are forming the salt bridges with the protein will remain bound to the protein when the bulk detergent is exchanged, and retain some of the stability. SMA has also been used in x-ray crystallography through the use of lipidic cubic phase (LCP) (Broecker, Eger et al. 2017) but so far there are no reports of its use in traditional vapour diffusion crystallization. This may be due to the lack of protein-protein interactions as the space between individual protein particles will be increased due to the size of the SMALP (~10nm)(Dorr, Scheidelaar et al. 2016). One way to overcome this problem would be to solubilise and purify in SMA and then switch over to a detergent more suitable for crystallography, using the sensitivity of the SMA polymer to divalent cations to remove it. Additionally it has been found that proteins within SMALPs are often more amenable to concentrating effectively than within detergents, which can be a major obstacle to generating crystals (Rothnie 2016). Although in this current study the yield of MRP4 was far lower with SMA than with C4C7, if the yield was improved this could become a viable option for x-ray crystallography.

Electron microscopy requires a far lower concentration of purified protein for structural analysis. The compatibility of SMA and C4C7 with negative stain EM was examined. SMA has been shown previously to be compatible with negative stain EM and is aided by the low electron density of SMA (Postis, Rawson et al. 2015).The negative stain of MRP4 in SMA in this study did not show a definite conclusion. Circular particles could be seen but if these were SMALPs, and contained MRP4, was unknown. This was the same conclusion for C4C7, as particles were seen varying between 7-14nm, but were not confirmed to be MRP4. However particles were seen in both the SMA and C4C7 showing that these novel solubilising agents are compatible with negative stain EM but need to be improved. The main improvement would come through increasing the purity of MRP4. The samples used in this study were about 70% (SMA) and 23- 40% (C4C7) pure. Excess SMA was removed prior to analysis as this could interact with the stain used causing aggregation

but the amount of C4C7 in the sample was unknown. Some of the background noise in the negative stain EM images may have come from excess C4C7 present. Running the purified MRP4 though gel filtration may help remove excess detergent but a 1 x CMC has to be kept. There are also many different types of stains that can be used for negative stain which can vary in pH. Interestingly the stain used in a previous study was 1% uranyl acetate which has a pH range of 4.2-4.9 (Postis, Rawson et al. 2015). SMA is known to precipitate out of solution at low pH, so it might be expected that protein purified within SMALPs would aggregate at this pH, however despite the low pH they were still able to produce a structure of AcrB (Postis, Rawson et al. 2015). Interestingly the XZ25010 SMA polymer showed better results than SMA 2000 with less aggregation and was used in the high resolution structure of the alternative complex III (Sun, Benlekbir et al. 2018). In this study uranyl acetate was also used. Using a negative stain that is closer to the pH in which SMA is stable may help protect the SMALPs creating better images. To attempt to address this the alternative stain gadolinium acetate was investigated, however it did not seem to offer any improvement. Recent studies investigating alternative polymer structures have developed polymers that are tolerant to acidic pH levels (Ravula, Hardin et al. 2017, Hall, Tognoloni et al. 2018, Ravula, Hardin et al. 2018), and this might provide a promising alternative approach.

One of the greatest downfalls of negative stain EM is the resolution. Cryo-EM has a far greater resolution than negative stain and with the advances in technology near atomic-resolution is now available. SMA polymers have been used in cyro-EM and were able to aid in a relatively high resolution structure of AcrB (Parmar, Rawson et al. 2018) and most recently a high resolution structure of the alternative complex III (Sun, Benlekbir et al. 2018). To understand the structure of MRP4 better producing a much more pure sample and using cryo-EM would be the best way, as this would also negate any issues with low pH..

Novel detergents such as Calixarenes cannot be used with all function techniques. They have a high absorbance at a wavelength of 280nm (the same as proteins) making the use of intrinsic

tryptophan fluorescence challenging. Unfortunately, for this reason the function of MRP4 purified within C4C7 could not be measured in this way. This also means that establishing base lines on gel filtration columns such as the AKTA purification systems can be troublesome as the UV detector measures at 280nm. This was shown in this study where the base line in figure 4.12.3.3 A was still increasing as the elution started, making identification of the peak corresponding to the membrane protein hard especially if the concentration is low. The SMA polymers are sensitive to divalent cations such as magnesium and calcium (Morrison, Akram et al. 2016) which causes the SMALP and the encapsulated protein to precipitate. This was problematic during this study as MRP4 is an ABC transporter and to measure ATPase activity magnesium is needed. It has also been suggested that ABC transporters may not be able to undergo complete conformational changes within a SMALP (Pollock, Lee et al. 2018). SMALP encapsulation may be able to produce a highly stable membrane protein presumably due to the lipids and the lateral pressure exerted by them, but the lateral pressure may actually be problematic. Membrane proteins normally reside in a fluid lipid environment allowing them to change conformation. Nevertheless, if SMA is putting too much pressure in the lipids surrounding the membrane protein it could not function properly. Within SMALPs the lipids in the centre of the disc have been shown to be fluid, but those around the outside of the disc which interact with the styrene groups of the polymer are much more ordered (Jamshad, Grimard et al. 2015). To date it has not been possible to determine if this is the case due to the requirement for magnesium.

One key way to overcome both of these problems in the future is the development of alternative polymers. New polymers have already been reported that can overcome the sensitivity to divalent cations such as the Diisobutylene/Maleic Acid (DIBMA) Copolymer (Oluwole, Klingler et al. 2017). Other new SMA polymers have been produced that can give larger disc sizes that may allow more movement within the lipid disc (Craig, Clark et al. 2016). The actual transporter function of MRP4 cannot be assessed within SMALPs as there is no confined space for the molecule to be transported into. To do this would require MRP4 to have to be reconstituted into liposomes. Again, the sensitivity to divalent cations may be a way in which to try to achieve this in

the future. Therefore, in order to measure function of the SMA purified MRP4 a binding assay was used based upon tryptophan fluorescence quenching. This showed that MRP4 was able to bind fluo-cAMP in a dose-dependent manner, with a Kd of 1.65 µM. This value is lower than the value obtain in the VTA (5.5 µM) and previously reported values (Reichel, Masereeuw et al. 2007).

6 Conclusion

MRP4 was successfully expressed in *Sf* 9 insect cells*, P. pastoris* yeast cells and mammalian HEK cells. Optimised expression of MRP4 in *Sf* 9 cells increased the expression two fold. The yeast cell expression was increasing through optimisation but was still below *Sf* 9 expression levels. The functionality of MRP4 expressed in *Sf* 9 cells was examined using a fluorescent VTA. This proved MRP4 was able to transport fluo-cAMP in an ATP dependent and was functional. Novel solubilising agents, calixar detergents and SMA polymers, showed increased solubility efficiency compared to conventional detergents.

MRP4 was successfully purified using the novel solubilising agents, calixarene (C4C7) and SMA 2000, and kept in a stable state compared to a conventional detergent DDM. There was no aggregation during purification and MRP4 in the novel solubilising agents had a higher thermostability than in conventional detergents. Only SMA was able to be verified in producing a functional MRP4 after purification using an intrinsic tryptophan fluorescence quenching assay. As calixarenes are unable to be used in this assay the function of MRP4 in C4C7 was not assessed but in the future an ATPase assay could be carried out. Preliminary negative stain EM images were taken and showed that improvements in sample preparation are required, but there is potential for its use to investigate the structure of MRP4.

7 Appendices

7.1 pFastBac MRP4-his$_6$ sequence

GACGCGCCCTGTAGCGGCGCATTAAGCGCGGCGGGTGTGGTGGTTACGCGCAGCGTGACCGCTACACTTG
CCAGCGCCCTAGCGCCCGCTCCTTTCGCTTTCTTCCCTTCCTTTCTCGCCACGTTCGCCGGCTTTCCCCGTCAA
GCTCTAAATCGGGGGCTCCCTTTAGGGTTCCGATTTAGTGCTTTACGGCACCTCGACCCCAAAAAACTTGAT
TAGGGTGATGGTTCACGTAGTGGGCCATCGCCCTGATAGACGGTTTTTCGCCCTTTGACGTTGGAGTCCAC
GTTCTTTAATAGTGGACTCTTGTTCCAAACTGGAACAACACTCAACCCTATCTCGGTCTATTCTTTTGATTTAT
AAGGGATTTTGCCGATTTCGGCCTATTGGTTAAAAAATGAGCTGATTTAACAAAAATTTAACGCGAATTTTA
ACAAAATATTAACGTTTACAATTTCAGGTGGCACTTTTCGGGGAAATGTGCGCGGAACCCCTATTTGTTTAT
TTTTCTAAATACATTCAAATATGTATCCGCTCATGAGACAATAACCCTGATAAATGCTTCAATAATATTGAAA
AAGGAAGAGTATGAGTATTCAACATTTCCGTGTCGCCCTTATTCCCTTTTTTGCGGCATTTTGCCTTCCTGTT
TTTGCTCACCCAGAAACGCTGGTGAAAGTAAAAGATGCTGAAGATCAGTTGGGTGCACGAGTGGGTTACA
TCGAACTGGATCTCAACAGCGGTAAGATCCTTGAGAGTTTTCGCCCCGAAGAACGTTTTCCAATGATGAGC
ACTTTTAAAGTTCTGCTATGTGGCGCGGTATTATCCCGTATTGACGCCGGGCAAGAGCAACTCGGTCGCCG
CATACACTATTCTCAGAATGACTTGGTTGAGTACTCACCAGTCACAGAAAAGCATCTTACGGATGGCATGA
CAGTAAGAGAATTATGCAGTGCTGCCATAACCATGAGTGATAACACTGCGGCCAACTTACTTCTGACAACG
ATCGGAGGACCGAAGGAGCTAACCGCTTTTTTGCACAACATGGGGGATCATGTAACTCGCCTTGATCGTTG
GGAACCGGAGCTGAATGAAGCCATACCAAACGACGAGCGTGACACCACGATGCCTGTAGCAATGGCAACA
ACGTTGCGCAAACTATTAACTGGCGAACTACTTACTCTAGCTTCCCGGCAACAATTAATAGACTGGATGGA
GGCGGATAAAGTTGCAGGACCACTTCTGCGCTCGGCCCTTCCGGCTGGCTGGTTTATTGCTGATAAATCTG
GAGCCGGTGAGCGTGGGTCTCGCGGTATCATTGCAGCACTGGGGCCAGATGGTAAGCCCTCCCGTATCGT
AGTTATCTACACGACGGGGAGTCAGGCAACTATGGATGAACGAAATAGACAGATCGCTGAGATAGGTGCC
TCACTGATTAAGCATTGGTAACTGTCAGACCAAGTTTACTCATATATACTTTAGATTGATTTAAAACTTCATT
TTTAATTTAAAAGGATCTAGGTGAAGATCCTTTTTGATAATCTCATGACCAAAATCCCTTAACGTGAGTTTTC
GTTCCACTGAGCGTCAGACCCCGTAGAAAAGATCAAAGGATCTTCTTGAGATCCTTTTTTTCTGCGCGTAAT
CTGCTGCTTGCAAACAAAAAAACCACCGCTACCAGCGGTGGTTTGTTTGCCGGATCAAGAGCTACCAACTC
TTTTTCCGAAGGTAACTGGCTTCAGCAGAGCGCAGATACCAAATACTGTCCTTCTAGTGTAGCCGTAGTTAG
GCCACCACTTCAAGAACTCTGTAGCACCGCCTACATACCTCGCTCTGCTAATCCTGTTACCAGTGGCTGCTG
CCAGTGGCGATAAGTCGTGTCTTACCGGGTTGGACTCAAGACGATAGTTACCGGATAAGGCGCAGCGGTC
GGGCTGAACGGGGGGTTCGTGCACACAGCCCAGCTTGGAGCGAACGACCTACACCGAACTGAGATACCTA
CAGCGTGAGCATTGAGAAAGCGCCACGCTTCCCGAAGGGAGAAAGGCGGACAGGTATCCGGTAAGCGGC
AGGGTCGGAACAGGAGAGCGCACGAGGGAGCTTCCAGGGGGAAACGCCTGGTATCTTTATAGTCCTGTC
GGGTTTCGCCACCTCTGACTTGAGCGTCGATTTTTGTGATGCTCGTCAGGGGGGCGGAGCCTATGGAAAAA
CGCCAGCAACGCGGCCTTTTTACGGTTCCTGGCCTTTTGCTGGCCTTTTGCTCACATGTTCTTTCCTGCGTTA
TCCCCTGATTCTGTGGATAACCGTATTACCGCCTTTGAGTGAGCTGATACCGCTCGCCGCAGCCGAACGACC
GAGCGCAGCGAGTCAGTGAGCGAGGAAGCGGAAGAGCGCCTGATGCGGTATTTTCTCCTTACGCATCTGT
GCGGTATTTCACACCGCAGACCAGCCGCGTAACCTGGCAAAATCGGTTACGGTTGAGTAATAAATGGATGC
CCTGCGTAAGCGGGTGTGGGCGGACAATAAAGTCTTAAACTGAACAAAATAGATCTAAACTATGACAATA
AAGTCTTAAACTAGACAGAATAGTTGTAAACTGAAATCAGTCCAGTTATGCTGTGAAAAAGCATACTGGAC
TTTTGTTATGGCTAAAGCAAACTCTTCATTTTCTGAAGTGCAAATTGCCCGTCGTATTAAAGAGGGGCGTGG
CCAAGGGCATGGTAAAGACTATATTCGCGGCGTTGTGACAATTTACCGAACAACTCCGCGGCCGGGAAGC
CGATCTCGGCTTGAACGAATTGTTAGGTGGCGGTACTTGGGTCGATATCAAAGTGCATCACTTCTTCCCGTA
TGCCCAACTTTGTATAGAGAGCCACTGCGGGATCGTCACCGTAATCTGCTTGCACGTAGATCACATAAGCA

CCAAGCGCGTTGGCCTCATGCTTGAGGAGATTGATGAGCGCGGTGGCAATGCCCTGCCTCCGGTGCTCGC
CGGAGACTGCGAGATCATAGATATAGATCTCACTACGCGGCTGCTCAAACCTGGGCAGAACGTAAGCCGC
GAGAGCGCCAACAACCGCTTCTTGGTCGAAGGCAGCAAGCGCGATGAATGTCTTACTACGGAGCAAGTTC
CCGAGGTAATCGGAGTCCGGCTGATGTTGGGAGTAGGTGGCTACGTCTCCGAACTCACGACCGAAAAGAT
CAAGAGCAGCCCGCATGGATTTGACTTGGTCAGGGCCGAGCCTACATGTGCGAATGATGCCCATACTTGA
GCCACCTAACTTTGTTTTAGGGCGACTGCCCTGCTGCGTAACATCGTTGCTGCTGCGTAACATCGTTGCTGC
TCCATAACATCAAACATCGACCCACGGCGTAACGCGCTTGCTGCTTGGATGCCCGAGGCATAGACTGTACA
AAAAAACAGTCATAACAAGCCATGAAAACCGCCACTGCGCCGTTACCACCGCTGCGTTCGGTCAAGGTTCT
GGACCAGTTGCGTGAGCGCATACGCTACTTGCATTACAGTTTACGAACCGAACAGGCTTATGTCAACTGGG
TTCGTGCCTTCATCCGTTTCCACGGTGTGCGTCACCCGGCAACCTTGGGCAGCAGCGAAGTCGAGGCATTT
CTGTCCTGGCTGGCGAACGAGCGCAAGGTTTCGGTCTCCACGCATCGTCAGGCATTGGCGGCCTTGCTGTT
CTTCTACGGCAAGGTGCTGTGCACGGATCTGCCCTGGCTTCAGGAGATCGGAAGACCTCGGCCGTCGCGG
CGCTTGCCGGTGGTGCTGACCCCGGATGAAGTGGTTCGCATCCTCGGTTTTCTGGAAGGCGAGCATCGTTT
GTTCGCCCAGGACTCTAGCTATAGTTCTAGTGGTTGGCTACGTATACTCCGGAATATTAATAGATCATGGA
GATAATTAAAATGATAACCATCTCGCAAATAAATAAGTATTTTACTGTTTTCGTAACAGTTTTGTAATAAAAA
AACCTATAAATATTCCGGATTATTCATACCGTCCCACCATCGGGCGCGGATCCCGGTCCGAAGCGCGCGGA
ATTCAAAGGCCTACGTCGACGAGCTCAACATGCTGCCCGTGTACCAGGAGGTGAAGCCCAACCCGCTGCA
GGACGCGAACCTCTGCTCACGCGTGTTCTTCTGGTGGCTCAATCCCTTGTTTAAAATTGGCCATAAACGGAG
ATTAGAGGAAGATGATATGTATTCAGTGCTGCCAGAAGACCGCTCACAGCACCTTGGAGAGGAGTTGCAA
GGGTTCTGGGATAAAGAAGTTTTAAGAGCTGAGAATGACGCACAGAAGCCTTCTTTAACAAGAGCAATCA
TAAAGTGTTACTGGAAATCTTATTTAGTTTTGGGAATTTTTACGTTAATTGAGGAAAGTGCCAAAGTAATCC
AGCCCATATTTTTGGGAAAAATTATTAATTATTTTGAAAATTATGATCCCATGGATTCTGTGGCTTTGAACAC
AGCGTACGCCTATGCCACGGTGCTGACTTTTTGCACGCTCATTTTGGCTATACTGCATCACTTATATTTTTAT
CACGTTCAGTGTGCTGGGATGAGGTTACGAGTAGCCATGTGCCATATGATTTATCGGAAGGCACTTCGTCT
TAGTAACATGGCCATGGGGAAGACAACCACAGGCCAGATAGTCAATCTGCTGTCCAATGATGTGAACAAG
TTTGATCAGGTGACAGTGTTCTTACACTTCCTGTGGGCAGGACCACTGCAGGCGATCGCAGTGACTGCCCT
ACTCTGGATGGAGATAGGAATATCGTGCCTTGCTGGGATGGCAGTTCTAATCATTCTCCTGCCCTTGCAAA
GCTGTTTTGGGAAGTTGTTCTCATCACTGAGGAGTAAAACTGCAACTTTCACGGATGCCAGGATCAGGACC
ATGAATGAAGTTATAACTGGTATAAGGATAATAAAAATGTACGCCTGGGAAAAGTCATTTTCAAATCTTATT
ACCAATTTGAGAAAGAAGGAGATTTCCAAGATTCTGAGAAGTTCCTGCCTCAGGGGGATGAATTTGGCTTC
GTTTTTCAGTGCAAGCAAAATCATCGTGTTTGTGACCTTCACCACCTACGTGCTCCTCGGCAGTGTGATCAC
AGCCAGCCGCGTGTTCGTGGCAGTGACGCTGTATGGGGCTGTGCGGCTGACGGTTACCCTCTTCTTCCCCT
CAGCCATTGAGAGGGTGTCAGAGGCAATCGTCAGCATCCGAAGAATCCAGACCTTTTTGCTACTTGATGAG
ATATCACAGCGCAACCGTCAGCTGCCGTCAGATGGTAAAAAGATGGTGCATGTGCAGGATTTTACTGCTTT
TTGGGATAAGGCATCAGAGACCCCAACTCTACAAGGCCTTTCCTTTACTGTCAGACCTGGCGAATTGTTAGC
TGTGGTCGGCCCCGTGGGAGCAGGGAAGTCATCACTGTTAAGTGCCGTGCTCGGGGAATTGGCCCCAAGT
CACGGGCTGGTCAGCGTGCATGGAAGAATTGCCTATGTGTCTCAGCAGCCCTGGGTGTTCTCGGGAACTCT
GAGGAGTAATATTTTATTTGGGAAGAAATACGAAAAGGAACGATATGAAAAAGTCATAAAGGCTTGTGCT
CTGAAAAAGGATTTACAGCTGTTGGAGGATGGTGATCTGACTGTGATAGGAGATCGGGGAACCACGCTGA
GTGGAGGGCAGAAAGCACGGGTAAACCTTGCAAGAGCAGTGTATCAAGATGCTGACATCTATCTCCTGGA
CGATCCTCTCAGTGCAGTAGATGCGGAAGTTAGCAGACACTTGTTCGAACTGTGTATTTGTCAAATTTTGCA
TGAGAAGATCACAATTTTAGTGACTCATCAGTTGCAGTACCTCAAAGCTGCAAGTCAGATTCTGATATTGAA
AGATGGTAAAATGGTGCAGAAGGGGACTTACACTGAGTTCCTAAAATCTGGTATAGATTTTGGCTCCCTTT
TAAAGAAGGATAATGAGGAAAGTGAACAACCTCCAGTTCCAGGAACTCCCACACTAAGGAATCGTACCTTC
TCAGAGTCTTCGGTTTGGTCTCAACAATCTTCTAGACCCTCCTTGAAAGATGGTGCTCTGGAGAGCCAAGAT
ACAGAGAATGTCCCAGTTACACTATCAGAGGAGAACCGTTCTGAAGGAAAAGTTGGTTTTCAGGCCTATAA
GAATTACTTCAGAGCTGGTGCTCACTGGATTGTCTTCATTTTCCTTATTCTCCTAAACACTGCAGCTCAGGTT

GCCTATGTGCTTCAAGATTGGTGGCTTTCATACTGGGCAAACAAACAAAGTATGCTAAATGTCACTGTAAAT
GGAGGAGGAAATGTAACCGAGAAGCTAGATCTTAACTGGTACTTAGGAATTTATTCAGGTTTAACTGTAGC
TACCGTTCTTTTTGGCATAGCAAGATCTCTATTGGTATTCTACGTCCTTGTTAACTCTTCACAAACTTTGCACA
ACAAAATGTTTGAGTCAATTCTGAAAGCTCCGGTATTATTCTTTGATAGAAATCCAATAGGAAGAATTTTAA
ATCGTTTCTCCAAAGACATTGGACACTTGGATGATTTGCTGCCGCTGACGTTTTTAGATTTCATCCAGACATT
GCTACAAGTGGTTGGTGTGGTCTCTGTGGCTGTGGCCGTGATTCCTTGGATCGCAATACCCTTGGTTCCCCT
TGGAATCATTTTCATTTTTCTTCGGCGATATTTTTTGGAAACGTCAAGAGATGTGAAGCGCCTGGAATCTAC
AACTCGGAGTCCAGTGTTTTCCCACTTGTCATCTTCTCTCCAGGGGCTCTGGACCATCCGGGCATACAAAGC
AGAAGAGAGGTGTCAGGAACTGTTTGATGCACACCAGGATTTACATTCAGAGGCTTGGTTCTTGTTTTTGA
CAACGTCCCGCTGGTTCGCCGTCCGTCTGGATGCCATCTGTGCCATGTTTGTCATCATCGTTGCCTTTGGGT
CCCTGATTCTGGCAAAAACTCTGGATGCCGGGCAGGTTGGTTTGGCACTGTCCTATGCCCTCACGCTCATG
GGGATGTTTCAGTGGTGTGTTCGACAAAGTGCTGAAGTTGAGAATATGATGATCTCAGTAGAAAGGGTCA
TTGAATACACAGACCTTGAAAAAGAAGCACCTTGGGAATATCAGAAACGCCCACCACCAGCCTGGCCCCAT
GAAGGAGTGATAATCTTTGACAATGTGAACTTCATGTACAGTCCAGGTGGGCCTCTGGTACTGAAGCATCT
GACAGCACTCATTAAATCACAAGAAAAGGTTGGCATTGTGGGAAGAACCGGAGCTGGAAAAAGTTCCCTC
ATCTCAGCCCTTTTTAGATTGTCAGAACCCGAAGGTAAAATTTGGATTGATAAGATCTTGACAACTGAAATT
GGACTTCACGATTTAAGGAAGAAAATGTCAATCATACCTCAGGAACCTGTTTTGTTCACTGGAACAATGAG
GAAAAACCTGGATCCCTTTAATGAGCACACGGATGAGGAACTGTGGAATGCCTTACAAGAGGTACAACTT
AAAGAAACCATTGAAGATCTTCCTGGTAAAATGGATACTGAATTAGCAGAATCAGGATCCAATTTTAGTGT
TGGACAAAGACAACTGGTGTGCCTTGCCAGGGCAATTCTCAGGAAAAATCAGATATTGATTATTGATGAAG
CGACGGCAAATGTGGATCCAAGAACTGATGAGTTAATACAAAAAAAAATCCGGGAGAAATTTGCCCACTG
CACCGTGCTAACCATTGCACACAGATTGAACACCATTATTGACAGCGACAAGATAATGGTTTTAGATTCAG
GAAGACTGAAAGAATATGATGAGCCGTATGTTTTGCTGCAAAATAAAGAGAGCCTATTTTACAAGATGGTG
CAACAACTGGGCAAGGCAGAAGCCGCTGCCCTCACTGAAACAGCAAAACAGGTATACTTCAAAAGAAATT
ATCCACATATTGGTCACACTGACCACATGGTTACAAACACTTCCAATGGACAGCCCTCGACCTTAACTATTTT
CGAGACAGCACTCGAGACCGGTCATCATCACCATCACCATTGAGTTTATCTGACTAAATCTTAGTTTGTATT
GTCATGTTTTAATACAATATGTTATGTTTGGGTCTAGAATTCGAAGCTTGTCGAGAAGTACTAGAGGATCAT
AATCAGCCATACCACATTTGTAGAGGTTTTACTTGCTTTAAAAAACCTCCCACACCTCCCCCTGAACCTGAAA
CATAAAATGAATGCAATTGTTGTTGTTAACTTGTTTATTGCAGCTTATAATGGTTACAAATAAAGCAATAGC
ATCACAAATTTCACAAATAAAGCATTTTTTTCACTGCATTCTAGTTGTGGTTTGTCCAAACTCATCAATGTAT
CTTATCATGTCTGGATCTGATCACTGCTTGAGCCTAGGAGATCCGAACCAGATAAGTGAAATCTAGTTCCAA
ACTATTTTGTCATTTTTAATTTTCGTATTAGCTTACGACGCTACACCCAGTTCCCATCTATTTTGTCACTCTTCC
CTAAATAATCCTTAAAAACTCCATTTCCACCCCTCCCAGTTCCCAACTATTTTGTCCGCCCACAGCGGGGCAT
TTTTCTTCCTGTTATGTTTTTAATCAAACATCCTGCCAACTCCATGTGACAAACCGTCATCTTCGGCTACTTTT
TCTCTGTCACAGAATGAAAATTTTTCTGTCATCTCTTCGTTATTAATGTTTGTAATTGACTGAATATCAACGCT
TATTTGCAGCCTGAATGGCGAATGG

7.2 pPICZαC MRP4-his$_6$ sequence

AGATCTAACATCCAAAGACGAAAGGTTGAATGAAACCTTTTTGCCATCCGACATCCACAGGTCCATTCTC
ACACATAAGTGCCAAACGCAACAGGAGGGGATACACTAGCAGCAGACCGTTGCAAACGCAGGACCTCCAC
TCCTCTTCTCCTCAACACCCACTTTTGCCATCGAAAAACCAGCCCAGTTATTGGGCTTGATTGGAGCTCGCTC
ATTCCAATTCCTTCTATTAGGCTACTAACACCATGACTTTATTAGCCTGTCTATCCTGGCCCCCCTG
GCGAGGTTCATGTTTGTTTATTTCCGAATGCAACAAGCTCCGCATTACACCCGAACATCACTCCAGATGA
GGGCTTTCTGAGTGTGGGGTCAAATAGTTTCATGTTCCCCAAATGGCCCAAAACTGACAGTTTAAACGCT
GTCTTGGAACCTAATATGACAAAAGCGTGATCTCATCCAAGATGAACTAAGTTTGGTTCGTTGAAATGCT
AACGGCCAGTTGGTCAAAAAGAAACTTCCAAAAGTCGGCATACCGTTTGTCTTGTTTGGTATTGATTGAC
GAATGCTCAAAAATAATCTCATTAATGCTTAGCGCAGTCTCTCTATCGCTTCTGAACCCCGGTGCACCTG
TGCCGAAACGCAAATGGGGAAACACCCGCTTTTTGGATGATTATGCATTGTCTCCACATTGTATGCTTCC
AAGATTCTGGTGGGAATACTGCTGATAGCCTAACGTTCATGATCAAAATTTAACTGTTCTAACCCCTACT
TGACAGCAATATATAAACAGAAGGAAGCTGCCCTGTCTTAAACCTTTTTTTTTATCATCATTATTAGCTT
ACTTTCATAATTGCGACTGGTTCCAATTGACAAGCTTTTGATTTTAACGACTTTTAACGACAACTTGAGA
AGATCAAAAAACAACTAATTATTCGAAACGATGAGATTTCCTTCAATTTTTACTGCTGTTTTATTCGCAG
CATCCTCCGCATTAGCTGCTCCAGTCAACACTACAACAGAAGATGAAACGGCACAAATTCCGGCTGAAGC
TGTCATCGGTTACTCAGATTTAGAAGGGGATTTCGATGTTGCTGTTTTGCCATTTTCCAACAGCACAAAT
AACGGGTTATTGTTTATAAATACTACTATTGCCAGCATTGCTGCTAAAGAAGAAGGGGTATCTCTCGAGA
AAAGAGAGGCTGAAGCATCGATGAATTCAAAGGCCTACGTCGACGAGCTCAACATGCTGCCCGTGTACCA
GGAGGTGAAGCCCAACCCGCTGCAGGACGCGAACCTCTGCTCACGCGTGTTCTTCTGGTGGCTCAATCCCT
TGTTTAAAATTGGCCATAAACGGAGATTAGAGGAAGATGATATGTATTCAGTGCTGCCAGAAGACCGCTCA
CAGCACCTTGGAGAGGAGTTGCAAGGGTTCTGGGATAAAGAAGTTTTAAGAGCTGAGAATGACGCACAG
AAGCCTTCTTTAACAAGAGCAATCATAAAGTGTTACTGGAAATCTTATTTAGTTTTGGGAATTTTTACGTTAA
TTGAGGAAAGTGCCAAAGTAATCCAGCCCATATTTTTGGGAAAAATTATTAATTATTTTGAAAATTATGATC
CCATGGATTCTGTGGCTTTGAACACAGCGTACGCCTATGCCACGGTGCTGACTTTTTGCACGCTCATTTTGG
CTATACTGCATCACTTATATTTTTATCACGTTCAGTGTGCTGGGATGAGGTTACGAGTAGCCATGTGCCATA
TGATTTATCGGAAGGCACTTCGTCTTAGTAACATGGCCATGGGGAAGACAACCACAGGCCAGATAGTCAAT
CTGCTGTCCAATGATGTGAACAAGTTTGATCAGGTGACAGTGTTCTTACACTTCCTGTGGGCAGGACCACT
GCAGGCGATCGCAGTGACTGCCCTACTCTGGATGGAGATAGGAATATCGTGCCTTGCTGGGATGGCAGTT
CTAATCATTCTCCTGCCCTTGCAAAGCTGTTTTGGGAAGTTGTTCTCATCACTGAGGAGTAAAACTGCAACT
TTCACGGATGCCAGGATCAGGACCATGAATGAAGTTATAACTGGTATAAGGATAATAAAAATGTACGCCTG
GGAAAAGTCATTTTCAAATCTTATTACCAATTTGAGAAAGAAGGAGATTTCCAAGATTCTGAGAAGTTCCTG
CCTCAGGGGGATGAATTTGGCTTCGTTTTTCAGTGCAAGCAAAATCATCGTGTTTGTGACCTTCACCACCTA
CGTGCTCCTCGGCAGTGTGATCACAGCCAGCCGCGTGTTCGTGGCAGTGACGCTGTATGGGGCTGTGCGG
CTGACGGTTACCCTCTTCTTCCCCTCAGCCATTGAGAGGGTGTCAGAGGCAATCGTCAGCATCCGAAGAAT
CCAGACCTTTTTGCTACTTGATGAGATATCACAGCGCAACCGTCAGCTGCCGTCAGATGGTAAAAAGATGG
TGCATGTGCAGGATTTTACTGCTTTTTGGGATAAGGCATCAGAGACCCCAACTCTACAAGGCCTTTCCTTTA
CTGTCAGACCTGGCGAATTGTTAGCTGTGGTCGGCCCCGTGGGAGCAGGGAAGTCATCACTGTTAAGTGC
CGTGCTCGGGGAATTGGCCCCAAGTCACGGGCTGGTCAGCGTGCATGGAAGAATTGCCTATGTGTCTCAG
CAGCCCTGGGTGTTCTCGGGAACTCTGAGGAGTAATATTTTATTTGGGAAGAAATACGAAAAGGAACGAT
ATGAAAAAGTCATAAAGGCTTGTGCTCTGAAAAAGGATTTACAGCTGTTGGAGGATGGTGATCTGACTGT
GATAGGAGATCGGGGAACCACGCTGAGTGGAGGGCAGAAAGCACGGGTAAACCTTGCAAGAGCAGTGTA
TCAAGATGCTGACATCTATCTCCTGGACGATCCTCTCAGTGCAGTAGATGCGGAAGTTAGCAGACACTTGT
TCGAACTGTGTATTTGTCAAATTTTGCATGAGAAGATCACAATTTTAGTGACTCATCAGTTGCAGTACCTCA
AAGCTGCAAGTCAGATTCTGATATTGAAAGATGGTAAAATGGTGCAGAAGGGGACTTACACTGAGTTCCT

AAAATCTGGTATAGATTTTGGCTCCCTTTTAAAGAAGGATAATGAGGAAAGTGAACAACCTCCAGTTCCAG
GAACTCCCACACTAAGGAATCGTACCTTCTCAGAGTCTTCGGTTTGGTCTCAACAATCTTCTAGACCCTCCTT
GAAAGATGGTGCTCTGGAGAGCCAAGATACAGAGAATGTCCCAGTTACACTATCAGAGGAGAACCGTTCT
GAAGGAAAAGTTGGTTTTCAGGCCTATAAGAATTACTTCAGAGCTGGTGCTCACTGGATTGTCTTCATTTTC
CTTATTCTCCTAAACACTGCAGCTCAGGTTGCCTATGTGCTTCAAGATTGGTGGCTTTCATACTGGGCAAAC
AAACAAAGTATGCTAAATGTCACTGTAAATGGAGGAGGAAATGTAACCGAGAAGCTAGATCTTAACTGGT
ACTTAGGAATTTATTCAGGTTTAACTGTAGCTACCGTTCTTTTTGGCATAGCAAGATCTCTATTGGTATTCTA
CGTCCTTGTTAACTCTTCACAAACTTTGCACAACAAAATGTTTGAGTCAATTCTGAAAGCTCCGGTATTATTC
TTTGATAGAAATCCAATAGGAAGAATTTTAAATCGTTTCTCCAAAGACATTGGACACTTGGATGATTTGCTG
CCGCTGACGTTTTTAGATTTCATCCAGACATTGCTACAAGTGGTTGGTGTGGTCTCTGTGGCTGTGGCCGTG
ATTCCTTGGATCGCAATACCCTTGGTTCCCCTTGGAATCATTTTCATTTTTCTTCGGCGATATTTTTTGGAAAC
GTCAAGAGATGTGAAGCGCCTGGAATCTACAACTCGGAGTCCAGTGTTTTCCCACTTGTCATCTTCTCTCCA
GGGGCTCTGGACCATCCGGGCATACAAAGCAGAAGAGAGGTGTCAGGAACTGTTTGATGCACACCAGGAT
TTACATTCAGAGGCTTGGTTCTTGTTTTTGACAACGTCCCGCTGGTTCGCCGTCCGTCTGGATGCCATCTGT
GCCATGTTTGTCATCATCGTTGCCTTTGGGTCCCTGATTCTGGCAAAAACTCTGGATGCCGGGCAGGTTGGT
TTGGCACTGTCCTATGCCCTCACGCTCATGGGGATGTTTCAGTGGTGTGTTCGACAAAGTGCTGAAGTTGA
GAATATGATGATCTCAGTAGAAAGGGTCATTGAATACACAGACCTTGAAAAAGAAGCACCTTGGGAATAT
CAGAAACGCCCACCACCAGCCTGGCCCCATGAAGGAGTGATAATCTTTGACAATGTGAACTTCATGTACAG
TCCAGGTGGGCCTCTGGTACTGAAGCATCTGACAGCACTCATTAAATCACAAGAAAAGGTTGGCATTGTGG
GAAGAACCGGAGCTGGAAAAAGTTCCCTCATCTCAGCCCTTTTTAGATTGTCAGAACCCGAAGGTAAAATT
TGGATTGATAAGATCTTGACAACTGAAATTGGACTTCACGATTTAAGGAAGAAAATGTCAATCATACCTCA
GGAACCTGTTTTGTTCACTGGAACAATGAGGAAAAACCTGGATCCCTTTAATGAGCACACGGATGAGGAAC
TGTGGAATGCCTTACAAGAGGTACAACTTAAAGAAACCATTGAAGATCTTCCTGGTAAAATGGATACTGAA
TTAGCAGAATCAGGATCCAATTTTAGTGTTGGACAAAGACAACTGGTGTGCCTTGCCAGGGCAATTCTCAG
GAAAAATCAGATATTGATTATTGATGAAGCGACGGCAAATGTGGATCCAAGAACTGATGAGTTAATACAA
AAAAAAATCCGGGAGAAATTTGCCCACTGCACCGTGCTAACCATTGCACACAGATTGAACACCATTATTGA
CAGCGACAAGATAATGGTTTTAGATTCAGGAAGACTGAAAGAATATGATGAGCCGTATGTTTTGCTGCAAA
ATAAAGAGAGCCTATTTTACAAGATGGTGCAACAACTGGGCAAGGCAGAAGCCGCTGCCCTCACTGAAAC
AGCAAAACAGGTATACTTCAAAAGAAATTATCCACATATTGGTCACACTGACCACATGGTTACAAACACTTC
CAATGGACAGCCCTCGACCTTAACTATTTTCGAGACAGCACTCGAGACCGGTCATCATCACCATCACCATTG
AGTTTATCTGACTAAATCTTAGTTTGTATTGTCATGTTTTAATACAATATGTTATGTTTGGGTCTAGATTCAC
GTGGCCCAGCCGGCCGTCTCGGATCGGTACCTCGAGCCGCGGCGGCCGCCAGCTTTCTAGAACAAAAACT
CATCTCAGAAGAGGATCTGAATAGCGCCGTCGACCATCATCATCATCATCATTGAGTTTGTAGCCTTAGACA
TGACTGTTCCTCAGTTCAAGTTGGGCACTTACGAGAAGACCGGTCTTGCTAGATTCTAATCAAGAGGATGT
CAGAATGCCATTTGCCTGAGAGATGCAGGCTTCATTTTTGATACTTTTTTATTTGTAACCTATATAGTATAGG
ATTTTTTTTGTCATTTTGTTTCTTCTCGTACGAGCTTGCTCCTGATCAGCCTATCTCGCAGCTGATGAATATCT
TGTGGTAGGGGTTTGGGAAAATCATTCGAGTTTGATGTTTTTCTTGGTATTTCCCACTCCTCTTCAGAGTAC
AGAAGATTAAGTGAGACCTTCGTTTGTGCGGATCCCCCACACACCATAGCTTCAAAATGTTTCTACTCCTTTT
TTACTCTTCCAGATTTTCTCGGACTCCGCGCATCGCCGTACCACTTCAAAACACCCAAGCACAGCATACTAA
ATTTTCCCTCTTTCTTCCTCTAGGGTGTCGTTAATTACCCGTACTAAAGGTTTGGAAAAGAAAAAAGAGACC
GCCTCGTTTCTTTTTCTTCGTCGAAAAAGGCAATAAAAATTTTTATCACGTTTCTTTTTCTTGAAATTTTTTTTT
TTAGTTTTTTTCTCTTTCAGTGACCTCCATTGATATTTAAGTTAATAAACGGTCTTCAATTTCTCAAGTTTCAG
TTTCATTTTTCTTGTTCTATTACAACTTTTTTTACTTCTTGTTCATTAGAAAGAAAGCATAGCAATCTAATCTA
AGGGGCGGTGTTGACAATTAATCATCGGCATAGTATATCGGCATAGTATAATACGACAAGGTGAGGAACT
AAACCATGGCCAAGTTGACCAGTGCCGTTCCGGTGCTCACCGCGCGCGACGTCGCCGGAGCGGTCGAGTT
CTGGACCGACCGGCTCGGGTTCTCCCGGGACTTCGTGGAGGACGACTTCGCCGGTGTGGTCCGGGACGAC
GTGACCCTGTTCATCAGCGCGGTCCAGGACCAGGTGGTGCCGGACAACACCCTGGCCTGGGTGTGGGTGC

GCGGCCTGGACGAGCTGTACGCCGAGTGGTCGGAGGTCGTGTCCACGAACTTCCGGGACGCCTCCGGGCC
GGCCATGACCGAGATCGGCGAGCAGCCGTGGGGGCGGGAGTTCGCCCTGCGCGACCCGGCCGGCAACTG
CGTGCACTTCGTGGCCGAGGAGCAGGACTGACACGTCCGACGGCGGCCCACGGGTCCCAGGCCTCGGAG
ATCCGTCCCCCTTTTCCTTTGTCGATATCATGTAATTAGTTATGTCACGCTTACATTCACGCCCTCCCCCCACA
TCCGCTCTAACCGAAAAGGAAGGAGTTAGACAACCTGAAGTCTAGGTCCCTATTTATTTTTTTATAGTTATG
TTAGTATTAAGAACGTTATTTATATTTCAAATTTTTCTTTTTTTTCTGTACAGACGCGTGTACGCATGTAACAT
TATACTGAAAACCTTGCTTGAGAAGGTTTTGGGACGCTCGAAGGCTTTAATTTGCAAGCTGGAGACCAACA
TGTGAGCAAAAGGCCAGCAAAAGGCCAGGAACCGTAAAAAGGCCGCGTTGCTGGCGTTTTTCCATAGGCT
CCGCCCCCCTGACGAGCATCACAAAAATCGACGCTCAAGTCAGAGGTGGCGAAACCCGACAGGACTATAA
AGATACCAGGCGTTTCCCCCTGGAAGCTCCCTCGTGCGCTCTCCTGTTCCGACCCTGCCGCTTACCGGATAC
CTGTCCGCCTTTCTCCCTTCGGGAAGCGTGGCGCTTTCTCAATGCTCACGCTGTAGGTATCTCAGTTCGGTG
TAGGTCGTTCGCTCCAAGCTGGGCTGTGTGCACGAACCCCCCGTTCAGCCCGACCGCTGCGCCTTATCCGG
TAACTATCGTCTTGAGTCCAACCCGGTAAGACACGACTTATCGCCACTGGCAGCAGCCACTGGTAACAGGA
TTAGCAGAGCGAGGTATGTAGGCGGTGCTACAGAGTTCTTGAAGTGGTGGCCTAACTACGGCTACACTAG
AAGGACAGTATTTGGTATCTGCGCTCTGCTGAAGCCAGTTACCTTCGGAAAAAGAGTTGGTAGCTCTTGAT
CCGGCAAACAAACCACCGCTGGTAGCGGTGGTTTTTTTGTTTGCAAGCAGCAGATTACGCGCAGAAAAAAA
GGATCTCAAGAAGATCCTTTGATCTTTTCTACGGGGTCTGACGCTCAGTGGAACGAAAACTCACGTTAAGG
GATTTTGGTCATGAGATC

7.3 pcDNA 3.1 MRP4-his$_6$ sequence

GACGGATCGG GAGATCTCCC GATCCCCTAT GGTCGACTCT CAGTACAATC TGCTCTGATG
CCGCATAGTTAAGCCAGTATCTGCTCCCTGCTTGTGTGTTGGAGGTCGCTGAGTAGTGCGCGAGCAAAATT
TAAGCTACAACAAGGCAAGGCTTGACCGACAATTGCATGAAGAATCTGCTTAGGGTTAGGCGTTTTGCGCT
GCTTCGCGATGTACGGGCCAGATATACGCGTTGACATTGATTATTGACTAGTTATTAATAGTAATCAATTAC
GGGGTCATTAGTTCATAGCCCATATATGGAGTTCCGCGTTACATAACTTACGGTAAATGGCCCGCCTGGCT
GACCGCCCAACGACCCCCGCCCATTGACGTCAATAATGACGTATGTTCCCATAGTAACGCCAATA
GGGACTTTCC ATTGACGTCA ATGGGTGGACTATTTACGGTAAACTGCCCACTTGGCAGTACATCAAGTGT
ATCATATGCC AAGTACGCCC CCTATTGACG TCAATGACGG TAAATGGCCC GCCTGGCATT
ATGCCCAGTACATGACCTTA TGGGACTTTC CTACTTGGCA GTACATCTAC GTATTAGTCA TCGCTATTAC
CATGGTGATG CGGTTTTGGC AGTACATCAA TGGGCGTGGA TAGCGGTTTG ACTCACGGGG
ATTTCCAAGT CTCCACCCCA TTGACGTCAA TGGGAGTTTG
TTTTGGCACCAAAATCAACGGGACTTTCCAAAATGTCGTAACAACTCCGCCCCATTGACGCAAATGGGCGG
TAGGCGTGTACGGTGGGAGGTCTATATAAGCAGAGCTCTCTGGCTAACTAGAGAACCCACTGCTTACTGGC
TTATCGAAATTAATACGACTCACTATAGGGAGACCCAAGCTGGCTAGCGTTTAAACTTAAGCTTGGTACCG
AGCTCGGATCCACTAGTCCAGTGTGGTGGAATTCAAAGGCCTACGTCGACGAGCTCAACATGCTGCCCGTG
TACCAGGAGGTGAAGCCCAACCCGCTGCAGGACGCGAACCTCTGCTCACGCGTGTTCTTCTGGTGGCTCAA
TCCCTTGTTTAAAATTGGCCATAAACGGAGATTAGAGGAAGATGATATGTATTCAGTGCTGCCAGAAGACC
GCTCACAGCACCTTGGAGAGGAGTTGCAAGGGTTCTGGGATAAAGAAGTTTTAAGAGCTGAGAATGACGC
ACAGAAGCCTTCTTTAACAAGAGCAATCATAAAGTGTTACTGGAAATCTTATTTAGTTTTGGGAATTTTTAC
GTTAATTGAGGAAAGTGCCAAAGTAATCCAGCCCATATTTTTGGGAAAAATTATTAATTATTTTGAAAATTA
TGATCCCATGGATTCTGTGGCTTTGAACACAGCGTACGCCTATGCCACGGTGCTGACTTTTTGCACGCTCAT
TTTGGCTATACTGCATCACTTATATTTTTATCACGTTCAGTGTGCTGGGATGAGGTTACGAGTAGCCATGTG
CCATATGATTTATCGGAAGGCACTTCGTCTTAGTAACATGGCCATGGGGAAGACAACCACAGGCCAGATAG
TCAATCTGCTGTCCAATGATGTGAACAAGTTTGATCAGGTGACAGTGTTCTTACACTTCCTGTGGGCAGGAC
CACTGCAGGCGATCGCAGTGACTGCCCTACTCTGGATGGAGATAGGAATATCGTGCCTTGCTGGGATGGC
AGTTCTAATCATTCTCCTGCCCTTGCAAAGCTGTTTTGGGAAGTTGTTCTCATCACTGAGGAGTAAAACTGC
AACTTTCACGGATGCCAGGATCAGGACCATGAATGAAGTTATAACTGGTATAAGGATAATAAAAATGTACG
CCTGGGAAAAGTCATTTTCAAATCTTATTACCAATTTGAGAAAGAAGGAGATTTCCAAGATTCTGAGAAGTT
CCTGCCTCAGGGGGATGAATTTGGCTTCGTTTTTCAGTGCAAGCAAAATCATCGTGTTTGTGACCTTCACCA
CCTACGTGCTCCTCGGCAGTGTGATCACAGCCAGCCGCGTGTTCGTGGCAGTGACGCTGTATGGGGCTGTG
CGGCTGACGGTTACCCTCTTCTTCCCCTCAGCCATTGAGAGGGTGTCAGAGGCAATCGTCAGCATCCGAAG
AATCCAGACCTTTTTGCTACTTGATGAGATATCACAGCGCAACCGTCAGCTGCCGTCAGATGGTAAAAAGA
TGGTGCATGTGCAGGATTTTACTGCTTTTTGGGATAAGGCATCAGAGACCCCAACTCTACAAGGCCTTTCCT
TTACTGTCAGACCTGGCGAATTGTTAGCTGTGGTCGGCCCCGTGGGAGCAGGGAAGTCATCACTGTTAAGT
GCCGTGCTCGGGGAATTGGCCCCAAGTCACGGGCTGGTCAGCGTGCATGGAAGAATTGCCTATGTGTCTC
AGCAGCCCTGGGTGTTCTCGGGAACTCTGAGGAGTAATATTTTATTTGGGAAGAAATACGAAAAGGAACG
ATATGAAAAAGTCATAAAGGCTTGTGCTCTGAAAAAGGATTTACAGCTGTTGGAGGATGGTGATCTGACTG
TGATAGGAGATCGGGGAACCACGCTGAGTGGAGGGCAGAAAGCACGGGTAAACCTTGCAAGAGCAGTGT
ATCAAGATGCTGACATCTATCTCCTGGACGATCCTCTCAGTGCAGTAGATGCGGAAGTTAGCAGACACTTG
TTCGAACTGTGTATTTGTCAAATTTTGCATGAGAAGATCACAATTTTAGTGACTCATCAGTTGCAGTACCTC
AAAGCTGCAAGTCAGATTCTGATATTGAAAGATGGTAAAATGGTGCAGAAGGGGACTTACACTGAGTTCC
TAAAATCTGGTATAGATTTTGGCTCCCTTTTAAAGAAGGATAATGAGGAAAGTGAACAACCTCCAGTTCCA
GGAACTCCCACACTAAGGAATCGTACCTTCTCAGAGTCTTCGGTTTGGTCTCAACAATCTTCTAGACCCTCCT
TGAAAGATGGTGCTCTGGAGAGCCAAGATACAGAGAATGTCCCAGTTACACTATCAGAGGAGAACCGTTC
TGAAGGAAAAGTTGGTTTTCAGGCCTATAAGAATTACTTCAGAGCTGGTGCTCACTGGATTGTCTTCATTTT
CCTTATTCTCCTAAACACTGCAGCTCAGGTTGCCTATGTGCTTCAAGATTGGTGGCTTTCATACTGGGCAAA
CAAACAAAGTATGCTAAATGTCACTGTAAATGGAGGAGGAAATGTAACCGAGAAGCTAGATCTTAACTGG
TACTTAGGAATTTATTCAGGTTTAACTGTAGCTACCGTTCTTTTTGGCATAGCAAGATCTCTATTGGTATTCT
ACGTCCTTGTTAACTCTTCACAAACTTTGCACAACAAAATGTTTGAGTCAATTCTGAAAGCTCCGGTATTATT

CTTTGATAGAAATCCAATAGGAAGAATTTTAAATCGTTTCTCCAAAGACATTGGACACTTGGATGATTTGCT
GCCGCTGACGTTTTTAGATTTCATCCAGACATTGCTACAAGTGGTTGGTGTGGTCTCTGTGGCTGTGGCCGT
GATTCCTTGGATCGCAATACCCTTGGTTCCCCTTGGAATCATTTTCATTTTTCTTCGGCGATATTTTTTGGAAA
CGTCAAGAGATGTGAAGCGCCTGGAATCTACAACTCGGAGTCCAGTGTTTTCCCACTTGTCATCTTCTCTCC
AGGGGCTCTGGACCATCCGGGCATACAAAGCAGAAGAGAGGTGTCAGGAACTGTTTGATGCACACCAGG
ATTTACATTCAGAGGCTTGGTTCTTGTTTTTGACAACGTCCCGCTGGTTCGCCGTCCGTCTGGATGCCATCT
GTGCCATGTTTGTCATCATCGTTGCCTTTGGGTCCCTGATTCTGGCAAAAACTCTGGATGCCGGGCAGGTTG
GTTTGGCACTGTCCTATGCCCTCACGCTCATGGGGATGTTTCAGTGGTGTGTTCGACAAAGTGCTGAAGTT
GAGAATATGATGATCTCAGTAGAAAGGGTCATTGAATACACAGACCTTGAAAAAGAAGCACCTTGGGAAT
ATCAGAAACGCCCACCACCAGCCTGGCCCCATGAAGGAGTGATAATCTTTGACAATGTGAACTTCATGTAC
AGTCCAGGTGGGCCTCTGGTACTGAAGCATCTGACAGCACTCATTAAATCACAAGAAAAGGTTGGCATTGT
GGGAAGAACCGGAGCTGGAAAAAGTTCCCTCATCTCAGCCCTTTTTAGATTGTCAGAACCCGAAGGTAAAA
TTTGGATTGATAAGATCTTGACAACTGAAATTGGACTTCACGATTTAAGGAAGAAAATGTCAATCATACCTC
AGGAACCTGTTTTGTTCACTGGAACAATGAGGAAAAACCTGGATCCCTTTAATGAGCACACGGATGAGGA
ACTGTGGAATGCCTTACAAGAGGTACAACTTAAAGAAACCATTGAAGATCTTCCTGGTAAAATGGATACTG
AATTAGCAGAATCAGGATCCAATTTTAGTGTTGGACAAAGACAACTGGTGTGCCTTGCCAGGGCAATTCTC
AGGAAAAATCAGATATTGATTATTGATGAAGCGACGGCAAATGTGGATCCAAGAACTGATGAGTTAATAC
AAAAAAAAATCCGGGAGAAATTTGCCCACTGCACCGTGCTAACCATTGCACACAGATTGAACACCATTATT
GACAGCGACAAGATAATGGTTTTAGATTCAGGAAGACTGAAAGAATATGATGAGCCGTATGTTTTGCTGCA
AAATAAAGAGAGCCTATTTTACAAGATGGTGCAACAACTGGGCAAGGCAGAAGCCGCTGCCCTCACTGAA
ACAGCAAAACAGGTATACTTCAAAAGAAATTATCCACATATTGGTCACACTGACCACATGGTTACAAACACT
TCCAATGGACAGCCCTCGACCTTAACTATTTTCGAGACAGCACTCGAGACCGGTCATCATCACCATCACCAT
TGAGTTTATCTGACTAAATCTTAGTTTGTATTGTCATGTTTTAATACAATATGTTATGTTTGGGTCTAGAATT
CGAAGCTTGTCGAGAAGTACTAGAGGATCATAATCAGCCATACCACATTTGTAGAGGTTTTACTTGCTTTAA
AAAACCTCCCACACCTCCCCCTGAACCTGAAACATAAAATGAATGCAATTGTTGTTGTTAACTTGTTTATTGC
AGCTTATAATGGTTACAAATAAAGCAATAGCATCACAAATTTCACAAATAAAGCATTTTTTTCACTGCATTCT
AGTTGTGGTTTGTCCAAACTCATCAATGTATCTTATCATGTCTGGATCTGATCACTGCTTGAGCCTAGGAGA
TCCGAACCAGATAAGTGAAATCTAGTTCCAAACTATTTTGTCATTTTTAATTTTCGTATTAGCTTACGACGCT
ACACCCAGTTCCCATCTATTTTGTCACTCTTCCCTAAATAATCCTTAAAAACTCCATTTCCACCCCTCCCAGTT
CCCAACTATTTTGTCCGCCCACAGCGGGGCATTTTTCTTCCTGTTATGTTTTTAATCAAACATCCTGCCAACTC
CATGTGACAAACCGTCATCTTCGGCTACTTTTTCTCTGTCACAGAATGAAAATTTTTCTGTCATCTCTTCGTTA
TTAATGTTTGTAATTGACTGAATATCAACGCTTATTTGCAGCCTGAATGGCGAATGGAATTCTGCAGATATC
CAGCACAGTGGCGGCCGCTCGAGGTGAGCAAGGGCGAGGAGCTGTTCACCGGGGTGGTGCCCATCCTGG
TCGAGCTGGACGGCGACGTAAACGGCCACAAGTTCAGCGTGCGCGGCGAGGGCGAGGGCGATGCCACCA
ACGGCAAGCTGACCCTGAAGTTCATCTGCACCACCGGCAAGCTGCCCGTGCCCTGGCCCACCCTCGTGACC
ACCCTGACCTACGGCGTGCAGTGCTTCAGCCGCTACCCCGACCACATGAAGCAGCACGACTTCTTCAAGTC
CGCCATGCCCGAAGGCTACGTCCAGGAGCGCACCATCTCCTTCAAGGACGACGGCACCTACAAGACCCGC
GCCGAGGTGAAGTTCGAGGGCGACACCCTGGTGAACCGCATCGAGCTGAAGGGCATCGACTTCAAGGAG
GACGGCAACATCCTGGGGCACAAGCTGGAGTACAACTACAACAGCCACAACGTCTATATCACCGCTGACA
AGCAGAAGAACGGCATCAAGGCCAACTTCAAGATCCGCCACAACATCGAGGACGGCAGCGTGCAGCTCGC
CGACCACTACCAGCAGAACACCCCCATCGGCGACGGCCCCGTGCTGCTGCCCGACAACCACTACCTGAGCA
CCCAGTCCGCCCTGAGCAAAGACCCCAACGAGAAGCGCGATCACATGGTCCTGCTGGAGTTCGTGACCGC
CGCCGGGATCACTCTCGGCATGGACGAGCTGTACAAGTAATCTAGAGGGCCCGTTTAAAC CCGCTGATCA
GCCTCGACTG TGCCTTCTAG TTGCCAGCCATCTGTTGTTT GCCCCTCCCC CGTGCCTTCCTTGACCCTGG
AAGGTGCCACTCCCACTGTC CTTTCCTAAT AAAATGAGGA AATTGCATCG CATTGTCTGAGTAGGTGTCA
TTCTATTCTG GGGGGTGGGG TGGGGCAGGA CAGCAAGGGGGAGGATTGGG AAGACAATAG
CAGGCATGCT GGGGATGCGG TGGGCTCTATGGCTTCTGAG GCGGAAAGAA CCAGCTGGGG
CTCTAGGGGG TATCCCCACGCGCCCTGTAG CGGCGCATTA AGCGCGGCGG GTGTGGTGGT
TACGCGCAGCGTGACCGCTA CACTTGCCAG CGCCCTAGCG CCCGCTCCTT
TCGCTTTCTTCCCTTCCTTTTCGCCACGT TCGCCGGCTT TCCCCGTCAA
GCTCTAAATCGGGGCATCCCTTTAGGGTTC CGATTTAGTG CTTTACGGCA CCTCGACCCCAAAAAACTTG
ATTAGGGTGA TGGTTCACGT AGTGGGCCATCGCCCTGATAGACGGTTTTT CGCCCTTTGA CGTTGGAGTC
CACGTTCTTT AATAGTGGACTCTTGTTCCA AACTGGAACA ACACTCAACC CTATCTCGGT
CTATTCTTTTGATTTATAAG GGATTTTGGG GATTTCGGCC TATTGGTTAA AAAATGAGCTGATTTAACAA

AAATTTAACG CGAATTAATT CTGTGGAATG TGTGTCAGTTAGGGTGTGGA AAGTCCCCAG
GCTCCCCAGG CAGGCAGAAG TATGCAAAGCATGCATCTCA ATTAGTCAGC AACCAGGTGT
GGAAAGTCCC CAGGCTCCCCAGCAGGCAGA AGTATGCAAA GCATGCATCT CAATTAGTCA
GCAACCATAGTCCCGCCCCT AACTCCGCCC ATCCCGCCCC TAACTCCGCC CAGTTCCGCCCATTCTCCGC
CCCATGGCTG ACTAATTTTT TTTATTTATG CAGAGGCCGAGGCCGCCTCT GCCTCTGAGC TATTCCAGAA
GTAGTGAGGA GGCTTTTTTGGAGGCCTAGG CTTTTGCAAA AAGCTCCCGG GAGCTTGTAT
ATCCATTTTCGGATCTGATC AGCACGTGTT GACAATTAAT CATCGGCATA GTATATCGGCATAGTATAAT
ACGACAAGGT GAGGAACTAA ACCATGGCCA AGTTGACCAGTGCCGTTCCG GTGCTCACCG
CGCGCGACGT CGCCGGAGCG GTCGAGTTCTGGACCGACCG GCTCGGGTTC TCCCGGGACT
TCGTGGAGGA CGACTTCGCCGGTGTGGTCC GGGACGACGT GACCCTGTTC
ATCAGCGCGGTCCAGGACCAGGTGGTGCCGGACAACACCCTGGCCTGGGTGTGGGTGCGCGGCCTGGAC
GAGCTGTACGCCGAGTGGTCGGAGGTCGTGTCCACGAACTTCCGGGACGCCTCCGGGCCGGCCATGACCG
AGATCGGCGAGCAGCCGTGGGGGCGGGAGTTCGCCCTGCGCGACCCGGCCGGCAACTGCGTGCACTTCG
TGGCCGAGGAGCAGGACTGACACGTGCTACGAGATTTCGATTCCACCGCCGCTTCTATGAAAGGTTGGGC
TTCGGAATCGTTTTCCGGGACGCCGGCTGGA TGATCCTCCAGCGCGGGGAT CTCATGCTGG
AGTTCTTCGC CCACCCCAAC TTGTTTATTGCAGCTTATAA TGGTTACAAA TAAAGCAATA GCATCACAAA
TTTCACAAATAAAGCATTTT TTTCACTGCA TTCTAGTTGT GGTTTGTCCA AACTCATCAATGTATCTTAT
CATGTCTGTA TACCGTCGAC CTCTAGCTAG AGCTTGGCGTAATCATGGTC ATAGCTGTTT CCTGTGTGAA
ATTGTTATCC GCTCACAATTCCACACAACA TACGAGCCGG AAGCATAAAG TGTAAAGCCT
GGGGTGCCTAATGAGTGAGC TAACTCACAT TAATTGCGTT GCGCTCACTG CCCGCTTTCCAGTCGGGAAA
CCTGTCGTGC CAGCTGCATT AATGAATCGG CCAACGCGCGGGGAGAGGCG GTTTGCGTAT
TGGGCGCTCT TCCGCTTCCT CGCTCACTGACTCGCTGCGC TCGGTCGTTC GGCTGCGGCG
AGCGGTATCA GCTCACTCAAAGGCGGTAAT ACGGTTATCC ACAGAATCAG GGGATAACGC
AGGAAAGAACATGTGAGCAA AAGGCCAGCA AAAGGCCAGG AACCGTAAAA
AGGCCGCGTTGCTGGCGTTT TTCCATAGGC TCCGCCCCCC TGACGAGCAT CACAAAAATCGACGCTCAAG
TCAGAGGTGG CGAAACCCGA CAGGACTATA AAGATACCAGGCGTTTCCCC CTGGAAGCTC
CCTCGTGCGC TCTCCTGTTC CGACCCTGCCGCTTACCGGA TACCTGTCCG CCTTTCTCCC TTCGGGAAGC
GTGGCGCTTTTCAATGCTC ACGCTGTAGG TATCTCAGTT CGGTGTAGGT CGTTCGCTCCAAGCTGGGCT
GTGTGCACGA ACCCCCCGTT CAGCCCGACC GCTGCGCCTTATCCGGTAAC TATCGTCTTG AGTCCAACCC
GGTAAGACAC GACTTATCGCCACTGGCAGC AGCCACTGGT AACAGGATTA GCAGAGCGAG
GTATGTAGGC GGTGCTACAG AGTTCTTGAA GTGGTGGCCT AACTACGGCT
ACACTAGAAGGACAGTATTT GGTATCTGCG CTCTGCTGAA GCCAGTTACC
TTCGGAAAAAGAGTTGGTAG CTCTTGATCC GGCAAACAAA CCACCGCTGG TAGCGGTGGTTTTTTTGTTT
GCAAGCAGCA GATTACGCGC AGAAAAAAAG GATCTCAAGA AGATCCTTTG ATCTTTTCTA
CGGGGTCTGA CGCTCAGTGG AACGAAAACTCACGTTAAGG GATTTTGGTC ATGAGATTAT
CAAAAAGGAT CTTCACCTAGATCCTTTTAA ATTAAAAATG AAGTTTTAAA TCAATCTAAA GTATATATGA
GTAAACTTGG TCTGACAGTT ACCAATGCTT AATCAGTGAG GCACCTATCTCAGCGATCTG TCTATTTCGT
TCATCCATAG TTGCCTGACT CCCCGTCGTGTAGATAACTA CGATACGGGA GGGCTTACCA TCTGGCCCCA
GTGCTGCAATGATACCGCGA GACCCACGCT CACCGGCTCC AGATTTATCA
GCAATAAACCAGCCAGCCGG AAGGGCCGAG CGCAGAAGTG GTCCTGCAAC
TTTATCCGCCTCCATCCAGT CTATTAATTG TTGCCGGGAA GCTAGAGTAA GTAGTTCGCCAGTTAATAGT
TTGCGCAACG TTGTTGCCAT TGCTACAGGC ATCGTGGTGTCACGCTCGTC GTTTGGTATG GCTTCATTCA
GCTCCGGTTC CCAACGATCAAGGCGAGTTA CATGATCCCC CATGTTGTGC AAAAAAGCGG
TTAGCTCCTTCGGTCCTCCG ATCGTTGTCA GAAGTAAGTT GGCCGCAGTG TTATCACTCATGGTTATGGC
AGCACTGCAT AATTCTCTTA CTGTCATGCC ATCCGTAAGATGCTTTTCTG TGACTGGTGA GTACTCAACC
AAGTCATTCT GAGAATAGTGTATGCGGCGA CCGAGTTGCT CTTGCCCGGC GTCAATACGG
GATAATACCGCGCCACATAG CAGAACTTTA AAAGTGCTCA TCATTGGAAA
ACGTTCTTCGGGGCGAAAAC TCTCAAGGAT CTTACCGCTG TTGAGATCCA GTTCGATGTAACCCACTCGT
GCACCCAACT GATCTTCAGC ATCTTTTACT TTCACCAGCGTTTCTGGGTG AGCAAAAACA
GGAAGGCAAA ATGCCGCAAA AAAGGGAATAAGGGCGACAC GGAAATGTTG AATACTCATA
CTCTTCCTTT TTCAATATTA TTGAAGCATT TATCAGGGTT ATTGTCTCAT GAGCGGATAC
ATATTTGAATTATTTAGAA AAATAAACAA ATAGGGGTTC CGCGCACATT TCCCCGAAAA GTGCCACCTG
ACGTC

8 References

Agez, M., P. Schultz, I. Medina, D. J. Baker, M. P. Burnham, R. A. Cardarelli, L. C. Conway, K. Garnier, S. Geschwindner, A. Gunnarsson, E. J. McCall, A. Frechard, S. Audebert, T. Z. Deeb, S. J. Moss, N. J. Brandon, Q. Wang, N. Dekker and A. Jawhari (2017). "Molecular architecture of potassium chloride co-transporter KCC2." Scientific Reports **7**.

Ahmad, M., M. Hirz, H. Pichler and H. Schwab (2014). "Protein expression in Pichia pastoris: recent achievements and perspectives for heterologous protein production." Applied Microbiology and Biotechnology **98**(12): 5301-5317.

Alam, A., R. Kung, J. Kowal, R. A. McLeod, N. Tremp, E. V. Broude, I. B. Roninson, H. Stahlberg and K. P. Locher (2018). "Structure of a zosuquidar and UIC2-bound human-mouse chimeric ABCB1." Proceedings of the National Academy of Sciences of the United States of America **115**(9): E1973-E1982.

Andrell, J. and C. G. Tate (2013). "Overexpression of membrane proteins in mammalian cells for structural studies." Molecular Membrane Biology **30**(1): 52-63.

Ashok, Y., R. T. Nanekar and V.-P. Jaakola (2013). "Crystallogenesis of Adenosine A(2A) Receptor-T4 Lysozyme Fusion Protein: A Practical Route for the Structure." G Protein Coupled Receptors: Structure **520**: 175-198.

Bayburt, T. H., Y. V. Grinkova and S. G. Sligar (2002). "Self-assembly of discoidal phospholipid bilayer nanoparticles with membrane scaffold proteins." Nano Letters **2**(8): 853-856.

Bayburt, T. H. and S. G. Sligar (2003). "Self-assembly of single integral membrane proteins into soluble nanoscale phospholipid bilayers." Protein Science **12**(11): 2476-2481.

Bayburt, T. H. and S. G. Sligar (2010). "Membrane protein assembly into Nanodiscs." Febs Letters **584**(9): 1721-1727.

Berger, I., D. J. Fitzgerald and T. J. Richmond (2004). "Baculovirus expression system for heterologous multiprotein complexes." Nature Biotechnology **22**(12): 1583-1587.

Bersch, B., J. M. Dorr, A. Hessel, J. A. Killian and P. Schanda (2017). "Proton-Detected Solid-State NMR Spectroscopy of a Zinc Diffusion Facilitator Protein in Native Nanodiscs." Angewandte Chemie-International Edition **56**(9): 2508-2512.

Bird, L. E., H. Rada, A. Verma, R. Gasper, J. Birch, M. Jennions, J. Loewe, I. Moraes and R. J. Owens (2015). "Green Fluorescent Protein-based Expression Screening of Membrane Proteins in Escherichia coli." Jove-Journal of Visualized Experiments(95).

Boekema, E. J., M. Folea and R. Kouril (2009). "Single particle electron microscopy." Photosynthesis Research **102**(2-3): 189-196.

Booth, P. J., S. L. Flitsch, L. J. Stern, D. A. Greenhalgh, P. S. Kim and H. G. Khorana (1995). "INTERMEDIATES IN THE FOLDING OF THE MEMBRANE-PROTEIN BACTERIORHODOPSIN." Nature Structural Biology **2**(2): 139-143.

Borst, P., C. de Wolf and K. van de Wetering (2007). "Multidrug resistance-associated proteins 3, 4, and 5." Pflugers Arch **453**(5): 661-673.

Broecker, J., B. T. Eger and O. P. Ernst (2017). "Crystallogenesis of Membrane Proteins Mediated by Polymer-Bounded Lipid Nanodiscs." Structure **25**(2): 384-392.

Bruce Alberts, D. B., Karen Hopkin, Alexander D Johnson, Alexander Johnson, Julian Lewis, Martin Raff, Keith Roberts, Peter Walter (2009). Essential Cell Biology, Garland Publishing.

Bruhn, H. (2005). "A short guided tour through functional and structural features of saposin-like proteins." Biochemical Journal **389**: 249-257.

Byme, B. (2015). "Pichia pastoris as an expression host for membrane protein structural biology." Current Opinion in Structural Biology **32**: 9-17.

Chae, P. S., K. Gotfryd, J. Pacyna, L. J. W. Miercke, S. G. F. Rasmussen, R. A. Robbins, R. R. Rana, C. J. Loland, B. Kobilka, R. Stroud, B. Byrne, U. Gether and S. H. Gellman (2010). "Tandem Facial Amphiphiles for Membrane Protein Stabilization." Journal of the American Chemical Society **132**(47): 16750-16752.

Chae, P. S., R. R. Rana, K. Gotfryd, S. G. F. Rasmussen, A. C. Kruse, K. H. Cho, S. Capaldi, E. Carlsson, B. Kobilka, C. J. Loland, U. Gether, S. Banerjee, B. Byrne, J. K. Lee and S. H. Gellman (2013). "Glucose-Neopentyl Glycol (GNG) amphiphiles for membrane protein study." Chemical Communications **49**(23): 2287-2289.

Chae, P. S., S. G. F. Rasmussen, R. R. Rana, K. Gotfryd, R. Chandra, M. A. Goren, A. C. Kruse, S. Nurva, C. J. Loland, Y. Pierre, D. Drew, J.-L. Popot, D. Picot, B. G. Fox, L. Guan, U. Gether, B. Byrne, B. Kobilka and S. H. Gellman (2010). "Maltose-neopentyl glycol (MNG) amphiphiles for solubilization, stabilization and crystallization of membrane proteins." Nature Methods **7**(12): 1003-U1090.

Chantemargue, B., F. Di Meo, K. Berka, N. Picard, H. Arnion, M. Essig, P. Marquet, M. Otyepka and P. Trouillas (2018). "Structural patterns of the human ABCC4/MRP4 exporter in lipid bilayers rationalize clinically observed polymorphisms." Pharmacological Research **133**: 318-327.

Chloupkova, M., A. Pickert, J. Y. Lee, S. Souza, Y. T. Trinh, S. M. Connelly, M. E. Dumont, M. Dean and I. L. Urbatsch (2007). "Expression of 25 human ABC transporters in the yeast Pichia pastoris and characterization of the purified ABCC3 ATPase activity." Biochemistry **46**(27): 7992-8003.

Cho, K. H., M. Husri, A. Amin, K. Gotfryd, H. J. Lee, J. Go, J. W. Kim, C. J. Loland, L. Guan, B. Byrne and P. S. Chae (2015). "Maltose neopentyl glycol-3 (MNG-3) analogues for membrane protein study." Analyst **140**(9): 3157-3163.

Claros, M. G. and G. Vonheijne (1994). "TOPPRED-II - AN IMPROVED SOFTWARE FOR MEMBRANE-PROTEIN STRUCTURE PREDICTIONS." Computer Applications in the Biosciences **10**(6): 685-686.

Craig, A. F., E. E. Clark, I. D. Sahu, R. Zhang, N. D. Frantz, M. S. Al-Abdul-Wahid, C. Dabney-Smith, D. Konkolewicz and G. A. Lorigan (2016). "Tuning the size of styrene-maleic acid copolymer-lipid nanoparticles (SMALPs) using RAFT polymerization for biophysical studies." Biochimica Et Biophysica Acta-Biomembranes **1858**(11): 2931-2939.

Dean, M. (2005). Genetics of ATP-binding cassette transporters. Phase Ii Conjugation Enzymes and Transport Systems. H. Sies and L. Packer. **400:** 409-429.

Dean, M., A. Rzhetsky and R. Allikmets (2001). "The human ATP-binding cassette (ABC) transporter superfamily." Genome Research **11**(7): 1156-1166.

Deisenhofer, J., O. Epp, K. Miki, R. Huber and H. Michel (1985). "STRUCTURE OF THE PROTEIN SUBUNITS IN THE PHOTOSYNTHETIC REACTION CENTER OF RHODOPSEUDOMONAS-VIRIDIS AT 3A RESOLUTION." Nature **318**(6047): 618-624.

Dilworth, M. V., M. S. Piel, K. E. Bettaney, P. Ma, J. Luo, D. Sharples, D. R. Poyner, S. R. Gross, K. Moncoq, P. J. F. Henderson, B. Miroux and R. M. Bill (2018). "Microbial expression systems for membrane proteins." Methods (San Diego, Calif.) **147**: 3-39.

Dorr, J. M., M. C. Koorengevel, M. Schafer, A. V. Prokofyev, S. Scheidelaar, E. A. van der Cruijsen, T. R. Dafforn, M. Baldus and J. A. Killian (2014). "Detergent-free isolation, characterization, and functional reconstitution of a tetrameric K+ channel: the power of native nanodiscs." Proc Natl Acad Sci U S A **111**(52): 18607-18612.

Dorr, J. M., S. Scheidelaar, M. C. Koorengevel, J. J. Dominguez, M. Schafer, C. A. van Walree and J. A. Killian (2016). "The styrene-maleic acid copolymer: a versatile tool in membrane research." Eur Biophys J **45**(1): 3-21.

Drew, D., D. J. Slotboom, G. Friso, T. Reda, P. Genevaux, M. Rapp, N. M. Meindl-Beinker, W. Lambert, M. Lerch, D. O. Daley, K. J. Van Wijk, J. Hirst, E. Kunji and J. W. De Gier (2005). "A scalable, GFP-based pipeline for membrane protein overexpression screening and purification." Protein Science **14**(8): 2011-2017.

El-Sheikh, A. A. K., J. van den Heuvel, E. Krieger, F. G. M. Russel and J. B. Koenderink (2008). "Functional role of arginine 375 in transmembrane helix 6 of multidrug resistance protein 4 (MRP4/ABCC4)." Molecular Pharmacology **74**(4): 964-971.

Ellinger, P., M. Kluth, J. Stindt, S. H. J. Smits and L. Schmitt (2013). "Detergent Screening and Purification of the Human Liver ABC Transporters BSEP (ABCB11) and MDR3 (ABCB4) Expressed in the Yeast Pichia pastoris." Plos One **8**(4).

Eshaghi, S., M. Hedren, M. I. A. Nasser, T. Hammarberg, A. Thornell and P. Nordlund (2005). "An efficient strategy for high-throughput expression screening of recombinant integral membrane proteins." Protein Science **14**(3): 676-683.

Fagerberg, L., K. Jonasson, G. von Heijne, M. Uhlen and L. Berglund (2010). "Prediction of the human membrane proteome." Proteomics **10**(6): 1141-1149.

Flayhan, A., H. D. T. Mertens, Y. Ural-Blimke, M. M. Molledo, D. I. Svergun and C. Loew (2018). "Saposin Lipid Nanoparticles: A Highly Versatile and Modular Tool for Membrane Protein Research." Structure **26**(2): 345-+.

Fleming, K. G., A. L. Ackerman and D. M. Engelman (1997). "The effect of point mutations on the free energy of transmembrane alpha-helix dimerization." Journal of Molecular Biology **272**(2): 266-275.

Fujiyoshi, Y. (2011). "Electron crystallography for structural and functional studies of membrane proteins." Journal of Electron Microscopy **60**: S149-S159.

Galian, C., F. Manon, M. Dezi, C. Torres, C. Ebel, D. Levy and J. M. Jault (2011). "Optimized purification of a heterodimeric ABC transporter in a highly stable form amenable to 2-D crystallization." PLoS One **6**(5): e19677.

Gao, M., D. W. Loe, C. E. Grant, S. P. C. Cole and R. G. Deeley (1996). "Reconstitution of ATP-dependent leukotriene C-4 transport by co-expression of both half-molecules of human multidrug resistance protein in insect cells." Journal of Biological Chemistry **271**(44): 27782-27787.

Garavito, R. M. and S. Ferguson-Miller (2001). "Detergents as tools in membrane biochemistry." Journal of Biological Chemistry **276**(35): 32403-32406.

Goldie, K. N., P. Abeyrathne, F. Kebbel, M. Chami, P. Ringler and H. Stahlberg (2014). "Cryo-electron microscopy of membrane proteins." Methods in molecular biology (Clifton, N.J.) **1117**: 325-341.

Gottesman, M. M., T. Fojo and S. E. Bates (2002). "Multidrug resistance in cancer: role of ATP-dependent transporters." Nat Rev Cancer **2**(1): 48-58.

Gulati, S., M. Jamshad, T. J. Knowles, K. A. Morrison, R. Downing, N. Cant, R. Collins, J. B. Koenderink, R. C. Ford, M. Overduin, I. D. Kerr, T. R. Dafforn and A. J. Rothnie (2014). "Detergent-free purification of ABC (ATP-binding-cassette) transporters." Biochemical Journal **461**: 269-278.

Hall, S. C. L., C. Tognoloni, J. Charlton, E. C. Bragginton, A. J. Rothnie, P. Sridhar, M. Wheatley, T. J. Knowles, T. Arnold, K. J. Edler and T. R. Dafforn (2018). "An acid-compatible co-polymer for the solubilization of membranes and proteins into lipid bilayer-containing nanoparticles." Nanoscale **10**(22): 10609-10619.

Hardy, D., R. M. Bill, A. Jawhari and A. J. Rothnie (2016). "Overcoming bottlenecks in the membrane protein structural biology pipeline." Biochem Soc Trans **44**(3): 838-844.

Hauser, A. S., S. Chavali, I. Masuho, L. J. Jahn, K. A. Martemyanov, D. E. Gloriam and M. M. Babu (2018). "Pharmacogenomics of GPCR Drug Targets." Cell **172**(1-2): 41-+.

Heydenreich, F. M., Z. Vuckovic, M. Matkovic and D. B. Veprintsev (2015). "Stabilization of G protein-coupled receptors by point mutations." Frontiers in Pharmacology **6**.

Hopkins, R. F. and D. Esposito (2009). "A rapid method for titrating baculovirus stocks using the Sf-9 Easy Titer cell line." Biotechniques **47**(3): 785-787.

Igonet, S., C. Raingeval, E. Cecon, M. Pucic-Bakovic, G. Lauc, O. Cala, M. Baranowski, J. Perez, R. Jockers, I. Krimm and A. Jawhari (2018). "Enabling STD-NMR fragment screening using stabilized native GPCR: A case study of adenosine receptor." Scientific Reports **8**.

Information, N. C. f. B. 2019, from https://pubchem.ncbi.nlm.nih.gov/compound/6076.

Invitrogen Bac-to-Bac Baculovirus Expression System.

Invitrogen pPICZα A, B, and C.

Jamshad, M., J. Charlton, Y. P. Lin, S. J. Routledge, Z. Bawa, T. J. Knowles, M. Overduin, N. Dekker, T. R. Dafforn, R. M. Bill, D. R. Poyner and M. Wheatley (2015). "G-protein coupled receptor solubilization and purification for biophysical analysis and functional studies, in the total absence of detergent." Biosci Rep **35**(2).

Jamshad, M., V. Grimard, I. Idini, T. J. Knowles, M. R. Dowle, N. Schofield, P. Sridhar, Y. Lin, R. Finka, M. Wheatley, O. R. T. Thomas, R. E. Palmer, M. Overduin, C. Govaerts, J.-M. Ruysschaert, K. J. Edler and T. R. Dafforn (2015). "Structural analysis of a nanoparticle containing a lipid bilayer used for detergent-free extraction of membrane proteins." Nano Research **8**(3): 774-789.

Jarvis, D. L. (2009). BACULOVIRUS-INSECT CELL EXPRESSION SYSTEMS. Guide to Protein Purification, Second Edition. R. R. Burgess and M. P. Deutscher. **463:** 191-222.

Jens Frauenfeld, R. L., Jean-Paul Armache, Andreas Sonnen, Fatma Guettou, Per Moberg, Lin Zhu, Caroline Jegerschöld, Ali Flayhan, John A.G. Briggs, Henrik Garoff, Christian Löw, Yifan Cheng, Pär Nordlund (2016). "A novel lipoprotein nanoparticle system for membrane proteins." Nature Methods **13**: 345-351.

Johnson, Z. L. and J. Chen (2017). "Structural Basis of Substrate Recognition by the Multidrug Resistance Protein MRP1." Cell **168**(6): 1075-+.

Kawate, T. and E. Gouaux (2006). "Fluorescence-detection size-exclusion chromatography for precrystallization screening of integral membrane proteins." Structure **14**(4): 673-681.

Kellosalo, J., T. Kajander, K. Kogan, K. Pokharel and A. Goldman (2012). "The Structure and Catalytic Cycle of a Sodium-Pumping Pyrophosphatase." Science **337**(6093): 473-476.

Killian, J. A. (2018). "The Styrene-Maleic Acid Copolymer: A Versatile Tool in Membrane Research." Biophysical Journal **114**(3): 402A-402A.

Kimple, M. E., A. L. Brill and R. L. Pasker (2013). "Overview of affinity tags for protein purification." Current protocols in protein science **73**: Unit 9.9-Unit 9.9.

Kobilka, B. K. (2007). "G protein coupled receptor structure and activation." Biochimica Et Biophysica Acta-Biomembranes **1768**(4): 794-807.

Kost, T. A., J. P. Condreay and D. L. Jarvis (2005). "Baculovirus as versatile vectors for protein expression in insect and mammalian cells." Nature Biotechnology **23**(5): 567-575.

Le Bon, C., A. Marconnet, S. Masscheleyn, J.-L. Popot and M. Zoonens (2018). "Folding and stabilizing membrane proteins in amphipol A8-35." Methods (San Diego, Calif.) **147**: 95-105.

le Maire, M., P. Champeil and J. V. Moller (2000). "Interaction of membrane proteins and lipids with solubilizing detergents." Biochimica Et Biophysica Acta-Biomembranes **1508**(1-2): 86-111.

Lee, S. C., B. C. Bennett, W. X. Hong, Y. Fu, K. A. Baker, J. Marcoux, C. V. Robinson, A. B. Ward, J. R. Halpert, R. C. Stevens, C. D. Stout, M. J. Yeager and Q. H. Zhang (2013). "Steroid-based facial

amphiphiles for stabilization and crystallization of membrane proteins." Proceedings of the National Academy of Sciences of the United States of America **110**(13): E1203-E1211.

Lee, S. C., T. J. Knowles, V. L. G. Postis, M. Jamshad, R. A. Parslow, Y. P. Lin, A. Goldman, P. Sridhar, M. Overduin, S. P. Muench and T. R. Dafforn (2016). "A method for detergent-free isolation of membrane proteins in their local lipid environment." Nature Protocols **11**(7): 1149-1162.

Lee, S. C. and N. L. Pollock (2016). "Membrane proteins: is the future disc shaped?" Biochemical Society Transactions **44**: 1011-1018.

Lefer, D. J., C. G. Nichols and W. A. Coetzee (2009). "Sulfonylurea Receptor 1 Subunits of ATP-Sensitive Potassium Channels and Myocardial Ischemia/Reperfusion Injury." Trends in Cardiovascular Medicine **19**(2): 61-67.

Leitz, A. J., T. H. Bayburt, A. N. Barnakov, B. A. Springer and S. G. Sligar (2006). "Functional reconstitution of beta(2)-adrenergic receptors utilizing self-assembling Nanodisc technology." Biotechniques **40**(5): 601-+.

Leslie, E. M., R. G. Deeley and S. P. C. Cole (2005). "Multidrug resistance proteins: role of P-glycoprotein, MRP1, MRP2, and BCRP (ABCG2) in tissue defense." Toxicology and Applied Pharmacology **204**(3): 216-237.

Li, C., P. C. Krishnamurthy, H. Penmatsa, K. L. Marrs, X. Q. Wang, M. Zaccolo, K. Jalink, M. Li, D. J. Nelson, J. D. Schuetz and A. P. Naren (2007). "Spatiotemporal coupling of cAMP transporter to CFTR chloride channel function in the gut epithelia." Cell **131**(5): 940-951.

Lichtenthaler, S. F., N. Ida, G. Multhaup, C. L. Masters and K. Beyreuther (1997). "Mutations in the transmembrane domain of APP altering gamma-secretase specificity." Biochemistry **36**(49): 15396-15403.

Lin, S. H. and G. Guidotti (2009). PURIFICATION OF MEMBRANE PROTEINS. Guide to Protein Purification, Second Edition. R. R. Burgess and M. P. Deutscher. **463:** 619-629.

Linton, K. J. (2007). Structure and Function of ABC Transporters.

Loll, P. J. (2014). "Membrane proteins, detergents and crystals: what is the state of the art?" Acta Crystallographica Section F-Structural Biology Communications **70**: 1576-1583.

Lund, S., S. Orlowski, B. Deforesta, P. Champeil, M. Lemaire and J. V. Moller (1989). "DETERGENT STRUCTURE AND ASSOCIATED LIPID AS DETERMINANTS IN THE STABILIZATION OF SOLUBILIZED CA-2+-ATPASE FROM SARCOPLASMIC-RETICULUM." Journal of Biological Chemistry **264**(9): 4907-4915.

Lyons, J. A., A. Boggild, P. Nissen and J. Frauenfeld (2017). "Saposin-Lipoprotein Scaffolds for Structure Determination of Membrane Transporters." Methods in enzymology **594**: 85-99.

Massimi, I., A. Ciuffetta, F. Temperilli, F. Ferrandino, A. Zicari, F. M. Pulcinelli and M. P. Felli (2015). "Multidrug Resistance Protein-4 Influences Aspirin Toxicity in Human Cell Line." Mediators of Inflammation.

Matar-Merheb, R., M. Rhimi, A. Leydier, F. Huche, C. Galian, E. Desuzinges-Mandon, D. Ficheux, D. Flot, N. Aghajari, R. Kahn, A. Di Pietro, J.-M. Jault, A. W. Coleman and P. Falson (2011). "Structuring Detergents for Extracting and Stabilizing Functional Membrane Proteins." Plos One **6**(3).

McDevitt, C. A., R. F. Collins, M. Conway, S. Modok, J. Storm, I. D. Kerr, R. C. Ford and R. Callaghan (2006). "Purification and 3D structural analysis of oligomeric human multidrug transporter ABCG2." Structure **14**(11): 1623-1632.

McKenzie, E. A. and W. M. Abbott (2018). "Expression of recombinant proteins in insect and mammalian cells." Methods (San Diego, Calif.) **147**: 40-49.

Meyer, T. H., P. M. Vanendert, S. Uebel, B. Ehring and R. Tampe (1994). "FUNCTIONAL EXPRESSION AND PURIFICATION OF THE ABC TRANSPORTER COMPLEX-ASSOCIATED WITH ANTIGEN-PROCESSING (TAP) IN INSECT CELLS." Febs Letters **351**(3): 443-447.

Mi, W., Y. Y. Li, S. H. Yoon, R. K. Ernst, T. Walz and M. F. Liao (2017). "Structural basis of MsbA-mediated lipopolysaccharide transport." Nature **549**(7671): 233-+.

Moraes, I., G. Evans, J. Sanchez-Weatherby, S. Newstead and P. D. S. Stewart (2014). "Membrane protein structure determination The next generation." Biochimica Et Biophysica Acta-Biomembranes **1838**(1): 78-87.

Morrison, K. A., A. Akram, A. Mathews, Z. A. Khan, J. H. Patel, C. M. Zhou, D. J. Hardy, C. Moore-Kelly, R. Patel, V. Odiba, T. J. Knowles, M. U. H. Javed, N. P. Chmel, T. R. Dafforn and A. J. Rothnie (2016). "Membrane protein extraction and purification using styrene-maleic acid (SMA) copolymer: effect of variations in polymer structure." Biochemical Journal **473**: 4349-4360.

Nagy, J. K., A. K. Hoffmann, M. H. Keyes, D. N. Gray, K. Oxenoid and C. R. Sanders (2001). "Use of amphipathic polymers to deliver a membrane protein to lipid bilayers." Febs Letters **501**(2-3): 115-120.

Oldham, M. L. and J. Chen (2011). "Snapshots of the maltose transporter during ATP hydrolysis." Proceedings of the National Academy of Sciences of the United States of America **108**(37): 15152-15156.

Oluwole, A. O., J. Klingler, B. Danielczak, J. O. Babalola, C. Vargas, G. Pabst and S. Keller (2017). "Formation of Lipid-Bilayer Nanodiscs by Diisobutylene/Maleic Acid (DIBMA) Copolymer." Langmuir **33**(50): 14378-14388.

Park, S. H., B. B. Das, F. Casagrande, Y. Tian, H. J. Nothnagel, M. Chu, H. Kiefer, K. Maier, A. A. De Angelis, F. M. Marassi and S. J. Opella (2012). "Structure of the chemokine receptor CXCR1 in phospholipid bilayers." Nature **491**(7426): 779-+.

Parmar, M., S. Rawson, C. A. Scarff, A. Goldman, T. R. Dafforn, S. P. Muench and V. L. G. Postis (2018). "Using a SMALP platform to determine a sub-nm single particle cryo-EM membrane protein structure." Biochimica Et Biophysica Acta-Biomembranes **1860**(2): 378-383.

Pham, P. L., A. Kamen and Y. Durocher (2006). "Large-scale Transfection of mammalian cells for the fast production of recombinant protein." Molecular Biotechnology **34**(2): 225-237.

Pollock, N. L., S. C. Lee, J. H. Patel, A. A. Gulamhussein and A. J. Rothnie (2018). "Structure and function of membrane proteins encapsulated in a polymer-bound lipid bilayer." Biochimica Et Biophysica Acta-Biomembranes **1860**(4): 809-817.

Postis, V., S. Rawson, J. K. Mitchell, S. C. Lee, R. A. Parslow, T. R. Dafforn, S. A. Baldwin and S. P. Muench (2015). "The use of SMALPs as a novel membrane protein scaffold for structure study by negative stain electron microscopy." Biochimica Et Biophysica Acta-Biomembranes **1848**(2): 496-501.

Prive, G. G. (2007). "Detergents for the stabilization and crystallization of membrane proteins." Methods **41**(4): 388-397.

Ravaud, S., M. A. Do Cao, M. Jidenko, C. Ebel, M. Le Maire, J. M. Jault, A. Di Pietro, R. Haser and N. Aghajari (2006). "The ABC transporter BmrA from Bacillus subtilis is a functional dimer when in a detergent-solubilized state." Biochemical Journal **395**: 345-353.

Ravna, A. W. and G. Sager (2008). "Molecular model of the outward facing state of the human multidrug resistance protein 4 (MRP4/ABCC4)." Bioorganic & Medicinal Chemistry Letters **18**(12): 3481-3483.

Ravula, T., N. Z. Hardin, S. K. Ramadugu, S. J. Cox and A. Ramamoorthy (2018). "Formation of pH-Resistant Monodispersed Polymer-Lipid Nanodiscs." Angewandte Chemie-International Edition **57**(5): 1342-1345.

Ravula, T., N. Z. Hardin, S. K. Ramadugu and A. Ramamoorthy (2017). "pH Tunable and Divalent Metal Ion Tolerant Polymer Lipid Nanodiscs." Langmuir **33**(40): 10655-10662.

Rawson, S., S. Davies, J. D. Lippiat and S. P. Muench (2016). "The changing landscape of membrane protein structural biology through developments in electron microscopy." Molecular Membrane Biology **33**(1-2): 12-22.

Rehan, S., V. O. Paavilainen and V. P. Jaakola (2017). "Functional reconstitution of human equilibrative nucleoside transporter-1 into styrene maleic acid co-polymer lipid particles." Biochimica Et Biophysica Acta-Biomembranes **1859**(5): 1059-1065.

Reichel, V., J. Klas, G. Fricker and R. Masereeuw (2010). "Fluo-cAMP is transported by multidrug resistance-associated protein isoform 4 in rat choroid plexus." Journal of Neurochemistry **115**(1): 200-208.

Reichel, V., R. Masereeuw, J. J. M. W. van den Heuvel, D. S. Miller and G. Fricker (2007). "Transport of a fluorescent cAMP analog in teleost proximal tubules." American Journal of Physiology-Regulatory Integrative and Comparative Physiology **293**(6): R2382-R2389.

Reid, G., P. Wielinga, N. Zelcer, M. De Haas, L. Van Deemter, J. Wijnholds, J. Balzarini and P. Borst (2003). "Characterization of the transport of nucleoside analog drugs by the human multidrug resistance proteins MRP4 and MRP5." Molecular Pharmacology **63**(5): 1094-1103.

Rius, M., J. Hummel-Eisenbeiss, A. F. Hofmann and D. Keppler (2006). "Substrate specificity of human ABCC4 (MRP4)-mediated cotransport of bile acids and reduced glutathione." American Journal of Physiology-Gastrointestinal and Liver Physiology **290**(4): G640-G647.

Rius, M., A. T. Nies, J. Hummel-Eisenbeiss, G. Jedlitschky and D. Keppler (2003). "Cotransport of reduced glutathione with bile salts by MRP4 (ABCC4) localized to the basolateral hepatocyte membrane." Hepatology **38**(2): 374-384.

Rosano, G. L. and E. A. Ceccarelli (2014). "Recombinant protein expression in Escherichia coli: advances and challenges." Frontiers in Microbiology **5**.

Rosenberg, M. F., Z. Bikadi, J. Chan, X. Liu, Z. Ni, X. Cai, R. C. Ford and Q. Mao (2010). "The Human Breast Cancer Resistance Protein (BCRP/ABCG2) Shows Conformational Changes with Mitoxantrone." Structure **18**(4): 482-493.

Rothnie, A. J. (2016). "Detergent-Free Membrane Protein Purification." Methods Mol Biol **1432**: 261-267.

Rubinstein, J. L. (2007). "Structural analysis of membrane protein complexes by single particle electron microscopy." Methods **41**(4): 409-416.

Russel, F. G. M., J. B. Koenderink and R. Masereeuw (2008). "Multidrug resistance protein 4 (MRP4/ABCC4): a versatile efflux transporter for drugs and signalling molecules." Trends in Pharmacological Sciences **29**(4): 200-207.

Sauna, Z. E., K. Nandigama and S. V. Ambudkar (2004). "Multidrug resistance protein 4 (ABCC4)-mediated ATP hydrolysis - Effect of transport substrates and characterization of the post-hydrolysis transition state." Journal of Biological Chemistry **279**(47): 48855-48864.

Scheidelaar, S., M. C. Koorengevel, J. D. Pardo, J. D. Meeldijk, E. Breukink and J. A. Killian (2015). "Molecular Model for the Solubilization of Membranes into Nanodisks by Styrene Maleic Acid Copolymers." Biophysical Journal **108**(2): 279-290.

Schymeinsky, J., H. Mayer, C. Tomsic, C. Tilp, J. D. Schuetz, Y. Cui, L. Wollin, F. Gantner and K. J. Erb (2013). "The Absence of Mrp4 Has No Effect on the Recruitment of Neutrophils and Eosinophils into the Lung after LPS, Cigarette Smoke or Allergen Challenge." Plos One **8**(4).

Scott, D. J., L. Kummer, D. Tremmel and A. Plueckthun (2013). "Stabilizing membrane proteins through protein engineering." Current Opinion in Chemical Biology **17**(3): 427-435.

Seddon, A. M., P. Curnow and P. J. Booth (2004). "Membrane proteins, lipids and detergents: not just a soap opera." Biochimica et Biophysica Acta (BBA) - Biomembranes **1666**(1–2): 105-117.

Shaikh, T. R., H. Gao, W. T. Baxter, F. J. Asturias, N. Boisset, A. Leith and J. Frank (2008). "SPIDER image processing for single-particle reconstruction of biological macromolecules from electron micrographs." Nature Protocols **3**(12): 1941-1974.

Shintre, C. A., A. C. W. Pike, Q. Li, J.-I. Kim, A. J. Barr, S. Goubin, L. Shrestha, J. Yang, G. Berridge, J. Ross, P. J. Stansfeld, M. S. P. Sansom, A. M. Edwards, C. Bountra, B. D. Marsden, F. von Delft, A. N. Bullock, O. Gileadi, N. A. Burgess-Brown and E. P. Carpenter (2013). "Structures of ABCB10, a human ATP-binding cassette transporter in apo- and nucleotide-bound states." Proceedings of the National Academy of Sciences of the United States of America **110**(24): 9710-9715.

Sinha, C., A. Ren, K. Arora, C.-S. Moon, S. Yarlagadda, W. Zhang, S. B. Cheepala, J. D. Schuetz and A. P. Naren (2013). "Multi-drug Resistance Protein 4 (MRP4)-mediated Regulation of Fibroblast Cell Migration Reflects a Dichotomous Role of Intracellular Cyclic Nucleotides." Journal of Biological Chemistry **288**(6): 3786-3794.

Skaar, K., H. J. Korza, M. Tarry, P. Sekyrova and M. Hogbom (2015). "Expression and Subcellular Distribution of GFP-Tagged Human Tetraspanin Proteins in Saccharomyces cerevisiae." Plos One **10**(7).

Stetsenko, A. and A. Guskov (2017). "An Overview of the Top Ten Detergents Used for Membrane Protein Crystallization." Crystals **7**(7).

Stroud, Z., S. C. L. Hall and T. R. Dafforn (2018). "Purification of membrane proteins free from conventional detergents: SMA, new polymers, new opportunities and new insights." Methods **147**: 106-117.

Sun, C., S. Benlekbir, P. Venkatakrishnan, Y. H. Wang, S. J. Hong, J. Hosler, E. Tajkhorshid, J. L. Rubinstein and R. B. Gennis (2018). "Structure of the alternative complex III in a supercomplex with cytochrome oxidase." Nature **557**(7703): 123-+.

Sun, Y.-L., A. Patel, P. Kumar and Z.-S. Chen (2012). "Role of ABC transporters in cancer chemotherapy." Chinese Journal of Cancer **31**(2): 51-57.

Tate, C. G. (2001). "Overexpression of mammalian integral membrane proteins for structural studies." Febs Letters **504**(3): 94-98.

Taylor, A. M., J. Storm, L. Soceneantu, K. J. Linton, M. Gabriel, C. Martin, J. Woodhouse, E. Blott, C. F. Higgins and R. Callaghan (2001). "Detailed characterization of cysteine-less P-glycoprotein reveals subtle pharmacological differences in function from wild-type protein." British Journal of Pharmacology **134**(8): 1609-1618.

Taylor, N. M. I., I. Manolaridis, S. M. Jackson, J. Kowal, H. Stahlberg and K. P. Locher (2017). "Structure of the human multidrug transporter ABCG2." Nature **546**(7659): 504-+.

Tribet, C., R. Audebert and J. L. Popot (1996). "Amphipols: Polymers that keep membrane proteins soluble in aqueous solutions." Proceedings of the National Academy of Sciences of the United States of America **93**(26): 15047-15050.

Tsybovsky, Y. and K. Palczewski (2014). "Expression, purification and structural properties of ABC transporter ABCA4 and its individual domains." Protein Expression and Purification **97**: 50-60.

Van Aubel, R., P. H. E. Smeets, J. van den Heuvel and F. G. M. Russel (2005). "Human organic anion transporter MRP4 (ABCC4) is an efflux pump for the purine end metabolite urate with multiple allosteric substrate binding sites." American Journal of Physiology-Renal Physiology **288**(2): F327-F333.

Van Aubel, R. A. M. H., P. H. E. Smeets, J. G. P. Peters, R. J. M. Bindels and F. G. M. Russel (2002). "The MRP4/ABCC4 gene encodes a novel apical organic anion transporter in human kidney

proximal tubules: Putative efflux pump for urinary cAMP and cGMP." Journal of the American Society of Nephrology **13**(3): 595-603.

van Geest, M. and J. S. Lolkema (2000). "Membrane topology and insertion of membrane proteins: Search for topogenic signals." Microbiology and Molecular Biology Reviews **64**(1): 13-+.

Vankeerberghen, A., H. Cuppens and J.-J. Cassiman (2002). "The cystic fibrosis transmembrane conductance regulator: an intriguing protein with pleiotropic functions." Journal of cystic fibrosis : official journal of the European Cystic Fibrosis Society **1**(1): 13-29.

Vatandoost J, D. B. (2017). "Stable and Transient Expression of Human Coagulation Factor IX in Mammalian Expression Systems; CHO Versus HEK Cells." Gene Cell Tissue.

Vonheijne, G. and Y. Gavel (1988). "TOPOGENIC SIGNALS IN INTEGRAL MEMBRANE-PROTEINS." European Journal of Biochemistry **174**(4): 671-678.

Wallin, E. and G. von Heijne (1998). "Genome-wide analysis of integral membrane proteins from eubacterial, archaean, and eukaryotic organisms." Protein Science **7**(4): 1029-1038.

Wilkens, S. (2015). "Structure and mechanism of ABC transporters." F1000prime reports **7**: 14-14.

Wittgen, H. G. M., J. J. M. W. van den Heuvel, E. Krieger, G. Schaftenaar, F. G. M. Russel and J. B. Koenderink (2012). "Phenylalanine 368 of multidrug resistance-associated protein 4 (MRP4/ABCC4) plays a crucial role in substrate-specific transport activity." Biochemical Pharmacology **84**(3): 366-373.

Wu, C. P., A. Klokouzas, S. B. Hladky, S. V. Ambudkar and M. A. Barrand (2005). "Interactions of mefloquine with ABC proteins, MRP1 (ABCC1) and MRP4 (ABCC4) that are present in human red cell membranes." Biochemical Pharmacology **70**(4): 500-510.

Wu, P., C. J. Oleschuk, Q. C. Mao, B. O. Keller, R. G. Deeley and S. P. C. Cole (2005). "Analysis of human multidrug resistance protein 1 (ABCC1) by matrix-assisted laser desorption ionization/time of flight mass spectrometry: Toward identification of leukotriene C4 binding sites." Molecular Pharmacology **68**(5): 1455-1465.

Zhang, Q., X. Ma, A. Ward, W.-X. Hong, V.-P. Jaakola, R. C. Stevens, M. G. Finn and G. Chang (2007). "Designing facial amphiphiles for the stabilization of integral membrane proteins." Angewandte Chemie-International Edition **46**(37): 7023-7025.

Zhang, S. S., N. N. Li, W. W. Zeng, N. Gao and M. J. Yang (2017). "Cryo-EM structures of the mammalian endo-lysosomal TRPML1 channel elucidate the combined regulation mechanism." Protein & Cell **8**(11): 834-847.

Zoonens, M., F. Giusti, F. Zito and J.-L. Popot (2007). "Dynamics of membrane Protein/Amphipol association studied by forster resonance energy transfer: Implications for in vitro studies of amphipol-stabilized membrane proteins." Biochemistry **46**(36): 10392-10404.